City Research Online

City St George's, University of London

Citation: Nassar, A-A. M. (1992). The strength and impact behaviour of intercritically annealed C-Mn-Al-Nb steels. (Unpublished Doctoral thesis, City, University of London)

This is the accepted version of the paper.

This version of the publication may differ from the final published version. To cite this item please consult the publisher's version.

Permanent repository link: https://openaccess.city.ac.uk/id/eprint/28540/

Copyright and Reuse: Copyright and Moral Rights remain with the author(s) and/or copyright holders. Copies of full items can be used for personal research or study, educational, or not-for-profit purposes without prior permission or charge, unless otherwise indicated, provided that the authors, title and full bibliographic details are credited, a hyperlink and/or URL is given for the original metadata page and the content is not changed in any way. For full details of reuse please refer to City Research Online policy.

City Research Online: http://openaccess.city.ac.uk/ publications@citystgeorges.ac.uk

THE CITY UNIVERSITY

LONDON

DEPARTMENT OF MECHANICAL ENGINEERING

&

AERONAUTICS

THE STRENGTH & IMPACT BEHAVIOUR OF INTERCRITICALLY ANNEALED C-Mn-Al-Nb STEELS

by

ABD-ALLAH MABROUK NASSAR

This thesis is submitted as a part of the requirements for the degree of Doctor of Philosophy.

June 1992

020220926

TO GOD THE ALL MIGHTY

TABLE OF CONTENTS

Page

TABLE OF CONTENTS 1

LIST OF FIGURES 6

LIST OF TABLES 14

LIST OF SYMBOLS 16

DECLARATION 18

ACKNOWLEDGMENTS 19

ABSTRACT 20

CHAPTER ONE 22

INTRODUCTION 22

CHAPTER TWO 24

LITERATURE SURVEY 24
- 2.1- INTRODUCTION. 24
- 2.2- PRODUCTION OF SHEET DUAL-PHASE STEELS. . 26
  - 2.2.1- INTERCRITICAL ANNEALING 28
  - 2.2.2- BOX-BATCH ANNEALING. 28
  - 2.2.3- CONTINUOUS-ANNEALING. 31
  - 2.2.4- AS-HOT-ROLLED DUAL-PHASE STEELS. . 35
- 2.3- CHARACTERISTICS OF SHEET DUAL-PHASE STEEL PRODUCED BY INTERCRITICAL ANNEALING. . . 46
  - 2.3.1- HEATING TEMPERATURE. 46
  - 2.3.2- HEATING TIME. 52
  - 2.3.3- ALLOYING ELEMENTS. 54
  - 2.3.4- COOLING RATE. 56
- 2.4- PHASE-TRANSFORMATION DURING INTERCRITICAL ANNEALING. 62
  - 2.4.1- FORMATION OF AUSTENITE DURING INTERCRITICAL ANNEALING HEAT-TREATMENT. 63
  - 2.4.2- CHANGE OF PROPERTIES OF FERRITE PHASE WITH INTERCRITICAL ANNEALING 74
- 2.5- ROLE OF ALLOYING ELEMENTS. 80
  - 2.5.1- Carbon. 81
  - 2.5.2- Manganese. 82
  - 2.5.3- Silicon. 83

2.5.4- MOLYBDENUM. 85
2.5.5- CHROMIUM. 86
2.6- ROLE OF MICROALLOYING ELEMENTS. 87
2.6.1- Hardenability of Austenite in the Intercritical Annealing Temperature Range. 91
2.6.2- NIOBIUM. 94
2.6.3- VANADIUM. 95
2.6.4- TITANIUM. 96
2.6.5- ALUMINIUM. 96
2.7- SELECTION PRINCIPLES 97
2.7.1- OPTIMUM VOLUME FRACTION. 97
2.7.2- SIZE AND SHAPE OF MARTENSITE PARTICLES. 97
2.7.3- MARTENSITE DISTRIBUTION. 98
2.7.4- MARTENSITE CARBON CONTENT. 98
2.7.5- PRECIPITATION REACTION. 98
2.7.6- GRAIN REFINEMENT. 98
2.8- STRUCTURE PROPERTY-RELATIONSHIP OF DUAL-PHASE STEELS. 100
2.8.1- STRENGTH. 100
2.8.2- DUCTILITY. 108
2.8.3- YIELD AND DEFORMATION BEHAVIOUR. . 113
2.8.4- IMPACT PROPERTIES. 116

CHAPTER THREE 120

EXPERIMENTAL PROCEDURE 120
3.1- MATERIAL PREPARATION 120
3.2- HEAT TREATMENT. 120
3.2.1- NORMALISING. 125
3.2.2- HEATING UP TO THE INTERCRITICAL ANNEALING TEMPERATURE 125
3.2.3- COOLING DOWN TO THE INTERCRITICAL ANNEALING TEMPERATURE 125
3.3- DETERMINATION OF MECHANICAL PROPERTIES . 132
3.3.1- ENGINEERING TENSILE PROPERTIES . . 132
3.3.2- IMPACT TEST 134
3.3.2.1- COOLING EQUIPMENT 134
3.3.2.2- DETERMINATION OF CRYSTALLINITY 138
3.3.3- MICRO-HARDNESS 139
3.4- MICRO-STRUCTURAL MEASUREMENTS 139
3.4.1- MECHANICAL POLISHING AND ETCHING . 140
3.4.2- FERRITE GRAIN SIZE. 140
3.4.3- VOLUME FRACTION OF PEARLITE . . . 141
3.4.4- GRAIN BOUNDARY CARBIDE THICKNESS. 141
3.5- GRAIN BOUNDARY CARBIDE DENSITY 142
3.6- SEGREGATION ANALYSIS. 142

CHAPTER FOUR 144

EXPERIMENTAL RESULTS 144

4.1- THE EFFECT OF MANGANESE LEVEL AND HOLDING TIME ON IMPACT AND TENSILE PROPERTIES . . 144
4.1.1- INTRODUCTION 144
4.1.2- MICRO-STRUCTURAL MEASUREMENTS. . . 145
4.1.3- IMPACT AND TENSILE BEHAVIOUR. . . 146
4.1.3.1- 0.56% Mn (C-Mn-Al-Nb STEEL). 146
4.1.3.2- 1% Mn (C-Mn Al-Nb steel). . 157
4.1.3.3- 1.49% Mn (C-Mn-Al-Nb STEEL). 165
4.1.4- COMPOSITIONAL CHANGES. 175
4.1.5- METALLOGRAPHY. 177
4.1.5.1- MICRO-STRUCTURAL CHANGES FOR 0.56% Mn AND 1% Mn STEELS . 177
4.1.5.1.1-COOLING DOWN TO THE INTERCRITICAL ANNEALING TEMPERATURE 177
4.1.5.1.2-HEATING UP TO THE INTERCRITICAL ANNEALING TEMPERATURE 177
4.1.5.2- METALLOGRAPHY of the 1.49% Mn STEEL 185
4.1.5.2.1-COOLING DOWN TO THE INTERCRITICAL ANNEALING TEMPERATURE 185
4.1.5.2.2-HEATING UP TO THE INTERCRITICAL ANNEALING TEMPERATURE 185
4.1.6- METALLOGRAPHY, MARTENSITE VOLUME FRACTION, AND MICROHARDNESS OF 0.56%Mn AND 1.49% Mn STEEL INTERCRITICAL ANNEALED FOR VARIOUS TIMES AND QUENCHED 194
4.1.6.1- METALLOGRAPHY OF 1.49%Mn STEEL 194
4.1.6.1.1-COOLING DOWN TO THE INTERCRITICAL ANNEALING TEMPERATURE 194
4.1.6.1.2-HEATING UP TO THE INTERCRITICAL ANNEALING 194
4.1.6.2- MARTENSITE VOLUME FRACTION. 199
4.1.6.3- MICRO-HARDNESS MEASUREMENTS. 202
4.1.6.4- CARBIDE DENSITY MEASUREMENTS. 205
4.2- THE EFFECT OF COOLING RATE AND HOLDING TIME ON IMPACT AND TENSILE PROPERTIES 207
4.2.1- INTRODUCTION. 207
4.2.2- MICROSTRUCTURAL MEASUREMENTS. . . 208
4.2.3- IMPACT AND TENSILE BEHAVIOUR. . . 212
4.2.4- COMPOSITIONAL CHANGES. 214
4.2.5- METALLOGRAPHY. 224
4.2.5.1- COOLING DOWN 224

4.2.5.2- HEATING UP. 224
4.3- THE EFFECT OF CARBON CONTENT AND HOLDING TIME ON IMPACT AND TENSILE PROPERTIES . . 232
4.3.1- INTRODUCTION. 232
4.3.2- MICRO-STRUCTURAL MEASUREMENTS: . . 233
4.3.3- IMPACT AND TENSILE BEHAVIOUR. . . 236
4.3.4- METALLURGY 246
4.3.4.1- COOLING DOWN. 246
4.3.4.2- HEATING UP. 246
4.4- THE EFFECT OF INTERCRITICAL ANNEALING TEMPERATURE AND HOLDING TIME ON IMPACT AND TENSILE PROPERTIES 250
4.4.1- INTRODUCTION. 250
4.4.2- MICROSTRUCTURAL MEASUREMENTS . . . 251
4.4.3- IMPACT AND TENSILE BEHAVIOUR. . . 252
4.4.4- METALLOGRAPHY. 263
4.4.4.1- COOLING DOWN. 263
4.4.4.2- HEATING UP. 263
4.5- THE EFFECT OF GRAIN SIZE AND HOLDING TIME ON IMPACT AND TENSILE PROPERTIES 268
4.5.1- INTRODUCTION. 268
4.5.2- MICROSTRUCTURAL MEASUREMENTS. . . 269
4.5.3- IMPACT AND TENSILE BEHAVIOUR. . . 272
4.5.3.1- THE FINER GRAINED (18 μm) PLAIN CARBON MANGANESE STEEL 272
4.5.3.2- THE COARSER GRAINED (37μm) PLAIN CARBON MANGANESE STEEL 272
4.5.4- METALLOGRAPHY. 289
4.5.4.1- Finer Grained (18 μm) Steel. 289
4.5.4.1.1- Cooling Down. . . 289
4.5.4.1.2- HEATING UP. 289
4.5.4.2- COARSER GRAINED (37μm) STEEL. 290
4.5.4.2.1- COOLING DOWN. . . . 290
4.5.4.2.2- HEATING UP. 290

CHAPTER FIVE 303

DISCUSSION 303
5.1- OVERVIEW. 303
5.2- CALCULATION OF LOWER YIELD STRENGTH (LYS). 307
5.3- RELATIONSHIP OF CHANGES IN GRAIN BOUNDARY CARBIDE THICKNESS TO IMPACT BEHAVIOUR. . 308
5.4- REFINEMENT of the GRAIN BOUNDARY CARBIDE. 314
5.5- MECHANISMS FOR MANGANESE DIFFUSION TO BOUNDARIES AND INTO AUSTENITE 320
5.6- IMPORTANCE OF PARTITIONING IN CONTROLLING TRANSFORMATION 322
5.6.1- COOLING DOWN FROM THE γ. 322

5.6.2- HEATING UP TO THE ITERCRITICAL ANNEALING TEMPERATURE 324
5.7- LITERATURE EXPERIMENTAL EVIDENCE FOR Mn DIFFUSION TO BOUNDARIES OR INTO THE γ . 324
5.8- PRESENT EVIDENCE FOR Mn DIFFUSION TO THE BOUNDARIES AND SEGREGATION INTO γ. . . . 326
5.9- THE EFFECT OF MANGANESE LEVEL ON IMPACT BEHAVIOUR. 330
5.9.1- CARBIDE THICKNESS After Normalising. 330
5.9.2- CARBIDE THICKNESS After Intercritical Annealing. 330
5.9.3- IMPACT PERFORMANCE FOR THE 0.56% Mn AND 1% Mn STEEL. 330
5.9.4- YIELD STRENGTH. 335
5.9.5- INTERCRITICAL ANNEALING OF THE 1.49% Mn STEEL. 335
5.9.5.1- IMPACT PERFORMANCE. . . . 335
5.9.5.2- YIELD STRENGTH. 341
5.9.6- MICROHARDNESS. 346
5.10- THE EFFECT OF COOLING RATE. 347
5.10.1- IMPACT PERFORMANCE. 347
5.10.2- YIELD STRENGTH. 348
5.11- THE EFFECT OF CARBON LEVEL. 351
5.11.1- IMPACT PERFORMANCE. 351
5.11.2- YIELD STRENGTH. 352
5.12- THE EFFECT OF HEATING TEMPERATURE. . . . 354
5.12.1- IMPACT PERFORMANCE. 354
5.12.2- YIELD STRENGTH. 355
5.13- THE EFFECT OF GRAIN SIZE. 357

CHAPTER SIX 361

CONCLUSIONS 361

CHAPTER SEVEN 365

FUTURE WORK 365

REFERENCES 367

PUBLICATION 384

LIST OF FIGURES

Figure 2.1- Automobiles Components Formed From V-Dual-Phase Steels. 25

Figure 2.2- Estimate of the Demand for HSLA Steels in the USA Automobile Industry. 27

Figure 2.3- Relationship Between Tensile Properties and Manganese Content. 30

Figure 2.4- Schematic Representation of Continuous Annealing Process. 32

Figure 2.5- Enrichment of Carbon and Manganese at Boundaries due to Coiling at High Temperature. 34

Figure 2.6- Schematic Representation of Laboratory Simulation of Hot-Strip Mill Processing. 38

Figure 2.7- Effect of Manganese Content on the Continuous Cooling Transformation Diagram 41

Figure 2.8- Upper Portion of CCT Diagrams for Steels in the Molybdenum and silicon Series. 43

Figure 2.9- Effect of Deformation on Continuous Cooling Transformation. 45

Figure 2.10- Effect of Intercritical Annealing Temperature on Properties of 48

Figure 2.11- Effect of Heating Temperature on Mechanical Properties of Two V-980X Steels. 49

Figure 2.12- Effect of Heating Time at 790°C on the Mechanical Properties of Two V-980X Steels. 54

Figure 2.13- Effect of Annealing Time on the Tensile Properties of, a- Mo-Nb Steel. b- Mo-V Steel. 55

Figure 2.14- The Effect of Cooling Rate on HSLA Steel After Contiuous Annealing. 57

Figure 2.15- The Effect of Cooling Rate After Intercritical Annealing on the Strength Properties of Cr-Steels. 59

Figure 2.16- Influence of Cooling Rate on the UTS X EL_T Product after Intercritical Annealing at 825°C. 60

Figure 2.17- a- Mn Partitioning by Grain Boundary Diffusion During I.A. b- Microstructure of 0.06C-1.5%Mn Steel I.A 1 hr at 740°C- Slow Cooled(4°C/in). 67

Figure 2.18- Detailed Microprobe Analysis of an Alloy 0.45%C-1.5%Mn Transformed for 5.37x106Sec (2 Month) at 728°C. 69

Figure 2.19- Austenite Formation Diagram for 0.12%C 1.5%Mn Steels. 71

Figure 2.20- Schematic Sequence Showing Likely Development of Austenite and Growth in MPDP Steels Annealed in the I.A. Temperature

Range. 73
Figure 2.21- Effect of Cooling Condition on Internal Friction. AC: Air Cooled. WQ: Water Quenched 76
Figure 2.22- Normal Stress-Strain Curves for GM-980X, SAE-980X, 980X, and Plain Carbon Steels. 88
Figure 2.23- Effect of Intercritical Annealing on Tensile Properties of Hot-Rolled Steels. 90
Figure 2.24- The 0.2% Flow Stress and the Tensile Strength as a Function of Percent Martensite for a Fe-Mn C Steels. 103
Figure 2.25- Yield (0.2%) and Tensile Strength of Ferrite-Martensite Steels. 107
Figure 2.26- Uniform and Total Elongation of Ferrite-Martensite Steels. 111
Figure 2.27a- Comparison of Observed n or True Uniform Strain with that of Mileko's Theory. 112
Figure 2.27b- Predicted n or True Uniform Strain as a Function of Tensile Strength for Various Ferrite Strengths. 112
Figure 2.28- Charpy Impact Energy as a Function of Temperature for as-Received, IDP, and ADP ADP Condition of a V-Steels., Filled Symbols are for Samples Tempered 1 hr at 300°C. 118
Fig.3.1- The Position of Charpy and Tensile Samples. 122
Fig.3.2- Cooling Curve for (Isoheat) Muffle Furnace. 123
Fig.3.3- Cooling Curve for (Isoheat) Air Circulating Furnace Used for the Intercritical Annealing. 124
Fig.3.4- Schematic Diagrams of Various Heat Treatment Used.(a)- Normalising., (b)- Heating Up., (c)- Cooling Down. 126
Fig.3.5- Schematic Diagrams of Various Heat Treatment Used for Plain Carbon Manganese Steel (Finer Grained). (a)- Normalising., (b)- Heating Up., (c)- Cooling Down. 128
Fig.3.6- Schematic Diagrams of Various Heat Treatment Used for Plain Carbon Manganese Steel (Corser Grained). (a)- Normalising., (b)- Heating Up., (c)- Cooling Down. 129
Fig.3.7- Diagram of the Position of the Temperature Measurements in the Plate. 131
Fig.3.8- Standard Tensile Sample. 133
Fig.3.9 a- Standard Charpy V-Notch Sample, b- Charpy V-Notch Impact Test. 135
Fig.3.10- Impact Sample Holder. 137
Fig.4.1a- Impact Transition Curves for 0.56%Mn SteelI.A. at 730°C for Various Times,

	Cooled at 7°C/min, Heating Up Cycle.	151
Fig 4.1b-	Fibrous Fracture Curves for 0.56%Mn Steel I.A. at 730°C for Various Times, Cooled at 7°C/min, Heating Up Cycle.	152
Fig.4.2a-	Impact Transition Curves for 0.56%Mn Steel I.A. at 730°C for Various, Times Cooled at 7°C/min, Cooling Down Cycle	153
Fig.4.2b-	Fibrous Fracture Curves for 0.56%Mn Steel I.A. at 730°C for Various Times, Cooled at 7°C/min, Cooling Down Cycle	154
Fig.4.3 -	The Effect of I.A. Time on the 54J ITT°C for the 0.56%Mn Steel.	155
Fig.4.4-	The Effect of I.A. Time on the Yield Strength for the 0.56%Mn Steel.	156
Fig.4.5a-	Impact Transition Curves for 1%Mn Steel I.A at 730°C for Various Times, Cooled at 7°C/min, Heating Up Cycle	159
Fig.4.5b-	Fibrous Fracture Curves for 1%Mn Steel I.A. at 730°C for Various Times, Cooled at 7°C/min, Heating Up Cycle.	160
Fig.4.6a-	Impact Transition Curves for 1%Mn Steel I.A. at 730°C for Various Times, Cooled at 7/°C, Cooling Down Cycle.	161
Fig.4.6b-	Fibrous Fracture Curves for 1%Mn Steel I.A. at 730°C for Various Times, Cooled at 7°C/min, Cooling Down Cycle.	162
Fig.4.7-	The Effect of I.A. Times on the 54J ITT°C for the 1%Mn Steel.	163
Fig. 4.8-	The Effect of I.A. Times on the Yield Strength for the 1%Mn Steel.	164
Fig.4.9a-	Impact Transition Curves for 1.49%Mn Steel I.A. at 730°C for Various Times, Cooled at 7°C/min, Heating Up Cycle.	167
Fig.4.9b-	Fibrous Fracture Curves for 1.49%Mn Steel I.A. at 730°C for Various Times, Cooled at 7°C/min, Heating Up Cycle.	168
Fig.4.10a-	ImpactTransition Curves for 1.49%Mn Steel I.A. at 730°C for Various Times, Cooled at 7°C/min, Cooling Down Cycle	169
Fig.4.10b-	Fibrous Fracture Curves for 1.49%Mn Steel I.A. at 730°C for Various Times, Cooled at 7°C/min, Cooling Down Cycle	170
Fig.4.11-	The Effect of I.A. Times on the 54J ITT°C for the 1.49%Mn Steel.	171
Fig.4.12-	The Effect of I.A. Times on the Yield Strength for the 1.49%Mn Steel.	172
Fig. 4.13-	The Effect of Manganese Level on the 54J ITT°C During I.A.	173
Fig.4.14-	The Effect of Manganese Level on the Yield Strength During I.A.	174
Fig.4.15-	Microstructure of the 0.56%Mn Steel. a-Normalised, b-I.A. for 30 min at 730°C, Cooled at 7°C/min, Cooling Down Cycle	179
Fig.4.15c-	Microstructure of the 0.56%Mn Steel I.A at 730°C for 15 Houres, Cooled at	

7°C/min, Cooling Down Cycle 180
Fig.4.16- Microstructure of the 1.0%Mn Steel. a-Normalised., b-I.A. for 30 min at 730°C, Cooled at 7°C/min, Cooling Down Cycle. 181
Fig.4.16c- Microstructure of the 1.0%Mn Steel I.A. at 730°C for 15 Houres, Cooled at 7°C/min, Cooling Down Cycle. 182
Fig.4.17- Microstructure of 0.56%Mn Steel I.A. at 730°C, Cooled at 7°C/min, Heating Up Cycle, a- for 30 min., b- for 15 hr. 183
Fig.4.18- Microstructure of 1.0%Mn Steel I.A. at 730°C, Heating Up Cycle. a- for 30 min., b- for 15 hr. 184
Fig.4.19 (1)- Microstructure of the 1.49%Mn Steel, a-Normalised., b-I.A for 30 min at 730°C, Cooled at 7°C/min, Cooling Down Cycle. 187
Fig.4.19 (1)c-Microstructure of the 1.49%Mn Steel I.A. at 730°C for 15 Houres, Cooling Down Cycle. 188
Fig.4.19 (2)- Microstructure of the 1.49%Mn Steel, a- Normalised., b- I.A for 30 min at 730°C, Cooled at 7°C/min, Cooling Down Cycle. 189
Fig.4.19 (2)c-Microstructure of the 1.49%Mn Steel I.A. at 730°C for 15 Houres, Cooling Down Cycle. 190
Fig.4.20 (1)- Microstructure of the 1.49%Mn Steel I.A. at 730°C, Cooled at 7°C/min, Heating Up Cyclea- for 30 min., b- for 15 hr. 191
Fig.4.20(2)- Microstructure of the 1.49%Mn Steel I.A. at 730°C, Cooled at 7°C/min, Heating Up Cycle, a- for 30 min., b- for 15 hr. 192
Fig.4.21- Martensite Formation After 15 Hours I.A., Heating Up Cycle. 193
Fig.4.22- Microstructure of 1.49%Mn Steel After I.A. at 730°C and Quenching, Cooling Down Cycle a- for 0 min., b- for 15 min.195
Fig.4.22- Microstructure of 1.49%Mn Steel After I.A. at 730°C and Quenching, Cooling Down Cycle, c- for 30 min., d- for 900 min. 196
Fig.4.23- Microstructure of 1.49%Mn Steel After I.A. at 730°C and Quenching, Heating Up Cycle a- for 0 min., b- for 15 min. 197
c- for 30 min., d- for 900 min. 198
Fig. 4.24- Influence of I.A. Time on Volume Fraction of austensite (Measured from Volume Fraction of Martensite Produced on Quenching V_{MQ}) for 1.49%Mn Steel. 200
Fig.4.25- The Influence of I.A. Time on Hardness of Ferrite and Martensite for 1.49%Mn Steel, Heatig up and Coolig Down Cycle. 204
Fig.4.26- The Effect of I.A. Time on the Nuclution Sites for 1,49% MnSteel. 206

Fig.4.27a- Impact Transition Curves for the 1.49%Mn Steel I.A. at 730°C for Various Times, Cooled at 0.8°C/min, Heating Up Cycle. 216
Fig.4.27b- Fibrous Fracture Curves for the 1.49%Mn Steel I.A. at 730°C for Various Times, Cooled at 0.8°C/min, Heating Up Cycle. 217
Fig.4.28a- Impact Transition Curves for 1.51%Mn Steel I.A. at 730°C for Various Times, Cooled at 0.8°C/min, Cooling Down Cycle.218
Fig.4.28b- Fibrous Fracture Curves for the 1.51%Mn Steel I.A. at 730°C for Various Times, Cooled at 0.8°C/min, Cooling Down Cycle.219
Fig.4.29- The Effect of I.A. Times on the 54J ITT°C for the 1.49%Mn Steel and the 1.51%Mn Steels, Cooled at 0.8°C/min. 220
Fig.4.30- The Effect of Cooling Rate After Different I.A. Times on 54J ITT°C for the 1.5%Mn Steels. 221
Fig.4.31- The Effect of I.A. Times on the Yield Strength for the 1.5%Mn Steels, Cooled at 0.8°C/min 222
Fig.4.32- The Effect of Cooling Rate After Different I.A. Times on the Yield Strength for the 1.5%Mn Steels. 223
Fig.4.33 (1)- Microstructure of the 1.51%Mn Steel a- Normalised., b- I.A. for 1 hr at 730°C, Cooled at 0.8°C/min, Cooling Down Cycle.226
Fig.4.33 (2)- Microstructure of the 1.51%Mn Steel a- Normalised., b- I.A. for 1 hr at 730°C, Cooled at 0.8°C/min, Cooling Down Cycle.227
Fig.4.34 (1)- Microstructure of the 1.49%Mn Steel a-Normalised., b-I.A. for 30 min at 730°C, Cooled at 0.8°C/min, (Heating Up Cycle. 228
Fig.4.34 (1)c-Microstructure of the 1.49%Mn Steel I.A. for 15 hr at 730°C, Cooled at 0.8°C/min, Heating up Cycle. 229
Fig.4.34 (2)- Microstructure of the 1.49%Mn Steel a- Normalised., b- I.A. for 30 min at 730°C, Cooled at 0.8°C/min, Heating Up Cycle. 230
Fig.4.34 (2)c-Microstructure of the 1.49%Mn Steel I.A. for 15 hr at 730°C, Cooled at 0.8°C/min Heating up Cycle. 231
Fig.4.35a- Impact Transition Curves for the 0.067%C Steel I.A. at 730°C for Various Times, Cooled at 7°C/min, Heating Up Cycle. 238
Fig.4.35b- Fibrous Fracture Curves for the 0.067%C Steel I.A. at 730°C for Various Times, Cooled at 7°C/min, Heating Up Cycle. 239
Fig.4.36a- Impact Transition Curves for the 0.067%C Steel I.A. at 730°C for Various Times, Cooled at 7°C/min, Cooling Down Cycle. 240
Fig. 4.36b- Fibrous Fracture Curves for the 0.067%C

Steel I.A. at 730°C for Various Times, Cooled at 7°C/min, Cooling Down Cycle. 241
Fig.4.37- The Effect of I.A. on the 54J ITT°C for the 0.067%C Steel. 242
Fig.4.38- The Effect of Carbon Level on the 54J ITT°C After Different I.A. Times for the 1.5%Mn Steels. 243
Fig.4.39- The Effect of I.A. Time on the Yield Strength for the 0.067%C Steel. 244
Fig.4.40- The Influence of I.A. Time on the Yield Strength for Two Different Carbon Levels for the 1.5%Mn Steel. 245
Fig.4.41- Microstructure of the 0.067 % C Steel a-Normalised, b-I.A. 30 min. Cooling Down Cycle. 247
Fig.4.41c- Microstructure of the 0.067%C Steel I.A. for 15 hr, Cooling Down Cycle. 248
Fig.4.42- Microstructure of the 0.067%C Steel a- I.A. 30 min., b- I.A. for 15 hr, Heating up Cycle. 249
Fig.4.43a- Impact Transition Curves for the 1.0%Mn Steel I.A. at 760°C for Various Times, Cooled at 7°C/min, Heating Up Cycle. 255
Fig.4.43b- Fibrous Fracture Curves for the 1.0%Mn Steel I.A. at 760°C for Various Times, Cooled at 7°C/min, Heating Up Cycle. 256
Fig.4.44a- Impact Transition Curves for the 1.0%Mn Steel I.A. at 760°C for Various Times, Cooled at 7°C/min, Cooling Down Cycle. 257
Fig.4.44b- Fibrous Fracture Curves for the 1.0%Mn Steel I.A. at 760°C for Various Times, Cooled at 7°C/min, Cooling Down Cycle 258
Fig. 4.45- The Effect of I.A. Times on the 54J ITT°C for the 1.0%Mn Steel I.A. at 760°C. 259
Fig.4.46- The Influence of Heating Temperature After Different I.A. Times on the 54J ITT°C for the 1% Mn Steel. 260
Fig.4.47- The Effect of I.A. Times on the Yield Strength of the 1.0%Mn Steel I.A. at 760°C. 261
Fig.4.48- The Effect of Heating Temperature After Different I.A. Time on the Yield Strength of the 1.0%Mn Strength. 262
Fig.4.49- Microstructure of the 1.0%Mn Steel a- Normalised., b-I.A. for 30 min. at 760°C Cooling Down Cycle. 265
Fig.4.49c- Microstructure of the 1.0%Mn Steel I.A. for 15 hr at 760°C. Cooling Down Cycle. 266
Fig.4.50- Microstructure of the 1.0%Mn Steel a- I.A. for 30 min., b- I.A. for 15 hr, at 760°C Heating Up Cycle 267
Fig.4.51a- Impact Transition Curves for the Plain Carbon Manganese Steel, (Fine Grain

Size), I.A.at 730°C,
Cooled at 7°C/min, Heating Up Cycle. 275
Fig.4.51b- Fibrous Fracture Curves for the Plain Carbon Manganese Steel, (Fine Grain Size), I.A. at 730°C, Cooled at 7°C/min, Heating Up Cycle. 276
Fig.4.52a- Impact Transition Curves for the Plain Carbon Manganese Steel, (Fine Grain Size), I.A., at 730°C, Cooled at 7°C/min, Cooling Down Cycle. 277
Fig.4.52b- Fibrous Fracture Curves for the Plain Carbon Manganese Steel, (Fine Grain Size), I.A., at 730°C, Cooled at 7°C/min, Cooling Down Cycle. 278
Fig.4.53- The Effect of I.A. Times on the 54J ITT°C for the Plain Carbon Mn Steel (Fine Grain Size). 279
Fig.4.54a- Impact Transition Curves for the Plain Carbon Mn Steel (Coarse Grain Size), I.A. at 730°C, Cooled at 7°C/min, Heating Up Cycle. 280
Fig.4.54b- Fibrous Fracture Curves for the Plain Carbon Mn Steel (Coarse Grain Size), I.A. at 730°C, Cooled at 7°C/min, Heating Up Cycle. 281
Fig.4.55a- Impact Transition Curves for the Plain Carbon Mn Steel (Coarse Grain Size), I.A at 730°C, Cooled at 7°C/min, Cooling Down Cycle. 282
Fig.4.55b- Fibrous Fracture Curves for the Plain Carbon Mn Steel (Coarse Grain Size), I.A. at 730°C, Cooled at 7°C/min, Cooling Down Cycle 283
Fig.4.56- The Effect of I.A Times on the 54J ITT°C for the Plain Carbon Mn Steel, Coarse Grain Size. 284
Fig.4.57- The Effect of Grain Size and I.A. Time on the 54J ITT°C of the Plain Carbon Manganese Steel. 285
Fig.4.58- The Effect of I.A. Time on the Yield Strength of the Finer Grained Size Plain Carbon Mn Steel. 286
Fig.4.59- The Effect of I.A. Time on the Yield Strength of the Coarser Grained Size Plain Carbon Mn Steel. 287
Fig.4.60- The Effect of Grain Size and I.A. Time on the Yield Strength of the Plain Carbon Mn Steel. 288
Fig.4.61 (1)- Microstructure of the Finer Grained Plain Carbon Manganese Steel. a- Normalised., b- I.A. at 730°C for 30min, Cooling Down Cycle. 291
Fig.4.61 (1)c-Microstructure of the Finer Grained Plain Carbon Manganese Steel.I.A. at 730°C for 15 hr,Cooling Down Cycle. 292

Fig.4.61(2)- Microstructure of the Finer Grained Plain Carbon Manganese Steel. a-Normalised., b- I.A. at 730°C for 30min, Cooling Down Cycle. 293
Fig.4.61(2)c- Microstructure of the Finer Grained Plain Carbon Manganese Steel. I.A. at 730°C for 15 hr, Cooling Down Cycle 294
Fig.4.62 (1)- Microstructure of the Finer Grained Plain Carbon Manganese Steel. a-I.A. at 730°C for 30 min., b-I.A. at 730°C for 15 hr.Heating Up Cycle. 295
Fig.4.62 (2)- Microstructure of the Finer Grained Plain Carbon Manganese Steel. a-I.A. at 730°C for 30 min., b-I.A. at 730°C for 15 hr, Heating Up Cycle. 296
Fig.4.63(1)- Microstructure of the Coarser Grained Plain Carbon Manganese Steel. a-Normalised., b-I.A. at 730°C for 30min, Cooling Down Cycle. 297
Fig.4.63(1)c- Microstructure of the Coarser Grained Plain Carbon Manganese Steel. I.A. at 730°C for 15 hr, Cooling Down Cycle. 298
Fig.4.63 (2)- Microstructure of the Coarser Grained Plain Carbon Manganese Steel. a-Normalised., b- I.A. at 730°C for 30min, Cooling Down Cycle. 299
Fig.4.63 (2)c-Microstructure of the Corser Grained Plain Carbon Manganese Steel. I.A. at 730°C for 15 hr, (Cooling Down Cycle). 300
Fig.4.64 (1)- Microstructure of the Corser Grained Plain Carbon Manganese Steel. a-I.A. at 730°C for 30 min., b-I.A. at 730°C for 15 hr. Heating Up Cycle. 301
Fig.4.64 (2)- Microstructure of the Corser Grained Plain Carbon Manganese Steel. a-I.A. at 730°C for 30 min., b-I.A. at 730°C for 15 hr. Heating Up Cycle. 302
Fig.5.1- The Effect of Carbide Thickness on ITT. 309
Fig.5.2- Refinement of Grain Boundary a-After Normalising.b- After 15 hr I.A. 311
Fig.5.3- The Effect of Carbide Thickness on ΔITT. 313
Fig.5.4- The Effect of Hardenability on Carbide Thickness. 315
Fig.5.5- The Proposed Mechanism for G.B.C Formation, and Growth. 316
Fig.5.6- Isotherm of the Fe-Mn-C System a- at 730°C b- at 760°C 323
Fig.5.7- Martensite Formation During Long Time I.A.(15hr), Heating Up Cycle. 337
Fig.5.8- The Effect of I.A. on Luder Extension. 342
Fig.5.9- The Effect of Martensite Volume Fraction on Yield Strength. 344

LIST OF TABLES

Table 3.1- The Chemical Composition Of Steels Used. 143
Table 3.2- Variation of Temperature Within the Plate Using the Muffel Furnace. 143
Table 3.3- Variation of Temperature Within the Plate Using Air-Circulating Furnace. 143
Table 4.1- The chemical composition of steel used for examining the influence of manganese level on intercritical annealing. 145
Table 4.2- Microstructural Measurements and Strength of 1.49% Mn Steels. 147
Table 4.3- Microstructural Measurements and Strength of the 1% Mn Steels. 148
Table 4.4- Microstructural Measurements and Strength of the 0.56% Mn steel. 149
Table 4.5- Average Mn and Si content of Ferrite and Pearlite Regions of C-Mn-Al-Nb Steels. 176
Table 4.6- Volume Fraction of Martensite, V_{MQ}, as a Function of I.A. Time. 201
Table 4.7- Micro-Hardness of Ferrite and Martensite after quenching for the 1.49% Mn. 203
Table 4.8- The Chemical Compsition of Steel Used for Examining the Influence of Cooling Rate on I.A. 210
Table 4.9- Microstructural Measurements and Strength of the 1.49% Mn Steel. 210
Table 4.10- Microstructural Measurements and Strength of the 1.51% Mn Steel. 211
Table 4.11- Average Mn and Si content of Ferrite and Pearlite Regions of C-Mn-Al-Nb Steels. 215
Table 4.12- The Chemical Composition of Steel Used for Examining the Influence of Carbon Level on I.A. 234
Table 4.13- Microstructural Measurements and Strength for the, 0.067% C Steel. 235
Table 4.14- The Chemical Composition of Steel Used for Examining the Influence of Heating Temperature on I.A. 251
Table 4.15- Microstructure Measurements and Strength of the 1% Mn Steel I.A at 760°C 254
Table 4.16- The Chemical Composition of Steel Used for Examining the Influence of Grain Size on I.A. 268
Table 4.17- Microstructural Measurements and Strength of the Finer Grained (18 µm) Plain Carbon Steel I.A.at 730°C 270
Table 4.18- Microstructural Measurements and Strength of the Coarser Grained (37 µm) Plain Carbon Steel I.A.at 730°C. 271
Table 5.1- Observed and Calculated ITT°C to Give

Impact Energy of 54J & Observed and Calculated Yield Strength for the 0.56% Mn Steel. 333
Table 5.2- Observed and Calculated ITT°C to Give Impact Energy of 54J & Observed and Calculated Yield Strength for the 1% Mn Steel. 334
Table 5.3- Observed and Caculated ITT'S to Give Impact Energy of 54J & Observed and Calculated Yield Strength for the 1.49% Mn Steel. 345
Table 5.4- Observed and Caculated ITT'S to Give Impact Energy of 54J & Observed and Calculated Yield Strength for 1.49% Mn Steel Heating Up to the Intercritical Annealing Temperature and Cooled at 0.8°C/min. 349
Table 5.5- Observed and Caculated ITT'S to Give Impact Energy of 54J & Observed and Calculated Yield Strength for 1.51% Mn Steel Cooling Down to the Intercritical Annealing Temperature and Cooled at 0.8°C/min. 350
Table 5.6- Observed and Caculated ITT'S to Give Impact Energy of 54J & Observed and Calculated Yield Strength for 0.067% C Steel. 353
Table 5.7- Observed and Caculated ITT'S to Give Impact Energy of 54J & Observed and Calculated Yield Strength for 1% Mn Steel Intercritically Annealed at 760°C. 356
Table 5.8- Observed and Caculated ITT'S to Give Impact Energy of 54J & Observed and Calculated Yield Strength for for Plain C-Mn Steel Intercritically Annealed at 730°C, (Finer Grain Size). 359
Table 5.9- Observed and Caculated ITT'S to Give Impact Energy of 54J & Observed and Calculated Yield Strength for for Plain C-Mn Steel Intercritically Annealed at 730°C, (Coarser Grain Size). 360

LIST OF SYMBOLS

The following is a list of abbreviations and symbols in this thesis.

ADP austenitic dual-phase (annealing in γ field).

BF bainite ferrite.

C carbon content of martensite.

CCT continuous cooling transformation.

d grain diameter (mean linear intercept).

e_c engineering strain of composite.

e_f engineering strain of ferrite.

e_m engineering strain of martensite.

EL_T total elongation.

FATT fibrous appearance transition temperature.

H_v vickers hardness.

I.A. intercritical annealing.

IDP intercritical dual phase (intercritical annealing in $\alpha+\gamma$ field)

ITT impact transition temperature.

K_y grain size strengthening factor.

MPDP manganese partitioning dual-phase.

N_f volume fraction of free nitrogen.

PF polygonal ferrite.

P pearlite volume fraction.

S_c nominal strength of composite.

S_f	nominal strength of ferrite.
S_m	nominal strength of martensite.
SEM	scanning electron microscope.
t	grain boundary carbide thickness.
Vm	volume fraction of martensite.
V_{MQ}	martensite volume fraction afterquenching.
V	volume fraction.
α	ferrite.
γ	austenite.
Δ_y	change in yield strength.
σ_y	lower yield stress (LYS).
σ_t	tensile stress.
σ_i	frictional stress.
σ_o	frictional stress of iron.

DECLARATION

I grant powers of discretion to the University Librarian to allow this thesis to be copied in whole or in part without further reference to me. This permission covers only single copies made for study purposes, subject to normal conditions of acknowledgement.

ACKNOWLEDGMENTS

I would like to thank my supervisor, Dr. B. Mintz for his help, continuous guidance, and encouragement during this research work.

I also wish to thank Professor G.T.S. Done for the provision of laboratory facilities, and to the staff of the Department of Mechanical Engineering.

I would also like to thank Mr. R. Vipond who never failed me when I sought his help.

Thanks are also due to British Steel for supplying the steels, in particular to Dr. W.B. Morrison and Dr. D. Crowther of Swinden Laboratories.

I would also like to express my thanks to the Egyptian Government for their financial support.

A special indebtedness is due to my family, especially my mother and my father who never managed to see the completion of this work, and to my wife for her support and encouragement.

I would also like to thank my friends Dr. G. Khalaf and Dr. N. Nassar for their help.

Finally, I wish to thank God for his mercies and blessings all the way long.

ABSTRACT

An investigation has been made into the influence of intercritical annealing on the tensile and impact properties of C-Mn-Al-Nb steels.

Three levels of manganese (1.5%, 1%, and 0.56%) were examined in an 0.1% C steel austenitised at 920°C followed by intercritical annealing at 730°C for various times. The cooling rate from 920°C to 730°C and from 730°C to room temperature was 7°C/minute. Intercritical annealing enabled Mn to diffuse to the α/α and/ or α/γ boundaries and into the newly formed γ causing the transformation temperature to be lowered, so refining the grain boundary carbides on cooling to room temperature. For the 1% Mn and 0.56% Mn steel, intercritical annealing resulted in improved impact toughness , compared to a normalising treatment due to this refinement of the carbides. The impact transition temperature (ITT) was lowered by as much as 35°C with no change in strength. Strength was little influenced by this heat treatment because grain size remained constant. The improvement in impact toughness was greater the longer the holding time at 730°C but was significant even after 15 minutes. Improvements occurred both on cooling from 920°C to the intercritical annealing (730°C) and on heating from room temperature to 730°C; the latter heat treatment being the more beneficial.

For the 1.5% Mn, intercritical annealing for long times introduced a high pearlite volume fraction and or small martensite colonies at the grain boundaries causing a deterioration in impact toughness compared to the normalised state.

Reducing the cooling rate to 0.8°C/minutes in the higher Mn (1.5%) steel again resulted in improved impact behaviour with no change in strength on intercritical annealing for long times. This is due to the slower cooling rate preventing martensite from forming, so allowing the carbide refinement on intercritical annealing to dominate the impact behaviour. Improvements occurred both on heating to and cooling down to the intercritical annealing temperature and were as much as a 60°C lowering of the ITT.

Reducing the C level to 0.067% C in the high Mn (1.5%) steel also gave rise to an improvement in impact behaviour with no significant change in strength even at the higher cooling rate. This is again believed to be due to the reduced C level preventing martensite from forming.

Raising the intercritical annealing temperature to 760°C in the 1% Mn steel produced similar improvements in impact behaviour to those obtained for the heating up cycle but only small improvements took place on cooling down. This

may be related to the higher intercritical annealing temperature delaying the γ/α transformation so reducing the amount of Mn able to diffuse along the α/α boundaries.

Finally, the effect of grain size on the impact and tensile properties of plain carbon manganese steel after intercritical annealing at 730°C was examined. Two grain sizes were studied (18μm, and 37μm). At the finer grain size the impact transition temperature (ITT) was reduced by as much as 15°C with no change in strength. The improvement in ITT was greater the longer the holding time at 730°C. Improvements occured both on cooling from the austenitising temperature (920°C) to intercritical annealing (730°C) and on heating from room temperature to 730°C, but the latter heat treatment was more beneficial. For the coarser grain size, there was no significant improvement in impact behaviour with intercritical annealing treatments. This is possibly due to a reduction in the Mn segregation along the boundaries caused by it's lower grain boundary surface area/ volume ratio.

The magnitude of the improvement in impact behaviour on intercritical annealing may also be related to the range of carbide thickness over which the improvements occur. Steels which on normalising have a carbide thickness in the range 0.55 μm to 0.25 μm are the ones which are likely to show the greatest improvements. Thus this treatment is best suited to thick plate.

CHAPTER ONE

INTRODUCTION

Dual phase steels have sparked a tremendous amount of research activity throughout the world in the past twenty years because of their striking mechanical properties such as continuous yielding, high initial work hardening rate, and an excellent combination of strength and ductility. However, research on dual phase steels has been concentrated on strip steels where ductility and strength are the most important properties. Because the dual phase steels market is directed towards strip steel there has been little interest in their impact behaviour.

However, recent work has shown that intercritical annealing may be used to improve the impact behaviour of plate steel[115]. The lowering of the impact transition temperature (ITT) is considered to be due to Mn segregation to the α/γ boundaries leading to refinement of the grain boundary carbides. It has been shown that reducing the grain boundary carbide thickness has a great influence in lowering the ITT's[92].

The present study has been instigated to examine the influence of manganese and carbon level, cooling rate, and intercritical annealing temperature on the strength and

impact behaviour of C-Mn-Nb-Al plate steels after intercritical annealing. In addition, the influence of grain size on intercritical annealing response has been examined in a plain C-Mn steel.

Intercritical annealing of plate steel is a topic which has not been addressed to a great extent in the literature, and the conditions used in the present work differ from most of the previous work in terms of plate thickness, heat treatment conditions, and in the final microstructure.

In the following chapters, the processing techniques for the dual phase steels, the role of alloying elements and phase transformation in dual phase heat treatments and the structure- property relationships for dual phase steels will be discussed.

By covering all the forementioned variables, it is hoped that a fuller understanding of the treatment will be obtained as well as the boundary conditions in which it can be used to advantage.

CHAPTER TWO

LITERATURE SURVEY

2.1- INTRODUCTION.

DUAL-PHASE STEELS.

Dual-phase steels are a new class of high strength low alloy steels characterised by a microstructure consisting of a dispersion of hard martensite particles in a soft, ductile ferrite matrix. These steels have a combination of strength, ductility, and formability that makes them attractive for weight-saving applications, and they have been used extensively in automobiles.

Dual-phase steels have the same ultimate tensile strength as HSLA steels but have far better formability. The superior formability of GM 980X[1] for example has substantially increased the utilization potential of high strength steels in the manufacture of automotive components.

Rashid[1] has cited the use of a vanadium strengthened (GM980X) dual-phase steel for manufacturing automotive components such as wheel discs, wheel rims, bumper face bars, bumper jack posts, pullies, and steering coupling reinforcements[2]. Figure 2.1 shows the components in a car which can be formed from these V-dual-phase steels. It has been also reported[3] that the automotive industry in the

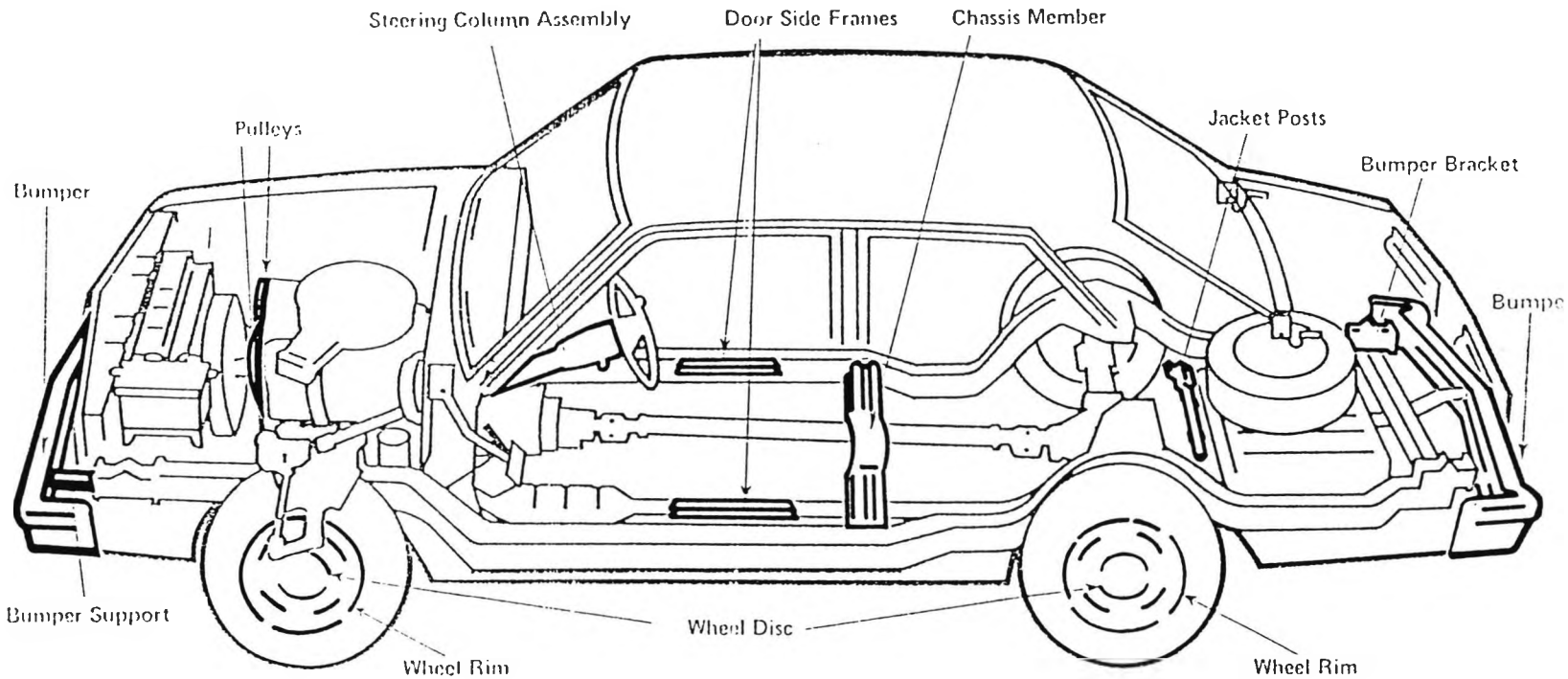

Figure 2.1- Automobiles Components Formed From V-Dual-Phase Steels.[2]

U.S.A. used 1 million tons of dual-phase steels in 1985, figure 2.2.

The term "dual-phase" refers to the presence of esentially two-phases, ferrite and martensite in the microstructure, although small amounts of bainite, pearlite and retained austenite may also be present. These steels have a number of unique properties which include:

1- Continuous yielding behaviour (no yield point).

2- A low 0.2% offset yield strength.

3- A high tensile strength.

4- A high work hardening rate.

5- An unusually high uniform and total elongation.

2.2- PRODUCTION OF SHEET DUAL-PHASE STEELS.

The duplex ferrite-martensite aggregates can be obtained in several ways.

2.2.1- Intercritical Annealing.

2.2.2- Box-Batch Annealing.

2.2.3- Continuous Annealing (Cold-Rolled Or Hot-Rolled).

2.2.4- As Hot-Rolled Directly.

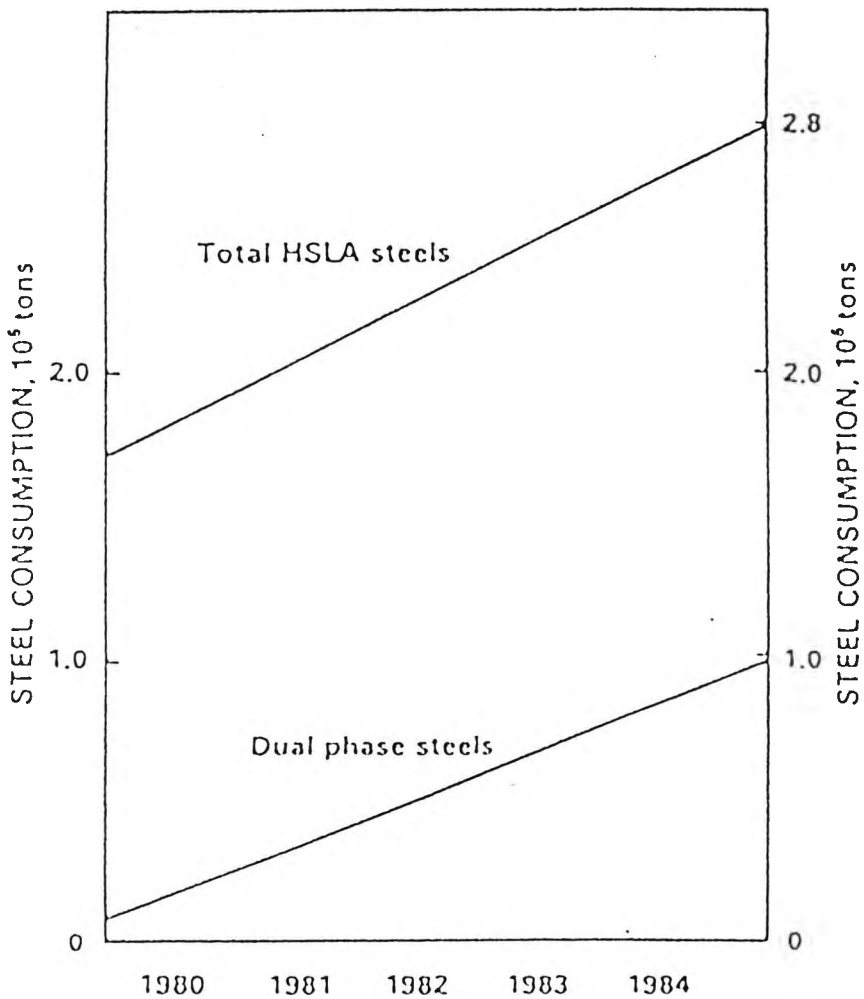

Figure 2.2- Estimate of the Demand for HSLA Steels in the USA Automobile Industry.[3]

2.2.1- INTERCRITICAL ANNEALING.

Dual-phase steels were first produced by heat-treatment[4,5]. The steel which has an initial ferrite plus carbide microstructure is heated into the intercritical region (730-850°C) where carbides dissolve leaving a mixture of ferrite plus carbon-rich austenite. On subsequent cooling at relatively moderate rates, depending on the steel alloy content, the carbon rich austenite has sufficient hardenability to transform to martensite.

2.2.2- BOX-BATCH ANNEALING.

In this technique the coiled hot-rolled or cold-rolled strip is heated into the intercritical temperature range (700-750°C) soaked for a relatively long period e.g 3-5 hr, then cooled slowly at 20°C/hr to room temperature.

Steels with high manganese contents, 0.06% C-2.5% Mn[6], 0.06%C-3%Mn[7] and 0.02%C-2.1% Mn[8] have been proposed for this technique.

The main advantages for this technique are:-

1- The availability of existing batch annealing facilities which can be adapted with little modification.

2- Avoiding substantial investment in new facilities.

The disadvantages of this technique are:-

1- A substantial price has to be paid for alloying additions to stabilize the austenite phase upon slow cooling.

2- It is difficult to obtain mechanical properties

throughout the coil[8,9], because of the large temperature difference existing from the middle to the outside of the coil.

Matsuoka.et al[10] have studied the mechanical properties of box-annealing steels. They reported that steels with high manganese content (greater than 2%) showed several peculiar characteristics after annealing in the temperature range 670°C to 750°C. The carbon content in this study was 0.06% and the manganese content, ranged from 0.6% to 3.3%. One of their results shown in Figure 2.3 reveals that, when the manganese content is greater than 2%, increasing the Mn content or annealing temperature raises the tensile strength, decreases the ductility, and has little influence on the yield strength. This behaviour was shown to be a direct result of the increase in the martensite volume fraction. Discontinuous yielding was also found to be eliminated when the annealing temperature was greater than 690°C and this has been confirmed by other work[6,8]. The change over from discontinuous to continuous yielding corresponds to in the region of 10-20% volume fraction martensite. In a 0.06%C-3% Mn steel, partitioning of manganese from ferrite to austenite is approximately 80% complete after 5 hours at 690°C[7]. Therefore, in order to obtain the dual-phase properties, the required heating temperature is usually greater than this lower limit of 700°C. The optimum annealing temperature range to obtain the best tensile properties is about 700°C to 730°C for an

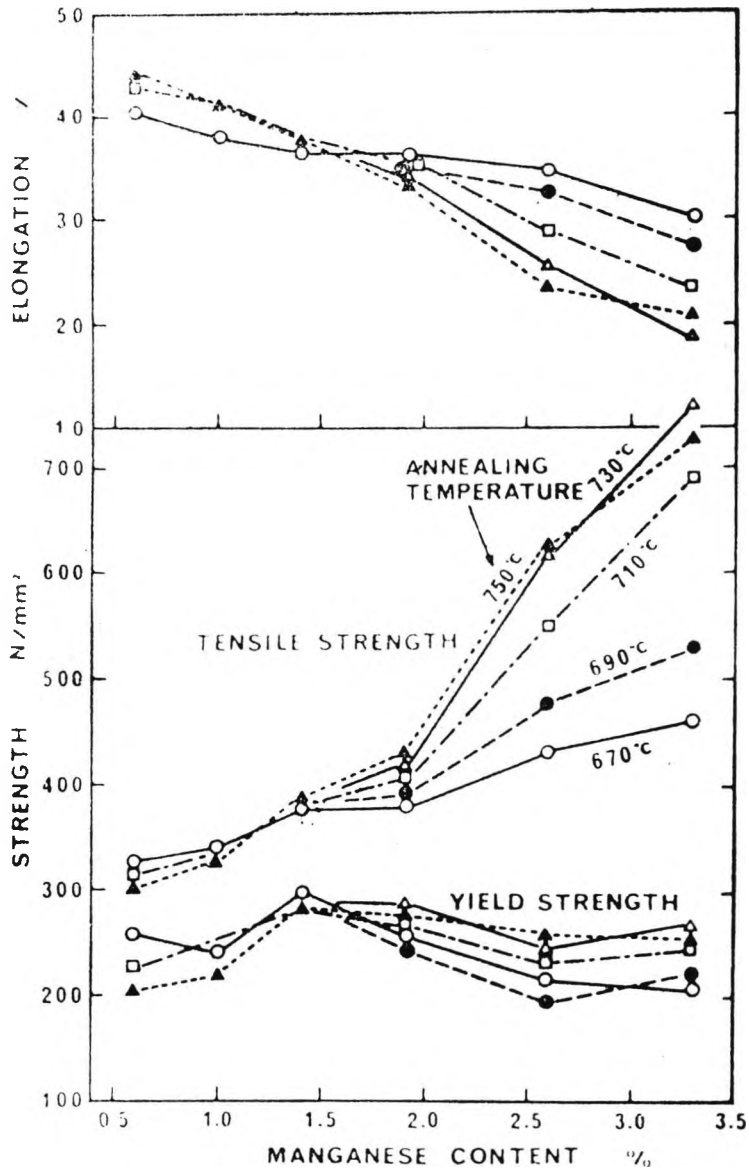

Figure 2.3- Relationship Between Tensile Properties and Manganese Content.[10]

0.06%C steel with greater than 2.5% Mn[6,7] (although pearlite or carbides may also be present after annealing).

At higher annealing temperatures, e.g, 770°C, because of the low carbon content, the hardenability of austenite is reduced, therefore, after slow cooling, the amount of martensite is decreased and the amount of bainite or pearlite is increased, resulting in a decrease in ultimate tensile strength[6].

2.2.3- CONTINUOUS-ANNEALING.

To produce dual-phase steels using this technique the hot-rolled or cold-rolled gauge strip is uncoiled and annealed for a short period of time, e.g, 2 or 3 minutes, then cooled to room temperature. On cooling, the steel can either be water-quenched, gas-quenched or air-cooled at preselected cooling rates. Water quenching is favoured when a high strength dual-phase steel is desired[11].

When ductility is required, a mild cooling (less than 30°C/sec) is preferred to reduce the amount of C in solution[12]. A cooling rate of about 10°C/sec has been shown to produce desirable dual-phase properties[13]. In general, the cooling rate required is dependent upon the thickness of the steel and the alloy content. Figure 2.4 shows a schematic representation of a continuous annealing process used for a cold-rolled grade of dual-phase steel.

The advantage of using continuous annealing techniques are:

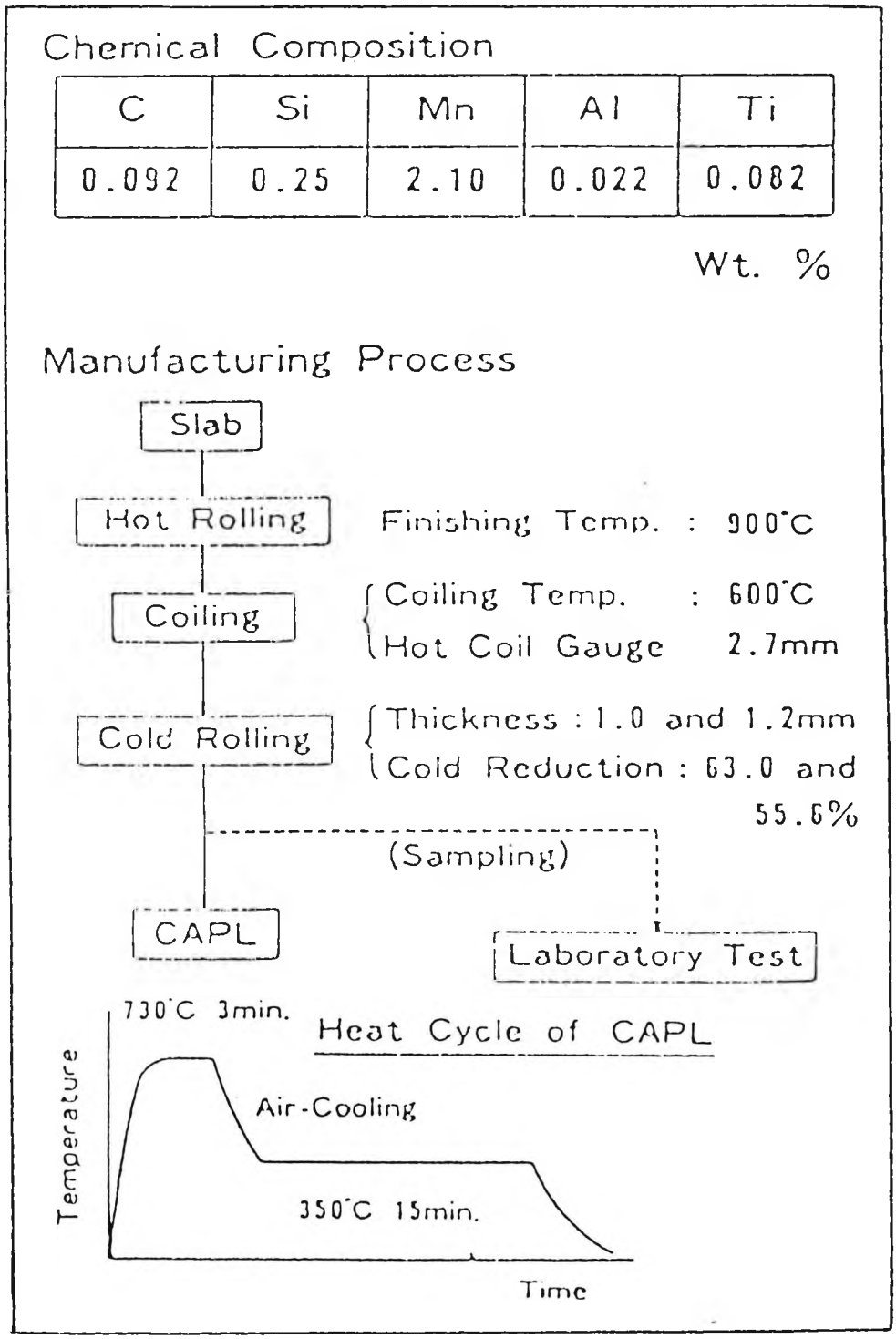

Figure 2.4- Schematic Representation of Continuous Annealing Process.[15]

1- This process may be used to produce both hot-rolled and cold-rolled gauges.
2- It requires only a modest addition of alloying elements.
3- It provides a high degree of uniformity of properties throughout the coil[9,12] .

This technique has the disadvantage in that, a modern continuous annealing line requires a substantial capital investment adding cost to the final product.

Several alloy systems have been proposed in order to optimize the manufacturing and control of strip thickness. These include 1.5%Mn-Si[12,14,15], 1.5%Mn-Si-V[9,11,16], 1.5%Mn-Si-V-Mo [13], and 1.2%Mn-Si-Cr (or Mo)[14]. In addition to alloy additions, the coiling temperature in the hot-rolling schedule prior to intercritical annealing has also been considered to be an important process parameter that can be varied so as to improve the hardenability of austenite[12]. For example, a high coiling temperature (750°C) leads to an enrichment in both carbon and manganese.

In contrast coiling at 600°C shows little tendency for the simultaneous enrichment of the elements C and Mn as shown in figure 2.5. Because of the further enrichment of C and Mn during the subsequent intercritical annealing, the austenite hardenability is further increased. This permits the use of a leaner chemistry of a 0.05%C-1.5%Mn or a 0.1%C-1.4%Mn for intercritical annealing followed by a mild cooling (10°C/sec).

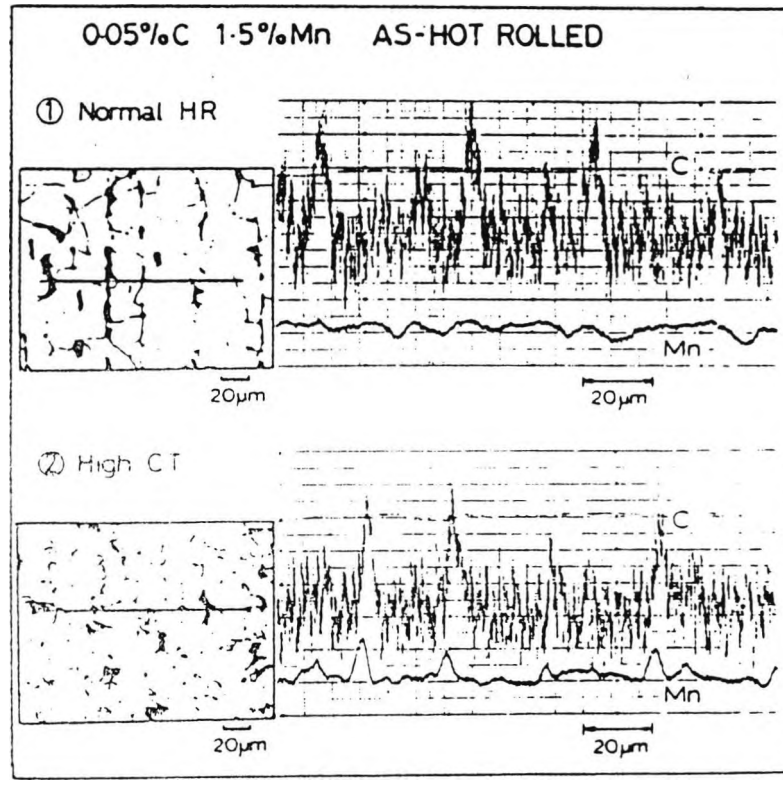

Figure 2.5-Enrichment of Carbon and Manganese at Boundaries due to Coiling at High Temperature.[12]

2.2.4- AS-HOT-ROLLED DUAL-PHASE STEELS.

The idea of obtaining a dual-phase microstructure without heat-treatment, that is, obtaining ferrite plus martensite in as hot-rolled strip, is an attractive one because of the potential savings of heat-treatment costs. To produce dual-phase steels directly off the hot strip mill using a conventional hot rolling cycle is more complicated than either of the two techniques mentioned before. In a continuous-annealing or a box-annealing process, the steel is heated into the intercritical region. Upon cooling, the phase-transformation occurs from a two-phase mixture (ferrite plus austenite) which makes it easy to control the amount of martensite in the steel (this being controlled by a fixed amount of austenite).

To produce the as-hot-rolled dual-phase steels, usually the slabs are reheated into the single austenite phase e.g, at 1200°C, hot rolled through several passes then coiled. After the finishing pass, the steel travels on the runout table for about 10 seconds before it reaches the coiling stand, the strip being cooled rapidly, at about 20-30°C/sec. After coiling, the steel is cooled slowly at a rate of 20-30°C/hr. Therefore transformation starts from a fully austenitic structure, and through continuous cooling, produces a structure containing 80-90% ferrite and 10-20% martensite.

The development and mill trials for producing the dual-phase steel directly off the hot-strip mill were first made

by Coldren et.al[17] using C-Mn-Si-Mo-Cr steels. The as rolled dual-phase steel concept is based on a low carbon, low alloy steel, that exhibits a special continuous cooling transformation (CCT) diagram figure 2.6 which includes the following:

1- An elongated ferrite C-curve, i.e, the ability to form very large amounts of polygonal ferrite (PF) over a reasonably wide range of cooling rates on the runout table.
2- A suppressed (delayed) pearlite (P) nose to ensure avoidance of pearlite formation during cooling to the coiling temperature.
3- A high pearlite finish temperature to avoid pearlite formation after coiling at temperatures up to 620°C.
4- A gap between the polygonal ferrite (PF) and bainitic ferrite (BF) regions to provide a temperature range of at least 75°C within which no further transformation occurs as in shown in figure 2.6.
5- Complete suppression of bainitic cementite nucleation during slow cooling after the polygonal ferrite has formed.

Precise control of the continuous cooling response of the deformed austenite is essential for obtaining the desired structure and mechanical properties. Several processing variables are important in determining the properties of the final product:

1- Soaking temperature.

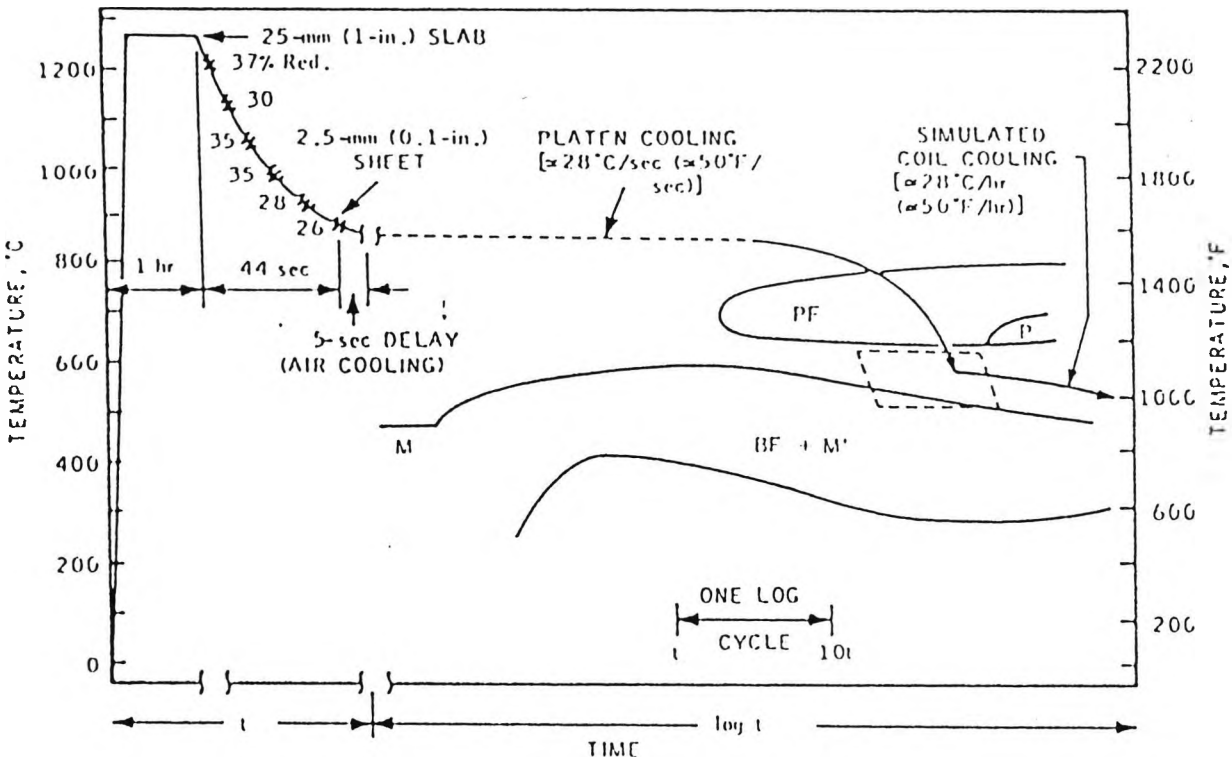

Figure 2.6- Schematic Representation of Laboratory Simulation of Hot-Strip Mill Processing.[17]

2- Hot rolling schedule.

3- Runout table cooling rate.

4- coiling temperature.

5- cooling rate after coiling.

During processing, the amount of polygonal ferrite and coiling temperature are usually determined by the controlled cooling rates on the runout table. If the coiling temperature is fixed, the microstructure and the mechanical properties of the strip will be dependent on the runout cooling rate[18]. If the cooling rate is too fast or the hardenability of steel is too high (the CCT curves are shifted to the right) only a small amount of polygonal ferrite is formed before coiling and transformation to bainitic ferrite occurs at a lower temperature. In early trials, the degrading of dual-phase properties, e.g, an increase in $\sigma y/\sigma u$ ratio or decrease in ductility, was found to be associated with the presence of pearlite, grain boundary carbides or bainitic constituents[9,12,17,18]. After the strip is coiled, it is assumed that the austenite to polygonal-ferrite transformation can be completed while the untransformed austenite phase, enriched with carbon and stabilised by the alloying elements, will be able to transform to martensite at lower temperatures.

The size, i.e, the temperature range, of the coiling windows (see dashed rectangular area in figure 2.6), is an important parameter that must be optimised and is based on adding alloying elements which will prevent the formation

of bainitic transformation products. For example figure 2.7, gives the CCT diagram for two steels with base composition of 0.05%C-1.0%Si-1.0%Cr and different manganese contents of 1.5% and 1.7% respectively. It can be seen from this figure that although the window for the 1.5% Mn steel is wide, coiling rate has to be closely controlled to give a ferrite-martensite microstructure on continuous cooling. However, for the 1.7% Mn steel, because the window size is very small and the bainite region is broad, a ferrite-martensite microstructure can not be obtained in a hot-strip mill. It should be noted that for the 1.5%Mn steel, when the cooling rate is appropriately adjusted to avoid the pearlite and bainite regions, the microstructure is not sensitive to the variations in coiling temperatures. Several compositions of steel, Mn-Si-Cr-Mo,[17,19,20], Mn-Si[12,21], Mn-Si-Cr-Mo[18] have been proposed for use in the as-hot-rolled dual-phase steel process. A typical material might have a carbon content of about 0.05% and manganese at about 1-1.5%. Among the alloying elements, manganese, silicon, chromium and molybdenum, molybdenum has been found to have the most pronounced effect in suppressing the pearlite transformation. Therefore, the addition of molybdenum provides a wide range of acceptable cooling rates allowing a large amount of polygonal ferrite to be formed without the formation of pearlite even at slow cooling rates.

Addition of molybdenum also has the advantage of stabilising the carbon enriched austenite phase to avoid

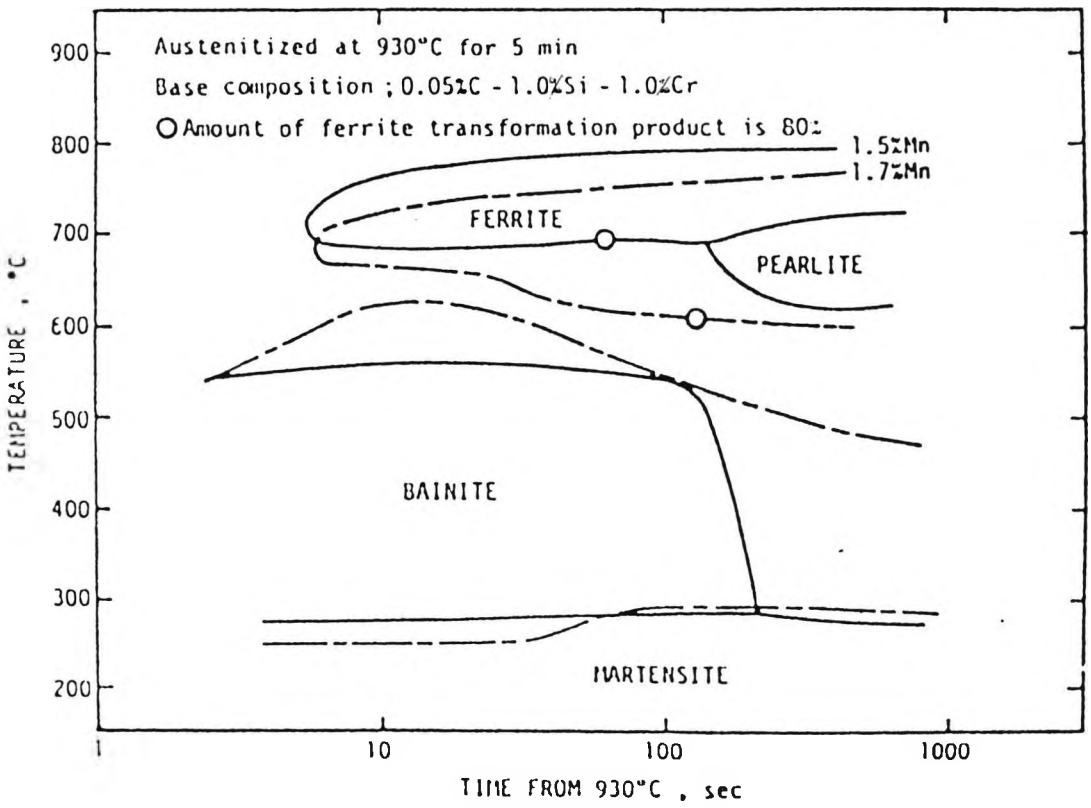

Figure 2.7- Effect of Manganese Content on the Continuous Cooling Transformation Diagram.[18]

the formation of bainite in the coil[14,20]. Silicon can also widen the range of allowable cooling rates but to a lesser extent than that shown by molybdenum as shown in figure 2.8. Chromium is considered to be beneficial.

In addition to the runout table control, the rolling schedule is also an important processing variable. The final structure is determined by the soaking temperature which is in the range 1000°C to 1200°C. It has been reported that if the austenite grain size before hot-rolling is too large (i.e, too a high soaking temperature) the bainite transformation may occur instead of the ferrite transformation[18].

If a low soaking temperature is used prior to rolling so that the austenite grain size remains fine, the resulting dual-phase steels are more structurally homogeneous. After soaking, the slabs are rolled through successively smaller gaps. Thus, in the austenite region, the large reduction ratio and the recrystallisation of the austenite phase generally results in grain refinement before the final pass. The fine grained austenite provides more nucleation sites, to accelerate ferrite formation and results in a homogeneous structure in dual-phase steels [12,18]. In general, a large amount of deformation below the recrystallisation region causes strain hardening. Therefore rolling in the recrystallisation region with a large reduction ratio is desirable for achieving effective grain refinement. When the strip runs through the last pass, the

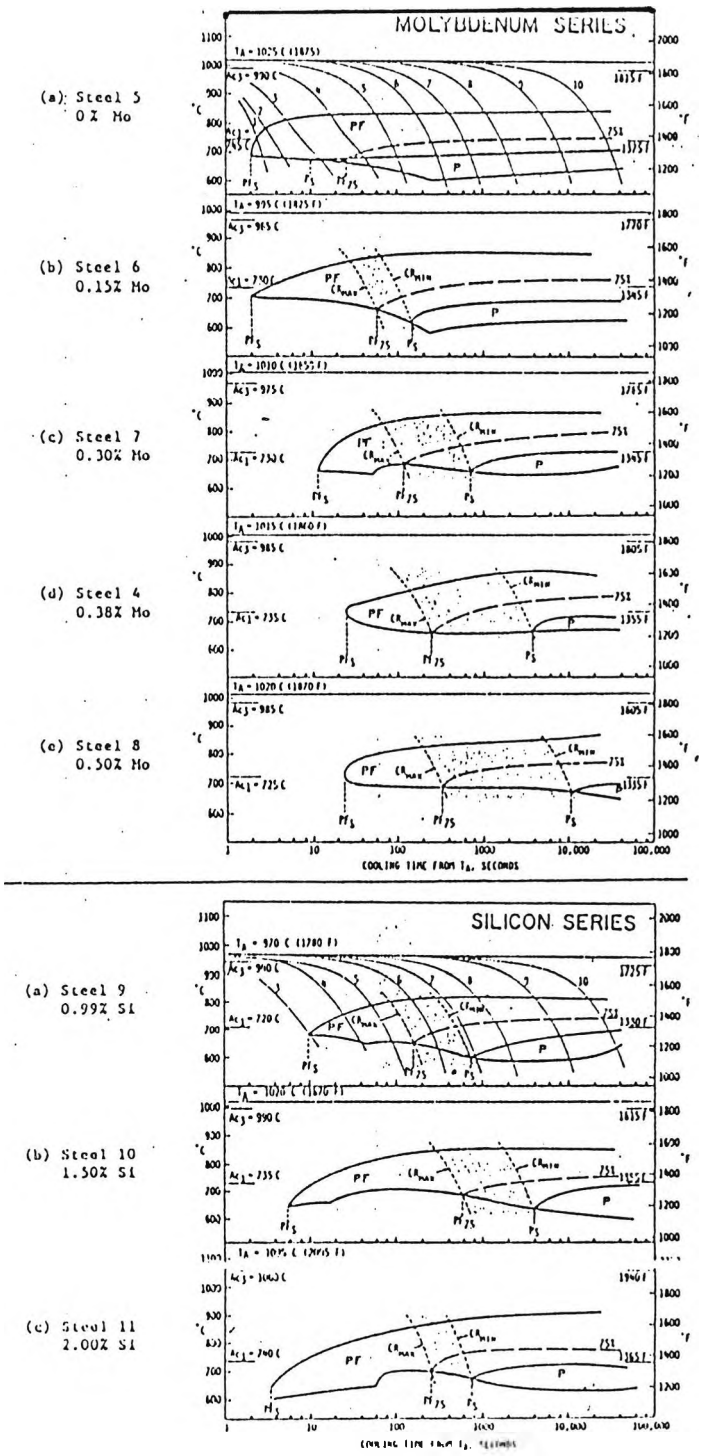

Figure 2.8- Upper Portion of CCT Diagrams for Steels in the Molybdenum and silicon Series.[20]

finish rolling temperature is an important factor controlling the strength-ductility combination of the final product. At low finish rolling temperature (below the Ar_3), a deformed ferrite structure may be produced which results in a decrease in ductility or an increase in $\sigma y/\sigma u$ ratio[17,18,21]. If the finish rolling temperature is too high, acicular ferrite may be obtained[21], which results in decreased ductility. In general, a finish rolling temperature just above the Ar_3 is desirable for obtaining good tensile properties.

One of the important features to take account of in the production of as-hot rolled dual-phase steels is that deformation of austenite reduces it's hardenability, i.e the CCT curves are shifted to the left. This means the transformation start and finish times are shortened as compared with the undeformed austenite phase[17,18,20].

It has been reported that for a steel containing 0.06%C, 1.2%Mn, 0.9%Si, 0.6%Cr, and 0.4%Mo, deformation of austenite will shift the ferrite-plus pearlite region to the left by about 2.5 orders of magnitude. This effect can be used to advantage in the production of dual-phase steels. The movement of the CCT curves to shorter times can promote rapid transformation of large amounts of polygonal ferrite during a short time cooling on the runout table. Figure 2.9 shows an example of the effect of deformation in moving the CCT curves to the left for the 1.5%Mn steel originally shown in the figure 2.7. It can be seen from the

figure 2.9 that for this steel, the deformation of austenite (solid curves) promotes polygonal ferrite formation. Additionally, the bainitic reaction is shifted to the left. Without deformation (dashed curves) the range of cooling rates that may be used to obtain 80% ferrite and 20% martensite is narrow. For deformed steel, because the bainitic region is shifted to the left, there exists a wide range of cooling rates. Therefore, dual-phase steels can be obtained using a more flexible runout table cooling pattern.

The advantages of producing As-hot-rolled dual-phase steels are:

1- No major capital investment is required.

2- No extra heat-treatment steps after hot-rolling are involved.

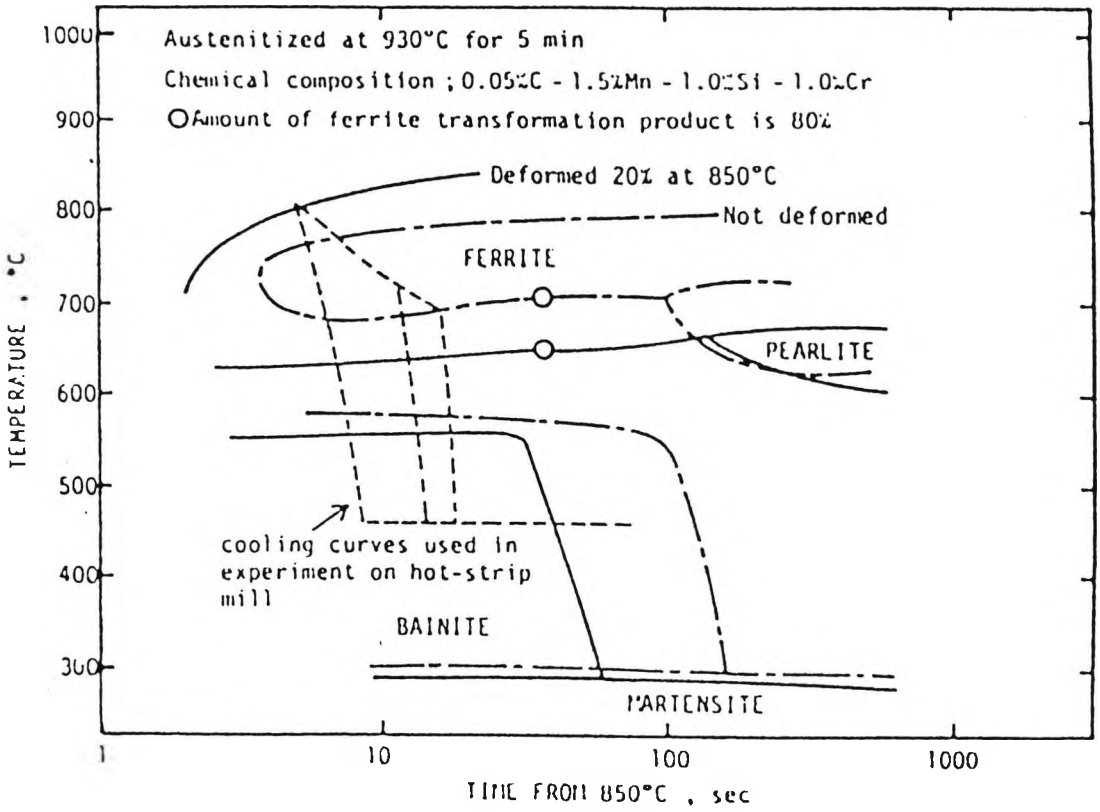

Figure 2.9- Effect of Deformation on Continuous Cooling Transformation.[18]

2.3- CHARACTERISTICS OF SHEET DUAL-PHASE STEEL PRODUCED BY INTERCRITICAL ANNEALING.

The characteristics of dual-phase steels produced by the intercritical annealing method depend on:

2.3.1- Heating Temperature.

2.3.2- Heating Time.

2.3.3- Alloying Elements.

2.3.4- Cooling Rate.

2.3.1- HEATING TEMPERATURE.

Many investigators have studied the effect of heating temperature during intercritical annealing on the strength, ductility and hardenability of the austenite formed, the amount of martensite formed after cooling, and the dissolution of carbides and nitrides in the as received steel. The results tend to often be contradictory due to the complexity of the processes.

Speich and Miller[22] have examined a C-Mn-Si hot rolled 13 mm thick plate intercritically annealed at 740°C,760°C and 780°C for 1 hour and water quenched. They reported that, both yield and tensile strength increased when the amount of martensite and carbon content of martensite phase increased. This was accompanied by a decrease in uniform elongation, total elongation, and reduction of area. The carbon content of the martensite which controls the hardness of the martensite depends primarily on the intercritical annealing temperature. For the same steel,

increasing the intercritical annealing temperature decreases the C content in the austenite while increasing the volume fraction of martensite. As martensite is the hard phase, the increase in martensite volume fraction has the greatest influence, leading to an increase in both yield and tensile strength. Morrow et.al.[23] have examined a C-Mn-Si-Mo-Al steel, hot-rolled to 2.5 mm thick strip and intercritically annealed at 790°C, 800°C, 815°C and 830°C for times of 15 sec or 1 min and air cooled. In contrast to Speich and Miller's work, they reported that, the overall strength level (yield and tensile) of this steel decreased slightly as the intercritical annealing temperature was increased, and this was accompanied by improved elongation at higher intercritical annealing temperatures as shown in figure 2.10. They suggested that, as the martensite volume fraction remained relatively constant, the decrease in strength and increase in total elongation was due to a slight coarsening of the grain size.

Rashid[24] has also found similar behaviour in a V-980X steel 3 mm thick strip intercritically annealed at temperatures in the range 700°C-850°C, for 10 min and air cooled. He reported that, the yield strength dropped with increasing annealing temperature, but the total elongation, and strain hardening exponent increased, while ultimate tensile strength remained the same after air cooling as shown in figure 2.11. He explained the improvement in

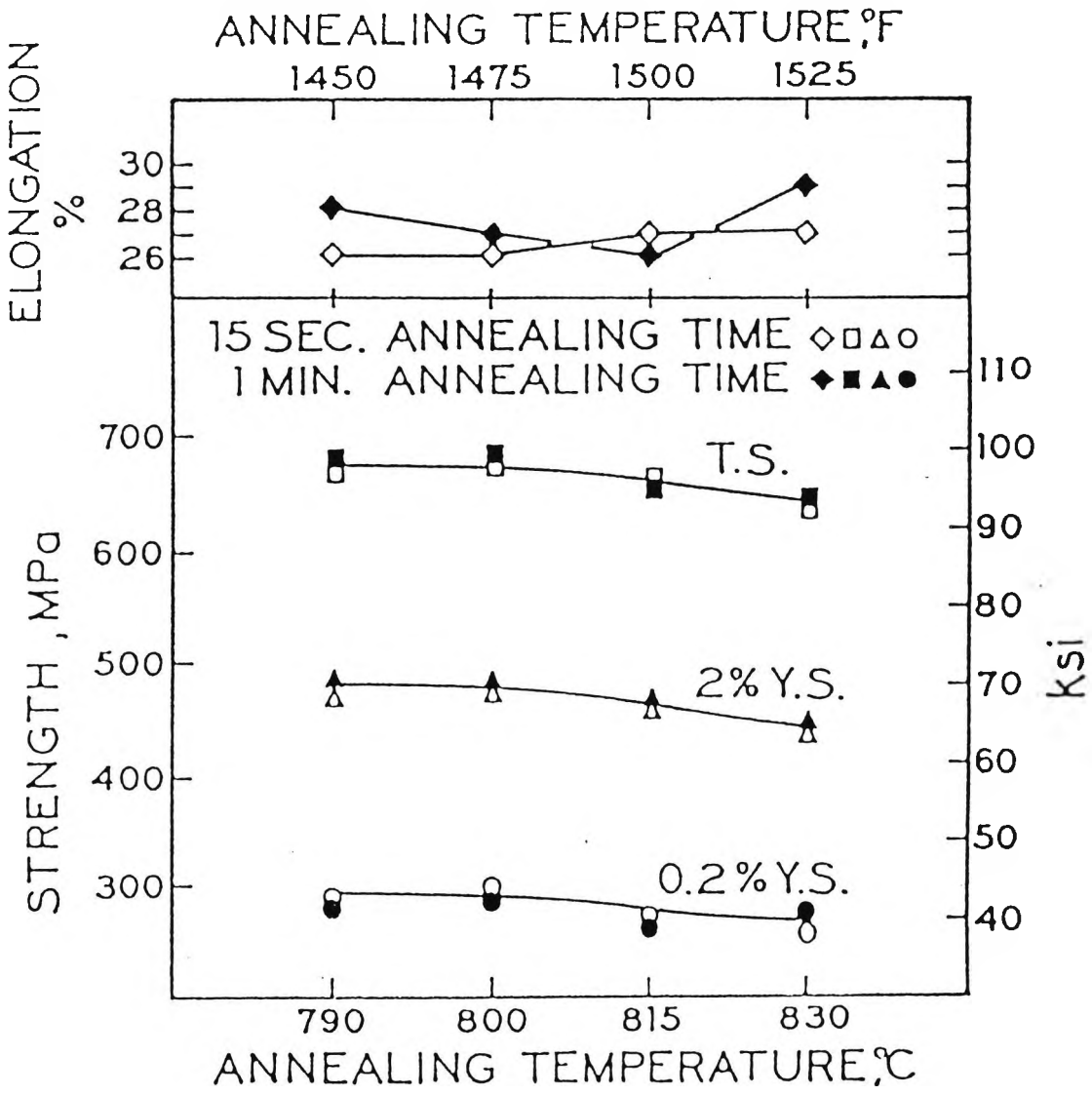

Figure 2.10- Effect of Intercritical Annealing Temperature on Tensile Properties of C-Mn-Si-Mo-Al Steel.[23]

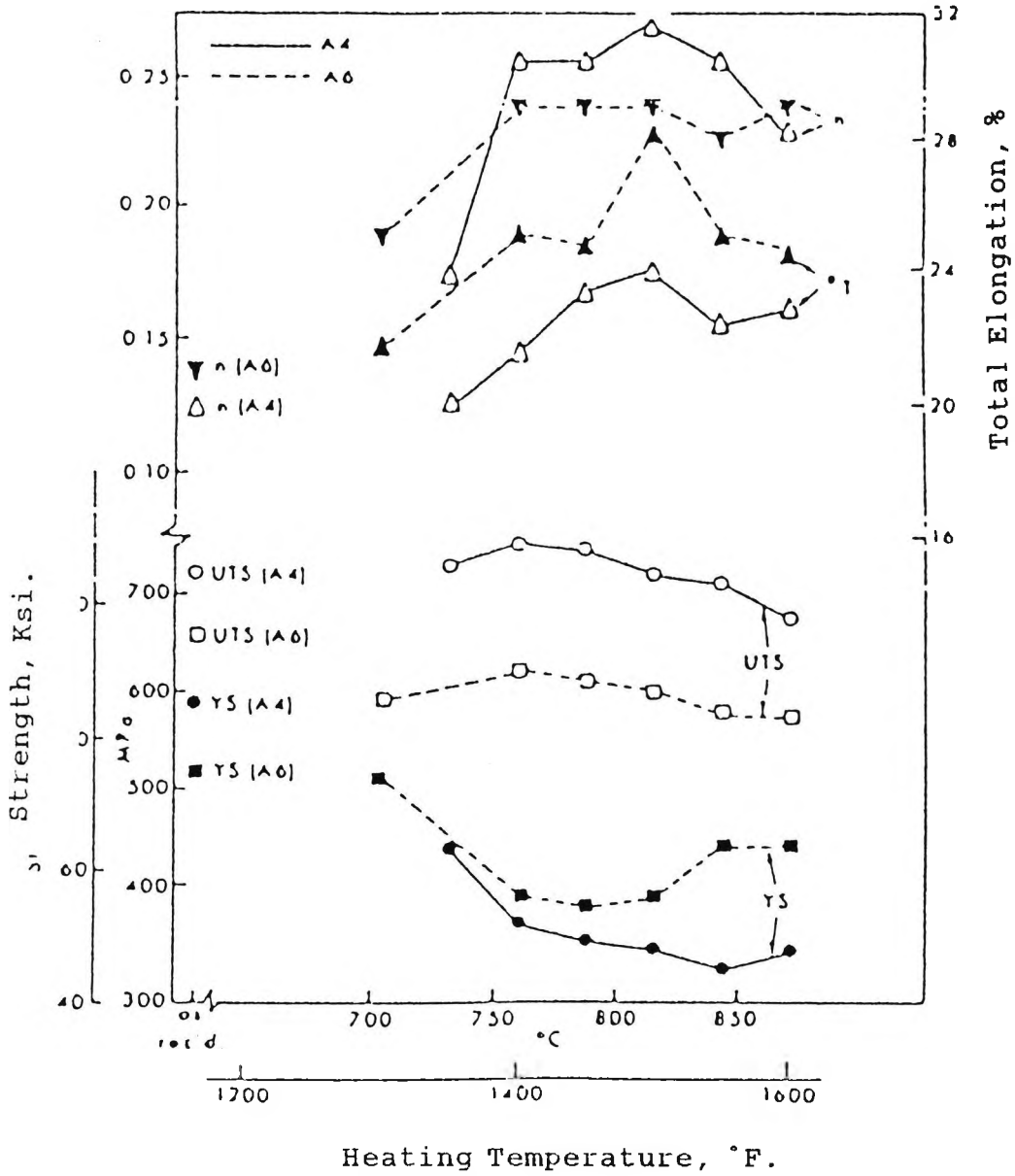

Figure 2.11-Effect of Heating Temperature on Mechanical Properties of Two V-980X Steels.[24]

ductility and fall in yield strength as being due to the dissolution of V(CN) during intercritical annealing resulting in a (clean), soft matrix. The ultimate tensile strength remained unchanged because of the counterbalancing effects between the strength increase produced by introducing martensite, and the decrease in strength due to loss of precipitation hardening.

Geib et.al.[25] have examined a Mn-Si-Nb hot rolled to 2 mm thick sheet and intercritically annealed at 760°C and 810°C for times ranging from 1-64 min, followed by oil quenching. They found that the hardenability of the austenite formed after intercritical annealing, decreases with increasing annealing temperature. The decrease in hardenability with increase in temperature is due to the lower carbon content of the austenite formed at higher temperatures, and this outweighs any increase in hardenability which may occur from resolution of niobium carbides. Martensite formed only in the carbon-enriched austenite after quenching from 760°C. At the higher temperature of 810°C, no martensite formed after oil quenching.

Priestner et.al.[26] have examined Mn-Si and Mn-Si-Nb-V specimens taken (10x10x5 mm), from hot rolled plates intercritically annealed in the temperature range 725°C to 835°C and found that, the hardenability of austenite formed at high temperature is lower than that of the austenite formed at lower temperature i.e. although the amount of

martensite transformed after quenching depended on cooling rate, at any cooling rate, the volume fraction of martensite increased with increase in annealing temperature.

Davies[27] examined a vanadium containing steel (1.65 mm thick sheet) intercritically annealed at 730°C to 815°C for 10 minutes followed by air cooling or brine quenching. He reported that, the amount of martensite formed, after air cooling from 730°C to 815°C is approximately constant, whereas the amount of martensite formed after brine quenching increases with increasing quenching temperature. He also reported that, the strength of dual phase steels is a function of percentage of martensite in the structure. Davies[28] in another investigation examined a series of C-Mn,-C-Mn-Mo, and C-Mn-Mo-Nb hot and cold rolled (1.2 mm) thick sheet intercritically annealed at 740°C to 840°C for 10 min, then brine quenched. He again emphasises that, the strength of a dual-phase structure is independent of the composition and strength of the martensite, being dependent only upon the ferrite grain size and the volume fraction of martensite. He also reported that, the yield strength and ultimate tensile strength increases with increasing intercritical annealing temperature, due to an increasing the volume fraction of martensite. Presumably although the amount of austenite increases with increasing intercritically annealing temperature, the ability to subsequentially form martensite on cooling to room

temperature is dependent on hardenability and cooling rate, and this must to a large degree account for the rather contradictory results.

2.3.2- HEATING TIME.

Okamoto et.al.[8] have reported that, the yield strength decreases with increasing holding time at the annealing temperature and the magnitude of the decrease depends on the annealing temperature. However tensile strength was found to increase with holding time. The yield strength was believed to decrease because more segregation of carbon from ferrite to austenite (martensite after cooling) took place leaving the ferrite matrix softer than before intercritical annealing. Tensile strength increased because the martensite became harder with increasing holding time. Similar results were also obtained by Rashid[24], who found for V-containing steels that, the yield strength decreased with increasing intercritical heating time at 790°C due to the V(CN) precipitates redissolving as shown in figure 2.12. However, in contrast to the previous work the ultimate tensile strength remained unchanged as shown in figure 2.13. The n value also increased with increasing heating time.

Morrow et.al.[23] examined two steels with the same base composition as that used in Rashid[24] investigation. The first steel had an addition of 0.1% Mo, and the second steel contained 0.21% Mo and 0.04% Nb. They again found

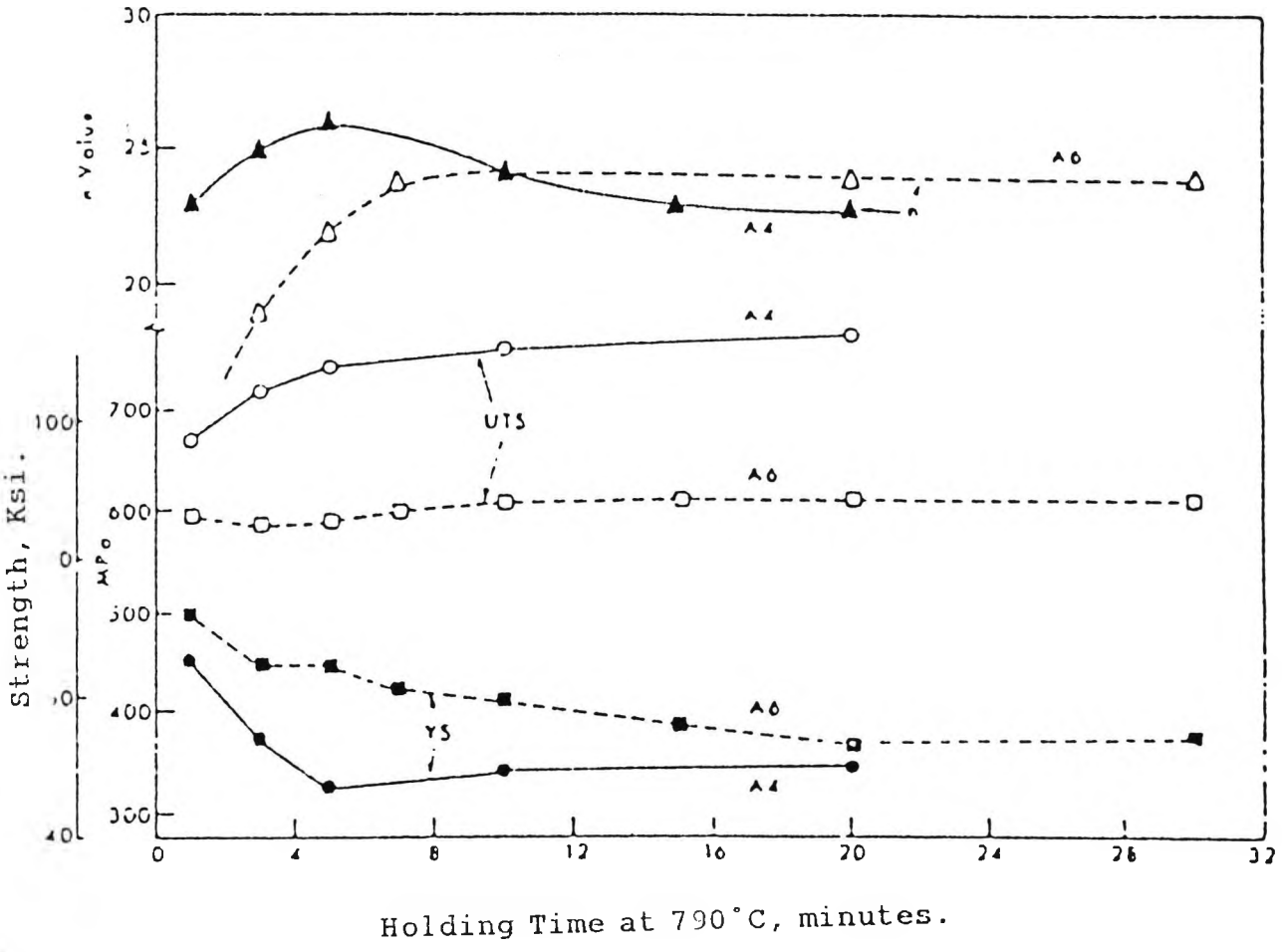

Figure 2.12- Effect of Heating Time at 790°C on the Mechanical Properties of Two V-980X Steels.[24]

very different behaviour. For the first steel, both yield strength and ultimate tensile strength increased with increasing heating time. The increase in yield with time was ascribed to the role of Mo as a ferrite stabilizer, increasing the C content of the ferrite, and the increase in ultimate was related to the increase in hardenability of the austenite. However, for the Mo-Nb containing steel the yield and tensile strength were insensitive to heating time, as shown in figure 2.13. This insensitivity, may due to the counterbalancing effects between the strength increase produced by Mo, and the loss of precipitation hardening from Nb(CN) as it redissolves during heating. Clearly again the complexity of the changes occurring during intercritical annealing make it very difficult to predict the changes in properties that occur with increase in intercritical annealing time.

2.3.3- ALLOYING ELEMENTS.

Alloying additions can be considered with respect to their effect on:

1- The hardenability of the austenite phase in the two-phase region.

2- The ductility of ferrite.

3- The continuous cooling transformation behaviour of the steel from the single phase austenite region.

The effect of alloying elements such as carbon, manganese, silicon, molybdenum, and chromium, will be

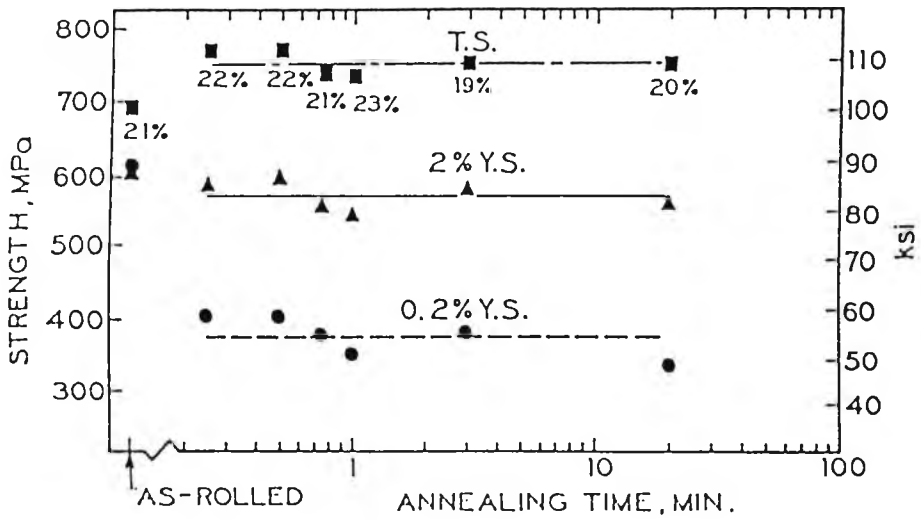

(a)

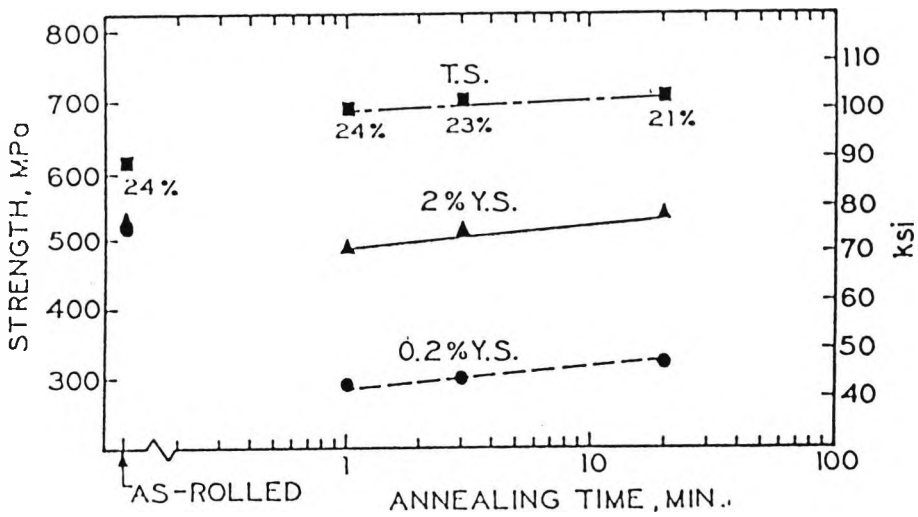

(b)

Figure 2.13- Effect of Annealing Time on the Tensile Properties of

a- Mo-Nb Steel.

b- Mo-V Steel.[23]

discussed in section 2.5.

2.3.4- COOLING RATE.

The cooling rate after annealing plays a very important role in determining a good balance of mechanical properties. Asamura[29] has reported that, the optimum cooling rate may vary, depending on the application of the product, as shown in figure 2.14. Repas[30] found that, an increased cooling rate promoted martensite formation and increased the tensile strength of dual-phase sheet steels. Rashid[13] has also reported for a vanadium steel that, the ultimate tensile strength increased with increasing cooling rate, while the yield strength decreased. Marder et.al.[31] have examined the influence of intercritical annealing using two different steel compositions, one a vanadium containing steel and the other a Molybdenum containing steel. They found that the yield and tensile strength of these steels increased with increase in the volume percent of the second phase in the microstructure. This in turn was controlled by the cooling rate from the annealing temperature, with the larger percentages occurring at the faster cooling rate for the Mo containing steel, but for the V- steel, the yield strength decreased at first, and then increased again, with increase in cooling rate. The ultimate tensile strength, increased with increase in cooling rate. Marder[32] in another investigation working with a Cr-steel reported that, the tensile strength

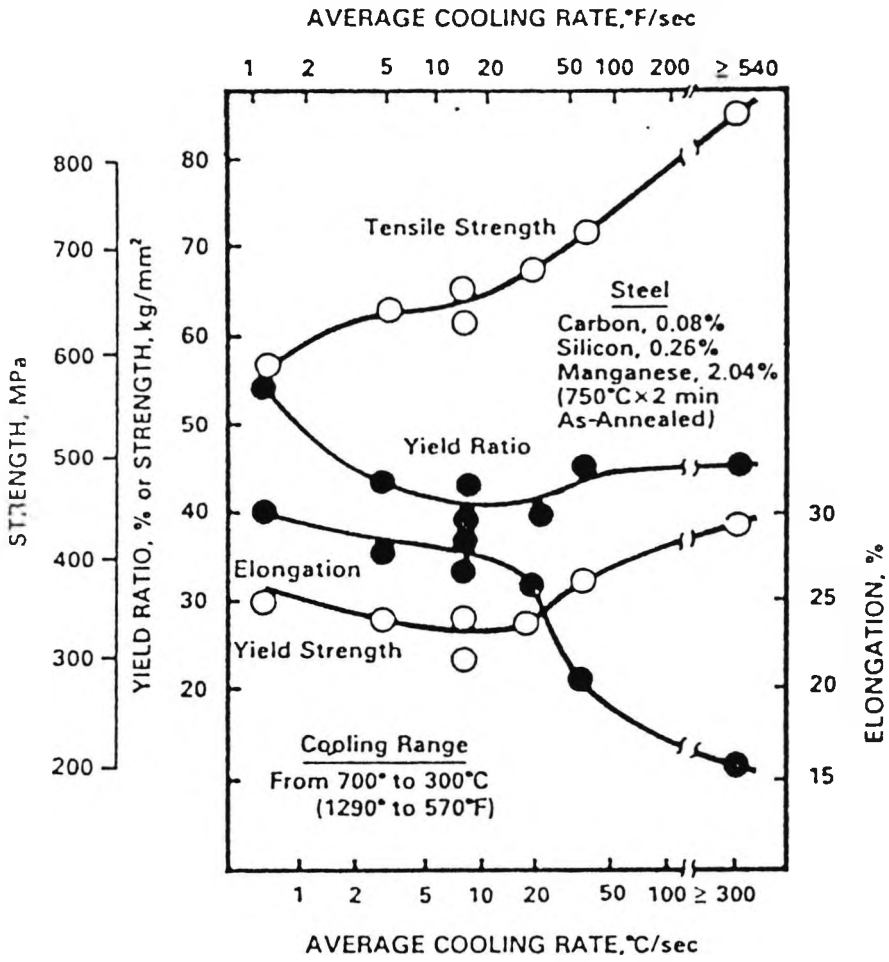

Figure 2.14- The Effect of Cooling Rate on HSLA Steel After Contiuous Annealing.[29]

increased with increasing cooling rate, but the yield strength first decreased and then again increased as the cooling rate increased as shown in Figure 2.15.

A minimum yield strength was observed when the volume percent of martensite was about (10-25%) as shown in Figure 2.15. Messien et.al.[33] examined a series of 18 low carbon steels(0.07%-0.1%) C. The steel also contained Mn (1%-1.7%), Si (0.2%-0.7%), P(0.010%-0.13%)/ and N(0.005-0.025%), and were intercritically annealed in the temperature range 700°C-850°C for 2-10 min and cooled at rates between 3.5°C/sec to 750°C/sec. They reported that increasing the cooling rate raises both the ultimate tensile strength (UTS) and the parameter (UTS X EL_t), (EL_t = total elongation) as long as the cooling rate is between (10-70) °C/sec, as shown in figure 2.16. This arises through the martensite volume fraction increasing with cooling rate. The use of faster cooling rates not only increases the ultimate tensile strength but also produces an important loss of ductility due to excessive amounts of martensite. They also developed a regression equation relating the cooling rate to the steel composition to give 5% martensite.

$$\mathrm{Log}C_R5M(°C/sec) = 4.93-1.7[Mn\%]-1.34[Si\%]-5.68[C\%] \quad \ldots\ldots 2.1$$

A regression equation was also developed relating the ultimate tensile strength to chemistry, grain size and cooling rate for 0.8, 1.05 and 1.4mm thick sheets.

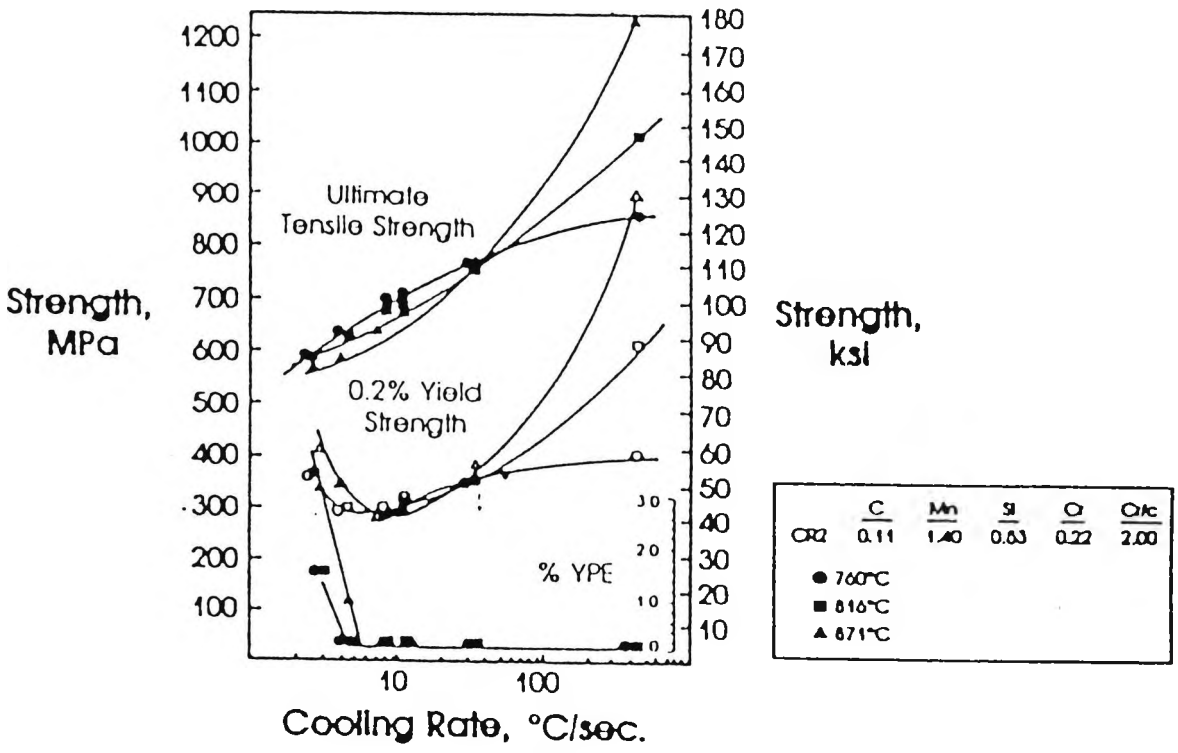

Figure 2.15- The Effect of Cooling Rate After Intercritical Annealing on the Strength Properties of Cr-Steels.[32]

		Thickness mm (in)	Anneal. time
Cold-rolled	A	.8 - 1.05 (.031-.041)	2'30"
	B	1.4 (.055)	3'30"
Hot-rolled	C	2.4 (.094)	4'30"
	D	3.2 (.126)	6'30"
	E	4.0 (.157)	6'30"

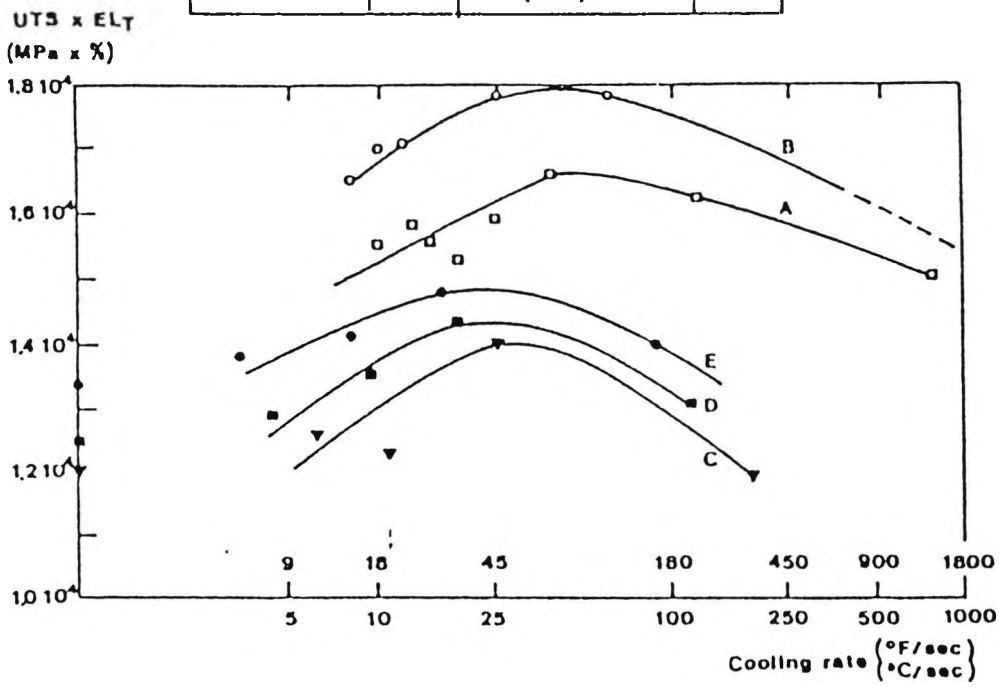

Figure 2.16- Influence of Cooling Rate on the UTS X EL_T Product after Intercritical Annealing at 825°C.[33]

$$UTS=71.6LogCR+955[C\%]+69.5[Mn\%]+1.31[Si\%]+9.4d^{-1/2}+70.8 \quad ..2.2$$

These relationships are valid only for steels cold-rolled and continuously annealed and with chemical compositions in the following range: [0.05-0.1]%C, [1-1.7]%Mn, and [0.2-0.7]%Si. They also developed a regression equation to calculate the cooling rate necessary to transform the austenite into martensite without any bainite formation as follows:

$$\log t_c^B = 3.274[C]+0.046[Si]+0.626[Mn]-1.818 \quad .....2.3$$

where

t^B_c = is the time in seconds, between the annealing temperature and 500°C.

[C] = is the carbon content of the austenite.

[Mn] and [Si]= the mean chemical contents of the steel, assuming that during a short continuous annealing treatment no diffusion of these elements will occur.

Tanaka[14] has studied the influence of alloying elements and cooling rate on the formation of dual-phase structures. He reported that, the logarithm of the critical cooling rate required for the formation of the dual-phase structure, decreases in a linear manner with increasing manganese equivalent, as expressed by:

$$LogCR(°C/sec) = -1.73Mneq(\%)+3.95 \quad .....2.4.$$

where

Mneq % = Mn(%) + 1.3 Cr(%) + 2.6 Mo(%).

2.4- PHASE-TRANSFORMATION DURING INTERCRITICAL ANNEALING.

The techniques for producing dual-phase steels have been discussed before.

It can be seen that the complexity involved in each manufacturing process is dependent on the mill processing parameters giving the required mechanical properties. Of the various techniques, the continuous annealing process has attracted most attention as a method for producing sheet steels because of several advantages which include short processing time and attainment of uniform properties along the coil length[34].

The processing parameters and the mechanical properties of continuously annealed dual-phase and other types of sheet steels have been documented in several important conferences[34-37].

For the continuous annealing technique the kinetics of the formation of austenite in the intercritical region is an important variable to be considered in the production of dual-phase steels.

The kinetics of formation of austenite during an austenitising process[38-43], and the subsequent kinetics of formation of proeutectoid ferrite have been studied by many workers[44-46].

2.4.1- FORMATION OF AUSTENITE DURING INTERCRITICAL ANNEALING HEAT-TREATMENT.

When a steel is heated into the single phase austenite region, the nucleation of austenite occurs at pearlite or at the carbide particles adjacent to ferrite grain boundaries [40,41,43,44]. The subsequent growth of austenite is presumably controlled by the diffusion of carbon through the austenite region. Substitutional alloying elements such as manganese which may decrease the carbon diffusion through the austenite usually decrease the growth of austenite[40-43].

Usually low carbon steels with substantial alloying elements, e.g. 1.5%Mn, are used when continuously annealed dual-phase steels are produced. The annealing temperature for this process is lower than that for full austenitisation, so that, the kinetics of austenite formation in the two phase region will be somewhat different. The rate controlling processes are dependent on the alloying elements partitioning from ferrite to austenite which, in turn, depends on the annealing temperature. The annealing temperature exerts its influence by controlling the temperature dependence of the diffusion coefficients of the various alloying elements, the concentration gradients and the amount of austenite formed in the two-phase region. Speich[47] has pointed out that during most of the intercritical annealing operations neither the true equilibrium nor the paraequilibrium[48,49]

(i.e. assuming no manganese redistribution occurs so that equilibrium is with respect to carbon rather than to manganese) condition can be achieved. This is particularly so when continuous-annealing is used.

The formation of austenite in low carbon, 1.5%Mn steels during intercritical annealing has been studied by several investigators[48,50,52].

In general when the steel is heated into the two phase region, the first step of phase transformation is the dissolution of pearlite and the separate carbide particles followed by the growth of austenite. The reaction curves usually show a sigmoidal shape indicating the nucleation and growth nature of the reaction[48,50,51].

Speich, Demurest and Miller[48] have postulated that the process of intercritical annealing can be separated into three stages:

1- Very rapid growth of austenite from the pearlite regions until dissolution is complete.
2- Slower growth of austenite into the ferrite regions
3- Very slow final equilibrium between ferrite and austenite.

According to these authors, during the first step (dissolution of pearlite), the nucleation of the austenite phase usually occurs instantaneously at the ferrite/ pearlite interface with essentially no nucleation barrier.

The subsequent growth of austenite into pearlite is controlled primarily by the carbon diffusion in the

austenite between adjacent pearlite cementite lamellae, which may be slowed down by the presence of substitutional alloying elements such as manganese. For example, between 740°C and the Ac_1 the time for dissolution of pearlite may range from 15 sec to 1 hr. The slow rate of pearlite dissolution at low intercritical annealing temperatures has also been observed by Garcia and Deardo[50,53]. A slight increase in temperature can cause a drastic increase in the dissolution rate of pearlite. For example at 780°C, the pearlite dissolution rate can be as great as three orders of magnitude higher than at 730°C [41,48].

After the dissolution of pearlite and cementite particles, the higher-carbon austenite phase is formed. If the specimen is annealed for a time longer than that required for pearlite dissolution, the austenite phase grows into the ferrite to achieve the equilibrium volume fraction of ferrite and austenite, as detailed by Speich et.al.[48]. During this stage, the growth rate of austenite is dependent on the diffusion of carbon and the partitioning of alloying elements between the ferrite and austenite [48,49,50,53]. It has been reported that at low temperature, e.g, at 725 [50,53] or 740°C, the growth of austenite occurs preferentially along the ferrite grain boundaries with the growth normal to the grain boundary being slow.

According to the analysis of Speich et.al.[48] during the second stage, the growth of austenite into the surrounding

ferrite may occur either with or without manganese redistribution. If no manganese redistribution occurs, a paraequilibrium condition (equilibrium with respect to carbon rather than to manganese) is established and the growth rate is controlled by carbon diffusion through the austenite phase. This occurs at higher temperatures of 850-900°C (above the Ae_3) for short exposure times, 2 to 9 sec. At low temperatures between 780-740°C partitioning of manganese may occur. Because the diffusion rate of manganese in ferrite is much faster than in austenite (about three orders of magnitude higher), the diffusion of manganese in ferrite can be rate controlling and the times for completion of this stage at low temperatures in the range 740 to 780°C are much longer ranging from 4-24 hours.

The grain boundary diffusion of manganese in ferrite has been considered by these authors as one of the possible mass transport mechanisms encouraging austenite growth at low temperatures. Because grain boundary diffusion is faster than volume diffusion, the manganese can diffuse down the ferrite grain boundary to austenite particles lying in the grain boundary. The transport of manganese to the austenite phase either by grain boundary diffusion or by volume diffusion in ferrite will result in a build-up of manganese concentration at the austenite/ferrite interface[48], see figure 2.17(a). (I.A. in the figure is intercritical annealing).

The build up of manganese concentration at the ferrite/

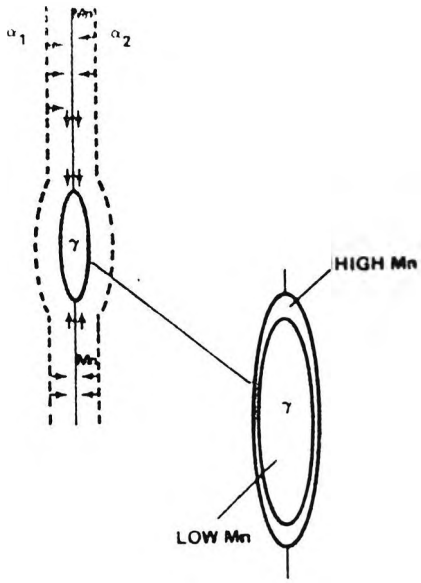

(a)

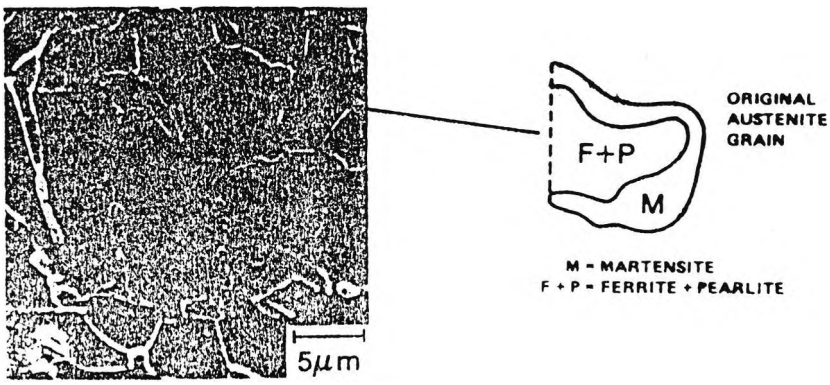

(b)

Figure 2.17- a- Mn Partitioning by Grain Boundary Diffusion During I.A.

b- Microstructure of 0.06C-1.5%Mn Steel I.A 1 hr at 740°C- Slow Cooled(4°C/in).[48]

austenite interface on annealing in the two-phase region has been reported earlier by Gilmour, Purdy and Kirkaldy[46]. These authors used two Fe-Mn-C alloys, annealed at 728°C for periods varying from 2 days to 2 months followed by water quenching. The manganese concentration profile across the ferrite/ austenite interface was investigated using an electron microprobe analytical technique.

One of their results is shown in figure 2.18 for a specimen annealed at 728°C for two months. According to these authors, the manganese concentration peak height across the ferrite/austenite interface increases with increasing annealing time.

The diffusion of manganese to the ferrite/austenite interface leads to the formation of a high manganese rim around the austenite phase figure 2.17(a). This rim has a higher hardenability than the central core, therefore upon cooling, it transforms to martensite and the central core transforms to ferrite and pearlite as shown in figure 2.17(b).

In the last stage of intercritical annealing, the manganese concentration gradient within the austenite will be eliminated by manganese diffusion through the austenite. The times for completion of the final equilibrium of ferrite and austenite are extraordinarily long, e.g, from 2000-4000 hours[48].

From the analysis of the kinetics of austenite formation,

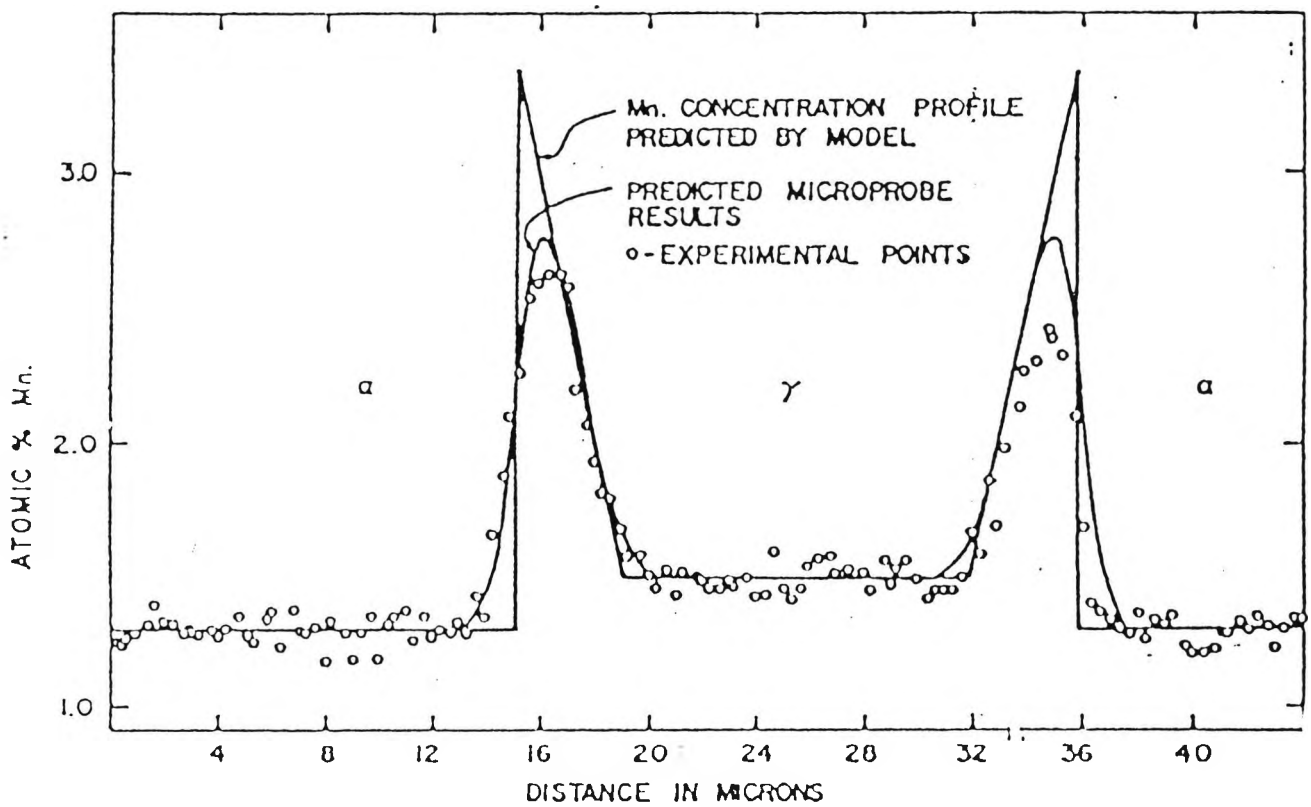

Figure 2.18- Detailed Microprobe Analysis of an Alloy 0.45%C-1.5%Mn Transformed for 5.37×10^6 Sec. (2 Month) at 728°C.[46]

Speich et.al.[48]. proposed an austenite formation diagram for a 0.12%C-1.5%Mn steel as shown in figure 2.19.

In this diagram the time for formation of various amounts of austenite and the controlling kinetic process at each stage for different temperatures, are shown. For example, at an annealing temperature of 780°C, the dissolution of pearlite (first stage) is completed in about 0.2 second to form 12% austenite. The subsequent growth of austenite into the ferrite phase initially is controlled by the carbon diffusion in austenite until about 20% austenite is formed after 6 seconds, then the growth of austenite is controlled by manganese diffusion in ferrite until just over 50% austenite is formed after 55 hr. The final stage is the equilibrium of manganese in austenite with final equilibrium being achieved after 3000 hr.

At temperatures higher than the Ae_3, the dissolution of pearlite is almost instantaneous. Carbon diffusion in austenite is the rate-controlling process for the growth of austenite and the manganese diffusion-controlled step is absent.

Navara and Harrysson[54] suggest that in Mn-containing steels, austenite forms by heterogeneous nucleation, most probably at grain boundary carbides, and subsequently grows by absorbtion of both carbon and manganese, supplied to the surface of the grain by both grain boundary and volume diffusion in the ferrite. The primary pearlite also transforms to austenite, but being less stable than the new

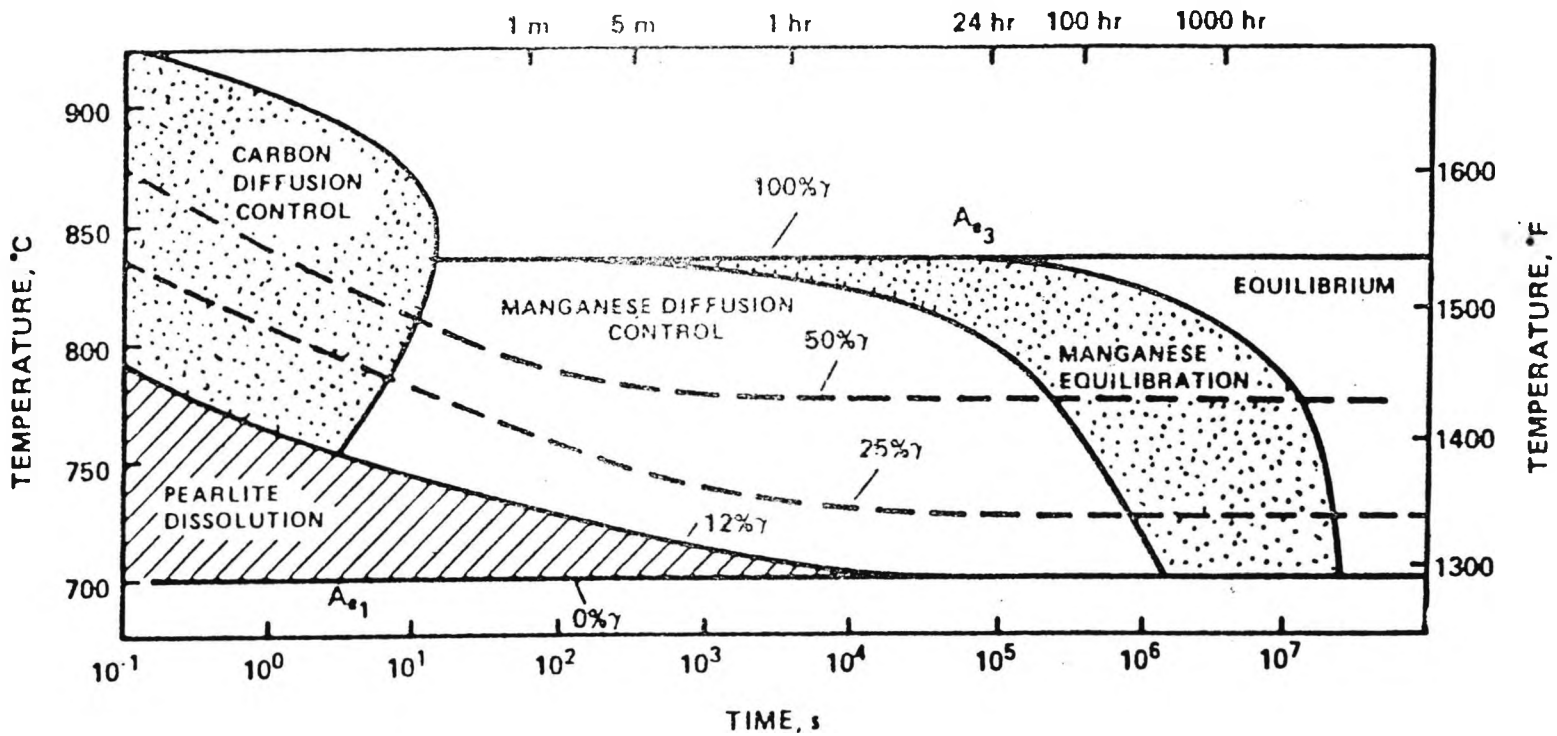

Figure 2.19- Austenite Formation Diagram for 0.12%C 1.5%Mn Steels.[48]

austenite nuclei which are rich in manganese from the start, dissolution can be a slow process, and they found residual pearlite even after a 12 hour treatment at 725°C.

More recent work by Navara et.al.[55] has indicated that austenite nucleation occurs at the ferrite/ferrite boundaries and is not dependent on the presence of cementite pearlite for nucleation. They noted that the formation of austenite is associated initially with migration of ferrite/ferrite grain boundaries and propose that the boundary migration is induced by manganese diffusion along the boundaries to provide the mechanism for rapidly transporting manganese into the growing austenite as shown in figure 2.20. (In the figure MPDP means manganese partitioning dual phase).

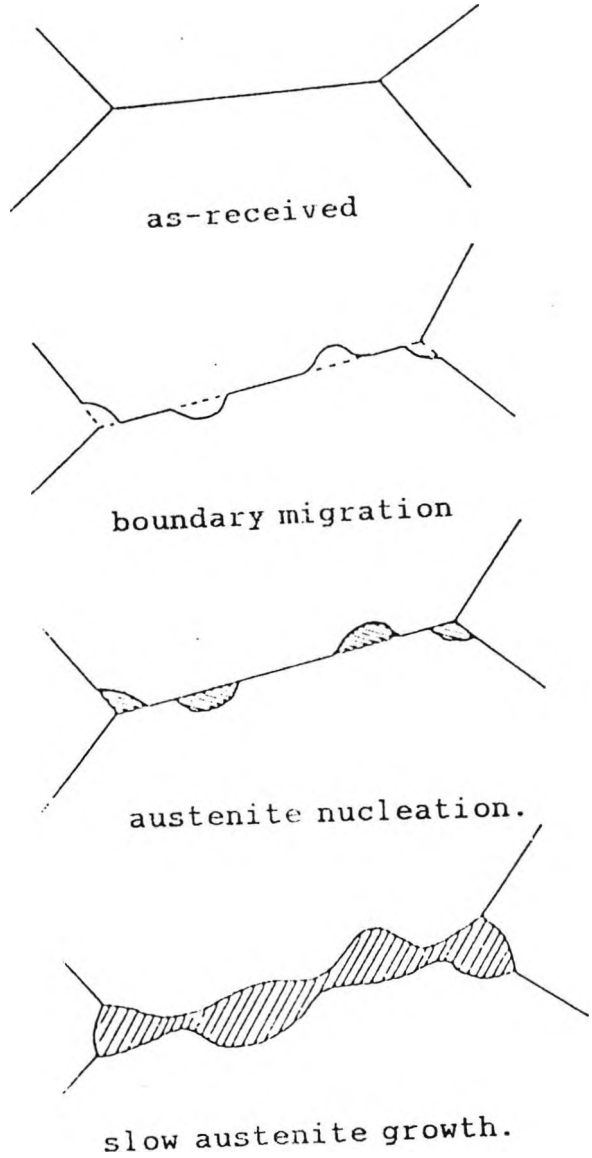

Figure 2.20- Schematic Sequence Showing Likely Development of Austenite and Growth in MPDP Steels Annealed in the I.A. Temperature Range.[55]

2.4.2- CHANGE OF PROPERTIES OF FERRITE PHASE WITH INTERCRITICAL ANNEALING.

It is believed that the ductility of the ferrite phase is very important in giving optimum ductility to a dual-phase steel and to ensure good ductility and formability the ferrite phase should be as ductile as possible.

It has been suggested that the improved ductility of continuously annealed dual-phase steels is related to a subtle change in either interstitial or precipitate content of the ferrite[56-58]. In general a "clean" ferrite matrix free from interstitial impurities and precipitates has been thought as the key factor contributing to the good ductility of dual phase steels[9,11,12,14,15]. However, since the most the attractive property of dual-phase steels is the superior strength/ductility combination, Lagneborg[59] has pointed out that the ductility improvement is usually gained at the expense of a reduction of strength. It is thus doubtful that an improvement in the combination of ductility and strength can be achieved by decreasing the interstitial content to very low levels.

Davies[56,60] has claimed that, since the ductility of dual-phase steels is sensitive to the strength and ductility of the ferrite matrix, it would be desirable to make the ferrite as strong as possible in keeping with a high ductility.

Davies[57], proposed that, for optimum ductility/strength combinations of dual-phase steels, very fine grained

(smaller than 5 micron) clean (low interstitial content) ferrite is required. Although, coarse grain sizes generally give high work hardening rates and hence better ductility[61] (i.e. uniform elongation), the high work hardening rate in dual phase steels is achieved through the presence of martensite. Finer grained steels giving higher strength levels as has been shown by Morrison[61] are preferred for dual phase steels.

In fact, during the intercritical annealing, the carbon content of ferrite may be lower than that of the original ferrite matrix in the as-received condition. The alloying elements may also decrease the carbon content of ferrite. For example, an addition of 1.5%Mn may lower the solubility of carbon in the ferrite from 0.02% to 0.005% at 760°C under equilibrium conditions[47].

Besides having a "clean" ferrite, the cooling rate has been reported to be an important parameter controlling the ductility of ferrite and hence dual-phase steels[14,12,15].

A mild cooling rate, e.g, air cooling, was believed to produce less solute carbon in the ferrite matrix than a drastic cooling such as water quenching. This had been noticed in results from internal friction measurements on several dual-phase steels annealed at 750°C for 2 minutes[12], see figure 2.21 In this figure, the internal friction maximum (Q^{-1}) times 10^{-4} gives an approximate solute carbon content of the ferrite. In higher alloyed steels the carbon content is less sensitive to the cooling

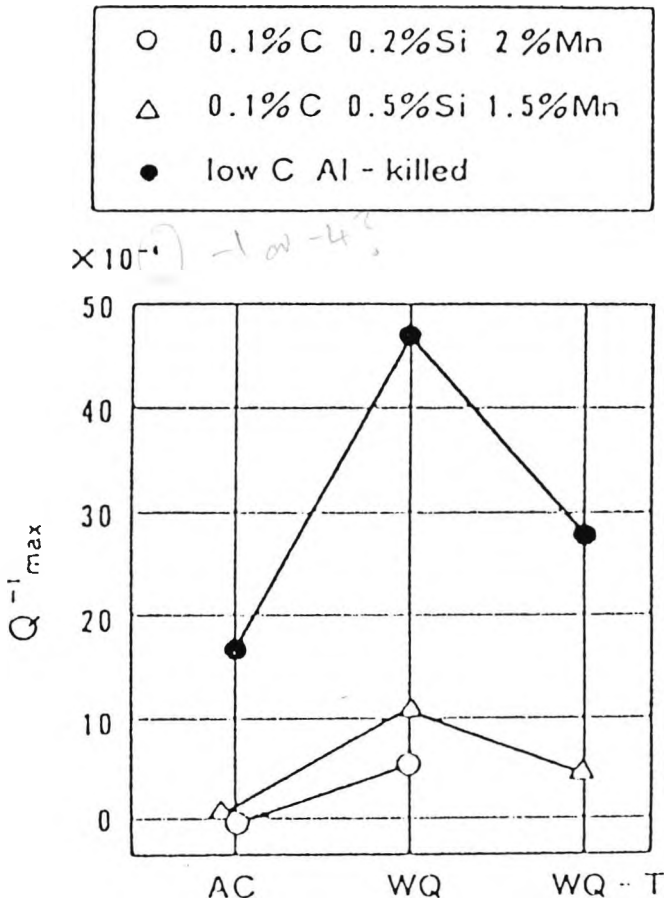

Figure 2.21- Effect of Cooling Condition on Internal Friction.[12]

AC: Air Cooled.

WQ: Water Quenched.

rate, for example, the difference in carbon content of ferrite between water-quenched and air-cooled specimens is only a few ppm for an 0.1%C -2%Mn -0.2%Si steel.

It has been proposed by Tanaka et.al.[14], that the beneficial (with respect to the properties of ferrite) substitutional alloying elements would be those which decrease the solute carbon content while not contributing any solid solution hardening to the ferrite matrix. Unfortunately most of the alloying elements do cause a hardening effect in the ferrite matrix[62], and thus decrease the ductility. The strength/ ductility balance of dual-phase steels is an important feature considered by most of the workers.

Masui and Takeshi[63] have reported that solid solution hardening using silicon and manganese resulted in the best combination of strength and ductility. Silicon has also been found by a number of investigators to be particularly useful in optimizing the best combination of strength/ ductility for dual-phase steels[63].

For dual-phase steels containing microalloying elements, the role of these elements during intercritical heat treatment is rather complex. Davies[57] has reported that, in several vanadium microalloyed specimens, after air cooling from different intercritical annealing temperatures the amount of martensite is approximately constant. This indicates that, some of the austenite from the higher annealing temperatures has transformed to ferrite prior to

the formation of martensite from the remainder of the austenite during air cooling. Matlock et.al.[64] have reported a similar phenomenon in Nb-bearing dual-phase steels, i.e, the ferrite was formed from austenite during cooling from the intercritical annealing temperature. The ferrite formed upon cooling was designated as "new ferrite" and the ferrite which existed during intercritical annealing was called "old ferrite " by these investigators. A special etching technique was developed by these workers, namely, an initial etch in nital followed by staining in an alkaline chromate solution, to differentiate the new and old ferrite. The alkaline chromate solution stains the martensite phase black, the old ferrite grey,and the new ferrite white. In the ferrite regions of Nb-bearing dual phase steels a very dense precipitate dispersion was observed under the transmission electron-microscope. Presumably, these precipitates were formed during the intercitical annealing treatment[65].

A precipitate-free zone in the new ferrite of Nb-dual phase steels around the martensite region was observed by Matlock et.al[64] in specimens cooled over a wide range of cooling rates, from 1000-12°C/sec. In contrast to this, in V-bearing dual-phase steels the new ferrite regions showed a dense precipitation on rapid cooling[66,67].

Another important factor influencing dual-phase steel properties is the 2% to 4% volume expansion that accompanies the austenite to martensite

transformation[68,69]. As a result of the transformation during cooling, the ferrite region adjacent to the transforming austenite is plastically deformed and remains "pre-yielded" and under compression which can be partially relieved by the generation of dislocations into the ferrite matrix immediately adjacent to the martensite region[70-73]. Consequently, the dislocation density at the ferrite/ martensite interface is higher than that in the interior of the ferrite grains. This has been observed by several investigators[6,9,14,74,75] using transmission electron microscopy.

It is generally believed that these transformation induced dislocations may account for the low yield strength continuous yielding and the low $\sigma y/\sigma u$ ratio observed for the dual-phase steels.

The details of these features will be discussed in the "structure property relationships" section (2.8).

2.5- ROLE OF ALLOYING ELEMENTS.

Alloying additions can be considered with respect to their effects on:

1- The hardenability of the austenite phase in the two-phase region.

2- The ductility of ferrite.

3- The continuous cooling transformation behaviour of steel from the single phase austenite region.

In commercial continuous annealing and the box-annealing processes, the steel is heated to the intercritical region and cooled at different cooling rates in order to obtain the desired tensile properties. The hardenability of austenite is of primary concern if the dual-phase structure is to be obtained as well as the need for high ductility which is controlled by the ferrite phase. The latter requires that a "clean" and soft ferrite matrix be produced by the heat-treatment. A proper matrix can be achieved by controlling the cooling rate and/or by the addition of alloying elements which reduce the carbon solubility in the ferrite.

The addition of silicon is a typical example of the latter. On some occasions, micro alloying elements, such as Nb, Ti, and V, are introduced during the steel making process. These elements may form carbides or carbonitrides in the ferrite matrix in the hot-rolled condition. Because the dissolution temperature of these precipitates are relatively high (dependent on the amount present), the

heating schedule in the two-phase region becomes an important processing variable.

In the production of as-hot-rolled dual-phase steels, the steel is usually reheated into the single phase austenite phase, hot-rolled through several passes, then coiled, and cooled to room temperature.

The phase transformation from a deformed austenite phase to ferrite plus martensite are more complicated than that in the continuous annealing and box-annealing processes. The effects of alloying elements on the hardenability of austenite, the ductility of ferrite and structure property relationship of dual-phase steels are summarised below.

2.5.1- Carbon.

The amount of carbon in dual-phase steels is governed by its effect on hardenability and control over the percentage of martensite formed. In general the carbon content is kept to less than 0.15% to ensure that the steels are weldable,[47] and also possess good ductility and toughness[76]. The carbon content in the martensite is determined by that of the austenite. It is desirable to maintain a carbon level of about 0.3% in the austenite, resulting in a dislocated martensitic structure. Higher carbon contents can drastically deteriorate the toughness of martensite[77], as twinned martensite is then formed. In order not to exceed this 0.3% C content, the carbon content of the alloy should be less than 0.1% C.

2.5.2- Manganese.

Manganese is the second most potent alloying element in increasing the hardenability of austenite[20]. Its addition provides the following benefits:

1- Mn refines the grain boundary carbide thickness[78] and hence improves impact toughness (1% increase in Mn refines the average carbides thickness as measured on the S.E.M.by 0.13 μm).

2- Besides refining the grain boundary carbides, it decreases the grain size, thus improving strength and impact properties at the same time[79,80].

Mintz[78,81] found a strong inter relationship between manganese and silicon on the impact transition temperature (ITT). Whereas manganese had only a small influence on the ITT of a Si killed steel, a very significant improvement in ITT occurred with a low silicon steel, a rise of 1% causing an approximate 40°C lowering in ITT after correcting for grain size and pearlite volume fraction. The decrease in ITT is believed[81] to be due predominantly to refining of grain boundary carbide thickness[79,82] and to the prevention of grain boundary segregation of the interstitials C and N by manganese.

3- Mn suppresses the temperature for the start of the ferrite reaction and hence promotes polygonal ferrite formation during continuous cooling from the single austenite phase region[17,18,20].

4- It stabilizes the austenite phase, by retarding the

bainite start and bainite finish reaction, therefore, avoiding the formation of bainite from the carbon enriched austenite on cooling.

5- Mn can decrease the carbon solubility in ferrite on intercritical annealing and hence promotes ductility while decreasing the yield strength of dual-phase steels[14]. It has been reported by Tanaka et.al.[21] that, in Cr-added as well as Mn-added dual-phase steels, when the alloy content is increased , the yield stress decreases, reflecting the decrease in C solubility in the ferrite.

2.5.3- Silicon.

Mintz[82] has shown that, increasing the silicon level from 0.03%-0.3% produced an improvement in impact behaviour by a 15 to 20 °C lowering of the ITT. It is believed that silicon reduces grain boundary segregation of C when present in sufficient amounts as is shown by the low Ky value found in silicon containing steels.

Mintz et.al.[81] using the field ion atom-probe have shown that Si segregates to the boundaries and because it increases the activity of N and C, would be expected to repel them from the boundaries. They also have shown that, the total interstitial segregation at the boundaries decreased from 2 to 1 atomic% on adding silicon.

The addition of silicon can also accelerate the formation of polygonal ferrite by shifting the pearlite transformation to higher temperatures during continuous

cooling from the single austenite phase region[18,20,76].

The ferrite promoting tendency has been reported to be greater at higher silicon levels[75].

Silicon in amounts around 2% promote a fine fibrous distribution of martensite in a continuous ferrite matrix [83].

Since silicon promotes a continuous ferrite matrix the connectivity of martensite particles can be avoided throughout the aggregate[84]. This may prevent continuous crack propagation in the early stages of plastic deformation and allows the ferrite to contribute its full ductility to the system. Additionally, silicon can provide the following benefits :

1- Increases the activity of C and hence promotes a more ductile ferrite[83,85,86].

2- Inhibits the formation of carbides, particulary Fe_3C at the ferrite/martensite interface[76], hence improving the ferrite/martensite interface (i.e. the martensite/ferrite interface is coherent while the carbide/ferrite interface is incoherent).

3- Refines the microstructure[18,76].

4- Increases the slope of Ae_3 line (hence allowing more flexibility in the intercritical heat treatment) by allowing a wider austenite/ferrite temperature range[76].

5- Increases the hardenability of austenite ensuring martensite formation[20,21,66].

2.5.4- MOLYBDENUM.

Molybdenum has been shown to have a very marked effect in suppressing the pearlite reaction-being more effective than either silicon or chromium[17,20]. The pearlite start curve on the CCT diagram can be shifted from 10 to 1000 seconds as molybdenum is raised from 0 to 0.5% in an 0.049%C-0.92%Mn-1.2%Si-0.5%Cr steel. The retarding effect of increasing the Mo level on polygonal ferrite formation can be seen from figure 2.8 to be less pronounced.

Consequently, a wide range of continuous cooling rates can be tolerated where ferrite formation will occur without any formation of pearlite during continuous cooling from the single austenite phase region.

Molybdenum is a strong carbide forming element[87], (i.e, Mo_2C). After annealing in the lower portion of the (austenite+ferrite) region the ferrite will be supersaturated with C in relation to its solubility at room temperature (carbon content in the ferrite is about 100-200 times greater than normal at room temperature). Hence, 0.38% Mo has been added to tie up this excess carbon in the ferrite in the form of alloy carbides. The addition of molybdenum can also:

1- Stabilize the remaining austenite during continuous cooling and suppress the start of the bainite transformation, thus ensuring that only the martensite transformation will occur[14,20,38,76].

2- Increase the slope of Ae_3 line[76].

3- Cause solid solution hardening[14].

2.5.5- CHROMIUM.

The addition of chromium is generally considered to:

1- Retard the bainite-start and bainite finish reaction[14].

2- Suppress the pearlite reaction (hence promoting the formation of polygonal ferrite during a continuous cooling from the austenite region)[17,20].

3- Promote the partitioning of carbon between austenite and ferrite hence deceasing the yield strength of the dual-phase steels)[14].

4- Stabilize the remaining austenite phase (thus, retarding the bainite formation)[14,20,76].

5- Increase the connectivity of martensite[76], an obvious disadvantage.

2.6- ROLE OF MICROALLOYING ELEMENTS.

Since Rashid[24] used a V-N strengthened HSLA steel to produce a dual-phase steel, the V and/ or Nb microalloying HSLA steels have been used by many investigators to study their structure-property relationships.

Hayami et.al.[15] have questioned Rashid's initial work[24] figure 2.22 which showed an improvement in ductility without a change in ultimate tensile strength. They believe that, this results come from the combined effect of an increase in the ductility of ferrite, a decrease in the strength of ferrite, and strengthening by martensite after intercritical annealing. They pointed out that the presence of V (CN) in the as-rolled HSLA steels may lead to a high yield and tensile strength with rather poor elongation; whereas, during intercritical annealing these carbonitride particles dissolve and after cooling may remain mostly in solution in ferrite resulting in a "cleaner" and softer ferrite matrix, and this is responsible for the enhanced ductility of the heat treated steel.

They postulated that the tensile strength remained the same because of counterbalancing effect between the strength increase produced by introducing martensite and the decrease in strength due to the loss of precipitation hardening.

To support this hypothesis, Hayami et.al.[15] demonstrated the effect of intercritical annealing on Si-Mn steels, figure 2.23. In Si-bearing steels, the ferrite matrix is

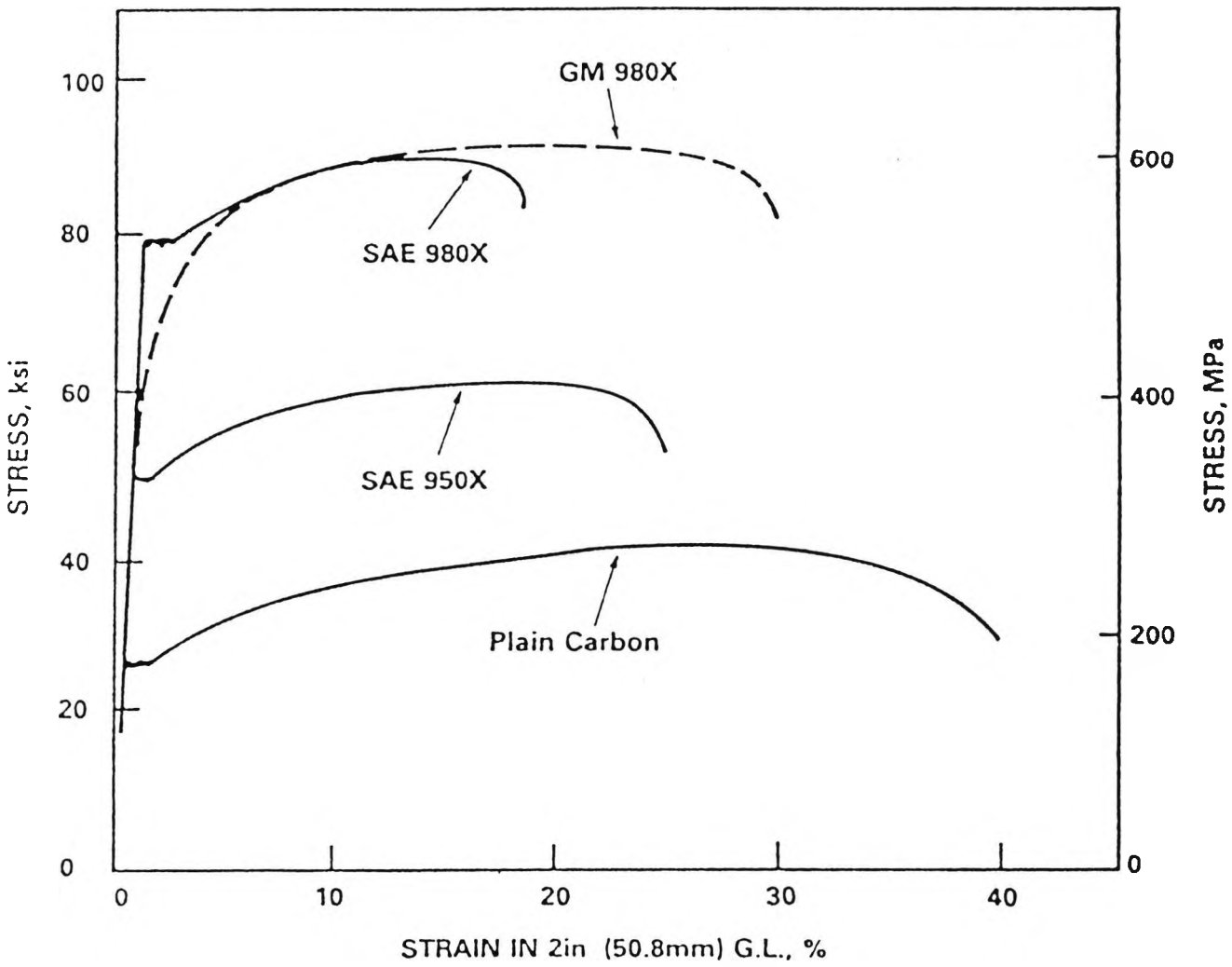

Figure 2.22- Normal Stress-Strain Curves for GM-980X, SAE-980X, 980X, and Plain Carbon Steels.[1]

relatively "clean" (i.e. precipitate free) in the as-rolled condition.

In figure 2.23 taken from Hayami et.al.[15] work, it can be seen that ductility improves only slightly whereas the UTS increases on intercritical annealing. Strength now increases because there is no V(CN) present to redissolve and hence the full potential of martensite strengthening can be obtained. Similarly, only a small improvement in ductility occurs because there are no precipitates which redissolve.

As expected, increasing the silicon level (steel B) reduces the C content producing a "cleaner" ferrite and encouraging a more stable austenite resulting in a dual-phase steel of somewhat higher elongation and ultimate tensile strength than given by (steel A).

In Rashid,s work[24], a high density of precipitates were observed in the ferrite in a SAE 980X steel in the as-received condition. After intercritical heat-treatment the volume fraction of precipitates decreased substantially and some of the precipitates were associated with strain contours when examined under the transmission electron microscope.

The latter effect suggests that these precipitates may either be coherent or semi-coherent with the ferrite matrix. The composition of the precipitates was not reported and, presumably, they were most likely to be vanadium carbides (or carbonitrides) or possibly aluminium

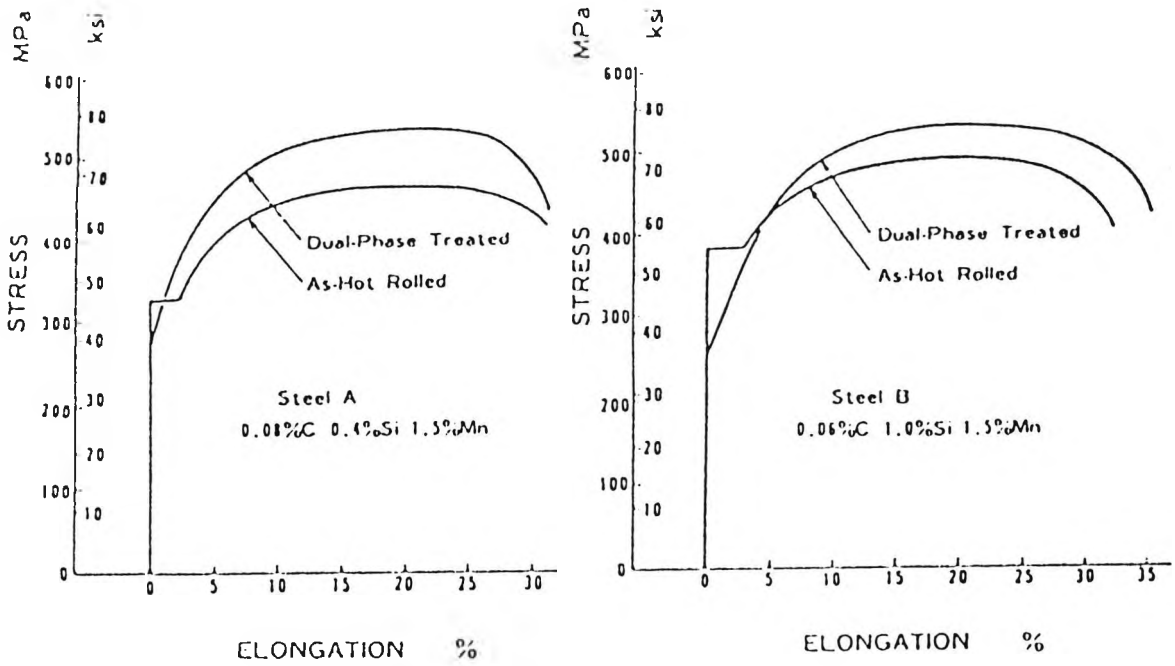

Figure 2.23- Effect of Intercritical Annealing on Tensile Properties of Hot-Rolled Steels.[15]

nitrides. Precipitates in the ferrite matrix for intercritically heat-treated V-bearing dual-phase steels have also been observed by other investigators[67,88].

In these two references studies[67,88], the specimens were intercritically annealed at 800°C for 10 minutes, then ice -brine quenched at a cooling rate of 1000°C/sec.

The precipitates were found both in the interior of ferrite grains and near the ferrite/martensite interface. The latter type of precipitate occurred in a narrow, localised zone, about 1-5 μm wide extending from the ferrite/ martensite interface into the ferrite region. This type of precipitate was not observed in a V-free steel under the same heat treatment conditions. According to these investigators the interface precipitates can possibly be cementite or vanadium carbides.

In contrast to Rashid,s[13,24] results, they[67,88] found the addition of vanadium did not improve the tensile strength. A lower strength and ductility were observed than for the vanadium-free dual phase steel which had been similarly heat-treated.

2.6.1- Hardenability of Austenite in the Intercritical Annealing Temperature Range.

So far, the cooling rate has been reported by many investigators to be one of the most important factors for achieving optimum properties and many studies have concentrated on the effect of cooling rate on the

structure-property relationships of dual-phase steels. Howerever, the hardenability of the austenite is important also and this depends on composition. The partitioning of alloying elements between ferrite and austenite during an intercritical annealing process usually is dependent on the diffusion of elements and the temperature used. The fact that equilibrium conditions, will not be reached for a short time intercritical anneal, means that the microstructure of a dual-phase steel subjected to continuous cooling from the two-phase region will be different from that of a fully austenitised material. During intercritical annealing, the presence of microalloying elements (Nb, V, Ti, and Mo) may either enhance the hardenability of austenite (dissolved in solution) or lessen the hardenability (in the form of undissolved particles). Since these elements are strong carbide formers if the temperature is not sufficiently high during the intercritical annealing, their reaction with carbon may also weaken the effectiveness of these elements on hardenability. The mutual interaction between microalloying elements and their effects on the hardenability of austenite has been reported by Eldis and Hagel[89]. In their study, a base composition of 0.1%C-1.47% Mn-0.11% Si-0.008% N and two temperatures 925°C and 1200°C (fully austenitic) were selected to study the effect of Mo, Nb, V and Ti additions on hardenability. They found that the addition of 0.3% Mo or 0.086% V is beneficial (i.e.

increases the hardenability) at both temperatures; 0.038% Nb gave rise to a improved hardenability at 1200°C and reduced hardenability at 925°C, 0.088% Ti decreases the hardenability at both temperatures. In addition to these observations on the effect of a single element,on hardenability two-way interactions and three-way interactions between these elements were also found. For example, at 1200°C, the addition of Ti and V was found to have a mutually beneficial effect when combined, i.e, each element increases the effectiveneness of the other. On the other hand, the combination of Ti and Nb results in a decrease of hardenability at this temperature. They also found that the addition of molybdenum was beneficial in most of the two-way and three-way interactions with Nb, V, and Ti. For example Mo + Nb + V at 1200°C and Mo + Nb at 925°C gives rise to a positive effect on hardenability.

One of the interesting results observed by Eldis and Hagel [89] is that a combination of Ti and Nb decreased the hardenability at 1200°C but gave a reversed result at 925°C. According to them these opposing effects at these two austenitising temperatures can possibly be due to a competition in their reaction with carbon. At 1200°C all of the 0.038% Nb is in solution and the addition of Ti leads to the removal of carbon from the solution (presumably forming titanium carbides) resulting in a decrease in hardenability. At 925°C which is lower than the dissolution temperature of niobium carbonitride, a large fraction of

Nb is in the form of undissolved particles. The addition of 0.088% Ti results in competition for carbon, and because Ti is the stronger carbide former, a resolution of part of Nb occurs and, hence, the hardenability is increased.

2.6.2- NIOBIUM.

In hot-rolled steels, Nb prevents recrystallisation of austenite so that pan-cake shaped grains result and fine grained ferrite is formed, leading to increased strength. Precipitation of Nb(CN) also prevents grain growth of austenite during normalising. The effectiveness of Nb as a grain refiner and precipitate strengthener depends upon the reheating temperature. At high temperature all the Nb will go into solution and on cooling, very fine precipitates form in the ferrite on phase transformation. The presence of niobium in dual-phase steels has been reported to refine the grain size and cause the precipitation of carbides or carbonitrides in the ferrite matrix[65,67,76,88,90]. Nb when dissolved in the solution can improve the hardenability of the austenite phase, however, a degradation of dual-phase properties may result if during the heating cycle the carbides or carbonitrides are not dissolved completely. However Nb has not been considered to improve the hardenability of austenite during the actual intercritical annealing treatment because any carbides present do not redissolve with time at temperature [65,91]. The difference in hardenability of the austenite phase at

different intercritical annealing temperatures in Nb microalloyed steels has been thought to be mainly attributable to the amount of Nb in solution in the austenite which does vary with the heat-treatment temperature.

2.6.3- VANADIUM.

The primary function of vanadium in HSLA steels is precipitation strengthening. The temperature at which V forms carbon rich precipitates is generally below 700°C, i.e during transformation, and particles are usually less than 30°Å in diameter. V is good for precipitation strengthening in as rolled steels and normalised steels and its effect can be enhanced by increasing the N content.

The presence of vanadium in dual-phase steels has been reported to refine the grain size and cause the precipitation of carbides or carbonitrides in the ferrite matrix[65,67,76,88,90].

It has been shown[88] that at higher intercritical annealing temperatures vanadium improves the hardenability of austenite significantly. Any vanadium precipitated in the austenite reduces the amount of vanadium available for precipitation in the ferrite on cooling and hence reduces the strength. At the lower intercritical annealing temperature less V is in solution in the ferrite and hence hardenability is reduced.

2.6.4- TITANIUM.

Titanium forms a nitride at very high temperatures and can therefore be used to reduce the grain growth of austenite during hot rolling of plates.

Titanium has been shown to increase the grain boundary carbide thickness and this would be expected to impair impact behaviour[92]. Titanium is also known to be an effective nitrogen scavenger removing nitrogen from solution in ferrite.

2.6.5- ALUMINIUM.

Aluminium as well as acting as a deoxidiser also combines with N to form AlN which can pin the grain boundaries, and result in a grain refinement of the ferrite. It's addition provides the following benefits:

1- Aluminium broadens the (austenite+ferrite) field when added to the Fe-C system. This facilitates practical control of the volume fraction and composition of the martensite produced.

2- Aluminium promotes a fine distribution of martensite in the ferrite matrix[93].

3- Aluminum improves the ferrite/martensite interface by inhibiting the formation of coarse carbides there during the final quench[83].

4- Aluminium increases the activity of carbon in ferrite[76,83] and should improve the ductility of ferrite.

2.7- SELECTION PRINCIPLES

The morphology of the phases in the duplex ferrite-martensite steels is critical to the mechanical properties produced by these steels. Consideration of parameters such as, size, shape and distribution of martensite particles as well ferrite have led to guidelines for developing desirable dual-phase structures[83].

2.7.1- OPTIMUM VOLUME FRACTION.

The volume fraction of the martensite particles is a primary factor in the mechanical properties of dual-phase steels. The amount of martensite present must exceed a lower limit (10% to 25%)[31] in order to achieve a substantial contribution to strengthening. At the same time, too much martensite in the composite would make the material brittle. If the volume fraction of martensite is in the optimum range the ferrite matrix can locally work harden upon failure of an adjacent martensite particle, and so transfer the load without failing in a brittle manner during the tensile test.

2.7.2- SIZE AND SHAPE OF MARTENSITE PARTICLES.

It has been shown that the morphology (size, shape, and distribution) of the constituents has a great effect on the tensile fracture behaviour and the ductility of dual phase steels[76,94].

2.7.3- MARTENSITE DISTRIBUTION.

A discontinuous, and randomly oriented martensite particle distribution in a continuous ferrite matrix gives the best mechanical properties for dual-phase steels.

2.7.4- MARTENSITE CARBON CONTENT.

Maintaining the carbon level below about 0.3% in austenite will result in dislocated lath martensite. Carbon levels above 0.3% in austenite will result in twinned plate martensite. Since higher carbon contents can drastically reduce the toughness of martensite[77], the average carbon content of the initial alloy must be kept sufficiently low to maintain carbon levels at or below about 0.3% in the austenite.

2.7.5- PRECIPITATION REACTION.

The nature of the interface at ferrite/martensite boundary is very important. The ferrite/martensite interface is coherent.However, if carbide particles (i.e. incoherent precipitates) should precipitate along this interface, then the steel will become more brittle). Therefore, the precipitation of a brittle incoherent phase at the ferrite/martensite interface is to be avoided.

2.7.6- GRAIN REFINEMENT.

In any alloy, grain refinement may serve as a strengthening mechanism and improve toughness. Thermal

cycling through the transformation when applied to intercritical annealing may also produce refinement in grain size[95].

2.8- STRUCTURE PROPERTY-RELATIONSHIP OF DUAL-PHASE STEELS.

In two-phase mixtures, the strengthening effects produced by introducing the second phase are generally dependent on several factors:

1- The amount, size, shape and distribution of the second phase.

2- The strength, ductility and strain-hardening properties of both the matrix and the second phase.

3- The crystallographic fit (coherency) between the constituent phases.

The martensite-ferrite dual-phase steels are usually treated as a composite material with strong, natural fibres of the martensite phase embedded in the soft ferrite matrix. For the analysis of mechanical behaviour of dual-phase steels, models based on the analysis of the behaviour of composite materials are commonly used.

However, there is no agreement among the different investigators as to the most useful model. In this section, the results from different workers of dual-phase steels will be discussed, in the following order, strength, ductility, and yield phenomenon and work-hardening behaviour.

2.8.1- STRENGTH.

The law of mixtures is generally applied as a model to analyse the strength of dual-phase steels as a function of the volume fraction of martensite. That is,

$$Sc = S_f V_f + S_m V_m \quad \text{..... 2.5}$$

where

S_c = tensile strength of composite.

S_f = tensile strength of ferrite.

S_m = tensile strength of martensite.

V_f = volume fraction of ferrite.

V_m = volume fraction of martensite.

According to this model, the strength of dual-phase is dependent on the strength of martensite and ferrite as well as on the amount of martensite. Since the strength of martensite is strongly dependent on the carbon content[39,96,97] and martensite is a much stronger phase than the ferrite, the strength of dual-phase steels is, therefore, sensitive to the carbon content of martensite. Because the interface between martensite and ferrite is coherent [76,98,99], one would expect substantial strengthening from the hard martensite phase. It is to be expected that the strength of dual-phase steels should increase with increase in the amount of martensite, the strength (carbon content) of martensite, and the strength of ferrite. This observation has been reported by a number of investigators[76,100,101,102].

Speich and Miller[22] studied the tensile properties of martensite-ferrite mixtures in a series of C-1.5%Mn steels quenched from several intercritical annealing temperatures. These authors found that the yield and the tensile strength of dual-phase steels are increased when either the volume

fraction or the strength (carbon content) of martensite is increased as shown in figure 2.24. For example, for a given volume fraction of martensite, the higher annealing temperature results in lower carbon content (and thus a lower strength) of martensite and thus the strength of dual-phase steels is decreased. For a given annealing temperature, as can be seen from figure 2.24, the strength of steel increases with the volume fraction of martensite, albeit nonlinearly. According to these authors, the nonlinear variation of strength with percent martensite can possibly be attributed to the variation in carbon content of martensite resulting from manganese segregation.

Tamura et.al.[102] have found empirically that, the law of mixtures can only be applied for the yield strength of a two-phase mixture when the yield strength of the hard phase is close to that of the softer phase, the ratio of the two being denoted as the parameter (c). When (c) is less than 3 the law of mixtures is nearly obeyed. When c is greater than 3, the yield strength of mixture starts to deviate strongly from the relationship.

Speich and Miller [22] following the analysis of Tamura et.al.[102] assumed that, the strain in the martensite phase is proportional to that of ferrite phase and that the law of mixtures applies for strain i.e

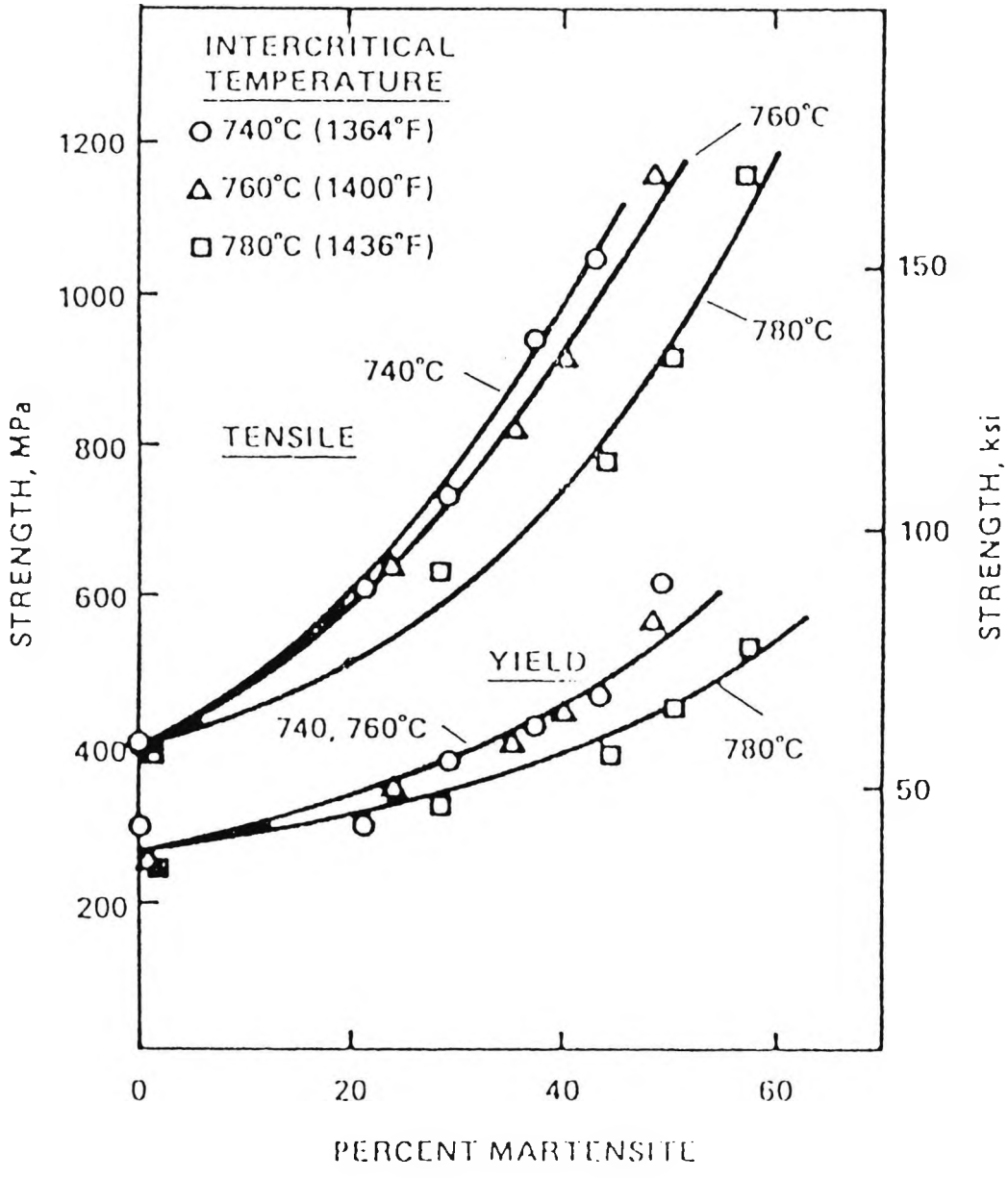

Figure 2.24- The 0.2% Flow Stress and the Tensile Strength as a Function of Percent Martensite for a Fe-Mn C Steels.[22]

$$e_c = e_f v_f + e_m v_m \quad \text{..... 2.6}$$

$$e_m / e_f = K$$

where

e_c = engineering strain of composite.

e_f = engineering strain of ferrite.

e_m = engineering strain of martensite.

These investigators found that K had a value that varied between 0.003 and 0.01 for austenite/martensite mixtures. From the above two equations, knowing a value for K (often taken as 0.01), it is possible to calculate the valus of e_f and e_m. They found that for a given K value the calculated values of e_f and e_m remain nearly constant with increase in martensite volume fraction; even through the uniform strain of the steel decreases with increasing percentage of martensite. The value for e_f corresponded to that obtained for a steel containing 100% ferrite and e_m corresponded to the yield strain of a steel containing 100% martensite. Therefore, they proposed a "Modified Law of mixtures" for the tensile strength of dual-phase steels

$$S_{t,c} = S_{t,f}V_f + S_{y,m}V_m \quad \text{..... 2.7}$$

where

$S_{t,c}$ = Tensile strength of the steel (composite).

$S_{t,f}$ = Tensile strength of the 100% ferrite.

$S_{y,m}$ = Yield strength of 100% martensite.

From the work of Leslie and Sober[103], the yield strength

of 100% martensite $S_{y,m}$ can be related to the carbon content of martensite, C_m, (in weight percent) using a linear equation.

$$S_{y,m} = 620 + 2585 \ C_m \quad \ldots\ldots\ldots\ldots\ldots\ldots\ldots\ldots 2.8$$

Using this expression, Speich and Miller[101] obtained an equation to correlate the tensile strength of dual phase steel to the carbon content of martensite and the volume fraction of martensite.

$$S_{t,c}=S_{t,f}+[(620 - S_{t,f})+2585 \ C_m]V_m \quad \ldots\ldots\ldots\ldots 2.9$$

For yield strength, these authors derived a similar linear regression expression from the experimental data.

$$S_{y,c} = S_{y,f}+[(325-S_{y,f})+1322C_m]V_m \quad \ldots\ldots\ldots\ldots\ldots\ldots\ldots 2.10$$

where

$S_{y,c}$ = yield strength of dual - phase.

$S_{y,f}$ = yield strength of 100% ferrite.

V_m = volume fraction of martensite.

C_m = weight percent carbon.

From these expressions, it can be clearly seen that, the strength of dual-phase steels will increase when either the carbon content or volume fraction of martensite is increased. Similar observations on the "carbon dependence" C_m on the strength of steel have also been reported by other workers[76,100,102].

In contrast to the results mentioned before, a number of workers have reported that the carbon content of martensite has no effect on the strength of dual-phase steels[57,58,104,105].

These papers illustrated that the tensile and yield strength of the martensite-ferrite mixture was linearly related only to the volume fraction of martensite. For example Davies[58] studied a series of Fe-Mn-C steels intercritically annealed at several temperatures for 10 minutes and then brine quenched. The tensile test results are presented in figure 2.25, and show that, both the tensile and yield strength of the dual-phase steels depend linearly on the volume fraction of martensite. Therefore, a least-squares technique was used to correlate the strength of steel to the volume fraction of martensite.

For the tensile strength, the expression obtained was[58]

$$S_{t,c} = 365 + 1630\ V_m \qquad \text{.....2.11.}$$

and for the yield strength

$$S_{y,c} = 103 + 1110\ V_m \qquad \text{.....2.12.}$$

From the law of mixtures

$$\begin{aligned} S_c &= S_f V_f + S_m V_m \\ &= S_f\ (1 - V_m) + S_m\ V_m \\ &= S_f + (S_m - S_f)\ V_m \end{aligned}$$

When the strength of the composite is a linear function of V_m, the term $(S_m - S_f)$ will be constant. The strength of ferrite, S_f, was assumed to be a constant. Therefore, Davies[58] concluded that the strength of dual-phase steels is only a linear function of V_m and is independent of the strength (carbon content) of martensite. His study indicated that the carbon content of martensite would increase with decreasing intercritical annealing

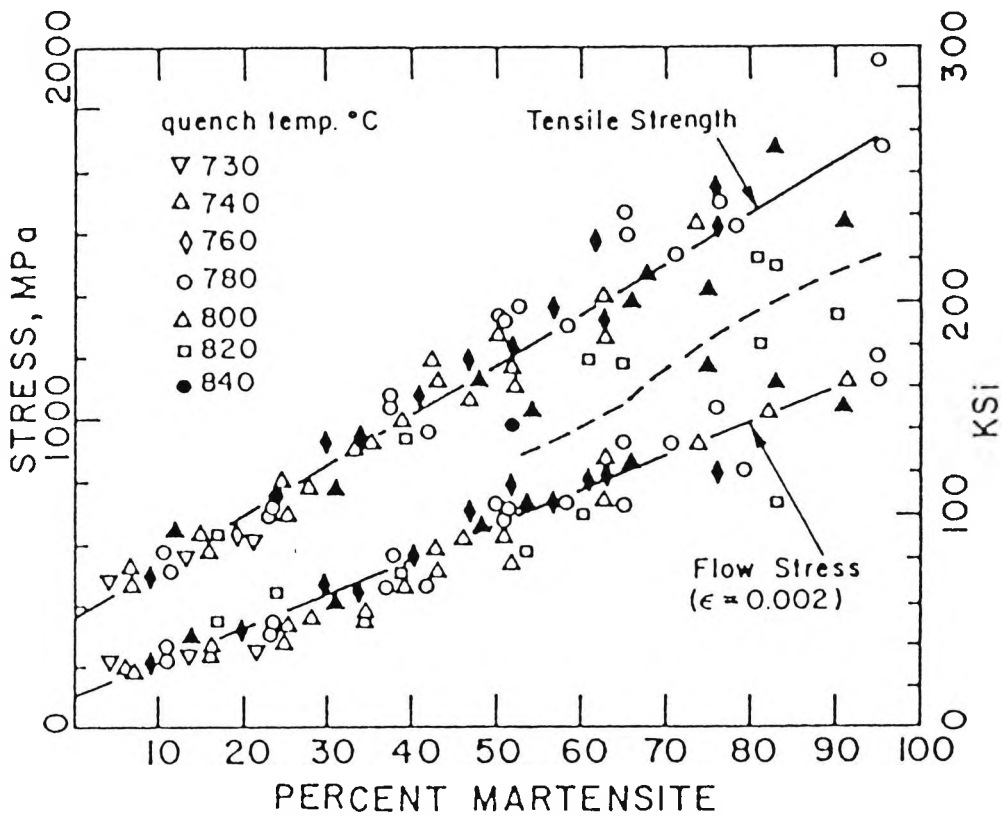

Figure 2.25- Yield (0.2%) and Tensile Strength of Ferrite-Martensite Steels.[56]

temperature. However, no effect of carbon content on the strength of martensite could be found. Some other workers[104,105] have also reported a similar linear relationship between the strength of steel and the amount of martensite with various correlation coefficients. The reasons why the strength of dual-phase steels is apparently independent of the carbon content of martensite is not clearly understood.

In a later review paper, Speich[47] pointed out that there is a very large scatter in the data of those workers who found a linear relationship between strength of steel and the volume faction of martensite. Therefore, it is possible that the effects of carbon content of martensite were masked in their work.

2.8.2- DUCTILITY.

The correlation of microstructure to the ductility is more difficult than that for strength. In general the ductility of dual-phase steels is governed by the ferrite phase, but may also be influenced by the properties of the martensite, the distribution of martensite islands in the ferrite matrix and the presence of retained austenite[47]. The correlation between microstructure and ductility will be discussed as follows:-

Speich and Miller[101] assumed that the strain in the martensite is proportional to that in the ferrite as follow:

$$e_m / e_f = K$$

, and from the law of mixtures the strain :

$$e_c = e_f V_f + e_m V_m \quad \ldots\ldots\ldots\ldots\ldots\ldots\ldots\ldots\ldots\ldots 2.6.$$

Combining these two equation the uniform elongation of the steel can be expressed as.

$$e_{u,c} = e_{u,f} V_f + e_{u,m} V_m$$

$$= e_{u,f}(1-V_m) + K\ e_{u,f} V_m$$

$$= e_{u,f}[1-(1-K)\ V_m] \quad \ldots\ldots\ldots\ldots\ldots\ldots\ldots\ldots 2.13.$$

where

$e_{u,f}$ = ferrite uniform elongation in percent engineering strain.

$e_{u,c}$ = composite uniform elongation in percent engineering strain.

$e_{u,m}$ = martensite uniform elongation in percent engineering strain

From this expression, the ratio of the uniform strain of steel to that of ferrite is obtained, i.e ,

$$e_{u,c} / e_{u,f} = 1 - (1-K)\ V_m$$

These authors found that the uniform elongation of ferrite, $e_{u,f}$ was a constant equal to 21.4% and that the uniform strain of steel was decreased slightly when the carbon content of martensite was increased. Therefore, a linear regression technique was used to find the relationship between ($e_{u,c}$ / $e_{u,f}$) , C_m and V_m. The empirical equation thus obtained was,

$$e_{u,c} / e_{u,f} = 1 - 2.2\ C_m\ V_m^{1/2} \quad \ldots\ldots\ldots\ldots\ldots\ldots\ldots\ldots 2.14.$$

where

C_m is the carbon percent in martensite.

For total elongation, a similar technique was used by these authors to find the correlations between ductility C_m and V_m. The empirical equation thus obtained was,

$e_{t,c} / e_{t,f} = 1 - 2.5\ C_m\ V_m^{1/2}$ 2.15

According to these two equations, the uniform and the total elongation of the steel is a linear function of $C_m\ V^{1/2}$ if $e_{u,f}$ and $e_{t,f}$ are constant. This can be seen from figure 2.26[101] where the experimental results are in good agreement with values predicted using a $C_m\ V_m^{1/2}$ relationship. From these two expressions it can be seen that the ductility of dual-phase steels is decreased when either the carbon content or the volume fraction of martensite is increased.

Davies[57,58] applied Mileiko,s theory to analyse experimental tensile date from a series of vanadium dual-phase steels and Fe-Mn C alloys. He found the theory and experimental results to be in good agreement as shown in figure 2.27.

From the results of different investigators, ductility has been shown to be dependent on the mechanical properties of the martensite and ferrite the volume fraction of martensite and the grain size.In addition, it may also be dependent on the shape,sizes and distribution of martensite[47,106].

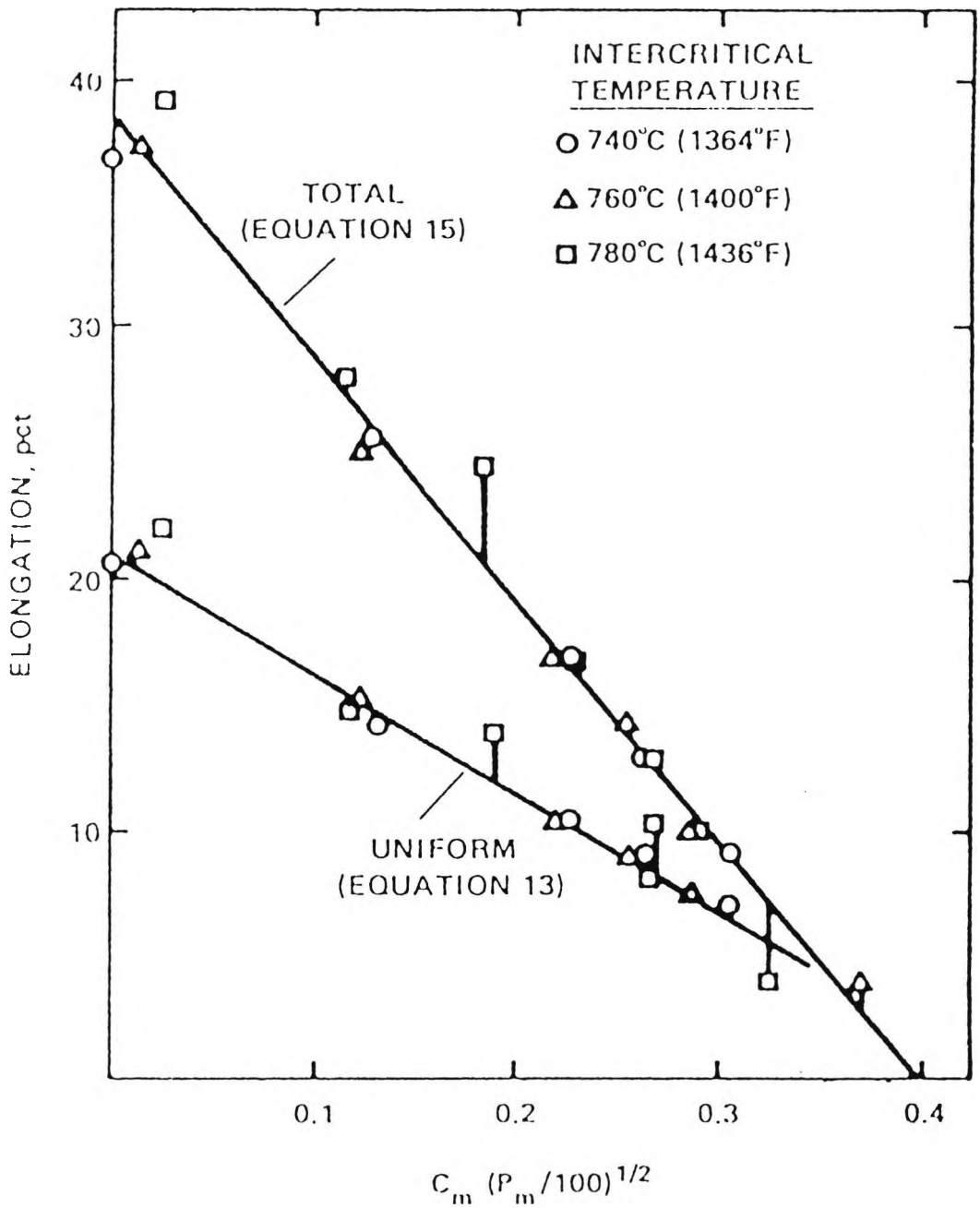

Figure 2.26- Uniform and Total Elongation of Ferrite-Martensite Steels.[22]

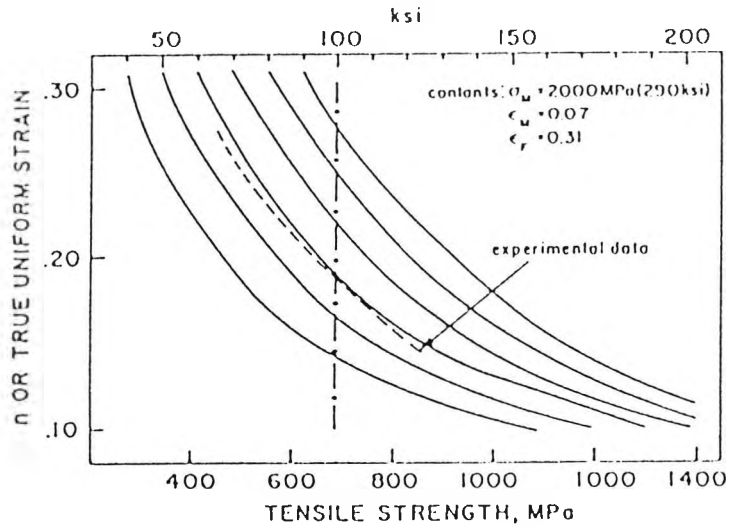

Figure 2.27a- Comparison of Observed n or True Uniform Strain with that of Mileko's Theory.[56]

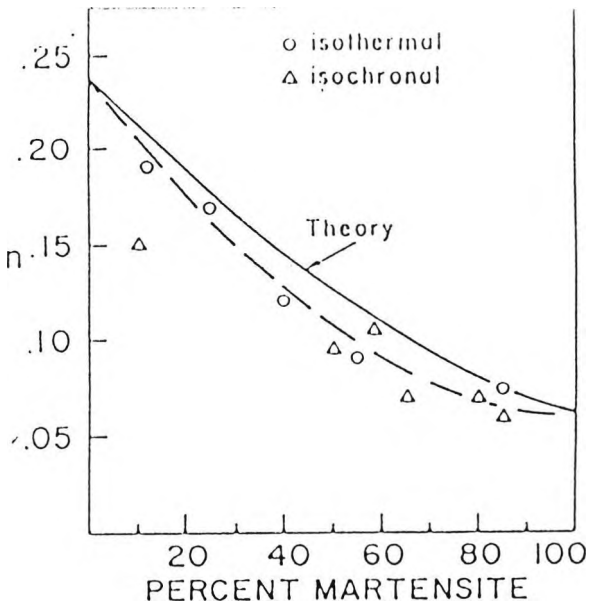

Figure 2.27b- Predicted n or True Uniform Strain as a Function of Tensile Strength for Various Ferrite Strengths.[56]

2.8.3- YIELD AND DEFORMATION BEHAVIOUR.

It has been reported by a number of investigators[9,13,14,70,101,104,107,108], that during tensile deformation steels having a martensite ferrite structure exhibit a continuous yielding behaviour (no yield point on tensile curve) at a low stress level. Some of the workers[13,70,108,109] have found that a minimum amount of martensite, from 3% to 15%, was required to produce the continuous yielding behaviour. Below this amount, discontinuous yielding occurs. In general, a material exhibits discontinuous yielding if:-

1- A low density of mobile dislocations are present prior to deformation.

2- A rapid dislocation multiplication occurs during deformation.

3- The dislocation velocity is significantly dependent on the applied stress.

The continuous yielding behaviour and low yield strength are usually attributed to a high density of mobile dislocations and the high residual stresses in the ferrite phase immediately adjacent to the martensite region. It will be noted that, these dislocation are generated due to the volume expansion which occurs during the austenite to martensite transformation [9,14,70,74,75,104]. Since the martensite transformation occurs at low temperature some investigators[9,70,104] believe that the dislocations generated will not be solute pinned and thus will be mobile. The

presence of mobile dislocations and residual stresses results in the low yield strength observed for dual-phase steels[70,101,104,110]. It has been observed that the yield point elongation (Luders strain) decreases with increasing amount of martensite.

When the martensite phase exceeds a critical amount, the steel yields continuously supporting the idea that the martensite particles are acting as slip initiation sites[9,70,104,109]. The martensite particles are, thus able to suppress discontinuous yielding[9,47,70].

Consequently, a uniform dispersion of martensite particles is thought to favour continuous yielding[70]. Because of the quenched-in mobile dislocations in the ferrite, during the plastic deformation, plastic flow may occur in the ferrite region prior to the gross yielding of martensite, thus leading to an inhomogeneous strain distribution[9,70,101]. Korlsson used a finite element method (F.E.M) to calculate the stain distribution in a martensite -ferrite mixture. Analytically, he found that the maximum strain areas are often located in the interior of ferrite region away from the martensite-ferrite interface. Their metallographic observation on polished specimens during tensile deformation verified this analysis. Korlsson pointed out that the (F.E.M) model predicts that at very early stages of deformation the strain distribution is very inhomogeneous, with the inhomogeneity being strongly dependent on the hardness of the phases.

The inhomogeneous strain between martensite and ferrite must result in an inhomogeneous stress distribution between these two phase. The effects of plastic incompatibility plus the pre-existing mobile dislocation and residual stress can be used to understand the high work hardening rate during the early stages of plastic deformation[9,70,101,111]. It has been suggested [9,70] that the high initial work hardening rate results when generated dislocations are immobilised by dislocation-dislocation interactions or by glide to a martensite-ferrite interface. Therefore, the stress required for continuation of the deformation in the steel increases rapidly to a level adequate for the nucleation and propagation of new, mobile dislocations.

Speich and Miller[101] proposed that the high work hardening rate at small plastic strain can possibly be attributed to three factors:

1- The residual stresses generated during the austenite to martensite transformation on quenching are relieved by small amounts of plastic deformation.

2- The dislocation density in the ferrite region is increased by the generation of dislocations.

3- The stresses created within the martensite region are compensated for by back stresses in the ferrite and these back stresses will restrict dislocation movement.

More fully, the work hardening of dual-phase steels can be separated into three stages[9,10,47,70,101].

In the first stage (from about 0.1 to 0.5 percent strain), the plastic deformation occurs in the ferrite region. The back stresses build up rapidly and the residual stresses are eliminated, therefore, the work hardening rate is high. The second stage (from 0.5 to 4 percent strain) is associated with the constrained deformation of ferrite caused by the presence of hard, undeformed martensite. The third stage (above 4 percent strain) begins with the formation of a dislocation cell structure. Further deformation is governed by dynamic recovery and cross-slip and yielding of the martensite.

2.8.4- IMPACT PROPERTIES.

Little research has been carried out specifically on the impact properties of dual-phase steels. Leslie et.al.[112] have noticed an improvement in impact behaviour of plate steel after a long time intercritical anneal.

The impact transition temperature (ITT) of an 0.1% C-Mn plain and 0.1% C-Mn-Al steels was decreased by 10°C-30°C by holding the steel at a constant temperature just above Ac_1 for a period of 24 hours. The reason for this improvement was not understood, although a U.S patent was taken out on the process in 1962[113]. Davies[28] has also shown that for a vanadium containing HSLA steel that both shelf energy and impact toughness improve on intercritical annealing both on heat treating into the ferrite+austenite field (IDP), or heating into the austenite and cooling through the two

phase region (ADP), as shown in figure 2.28. He reported, two possible explanations for this toughness improvement. This first one is based on the nature of the interface between the second phase and the matrix. The martensite will be coherent with the matrix[28,76], while the carbides will in general be incoherent with the ferrite lattice. During straining, dislocations will pile up at the carbide/ferrite interface leading to the nucleation of voids and fracture. On the other hand, dislocations, from the ferrite will be able to penetrate into the martensite (lath martensite with max.carbon 0.3%), albeit with difficulty giving a reduced strain concentration so that fracture will occur at higher strains.

The second explanation is based on the changes in matrix properties. The ferrite in dual phase structure has, as indicated by the flow stress data, a low strength and should be tough (resistance to crack propagation). In the conventional steel the ferrite is strengthened by carbonitride precipitates which in general degrade impact properties.

In general for ferrite/pearlite steels there are three main parameters affecting the impact transition temperature (ITT), ferrite grain size, pearlite volume fraction, and grain boundary carbides. For ferrite/pearlite steels, Mintz et.al.[114] proposed the following equation to predict ITT.

$$54J\ ITT°C = 161t_c^{1/2}-11.7d^{-1/2}+18\%P_e^{1/3}+0.47\ \Delta y+C \qquad 2.16.$$

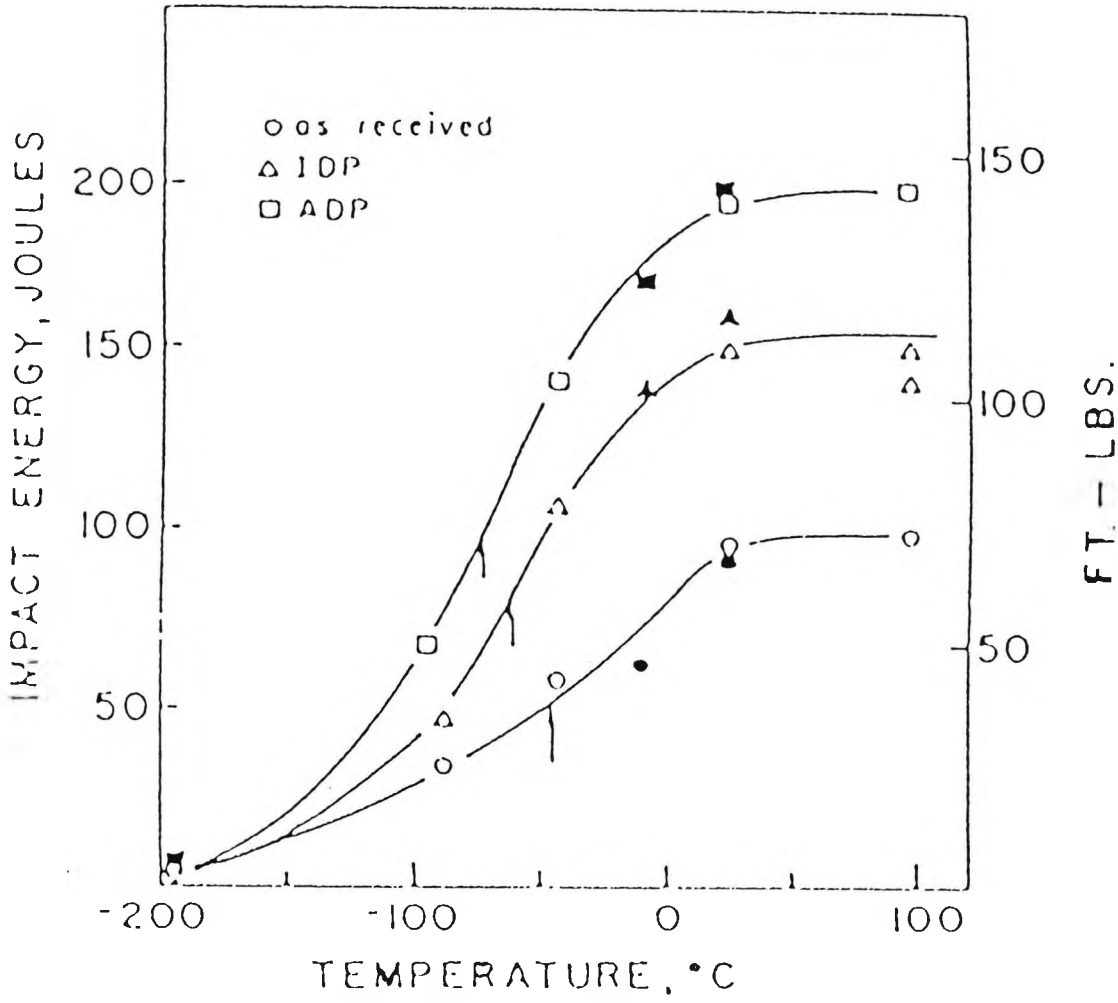

Figure 2.28- Charpy Impact Energy as a Function of Temperature for as-Received, IDP, and ADP ADP Condition of a V-Steels.[5]

Filled Symbols are for Samples Tempered 1 hr at 300°C.

where

Δy is the precipitation and solid solution hardening component obtained by subtraction of the actual LYS from that calculated using the regression equation.

$$LYS = 43.1\% Mn + 83\% Si + 15.4\ d^{-1/2} + 105 \quad \ldots\ldots\ldots\ldots\ldots \quad 2.17.$$

which was obtained for non-precipitation hardening steels.

t_c = grain boundary carbide thickness, µm

d = grain diameter, mm.

P_c = pearlite volume fraction.

In a recent study Mintz et.al.[115], examined C-Mn, C-Mn-Al, and C-Mn-Al-Nb plate steels intercritically annealed at 730°C. They found that, the impact transition temperature was decreased by about (20°C-30°C), without change in strength. They explained this improvement as follow; during intercritical annealing manganese segregates to grain boundaries, and hence refines the grain boundary carbides leading to lower impact transition temperatures.

CHAPTER THREE

EXPERIMENTAL PROCEDURE

3.1- MATERIAL PREPARATION.

The steels used in this investigation were supplied as 12-15 mm thick hot-rolled plates from British Steel with different chemical compositions as shown in table 3.1. The steels were vacuum melted.

For each steel, the plate was cut into small pieces (15x10 cm), and heat-treated.

3.2- HEAT TREATMENT.

The plates were heat-treated using two furnaces; a muffle furnace (Isoheat type 810) for austenitisation and an air circulating furnace (Isoheat type 815) for intercritical annealing. Each one of these two furnaces was fitted with a microprocessor based 3-term controller. In all heat treatments, to check cooling and heating rates a chromel-alumel[116,117] thermocouple connected to a potentiometer was placed at the center of each block, figure 3.1. All plate blocks had a hole drilled from one side to the center, so that a thermocouple could be inserted for temperature measurement. The furnaces were set at the required temperature and switched on. Before heat treatment, a

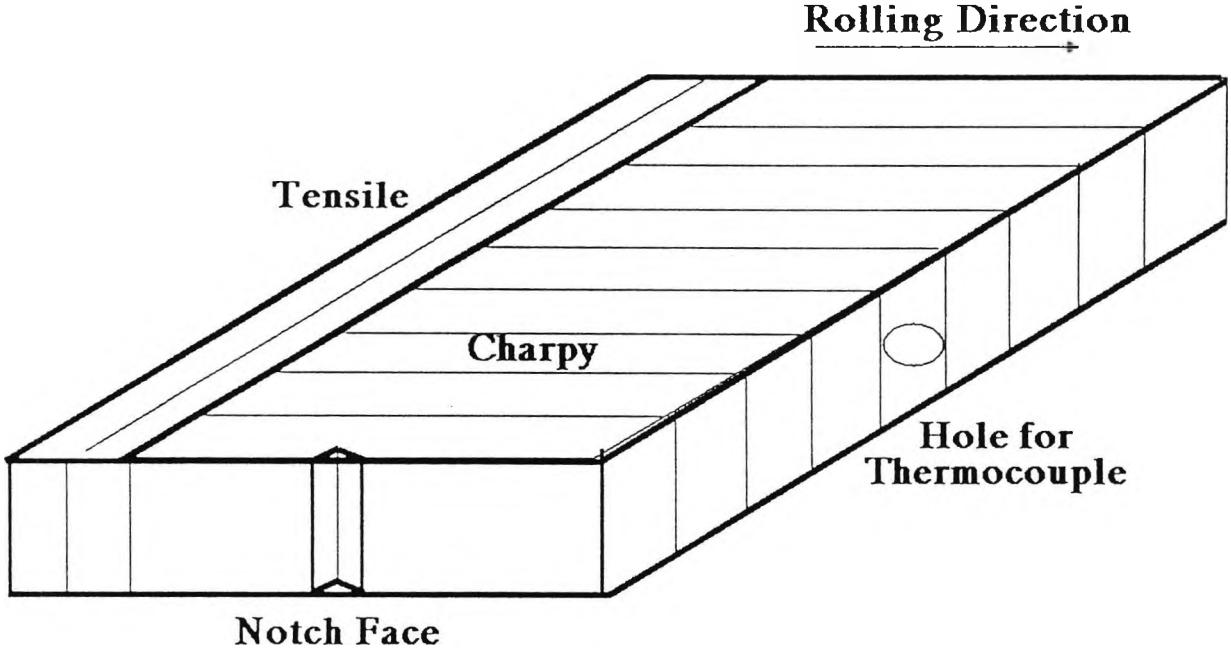

Fig.3.1- The Position of Charpy and Tensile Samples.

cooling curve for each furnace was obtained and the gradient between 800°C and 400°C, figure 3.2, and figure 3.3 was taken as the average cooling rate for the two furnaces. The plate with attached thermocouple was introduced into the austenitising furnace when the furnace temperature reached the temperature range 300-400°C. For the intercritical annealing furnace the plate was introduced at a temperature depending on the type of intercritical annealing condition. For example, during the "cooling down cycle" intercritical annealing treatment at 730°C, the plate was transfered from the muffle furnace when the plate temperature was about 740°C to the intercritical annealing furnace set at 730°C. The plate temperature fell to 730°C during transferrence, the transfer taking a few seconds. For the "heating up cycle" intercritical annealing treatment at 730°C, the intercritical annealing furnace temperature was about 300-400°C, when the plate was introduced to the furnace.

The various heat treatments given are shown schematically in figure 3.4, and are given in detail below.

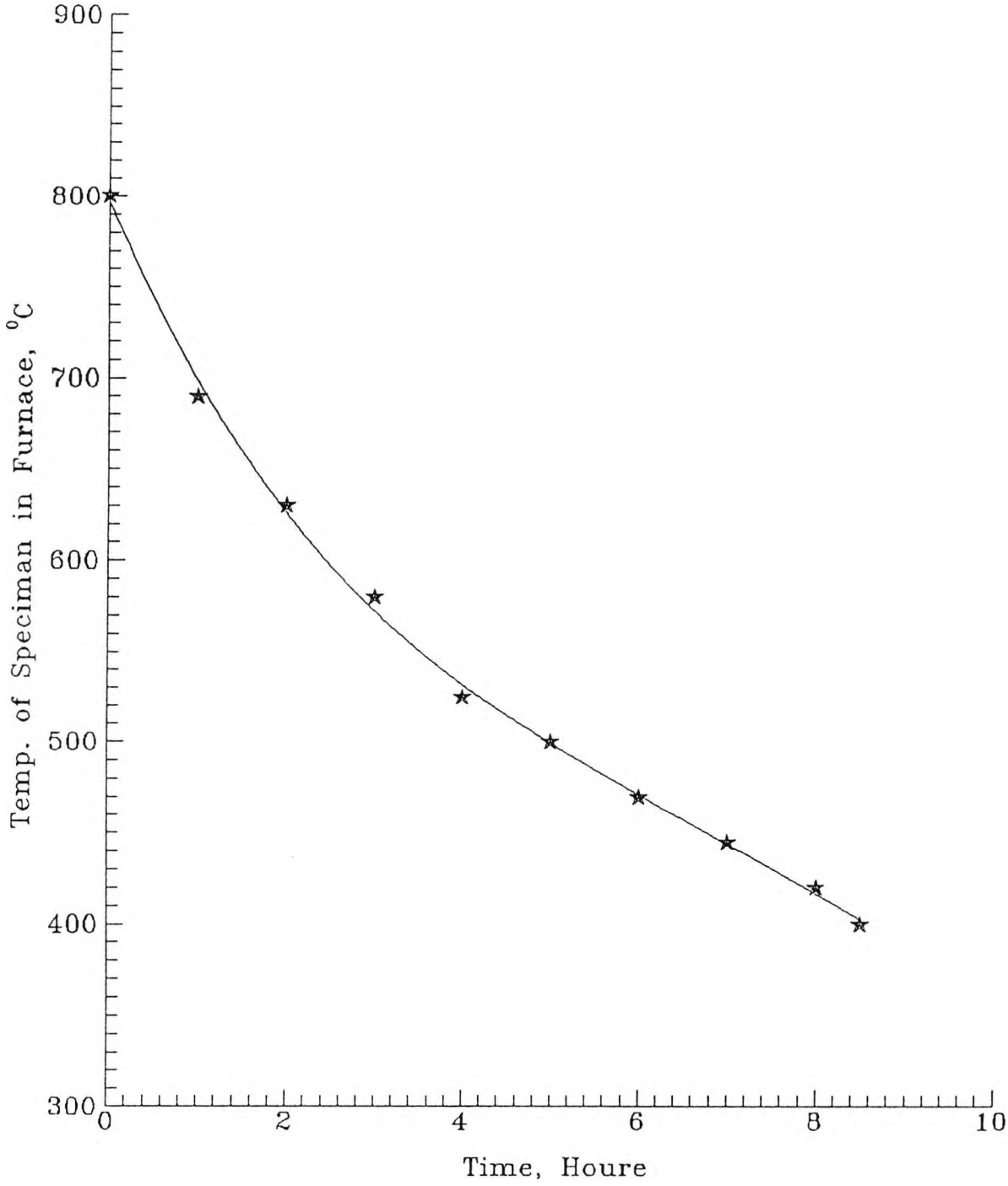

Fig.3.2- Cooling Curve for (Isoheat) Muffle Furnace.

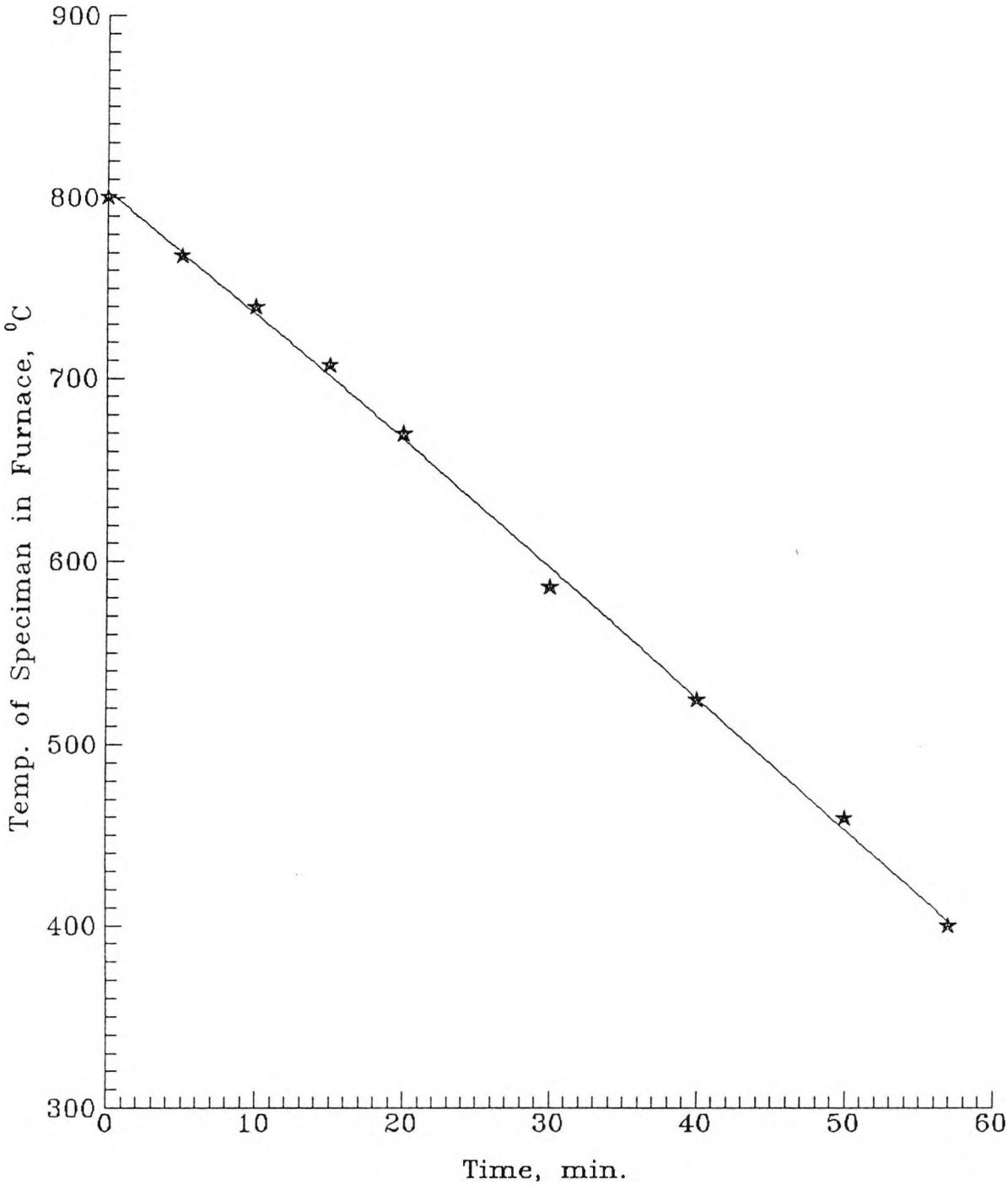

Fig.3.3- Cooling Curve for (Isoheat) Air Circulating Furnace Used for the Intercritical Annealing.

3.2.1- NORMALISING.

One plate from each group was austenitised at 920°C for 45 minutes, followed by cooling at (7°C/min or 0.8°C/min) to room temperature as shown in figure 3.4.a.

The cooling rate quoted is the average cooling rate in the temperature range from 800°C to 400°C.

3.2.2- HEATING UP TO THE INTERCRITICAL ANNEALING TEMPERATURE.

Plates were austenitised at 920°C for 45 minutes, followed by cooling at (7°C/min or 0.8°C/min) to room temperature. The plates were then reheated to 730°C and intercritically annealed at 730°C for different times (15, 30,60 and 900) minutes, and finally cooled at 7°C/min or 0.8°C/min, as shown in figure 3.4.b.

The cooling rate 7°C/min is equivalent to air cooling 70 mm thick plate, and the cooling rate 0.8°C/min is equivalent to air cooling 500 mm thick plate.

3.2.3- COOLING DOWN TO THE INTERCRITICAL ANNEALING TEMPERATURE.

The plates were austenitised at 920°C for 45 min, cooled at (7°C/min or 0.8°C/min) to 730°C, followed by intercritical annealing at 730°C for different times (15, 30, 60, and 900) minutes and finally cooled at (7°C/min or 0.8°C/min) to room temperature, as shown in figure 3.4.c.

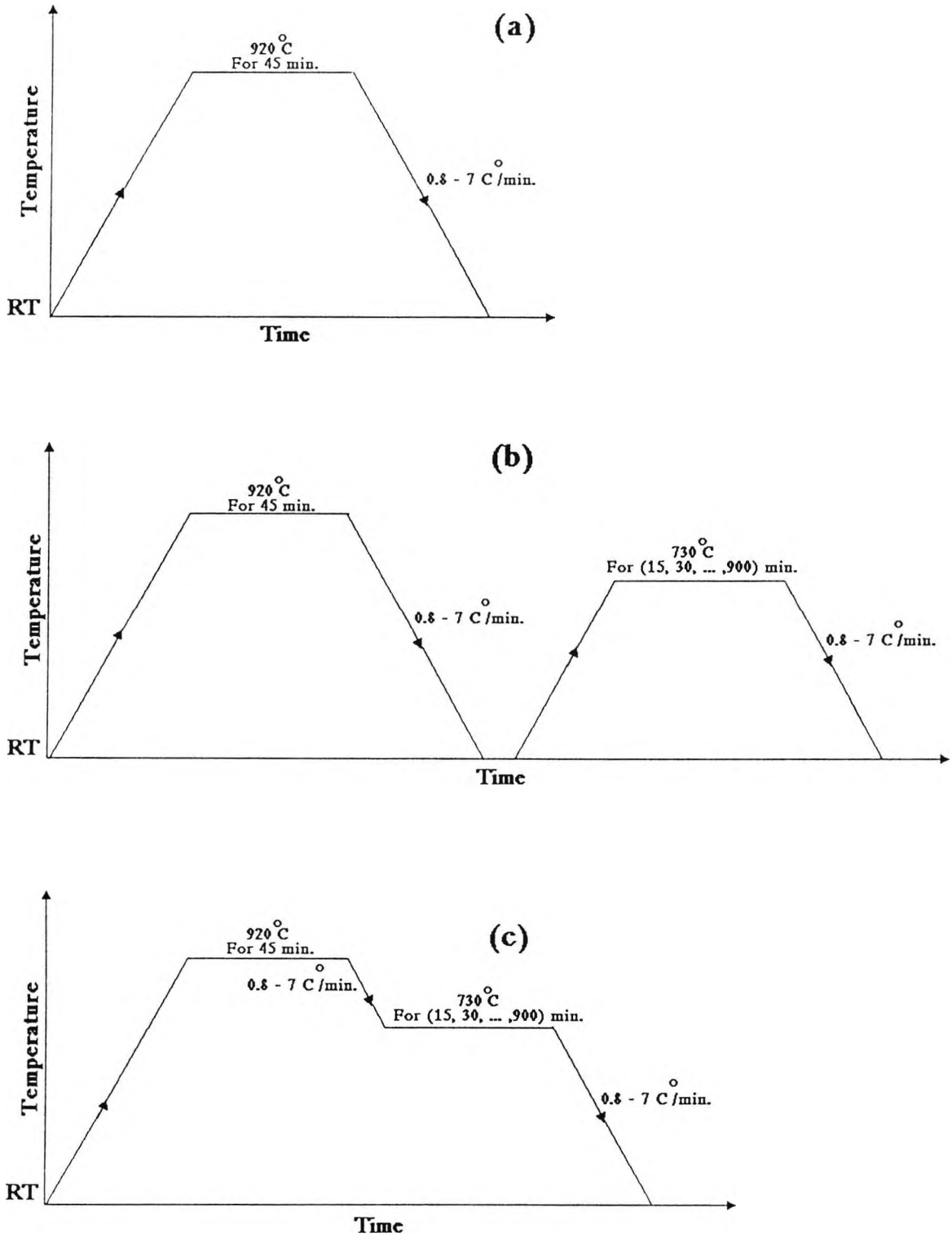

Fig.3.4- Schematic Diagrams of Various Heat Treatment Used.

(a)- Normalising., (b)- Heating Up., (c)- Cooling Down.

To study the influence of heating temperature on intercritical annealing, two intercritical annealing temperatures were examined, 730°C and 760°C.

In addition to these heat-treatments, the influence of grain size on intercritical annealing was examined using a plain C-Mn steel, which had been supplied in the controlled rolled condition so that it would have a fine grain size. Two different grain sizes, 18 um and 37 um, were achieved by austenitising the plain C-Mn steel at 865°C for 30 minutes, and 1050°C for 1 hour respectively as shown in figure 3.5 and figure 3.6.

The normalised (Fig. 3.5a and 3.6a) and intercritical annealed condition both on heating (Fig. 3.5b and 3.6b) and cooling down (Fig. 3.5c and 3.6c) to the intercritical annealing temperature of 730°C were examined.

In order to follow the changes in micro-structure with intercritical annealing time, small samples (2.5 x 2.5 Cm) were intercritically annealed as in sections 3.2.2, and 3.2.3 for times from 0, to 900 min and quenched after intercritical annealing in ice brine.

After heat-treatment, the properties studied included mechanical properties, micro-structural measurements, microhardness, and manganese segregation. The experimental technique employed for these studies are detailed in the following sections.

The variation in temperature within the plate was measured at furnace temperatures of 730°C and 920°C using

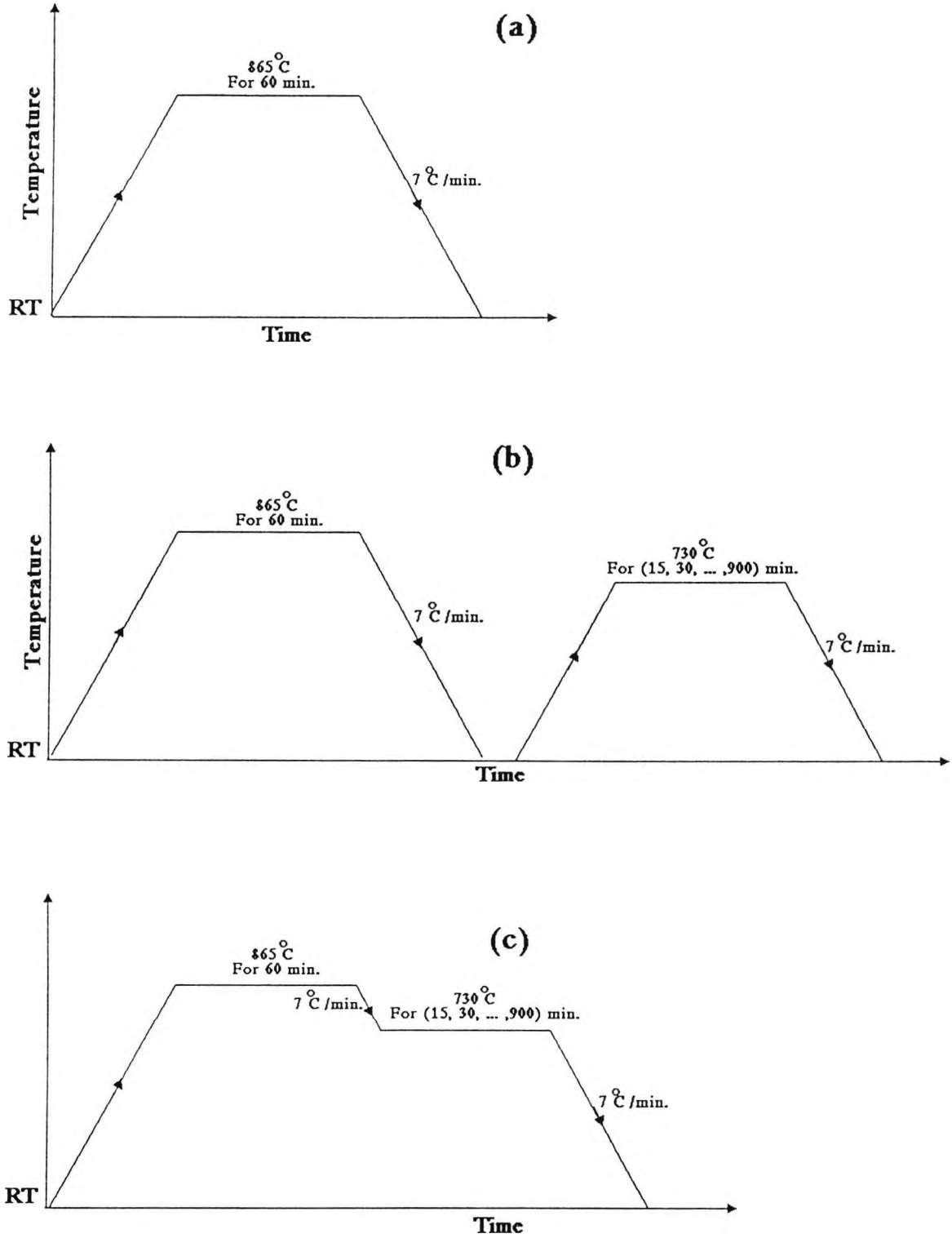

Fig.3.5- Schematic Diagrams of Various Heat Treatment Used for Plain Carbon Manganese Steel (Finer Grained).

(a)- Normalising., (b)- Heating Up., (c)- Cooling Down.

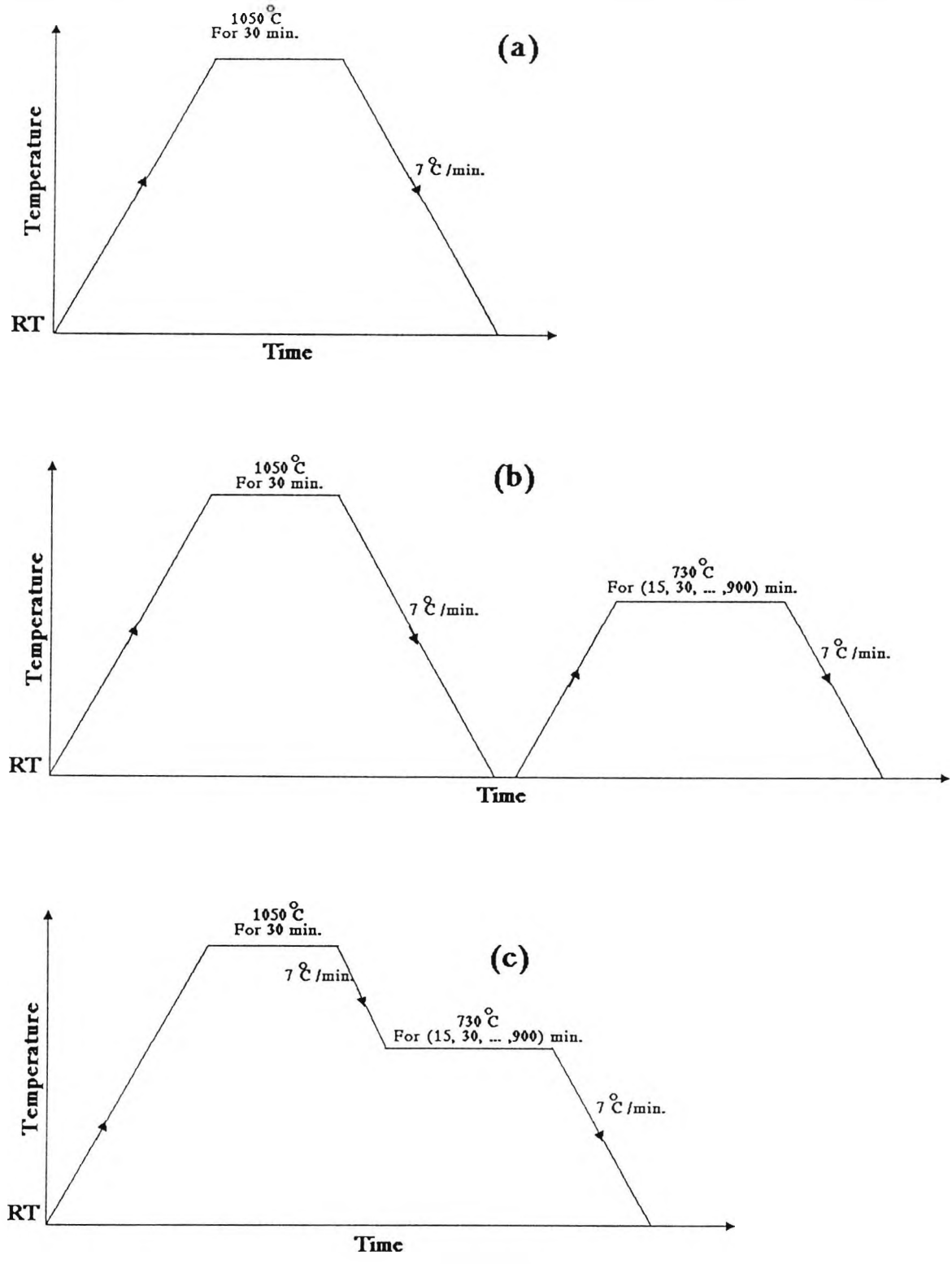

Fig.3.6- Schematic Diagrams of Various Heat Treatment Used for Plain Carbon Manganese Steel (Corser Grained).

(a)- Normalising., (b)- Heating Up., (c)- Cooling Down.

a plate 150x100 mm in which three holes at a distance of 35mm apart were drilled along the length. The holes were drilled to a depth of 25 mm and the temperature within the plate measured using thermocouples as shown in figure 3.7. The readings were also taken at a depth of 50 mm and 75 mm and the results are tabulated in table 3.2, and table 3.3 respectively. The maximum error was ±3°C at 730°C and ± 4°C at 920 °C for the muffle furnace, and ± 1°C for the air circulating furnace.

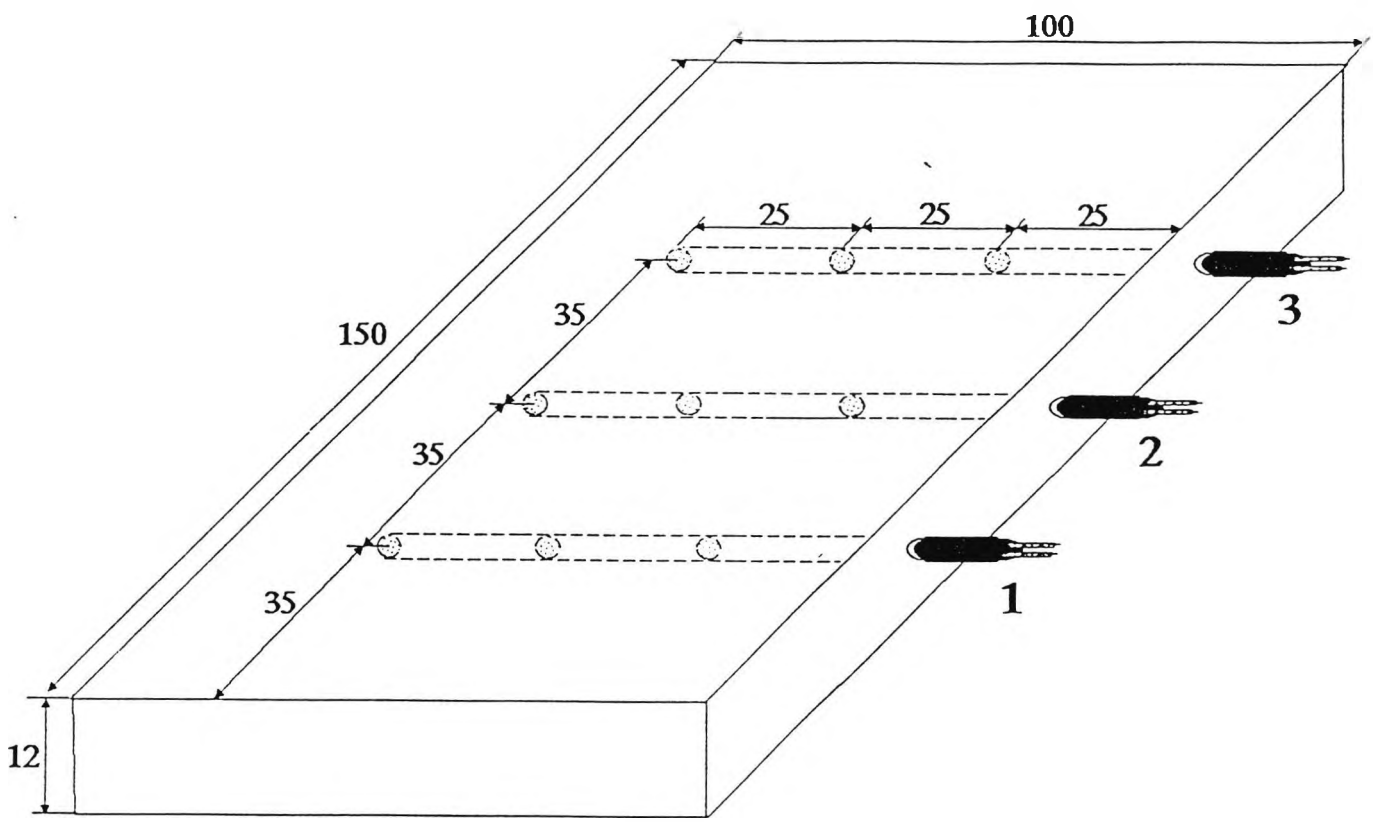

Fig.3.7- Diagram of the Position of the Temperature Measurements in the Plate.

3.3- DETERMINATION OF MECHANICAL PROPERTIES.

3.3.1- ENGINEERING TENSILE PROPERTIES.

Tensile specimens were cut from each heat treated plate in a direction perpendicular to the rolling direction (i.e transverse). Standard tensile specimens with 5 mm diameter were machined according to B.S.18 part2[118], as shown in figure 3.8. The specimens were pulled to fracture using either an Instron universal testing instrument (floor model TT-C AO141), or a LLOYD 1M 30K tensile machine. An Instron strain gauge extensometer G-51-14M, covering a gauge length of 25 mm was fitted to the specimen. Samples were strained at an average strain rate of $1.7 \times 10^{-3} S^{-1}$. In this way stress-strain graphs could be obtained for each sample. All the tests were carried out at room temperature at a cross head speed of 2.54 mm/min (equivalent to a strain rate of $1.7 \times 10^{-3} S^{-1}$). After tensile testing, the load and elongation data were read from the chart recording. Using the original cross-sectional area, the engineering stress was calculated from the load. Lower yield strength (YS) and ultimate tensile strength (UTS) were determined for each sample.

Lower yield strength was taken as the average value of the stress in the Luders extension.

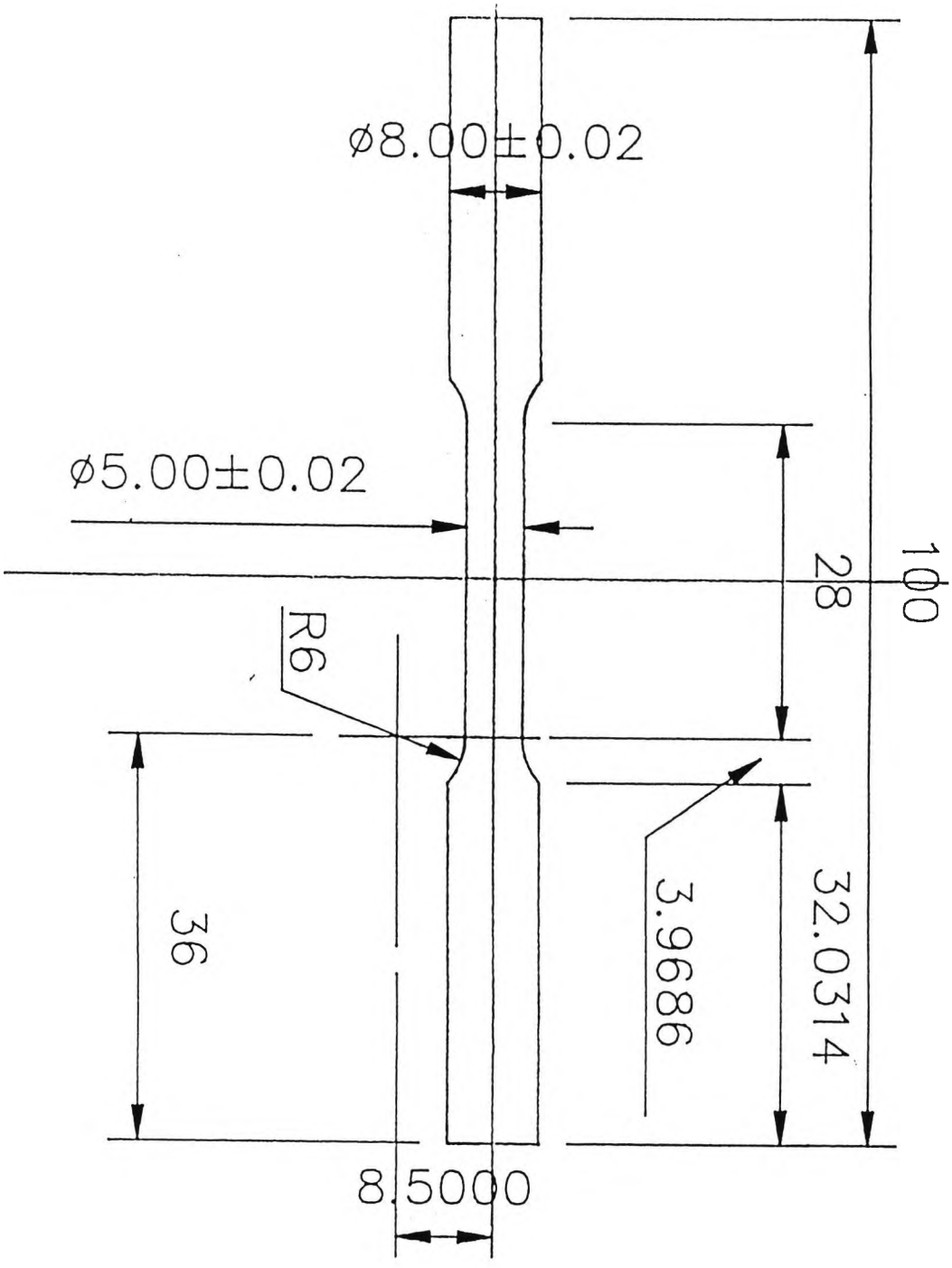

Fig.3.8- Standard Tensile Sample.

3.3.2- IMPACT TEST.

Charpy V-notch impact specimens were cut in a direction parallel to the rolling direction as shown in fig 3.9. They were machined according to B.S 131, part 2, with the square section (10x10 mm) containing a 45° V-notch (perpendicular to the plate thickness and rolling direction), having a depth of 2 mm and a root radius of 0.25 mm as shown in figure 3.9(a).

The specimen is supported as a beam in a horizontal position and is loaded behind the notch by the impact of a heavy swinging pendulum as shown in figure 3.9(b).

An Avery-Denison, Izod, Charpy Impact Machine, No 6703/A/31045 was used at all times calibrated to B.S.131[119] part 4 having a striking velocity of 5 m/s and a capacity of 300 J. The specimen is forced to bend and fracture. Charpy specimens were tested at different temperatures to determine the ductile-brittle transition curves. For each specimen, the absorbed impact energy was recorded and plotted versus the test temperature, and the percentage cleavage fracture in the fracture surface was estimated,as discussed later. The percentage cleavage fracture was then plotted versus the temperature and the fracture-appearance-transition-temperature (FATT) was determined by interpolation at 50% cleavage fracture.

3.3.2.1- COOLING EQUIPMENT.

In order to obtain a ductile-brittle curve for each heat-treatment various cooling baths were used to achieve

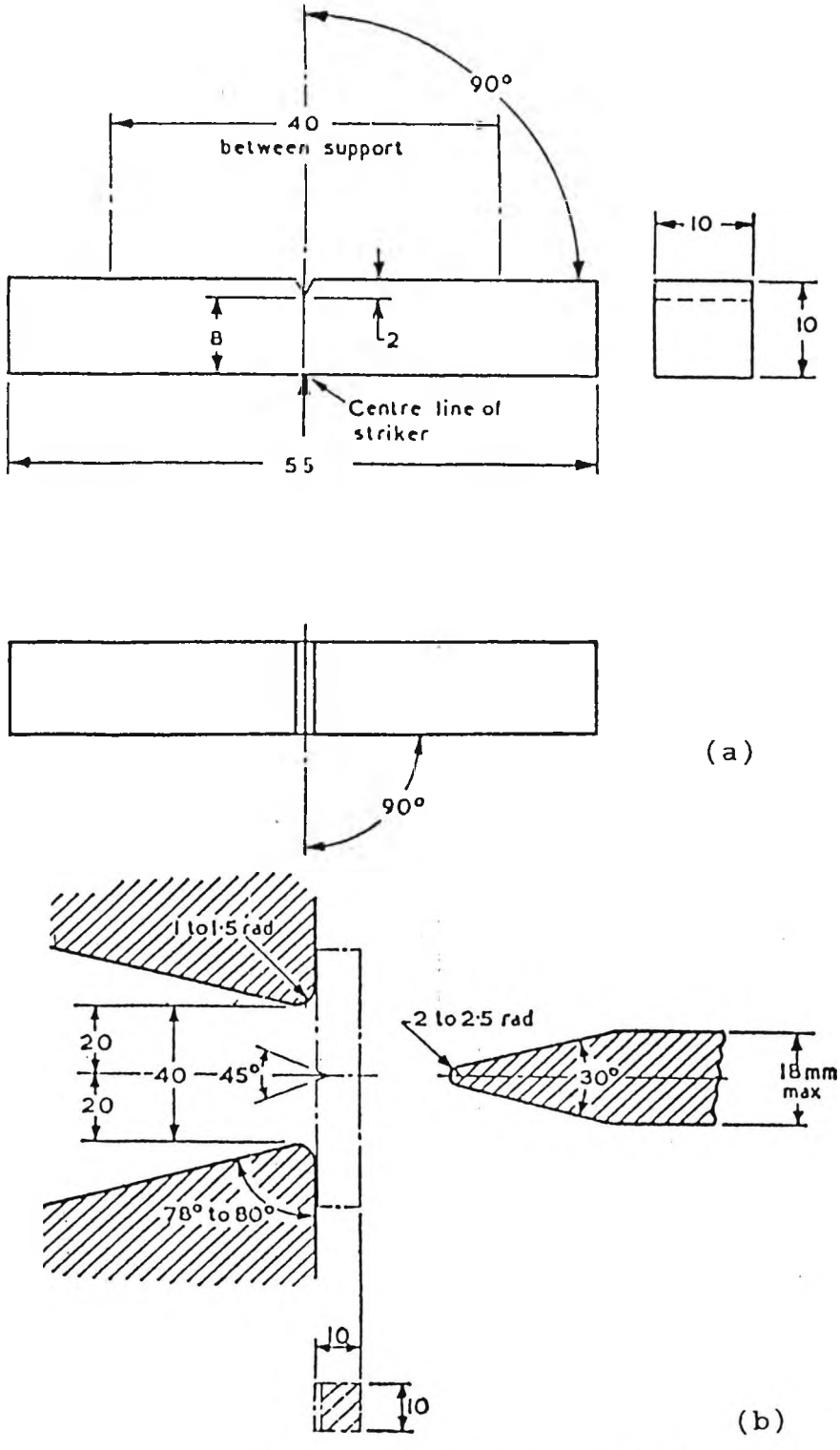

All dimensions are in millimetres unless otherwise stated

Fig.3.9 a- Standard Charpy V-Notch Sample

b- Charpy V-Notch Impact Test.

different test temperatures. According to B.S 131 part2[119], in all cases the period of immersion of the test piece and the holder in the bath at the required temperature must not be less than 10 minutes and the test piece must be broken within 5 sec from the time of removal from the bath.
A holder/carrier was designed figure 3.10 to reduce the fracture time to less than 5 seconds.

The following cooling media were used for the various temperatures.

1- Temperatures between 10°C to 35°C.

Samples were placed in a stainless steel beaker having at least 100 mm of water after which the container was immersed in a larger water bath. This was heated to the required temperature ensuring a constant distribution of heat using a magnetic stirrer. A 0°C to 200°C mercury thermometer manufactured to B.S. 1704 was used to record the temperature.

2- Temperatures between 0°C to 10°C.

Samples were placed in a stainless steel beaker having a mixture of ice/water. A alcohol thermometer manufactured to B.S 1704 was used to measure the temperature. Alcohol thermometers can be used over a temperature range from (-140 to +35°C).

3- Temperatures between -10°C to -140°C.

An Amsler TV742 cooling chamber containing liquid nitrogen

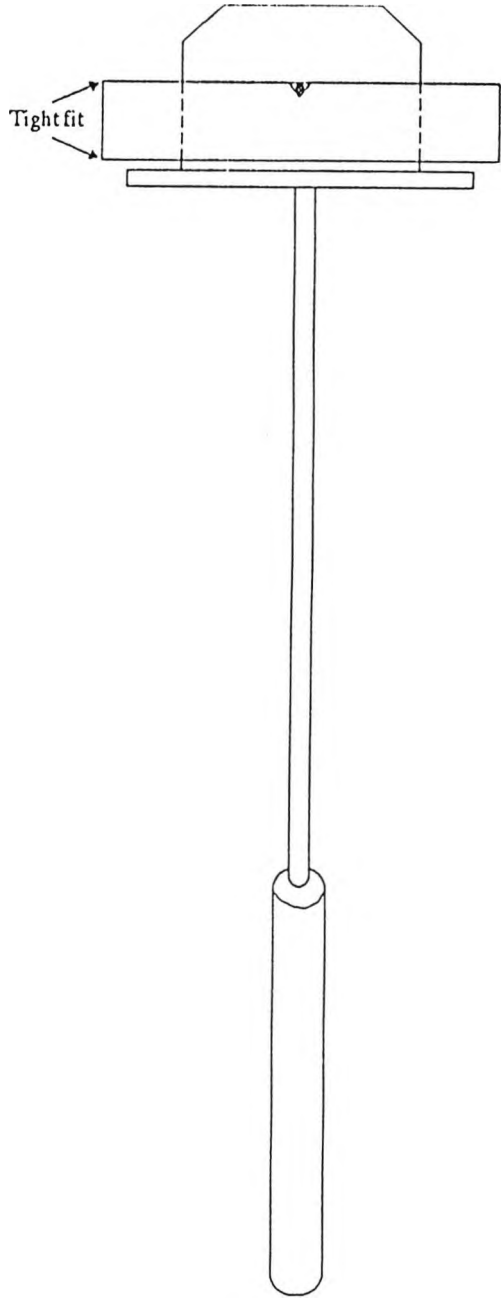

Fig.3.10 Impact Sample Holder.

which circulates around an isopentane chamber was employed.

The samples were placed in the isopentane chamber which has a stirring device keeping the temperature constant at all times. The liquid nitrogen is circulated around the isopentane chamber with the aid of a pump which was controlled by means of cut-off switch. The switch was set so as to stop the flow of liquid nitrogen around the isopentane chamber when the desired temperature was achieved. The alcohol thermometer was used to measure the temperature in the isopentane chamber.

3.3.2.2- DETERMINATION OF CRYSTALLINITY[120].

When a notched bar test piece of a metal is broken by impact, the individual crystals may fracture either by cleavage or by shear and for steel both modes may occur in the same fracture.

In cleavage, the crystals fracture on crystallographic planes which in coarse grained material appear as bright sparkling facets, giving the appearance known as "crystalline". In the shear mode the crystals elongate and deform,producing a silky texture described as "fibrous".

The fibrous appearance transition temperature (FATT)[79,92] normally taken as the temperature which gives a 50% fibrous and 50% brittle fracture, is another indication of the impact behaviour of a material. Similar equations[80,121] relating both impact energy and fibrous fracture to micro- structural parameters can be obtained.

The percentage of crystallinity is defined[119] as the total area of the crystalline portion of the fractured test piece expressed as a percentage of the original cross-sectional area of the test piece below the notch.

A binocular microscope (x10) was used to determine the percentage of fibrous fracture using a graduated transparent rule. The percentage of fibrous fraction was derived using the equation below. Thus by plotting a graph of percentage of fibrous fracture against impact temperature the values of 50% FATT can be determined for each heat treatment.

100 (1 - crystalline area in mm^2/ 80 mm^2) per cent

3.3.3- MICRO-HARDNESS.

The Leco microhardness testing machine was used to measured the microhardness of ferrite and martensite. The impression was taken at the center of the ferrite grain and at the center of the martensite colony. The average of 10 measurements for each sample was taken. The load used was 5 gram.

3.4- MICRO-STRUCTURAL MEASUREMENTS.

The following micro-structural measurements were made in order to corelate the micro-structure to the tensile and impact properties.

Ferrite grain size (d), percentage of pearlite (%p), percentage of martensite (%M) and grain boundary carbide thickness (t_c).

3.4.1- MECHANICAL POLISHING AND ETCHING.

The broken charpy samples were cut to a smaller size (10 x10x5mm) so that micro-structural observations could be carried out both optically and using the SEM. The face opposite to the notch was examined. The samples were mounted in bakelite and mechanically polished using successively finer abrasive paper followed by six and one micron diamond paste on a cloth covered wheel.

For SEM work, these samples were etched lightly in a 2% nital solution and the polishing process was repeated.

The final etching treatments used for the various measurements is as follows:

1- 2 % nital solution (2% nitric acid in alcohol) for measurements of ferrite grain size.

2- 5% picral solution (5% picric acid in alcohol) for measurement of percentage of pearlite.

3- A mixture of 70% picral and 30% nital solution for measurement of grain boundary carbide thickness and density.

4- Mixture of 50% picral and 50% nital solution for measurement of martensite.

3.4.2- FERRITE GRAIN SIZE.

The mean linear intercept method was used to measure the ferrite grain size. This was done by securing a micrometer stage onto a Vickers optical microscope fitted with a cross wire. The micrometer moved the stage and 1000 ferrite grains were intercepted on each sample in order to obtain an average

grain size, [relative error[122] of 2.5%].

3.4.3- VOLUME FRACTION OF PEARLITE.

The volume fraction of pearlite was measured by point counting at least seven hundred counts being made [relative error[122] of 2.5%]. A Swift point counter model F.415C (No.1) attached to the Vickers optical microscope was employed.

3.4.4- GRAIN BOUNDARY CARBIDE THICKNESS.

The grain boundary carbide thickness was measured using the method of Mintz et.al[80] on a Jeol JSM T 100 scanning electron microscope working at 25 Kv. Measurements were made with 45° tilt. For each specimen the thickness of one hundred grain boundary carbides was measured. In order to achieve consistent results, the rules listed below were followed when measuring carbide thickness.

1- Measurement was taken at the thickest part of the carbide, perpendicular to the grain boundary direction.

2- Only isolated grain boundary carbides and carbides at the tail of pearlite colonies were measured.

3- Carbides at triple grain boundary intersections were measured across the thickest limb.

4- Where a number of carbides occurred in close proximity, only the largest two were measured.

Measurement was simply achieved using a short length of transparent ruler held against the cathode ray screen. From the measured results, the mean value was calculated for the

complete set of one hundred values.

3.5- GRAIN BOUNDARY CARBIDE DENSITY.

The grain boundary carbide density was measurement on the SME using the method of Mintz et.al[118]. The number of grain boundary carbides intersected in a linear traverse were noted and the carbide density (i.e. number of carbides intersected divided by the length of traverse) calculated. At least 100 carbides were counted.

3.6- SEGREGATION ANALYSIS.

In order to follow the progress of manganese diffusion from ferrite to austenite during intercritical annealing, a Jeol JSM-840A scanning electron microscope with a Link analytical system AN 10/85 with a solid state SiOLi EDS detector was used. A fully quantitative analysis package (ZF4) using a least square fit followed by ZAF correction was employed. The microscope was used at 15 kV with a probe current of $3x10^{-9}$A.

Specimens were placed flat to the horizontal at a working distance of 39 mm and the inclined angle of spectrum was 40°.

Spot analysis having a spot diameter of 1 μm was used at 30 K magnification. Each analysis was made at approximately the center of the ferrite or pearlite/martensite grain for a time of 100 s (with a dead time of 22%) using a count rate of 2400 counts/second.

Table 3.1 The Chemical Composition Of Steels Used.

Steel	C	Mn	Si	S	P	Al	Nb	N
1.51% Mn Steel	0.100	1.51	0.43	0.005	0.010	0.040	0.020	0.0025
1.49% Mn steel	0.096	1.49	0.41	0.003	0.010	0.016	0.027	0.0050
1.0% Mn steel	0.083	1.00	0.29	0.004	0.010	0.028	0.026	0.0050
0.56% Mn steel	0.098	0.56	0.32	0.003	0.010	0.030	0.026	0.0053
1.41% Mn Steel	0.067	1.41	0.28	0.006	0.009	0.041	0.030	0.0100
Plain C-Mn steel	0.110	0.62	0.32	0.005	0.009	0.008	-	0.0039

Table 3.2- Variation of Temperature Within the Plate Using the Muffel Furnace.

Furnace Temperature Reading °C	Temperature at position 1	Temperature at position 2	Temperature at position 3	Depth m m
730	725	729	730	25
730	729	730	731	50
730	731	731	732	75
920	916	918	921	25
920	918	920	923	50
920	921	922	924	75

Table 3.3- Variation of Temperature Within the Plate Using Air- Circulating Furnace

Furnace Temperature Reading °C	Temperature at position (1)	Temperature at position (2)	Temperature at position (3)	Depth m m
730	729	730	731	25
730	730	730	731	50
730	731	730	731	75

CHAPTER FOUR

EXPERIMENTAL RESULTS

4.1- THE EFFECT OF MANGANESE LEVEL AND HOLDING TIME ON IMPACT AND TENSILE PROPERTIES.

4.1.1- INTRODUCTION.

Previous work by Mintz and Kolahi-Aval[115] has shown that, the intercritical annealing of C-Mn-Al-Nb steels can improve the impact performance (lower the ITT) by about 20-40°C with no change in strength.

The present investigation is a continuation of this work. The aim of this investigational section is to study the effect of manganese level, and holding time at 730°C on the impact and tensile properties of C-Mn-Al-Nb steels. The influence of intercritical annealing on both cooling down from the austenitising temperature to the intercritical annealing temperature, and heating directly to the intercritical annealing temperature will be examined. In addition the changes in micro-structure with intercritical annealing time will be investigated.

Three levels of manganese were used 0.56%, 1% and 1.49% Mn. The chemical composition of these steels are given in table (4.1). The holding time varied from 15 minutes to 15 hours. The cooling rate in all cases was 7°C/min

(equivalent to air cooling of 70 mm thick plate).

Plates were also normalised and cooled at 7°C/min to room temperature.

Table 4.1- The chemical composition of steel used for examining the influence of manganese level on intercritical annealing.

Steel	C	Mn	Si	S	P	Al	Nb	N
1.49% Mn	0.1	1.49	0.41	0.003	0.010	0.016	0.027	0.0050
1% Mn	0.08	1.0	0.29	0.004	0.010	0.028	0.026	0.0050
0.56% Mn	0.1	0.56	0.32	0.003	0.010	0.030	0.026	0.0053

4.1.2- MICRO-STRUCTURAL MEASUREMENTS.

The micro-structural data, i.e, grain size, pearlite volume fraction and grain boundary carbide thickness measurements are listed in tables 4.2, 4.3, and 4.4 for the 1.49%, 1%, and 0.56%Mn steels respectively.

Little change in grain size was observed with intercritical annealing time. The pearlite volume fraction increased slightly with increasing intercritical annealing time.

The grain boundary carbides for all the three steels examined were fine after the long time (15 hr) intercritical annealing treatment, independent of whether the intercritical annealing temperature was approached by

heating-up or by cooling-down. Of most interest in the present investigation, was the observation that intercritical annealing can produce a marked refinement in carbide thickness after only 15 minutes of intercritical annealing time both on heating up and on cooling down to the intercritical annealing temperature. Increasing intercritical annealing time resulted in a significant refinement of the grain boundary carbides.

4.1.3- IMPACT AND TENSILE BEHAVIOUR.

4.1.3.1- 0.56% Mn (C-Mn-Al-Nb STEEL).

Impact transition curves and fibrous fracture curves after normalising and intercritical annealing are given in Figure 4.1 and Figure 4.2, for heating up directly to the intercritical annealing temperature and cooling down to the intercritical annealing temperature respectively. The effect of intercritical annealing holding time at 730°C on 54J ITT °C is shown in Figure 4.3 for both heating up directly to the intercritical annealing temperature and cooling down to the intercritical annealing temperature. In the former instance, the starting microstructure was ferrite plus pearlite (F+P), and for the latter case the starting microstructure was ferrite plus austenite (F+A). Comparing with the normalised condition, drops in impact transition temperature (ITT) of 18°C after 15 minutes, and 34°C after 15 hours were found after heating up directly to the intercritical annealing temperature.

Table 4.2- Microstructural Measurements and Strength of 1.49% Mn Steels.

Specimen No.	Ferrite Grain Size µm	Ferrite Grain Size $d^{-1/2}$ $mm^{-1/2}$	Pearlite Volume Fraction %	Grain Boundary Carbide Thickness µm	54J ITT °C	σ_Y MPa	σ_s MPa
5N	9.2	10.4	14	0.24	-80	341	479
51C	9.2	10.4	16	0.23	-82	344	481
53C	9.1	10.5	16	0.22	-82	343	480
56C	8.9	10.6	15	0.17	-72	343	478
59C	8.4	10.9	16	0.15	-70	327	468
51H	10.6	9.7	20	0.24	-85	322	476
53H	9.6	10.2	21	0.21	-85	332	487
56H	9.4	10.3	28	0.18	-78	332	496
59H	8.1	11.1	30	0.16	-61	302	508

5N =normalised.

51C,53C,56C,and 59C are for samples cooled down to the intercritical annealing temperature and held for 15,30,60, and 900 minutes respectively. 51H,53H,56H,and 59H are for samples heated directly to the intercritical annealing temperature and held for 15,30,60,and 900 minutes respectively.

Table 4.3- Microstructural Measurements and Strength of the 1% Mn Steels.

Specimen No.	Ferrite Grain Size µm	Ferrite Grain Size $d^{-1/2}$ $mm^{-1/2}$	Pearlite Volume Fraction %	Grain Boundary Carbide Thickness µm	54J ITT °C	σ_Y MPa	σ_s MPa
3N	11.0	9.5	9	0.35	-59	293	410
31C	10.4	9.8	8	0.25	-79	313	428
32C	9.90	10.3	10	0.23	-85	309	428
31H	10.1	9.9	9.5	0.27	-87	297	418
32H	10.3	9.9	14	0.22	-89	301	432

3N = normalised.

31C, and 32C, are for samples cooled down to the intercritical annealing temperatures and held for 30, and 900 minutes respectively.

31H, 32H are for samples heated directly to intercritical annealing temperature and held for 30, and 900 minutes respectively.

Table 4.4 Microstructural Measurements and Strength of the 0.56% Mn steel.

Specimen No.	Ferrite Grain Size µm	Ferrite Grain Size $d^{-1/2}$ $mm^{-1/2}$	Pearlite Volume Fraction %	Grain Boundary Carbide Thickness µm	54J ITT °C	σ_Y MPa	σ_s MPa
4N	13.7	8.5	11.0	0.48	-18	265	389
41C	14.0	8.4	11.5	0.45	-34	287	405
43C	14.7	8.3	12.0	0.43	-38	287	403
46C	14.6	8.3	12.0	0.38	-40	272	396
49C	13.3	8.7	12.5	0.35	-42	289	416
41H	12.7	8.9	11.o	0.44	-36	268	410
43H	12.8	8.8	11.5	0.40	-38	270	415
46H	13.0	8.8	12.0	0.40	-43	276	421
49H	13.4	8.7	13.0	0.34	-54	280	430

4N = normalised.

41C, 43C, 46C, and 49C are for the samples cooled down to the intercritical annealing temperature and held for 15, 30, 60, and 900 minutes respectively.

41H, 43H, 46H, and 49H are for samples heated directly to the intercritical annealing temperature and held for 15, 30, 60, and 900 minutes respectively.

A drop in impact transition temperature of 16°C and 25°C was found after cooling down to the intercritical annealing temperature and holding for 15 minutes and 15 hours respectively.

Tensile data (yield strength and ultimate tensile strength) and 54J ITT°C are listed together with microstructural data in table 4.2. Figure 4.4 shows the effect of intercritical annealing holding time on lower yield strength. It can be seen that intercritical annealing leads to very little change in yield strength yet gives improved impact behaviour compared to a standard normalising treatment.

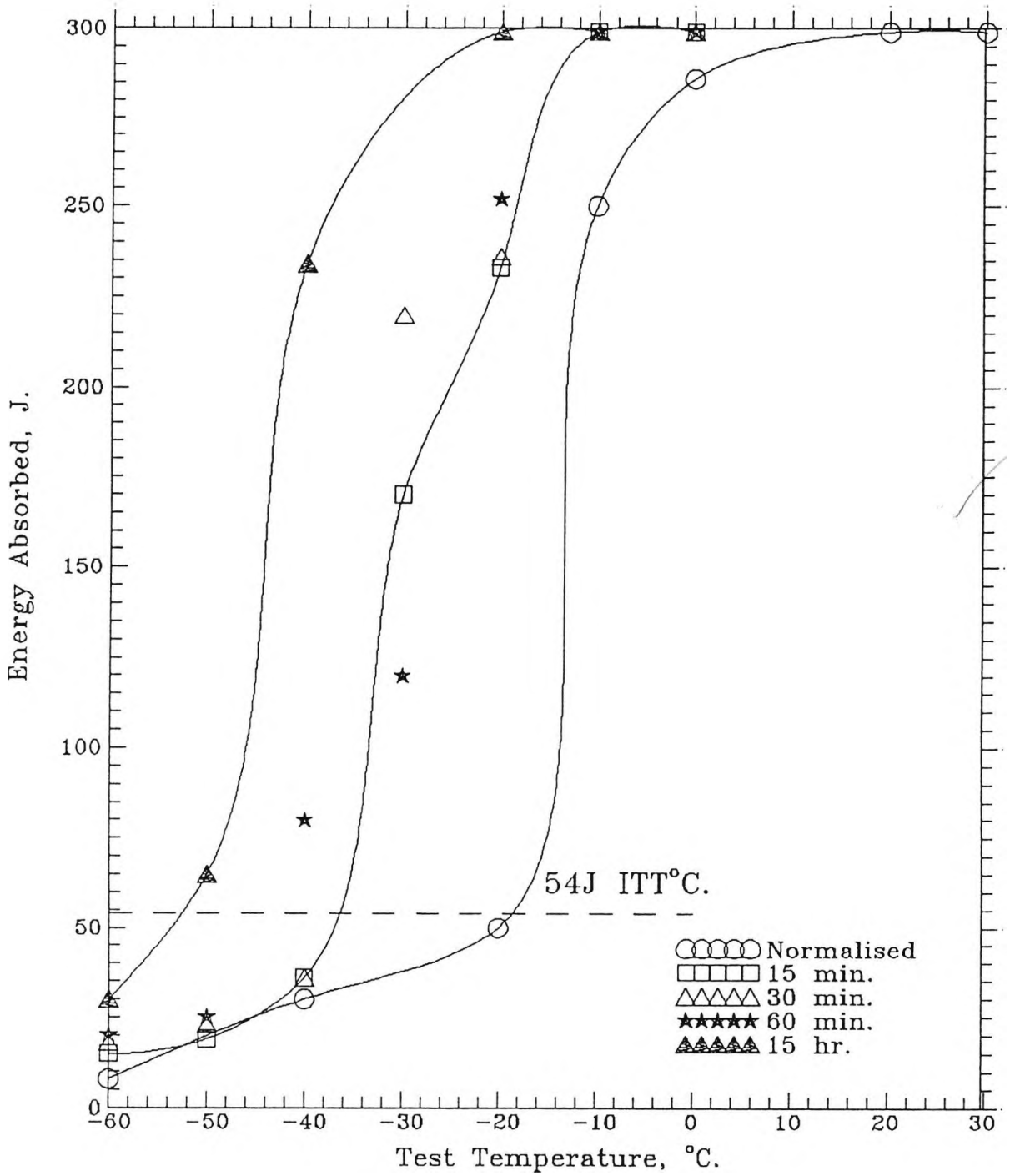

Fig.4.1a- Impact Transition Curves for 0.56%Mn Steel I.A. at 730°C for Various Times, Cooled at 7°C/min, Heating Up Cycle.

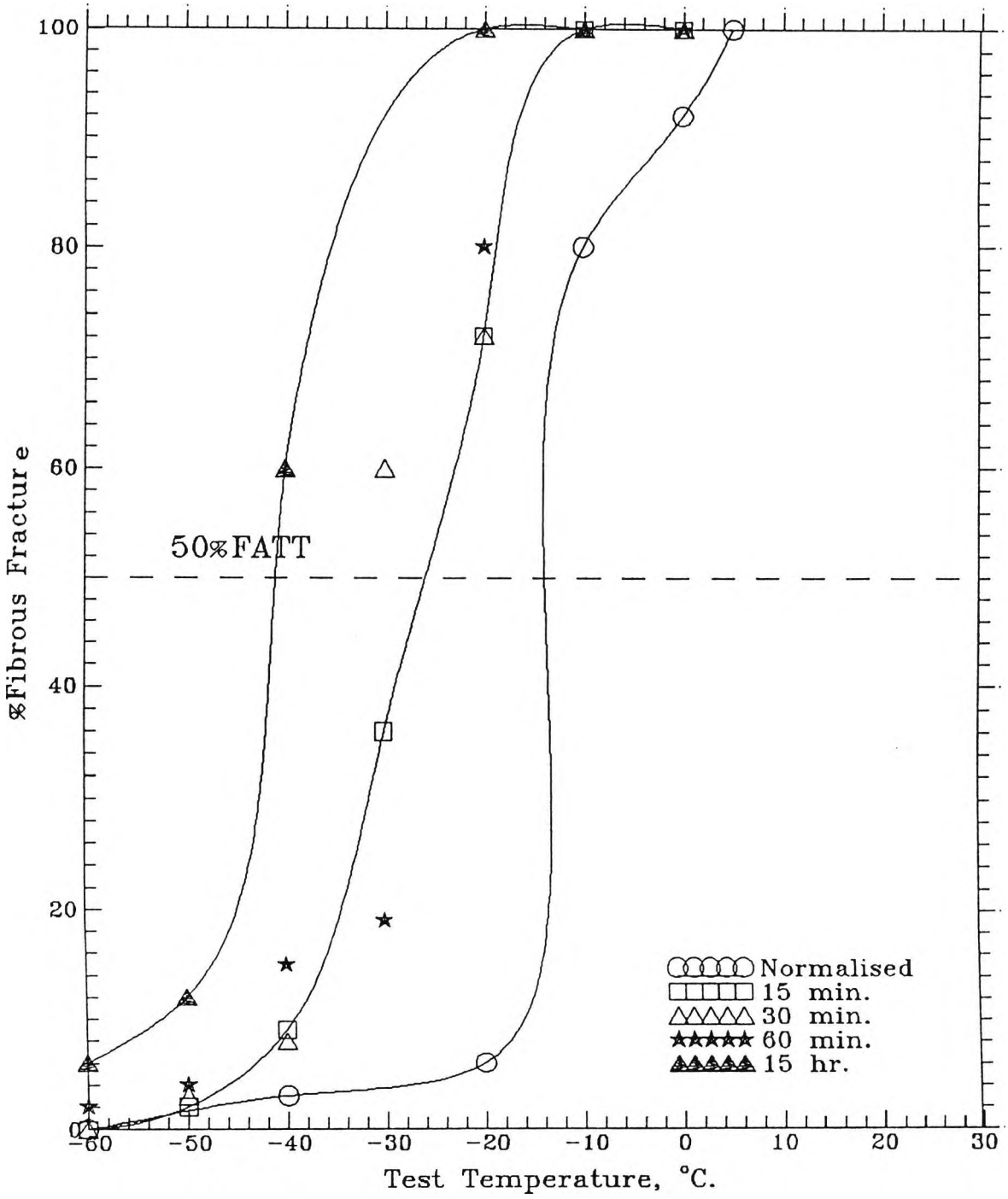

Fig 4.1b- Fibrous Fracture Curves for 0.56%Mn Steel I.A. at 730°C for Various Times, Cooled at 7°C/min, Heating Up Cycle.

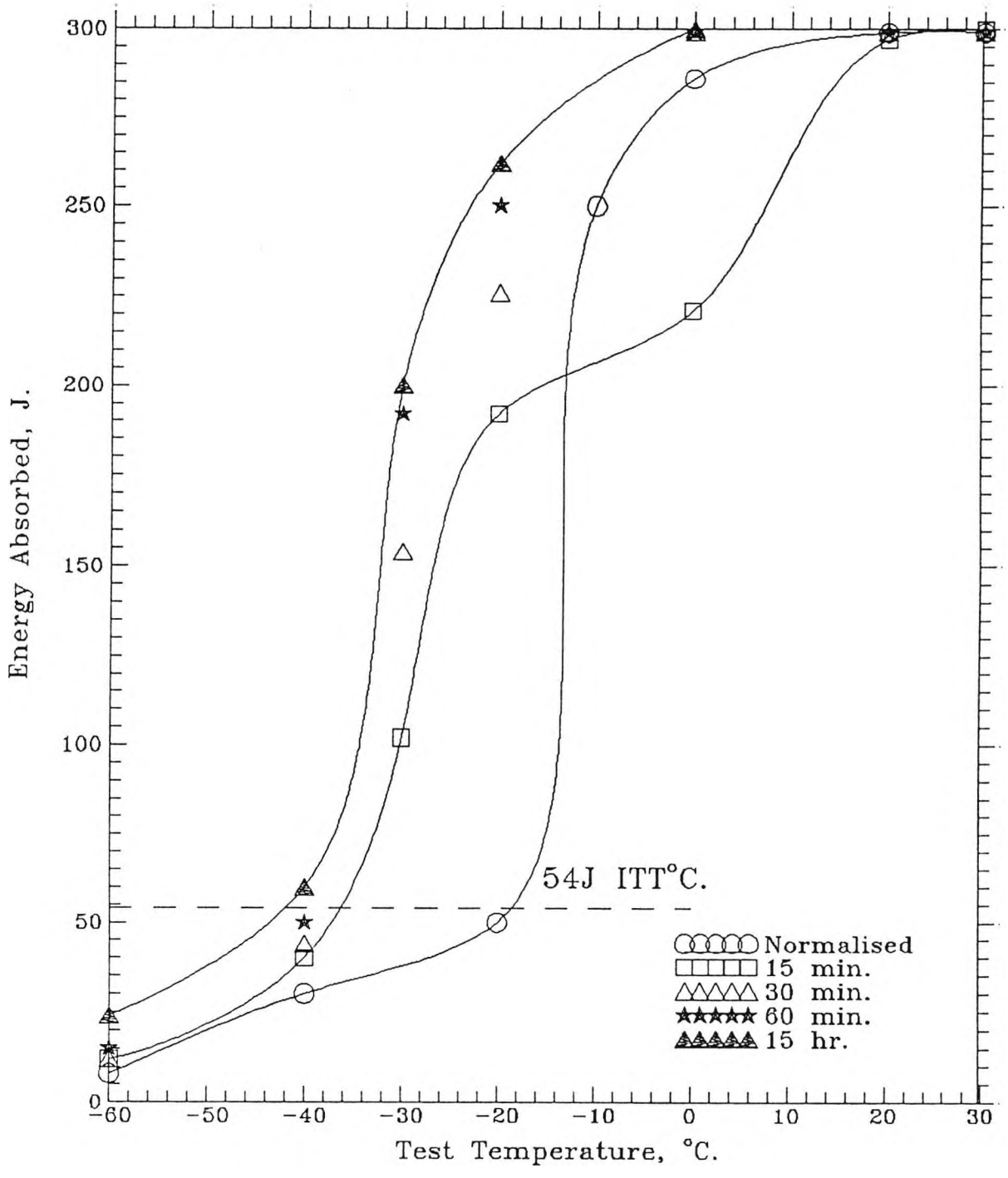

Fig.4.2a- Impact Transition Curves for 0.56%Mn Steel I.A. at 730°C for Various, Times Cooled at 7°C/min, Cooling Down Cycle.

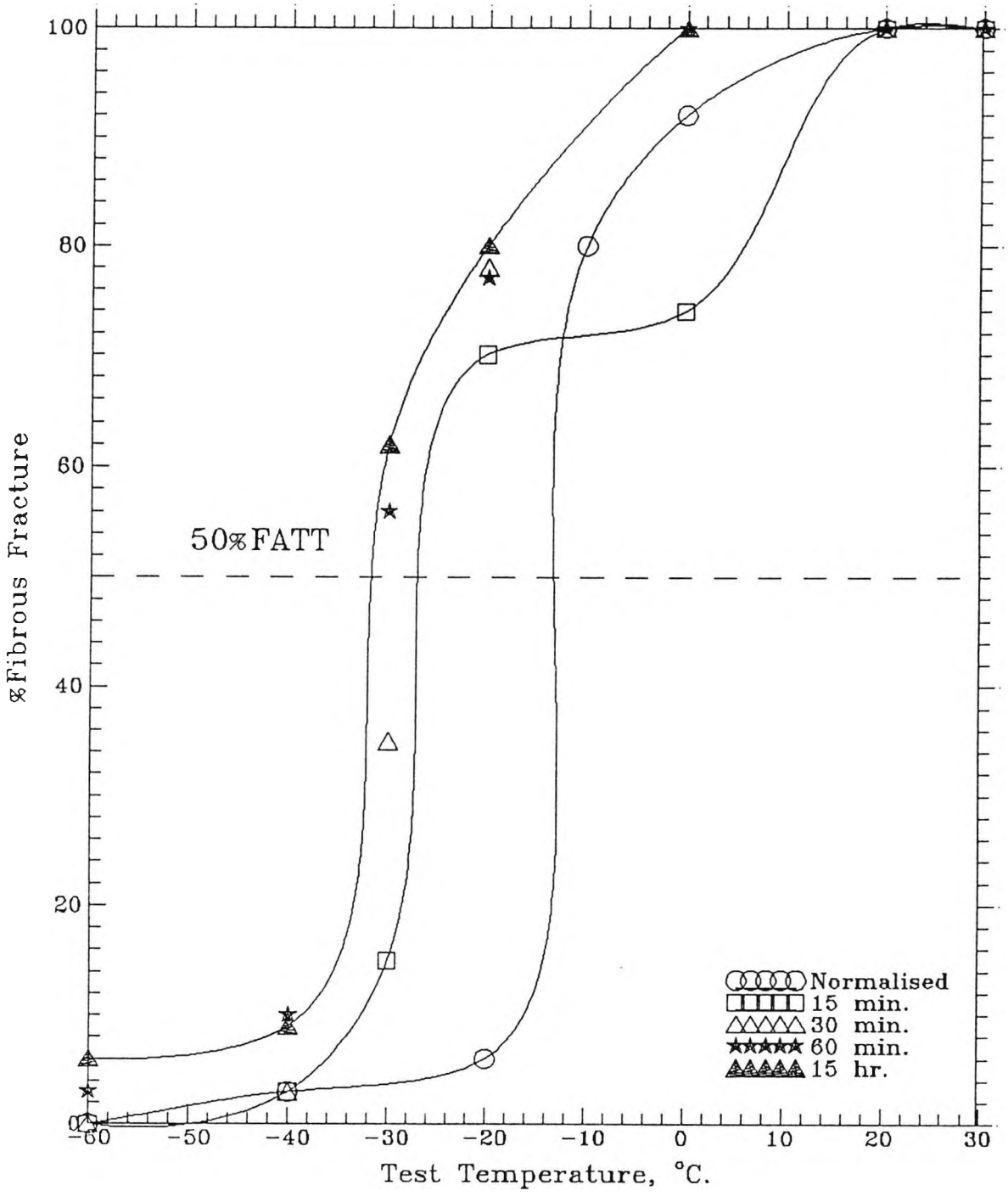

Fig.4.2b- Fibrous Fracture Curves for 0.56%Mn Steel I.A. at 730°C for Various Times, Cooled at 7°C/min, Cooling Down Cycle.

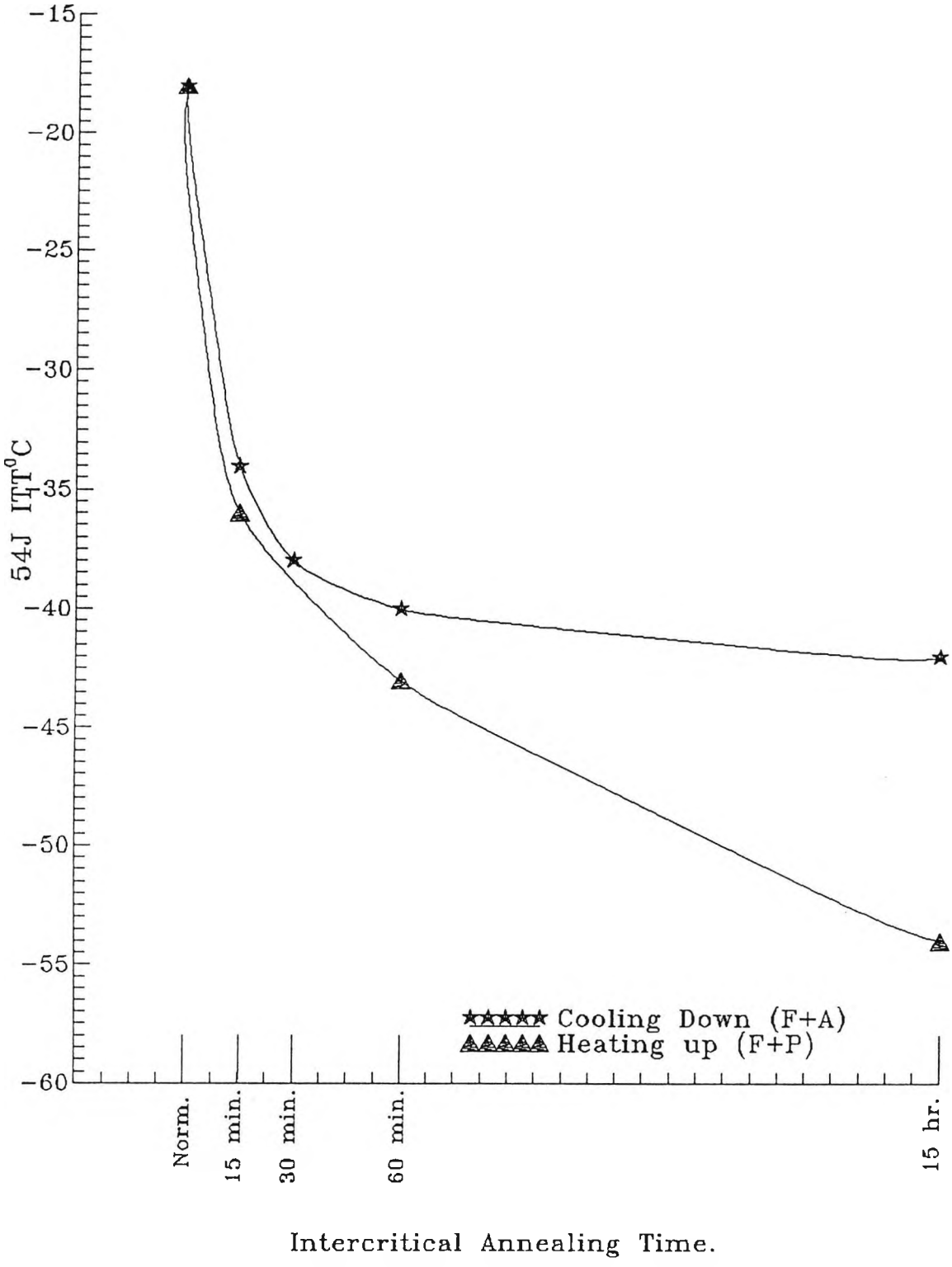

Fig.4.3 - The Effect of I.A. Time on the 54J ITT°C for the 0.56%Mn Steel.

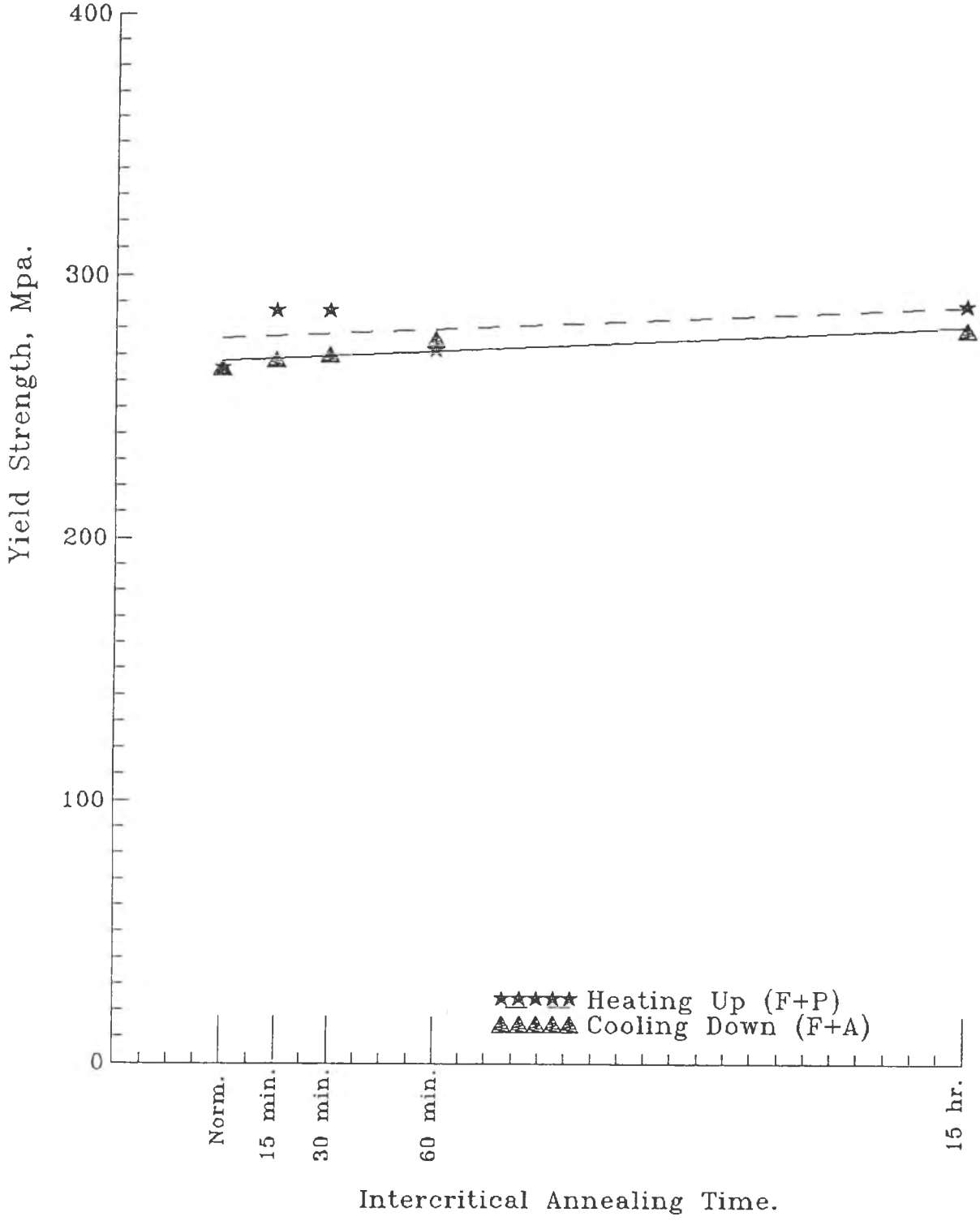

Fig.4.4- The Effect of I.A. Time on the Yield Strength for the 0.56%Mn Steel.

4.1.3.2- 1% Mn (C-Mn Al-Nb steel).

Impact transition curves and fibrous fracture curves after normalising and intercritical annealing are given in Figure 4.5 and Figure 4.6 for heating up directly to the intercritical annealing temperature, and cooling down to the intercritical annealing temperature respectively. The effect of intercritical annealing holding time at 730°C on 54J ITT °C is shown in Figure 4.7 both, for heating up directly to the intercritical annealing temperature and, cooling down to the intercritical annealing temperature. Again in the former instance, the intercritical annealing starting microstructure was ferrite (F+P), and in the latter case the starting microstructure was ferrite and austenite (F+A).

Tensile data (yield strength and ultimate tensile strength) and 54J ITT °C are listed together with microstructural data in table 4.3. Figure 4.8 shows the effect of intercritical annealing holding time on lower yield strength, for both heating up directly to the intercritical annealing temperature, and for cooling down to the intercritical annealing temperature.

As for the lower Mn steel, it can be seen that, intercritical annealing gives improved impact behaviour compared to a standard normalising treatment with no significant change in strength.

However, the degree of improvement for this 1%Mn steel is more marked than observed in the 0.56% Mn steel. For

example, on heating up to the intercritical annealing temperature and holding for 30 minutes, the drop in ITT compared to a simple normalising treatment was 20°C for the 0.56%Mn steel, and 28°C for the 1%Mn steel. Similar improvements were noted on cooling down, the ITT being lowered by 20°C for 0.56%Mn steel compared to 26°C for the 1%Mn steel.

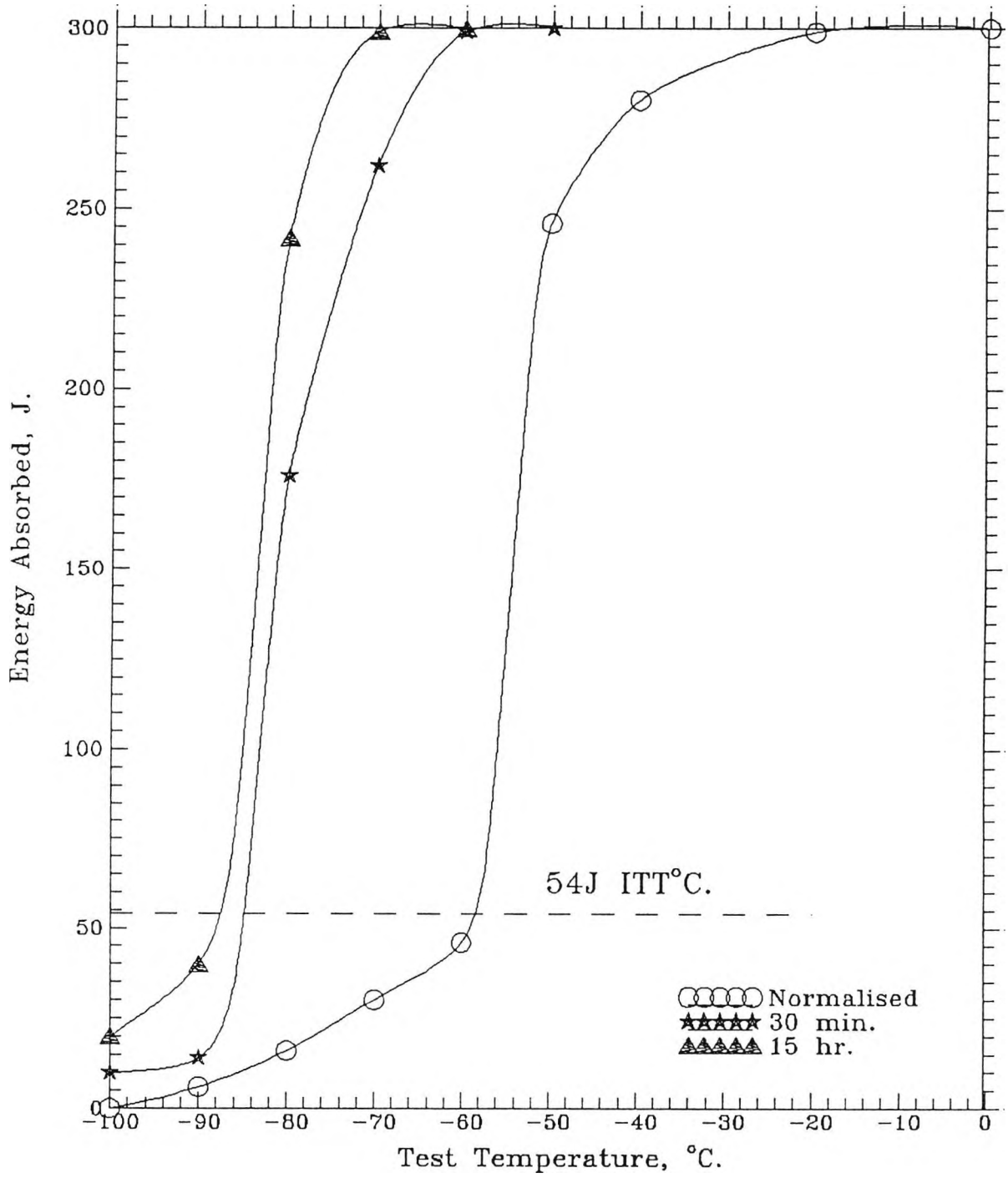

Fig.4.5a- Impact Transition Curves for 1%Mn Steel Intercritically Annealed at 730°C for Various Times, Cooled at 7°C/min, Heating Up Cycle.

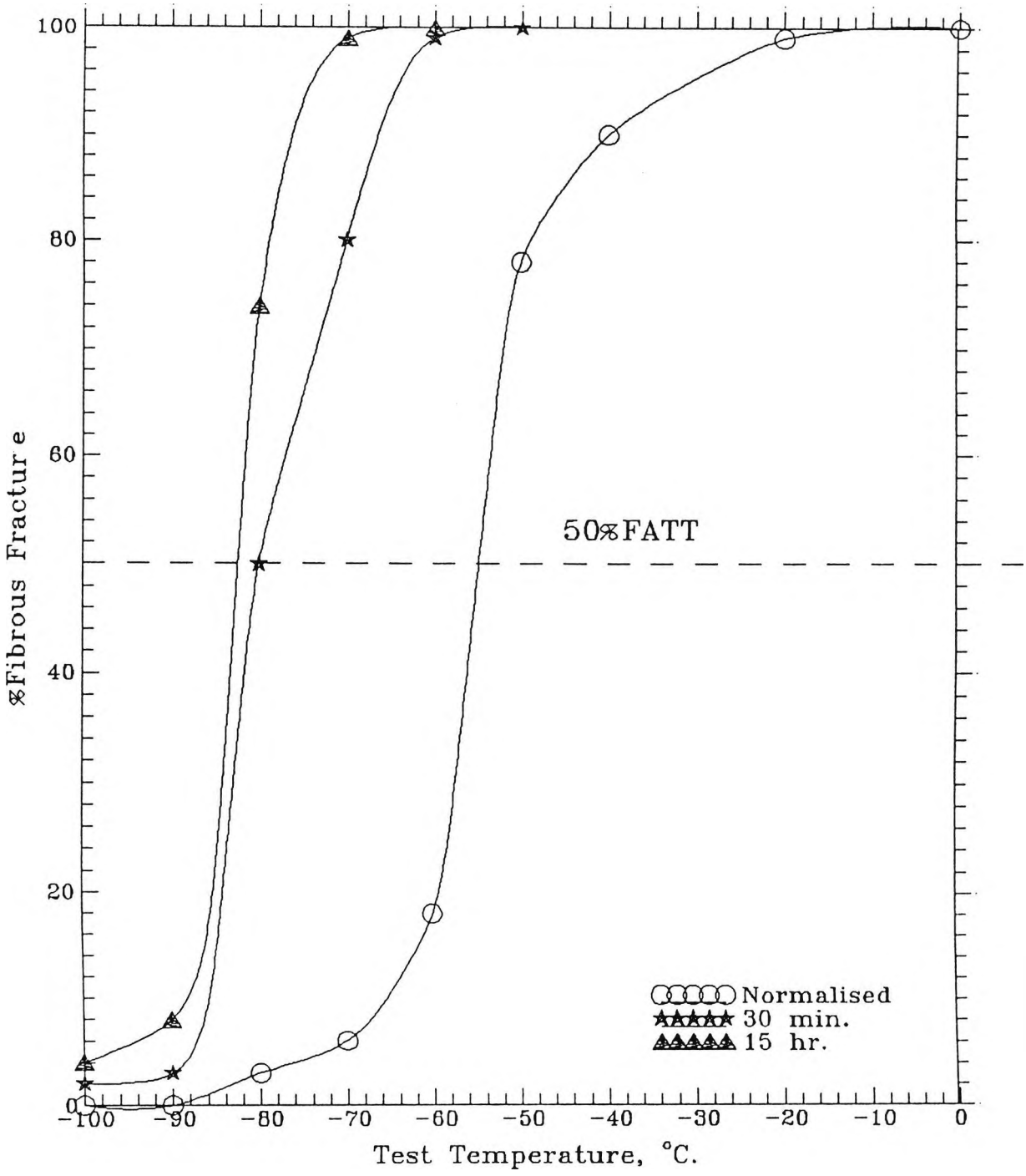

Fig.4.5b- Fibrous Fracture Curves for 1%Mn Steel I.A. at 730°C for Various Times, Cooled at 7°C/min, Heating Up Cycle.

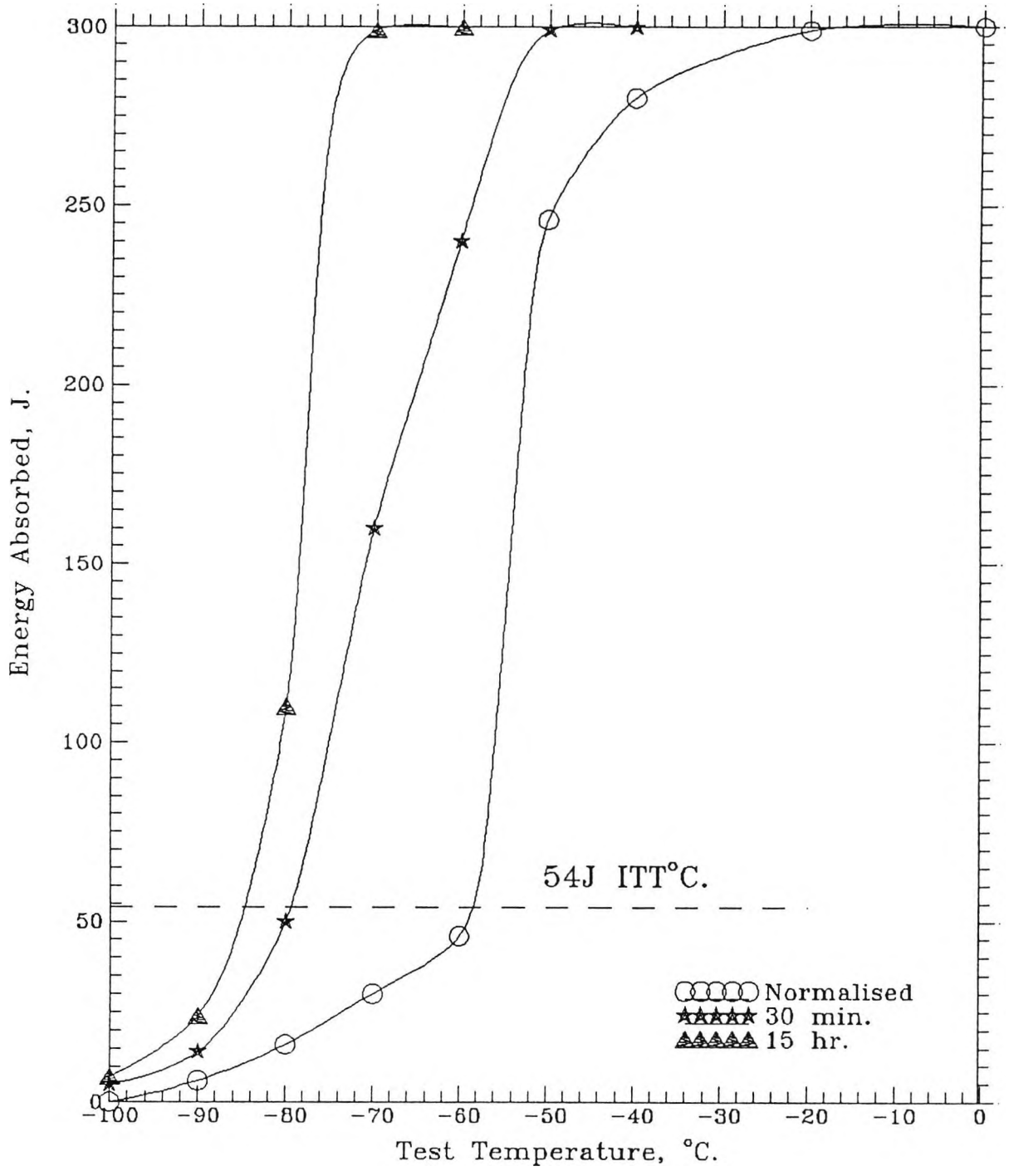

Fig.4.6a- Impact Transition Curves for 1%Mn Steel I.A. at 730°C for Various Times, Cooled at 7/°C, Cooling Down Cycle.

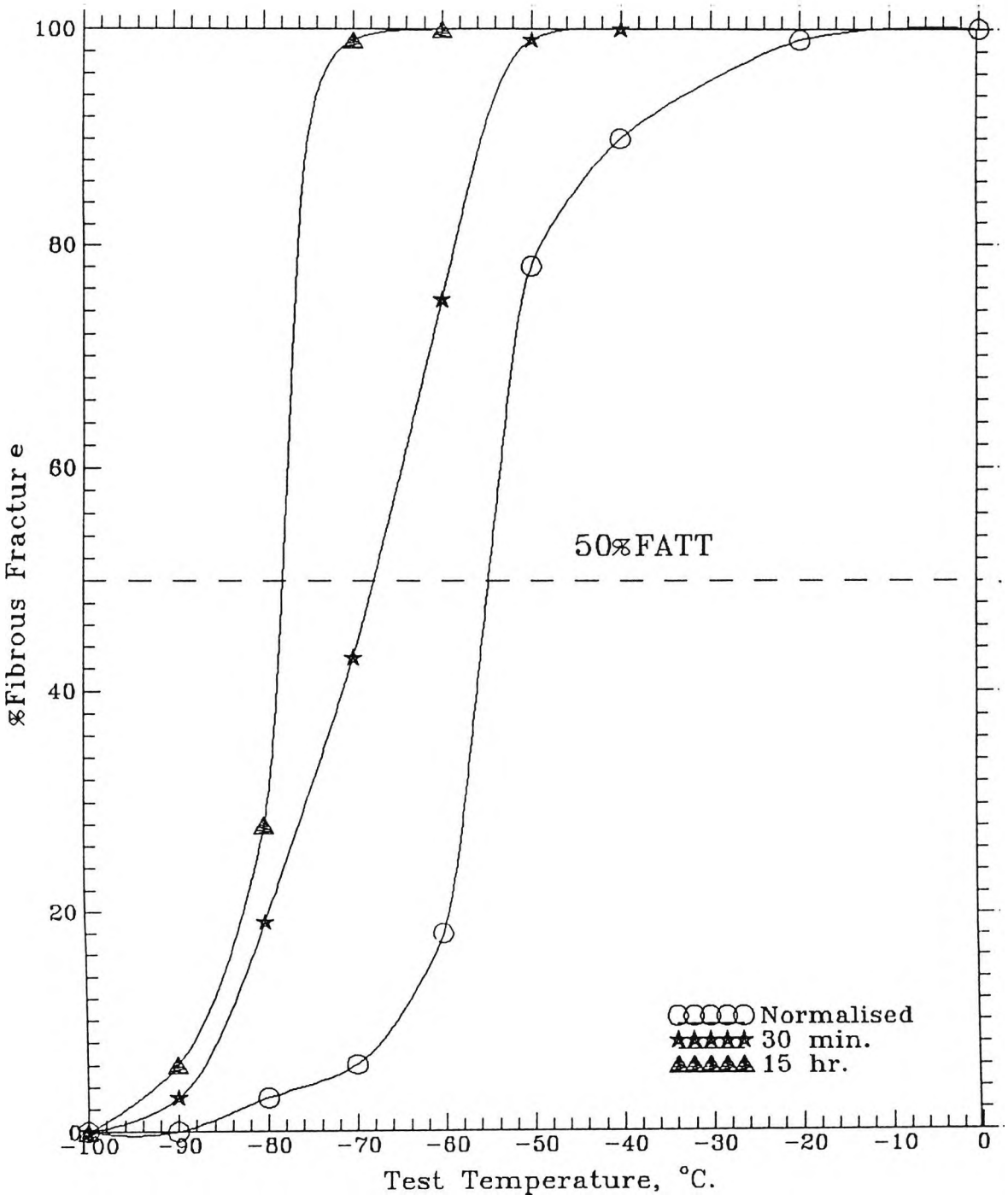

Fig.4.6b- Fibrous Fracture Curves for 1%Mn Steel I.A. at 730°C for Various Times, Cooled at 7°C/min, Cooling Down Cycle.

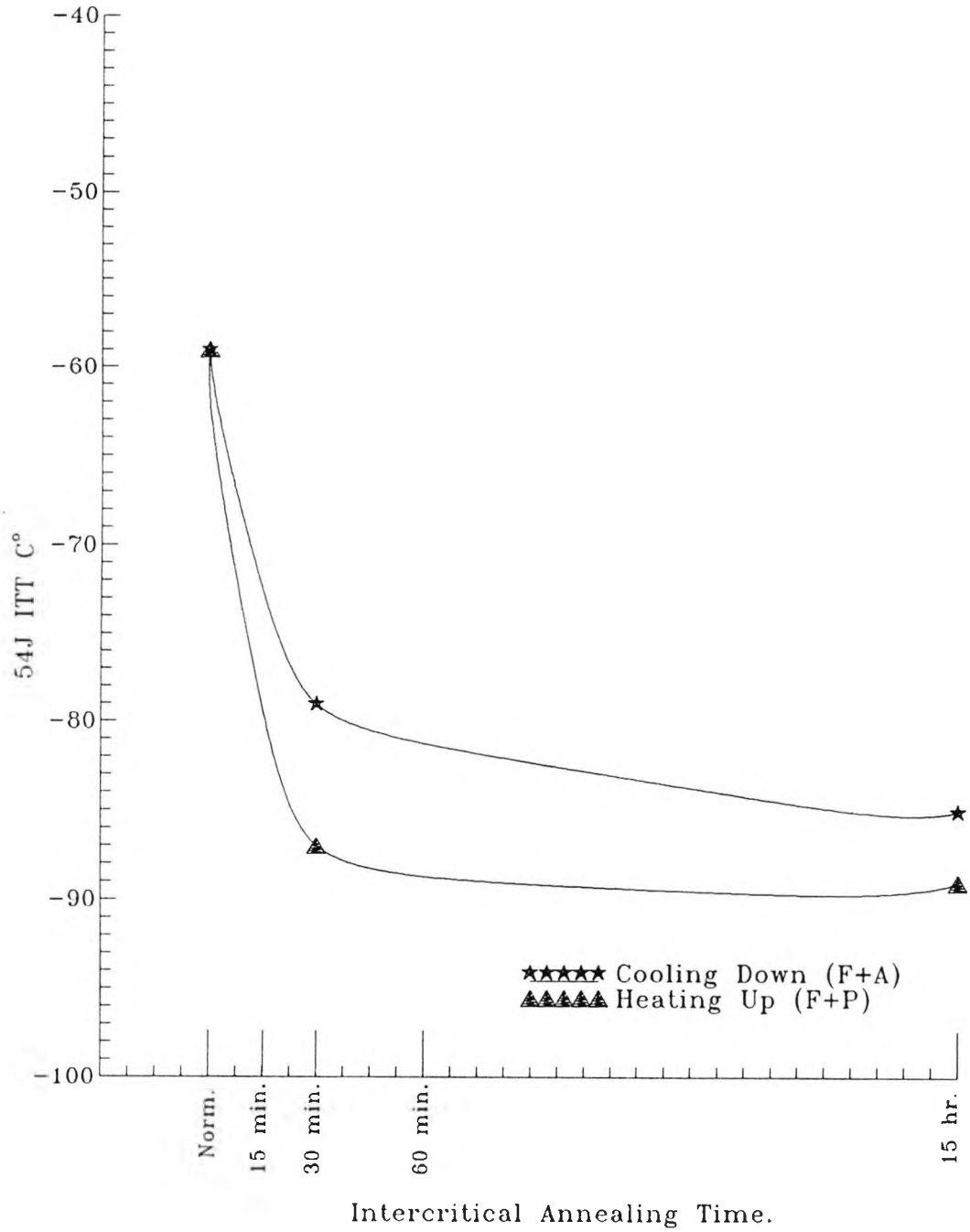

Fig.4.7- The Effect of I.A. Times on the 54J ITT°C for the 1%Mn Steel.

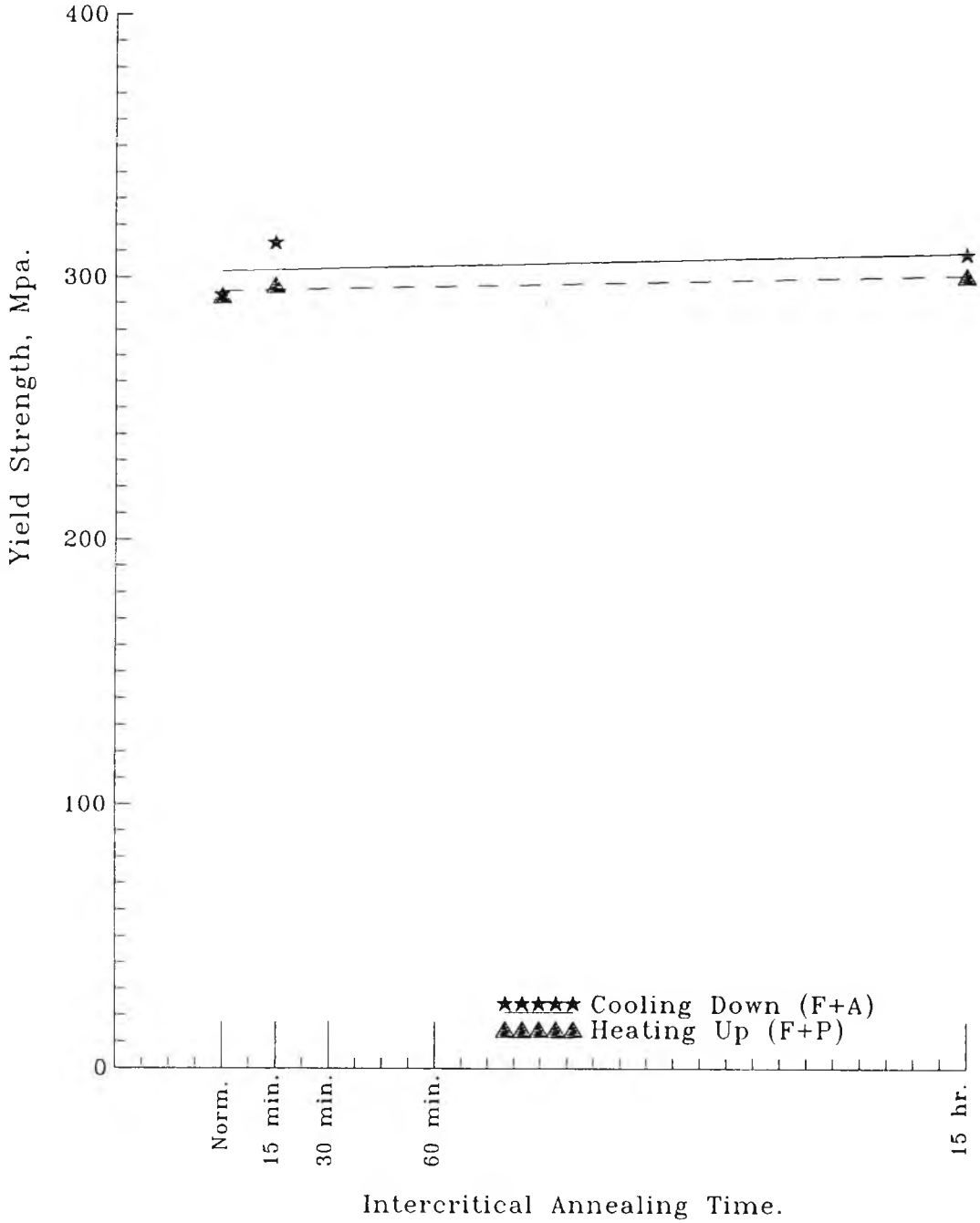

Fig. 4.8- The Effect of I.A. Times on the Yield Strength for the 1%Mn Steel.

4.1.3.3- 1.49% Mn (C-Mn-Al-Nb STEEL).

Impact transition curves after normalising and intercritical annealing are given in Figure 4.9 and Figure 4.10 for heating up directly to the intercritical annealing temperature, and cooling down to the intercritical annealing temperature respectively. The effect of intercritical annealing holding time at 730°C on 54J ITT °C is shown in Figure 4.11. On heating up directly to the intercritical annealing temperature, the starting microstructure was ferrite plus pearlite (F+P),while for cooling down to the intercritical annealing temperature the starting microstructure was ferrite plus austenite (F+A).

Tensile data (yield strength and ultimate tensile strength) and 54J ITT°C are listed together with the microstructural data in table 4.4. Figure 4.12 shows the effect of intercritical annealing holding time on lower yield strength for heating up directly to the intercritical annealing temperature and for cooling down to the intercritical annealing temperature.

For this steel, it can be seen that, in contrast to the two other steels, there was no significant change in impact behaviour after 15 minutes. Furthermore, the impact resistance started to deteriorate after 30 minutes and became worse with increasing intercritical annealing time. It can be seen that the yield strength decreased with increasing holding time.

Figure 4.13 summarises the effect of manganese level on

impact properties during intercritical annealing. From this Figure it can be seen that increasing the manganese level from 0.56% to 1% improved the impact performance (lowers the ITT), while when the Mn level reached 1.49% the impact performance started to deteriorate.

Figure 4.14 summarises the effect of Mn level on yield strength. It can be seen that, increasing the manganese level increases the strength of the steel on normalising and after short intercritical annealing time. For the 0.56% and 1% Mn steels increasing the holding time at the intercritical annealing temperature produced a small increase in strength. When the manganese level reached 1.49%, yield strength again showed little change after short time treatments, but after holding for long times at the intercritical annealing temperature the yield strength actually decreased.In all cases even for the high manganese steel after holding for long times at the intercritical annealing temperature, yield points and Luders extensions were observed.

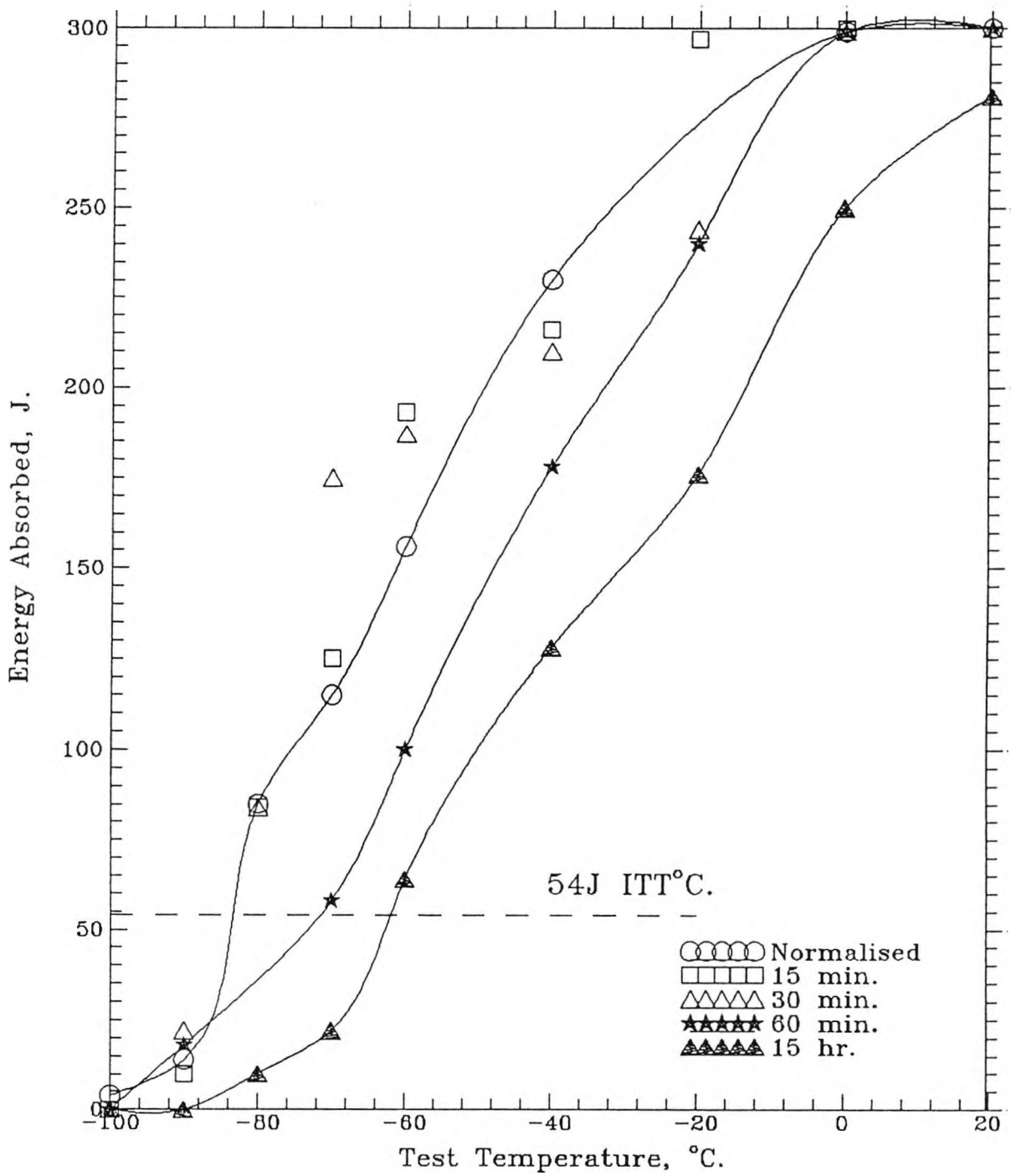

Fig.4.9a- Impact Transition Curves for 1.49%Mn Steel I.A. at 730°C for Various Times, Cooled at 7°C/min, Heating Up Cycle.

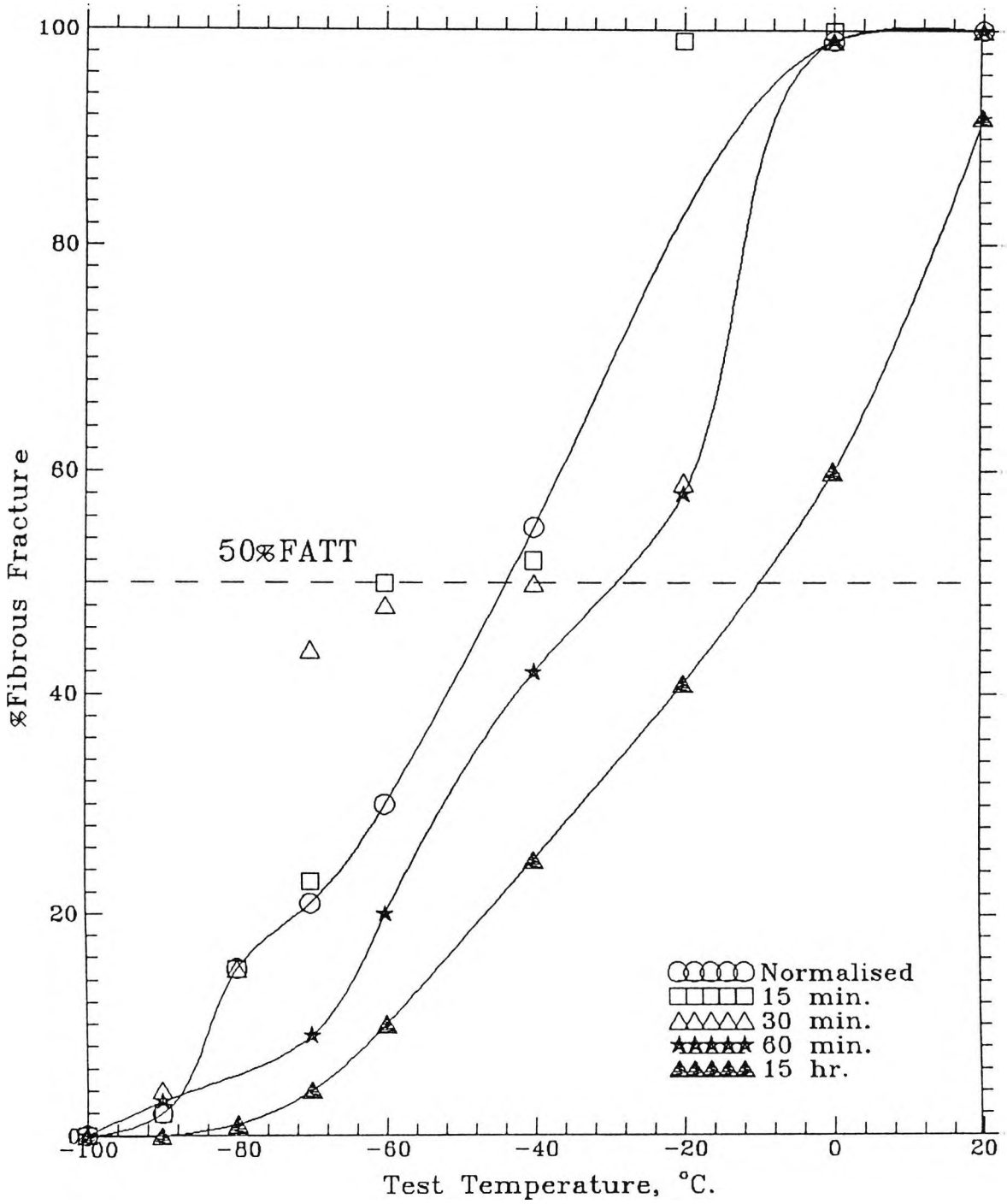

Fig.4.9b- Fibrous Fracture Curves for 1.49%Mn Steel I.A. at 730°C for Various Times, Cooled at 7°C/min, Heating Up Cycle.

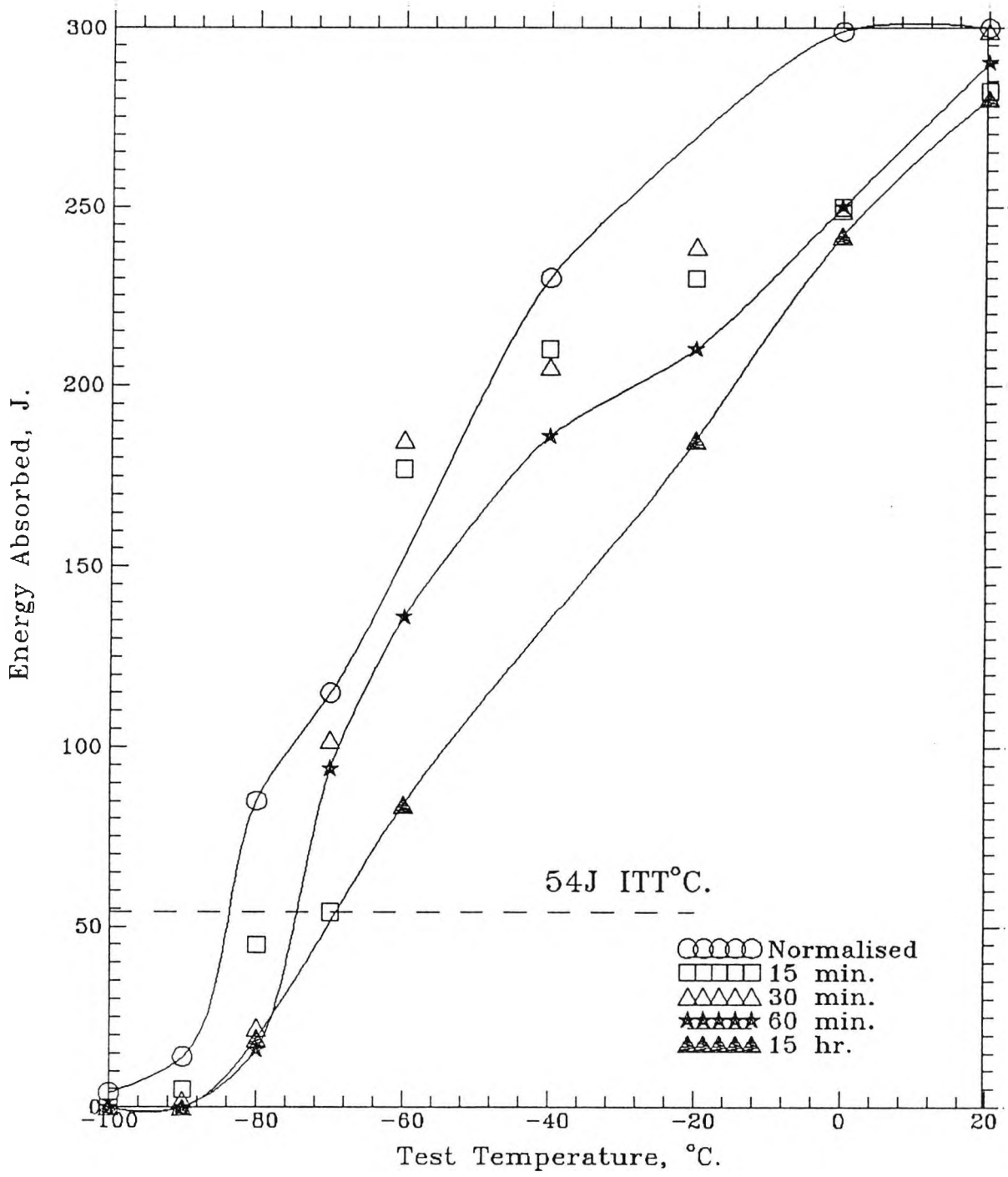

Fig.4.10a- ImpactTransition Curves for 1.49%Mn Steel I.A. at 730°C for Various Times, Cooled at 7°C/min, Cooling Down Cycle.

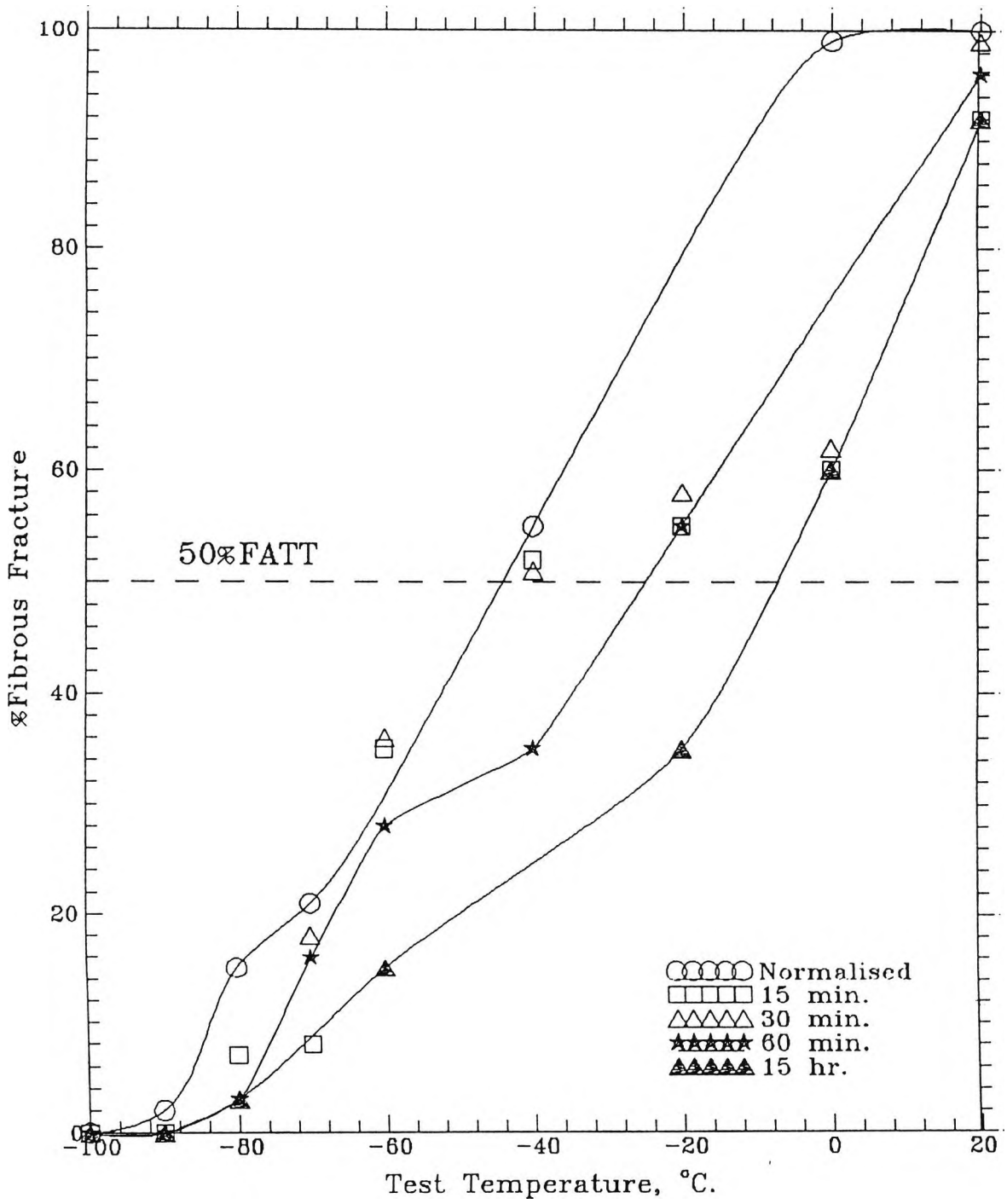

Fig.4.10b- Fibrous Fracture Curves for 1.49%Mn Steel I.A. at 730°C for Various Times, Cooled at 7°C/min, Cooling Down Cycle.

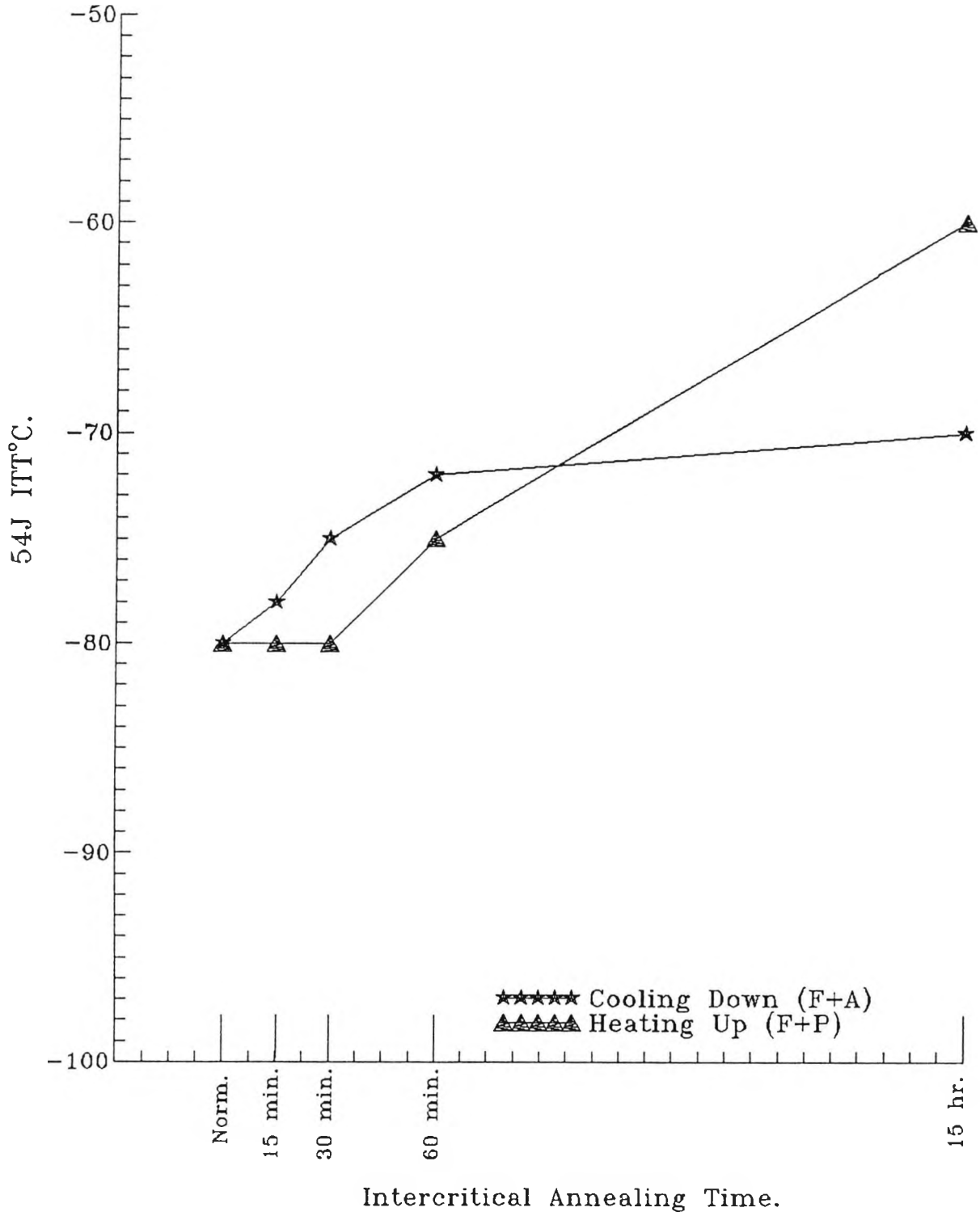

Fig.4.11- The Effect of I.A. Times on the 54J ITT°C for the 1.49%Mn Steel.

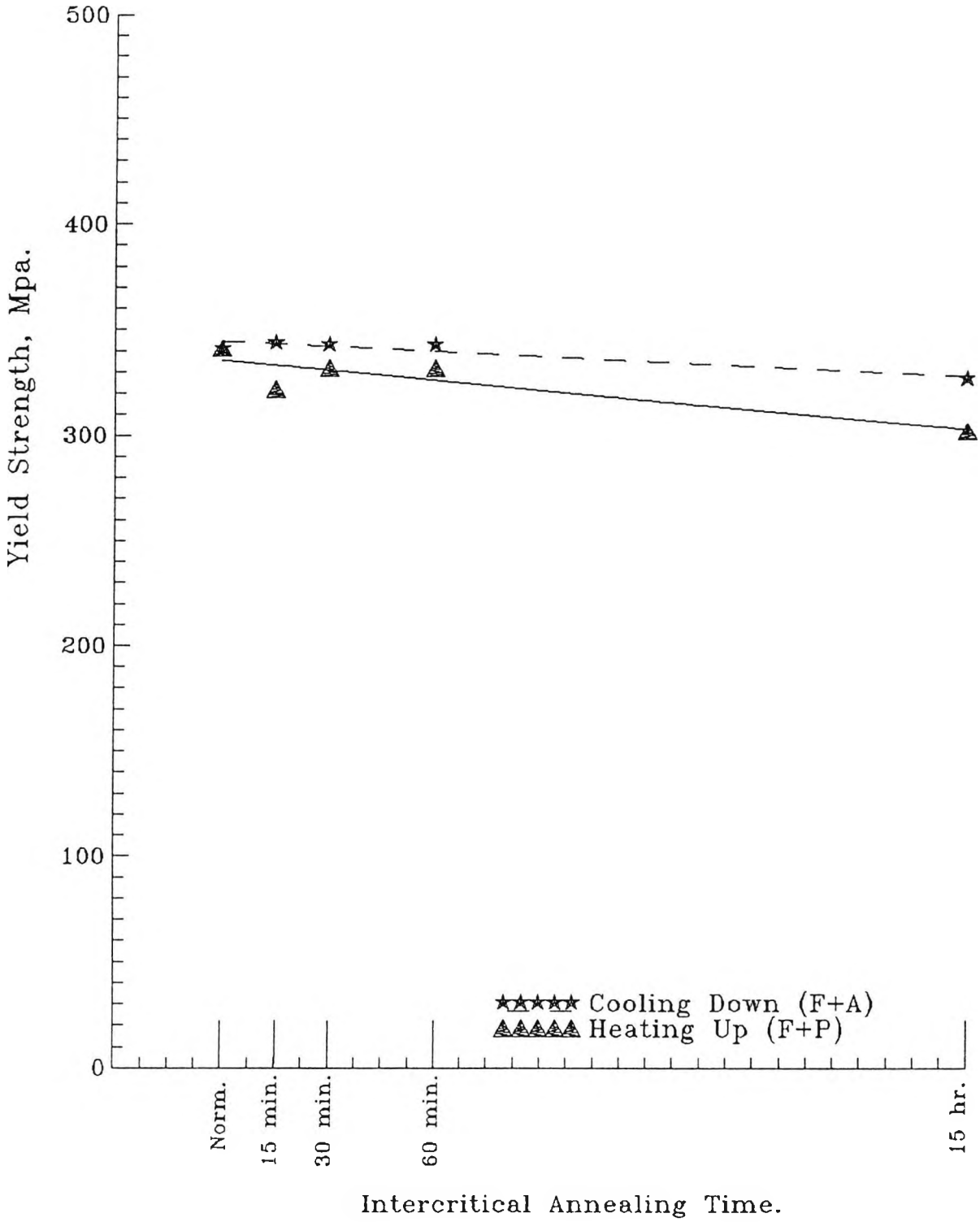

Fig.4.12- The Effect of I.A. Times on the Yield Strength for the 1.49%Mn Steel.

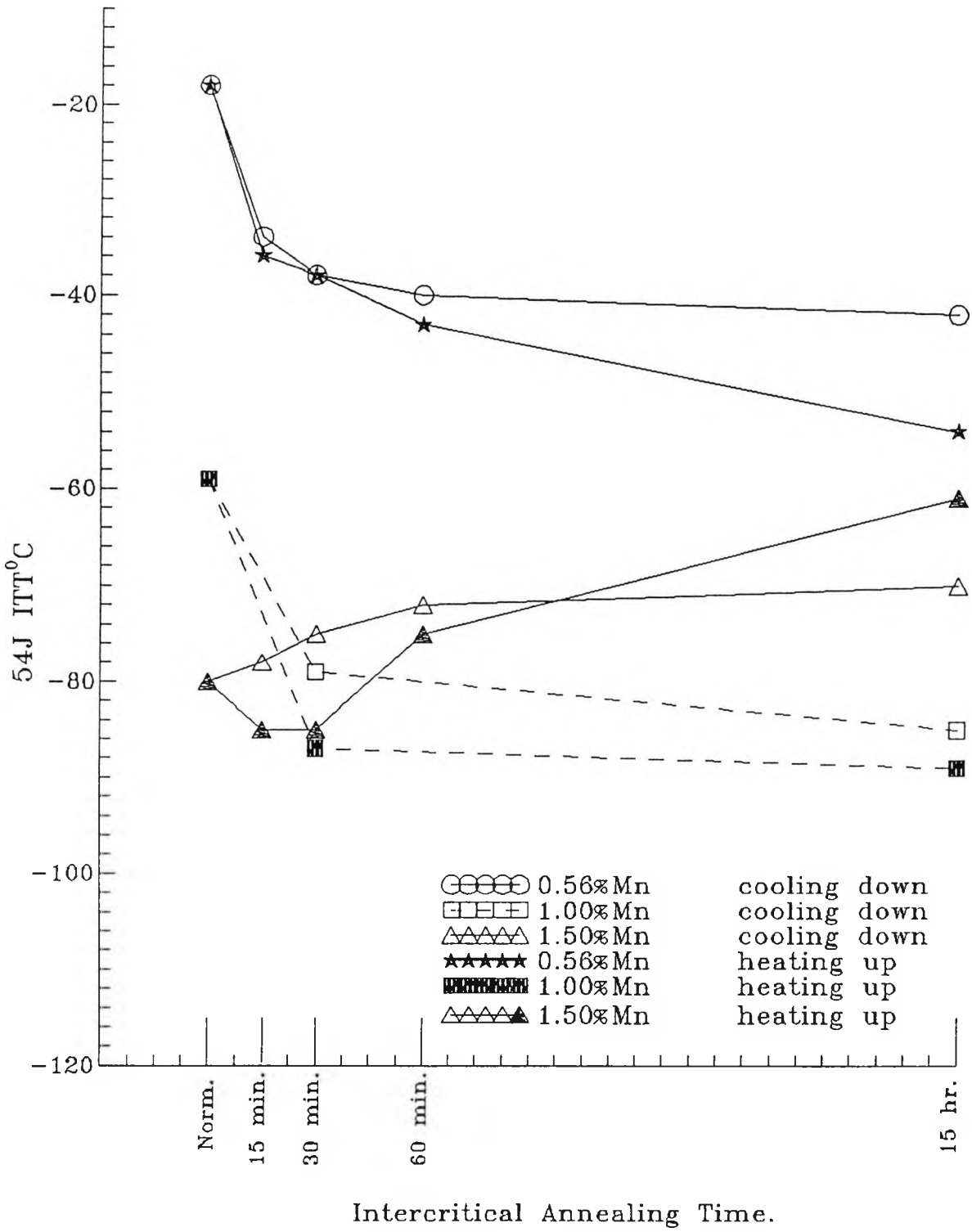

Fig. 4.13- The Effect of Manganese Level on the 54J ITT°C During I.A.

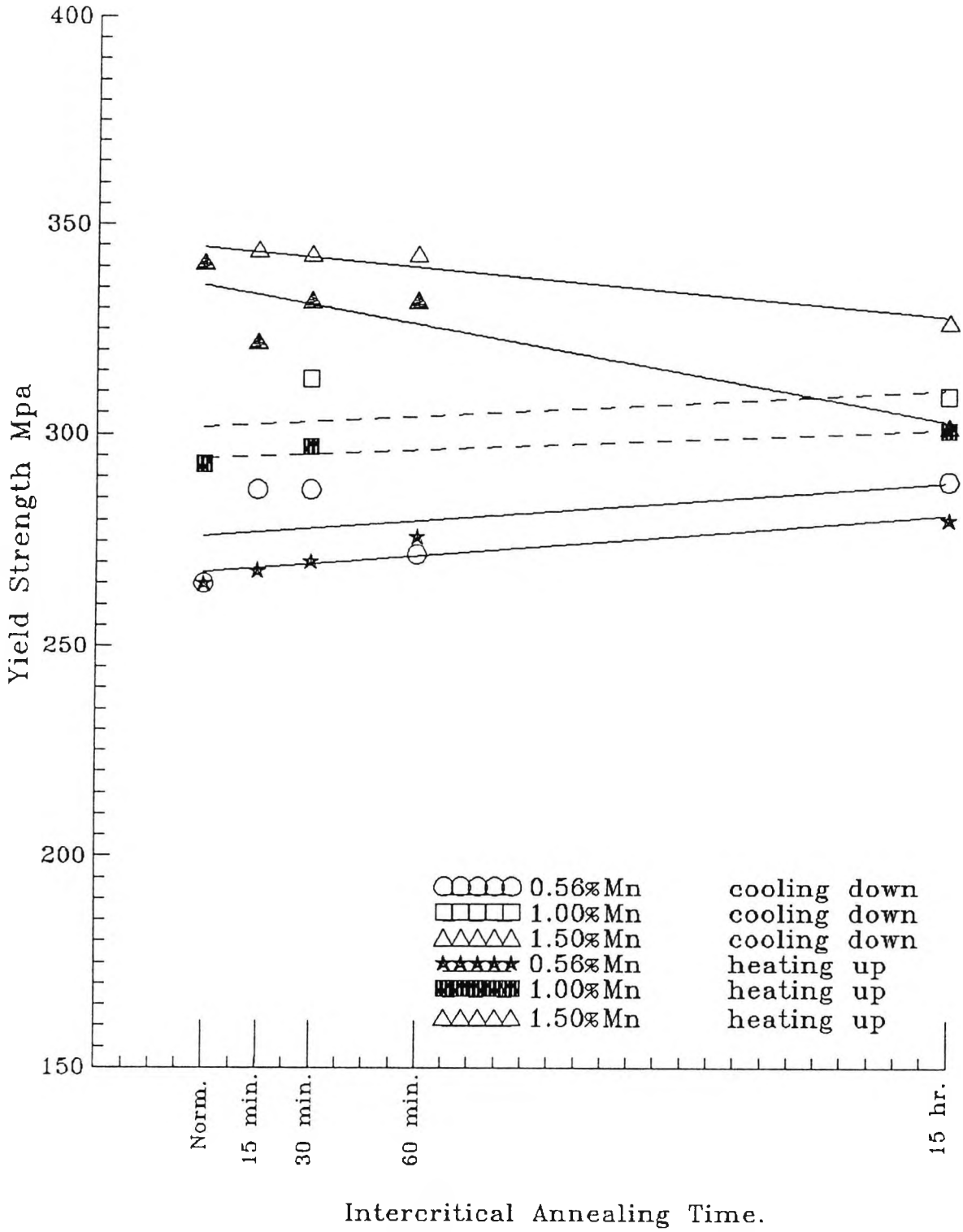

Fig.4.14- The Effect of Manganese Level on the Yield Strength During I.A.

4.1.4- COMPOSITIONAL CHANGES.

Manganese content measured at the centre of the pearlite colonies was found to have increased after holding for 15 hr at 730°C, as shown in table 4.5. Slightly more partitioning of manganese was observed on heating up than on cooling down. Silicon content was also measured at the center of the pearlite colonies and was found to decrease with intercritical annealing time.

Table 4.5. Average Mn and Si content of Ferrite and Pearlite Regions of C-Mn-Al-Nb Steels.

Heat Treatment	Holding Time Minutes	Mn %		Si %	
		In Ferrite	In Pearlite	In Ferrite	In Pearlite
1.5% Mn Steel					
Normalised	-	1.47	1.56	0.42	0.4
Reheated to 730°C	900	1.36	2.2	0.45	0.36
Cooled to 730°C	900	1.42	1.93	0.44	0.37
1% Mn Steel					
Normalised	-	0.92	1.18	0.24	0.23
Reheated to 730°C	900	0.92	1.61	0.3	0.213
Cooled to 730°C	900	1.02	1.63	0.283	0.224
0.56% Mn Steel					
Normalised	-	0.60	0.70	0.305	0.29
Reheated to 730°C	900	0.57	0.78	0.325	0.257
Cooled to 730°C	900	0.58	0.76	0.315	0.265

4.1.5- METALLOGRAPHY.

The change in microstructure with intercritical annealing time was followed by taking a series of optical photographs of the microstructure of samples cooled at 7°C/min to room temperature after intercritical annealing for various times.

4.1.5.1- MICRO-STRUCTURAL CHANGES FOR 0.56% Mn AND 1% Mn STEELS.

Figure 4.15(a), and Figure 4.16(a) show the microstructure of the 0.56% Mn and 1% Mn steels respectively after normalising.

It can be seen that, the structure consists of equiaxed ferrite grains plus banded pearlite colonies.

4.1.5.1.1- COOLING DOWN TO THE INTERCRITICAL ANNEALING TEMPERATURE.

Figure 4.15 (b,c) and Figure 4.16 (b,c) show the microstructure of the 0.56% Mn and 1% Mn steels respectively after intercritical annealing at 730°C for 30 minutes and 15 hours. It can be seen that, the size of the pearlite colonies increases with increasing holding time.

4.1.5.1.2- HEATING UP TO THE INTERCRITICAL ANNEALING TEMPERATURE.

Figure 4.17 (a,b) and Figure 4.18 (a,b) show the microstructure of the 0.56% Mn and 1% Mn steels after

intercritical annealing at 730°C for 30 minutes and 15 hours respectively. It can be seen that, new small pearlite colonies were observed after 30 minutes, and their size and coverage of grain boundaries increased with increasing intercritical annealing time.

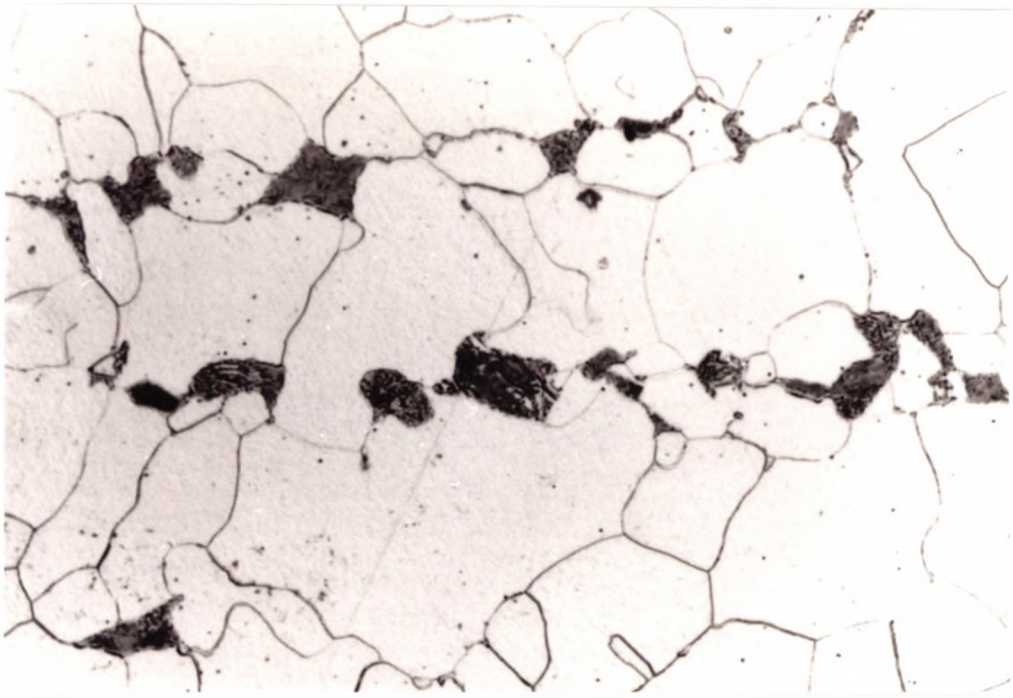

-a- x 900

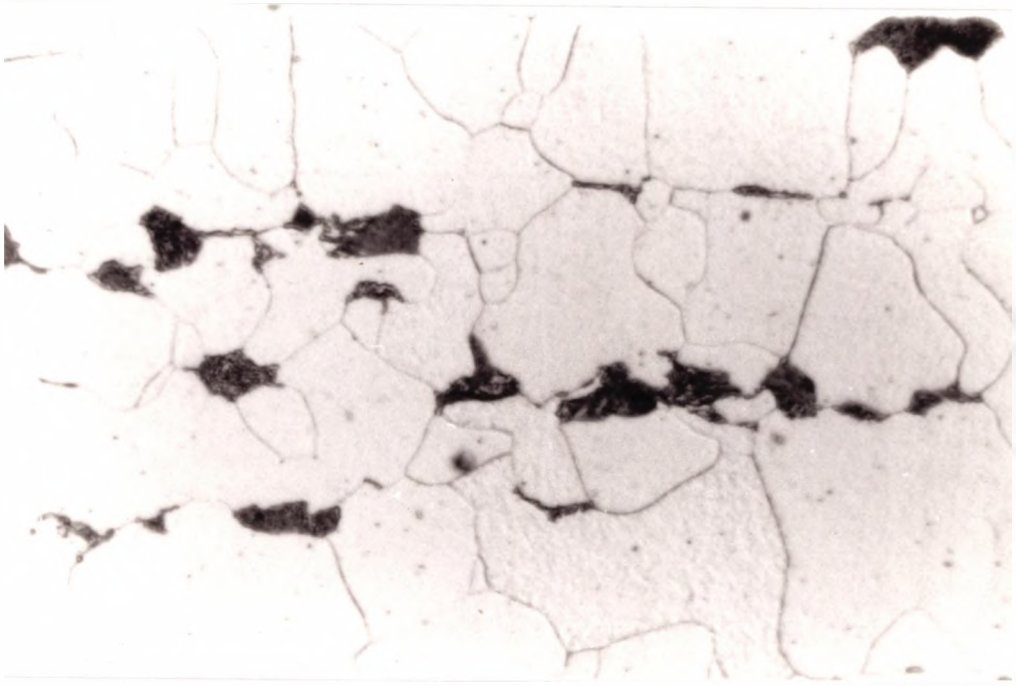

-b- x 900

Fig.4.15- Microstructure of the 0.56%Mn Steel.

a- Normalised, b- I.A. for 30 min at 730°C,

Cooled at 7°C/min, Cooling Down Cycle.

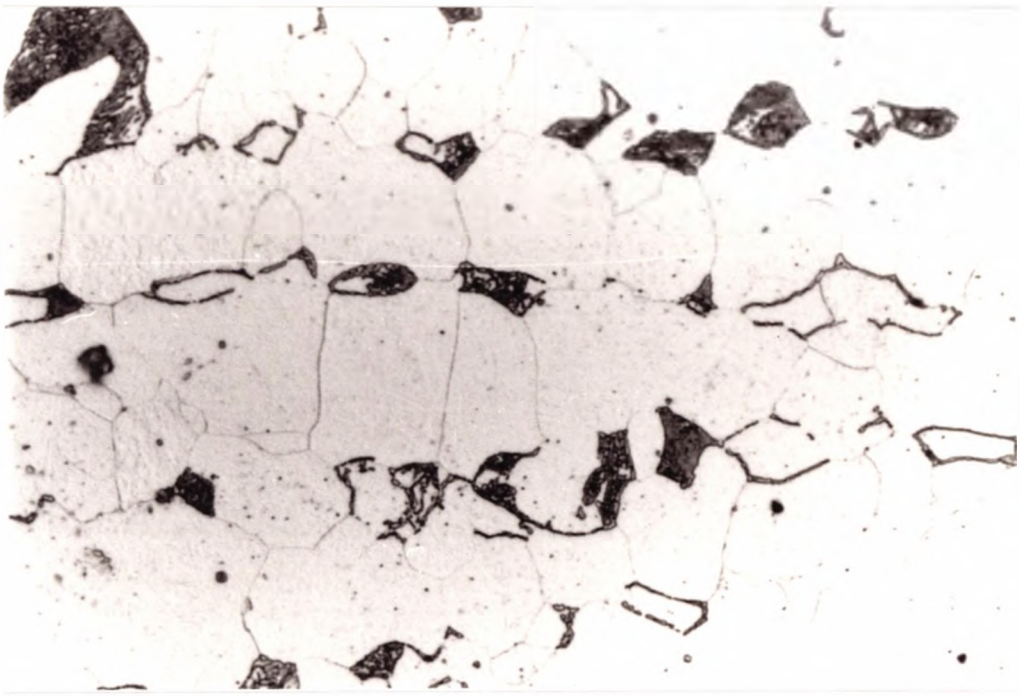

-c- x 900

Fig.4.15c- Microstructure of the 0.56%Mn Steel I.A at 730°C for 15 Houres, Cooled at 7°C/min, Cooling Down Cycle.

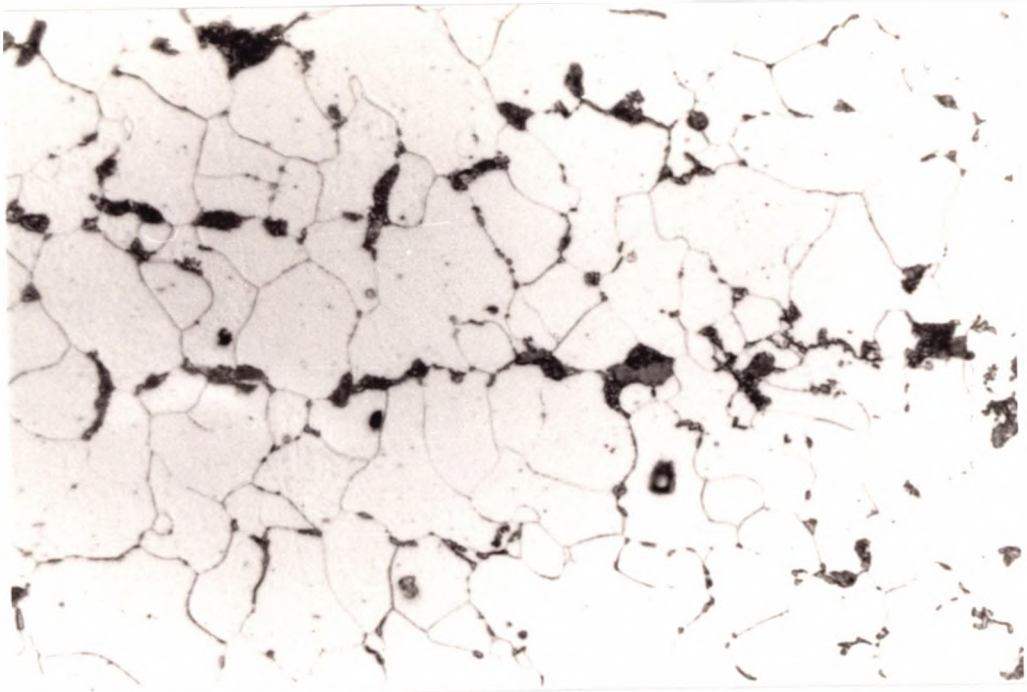

-a- x 900

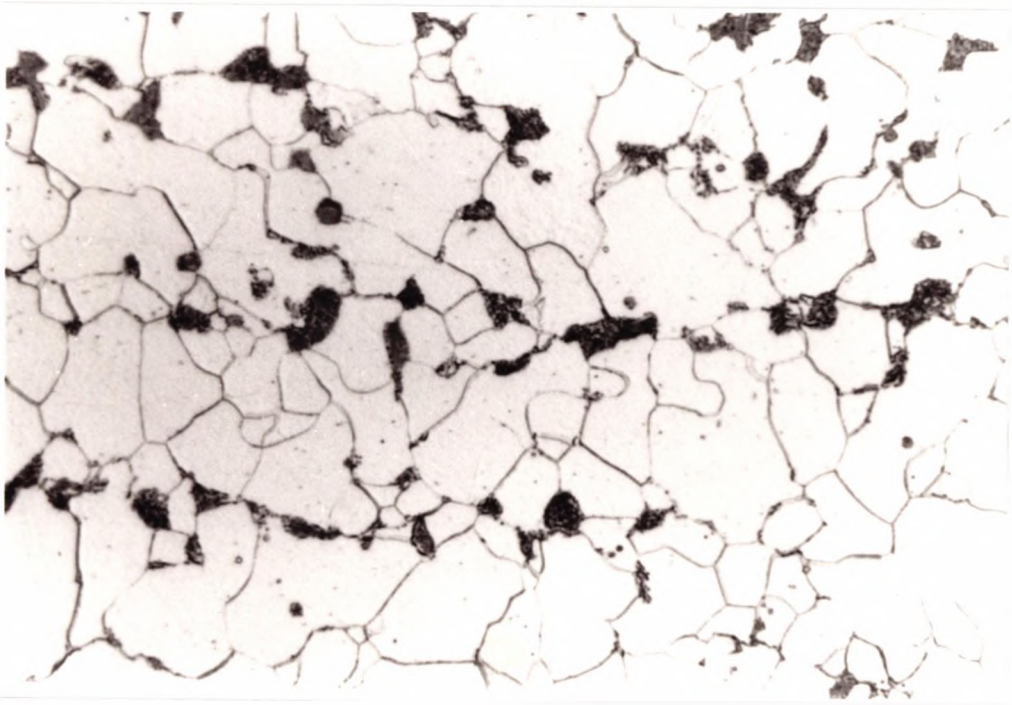

-b- x 900

Fig.4.16- Microstructure of the 1.0%Mn Steel.

a- Normalised., b- I.A. for 30 min at 730°C,

Cooled at 7°C/min, Cooling Down Cycle.

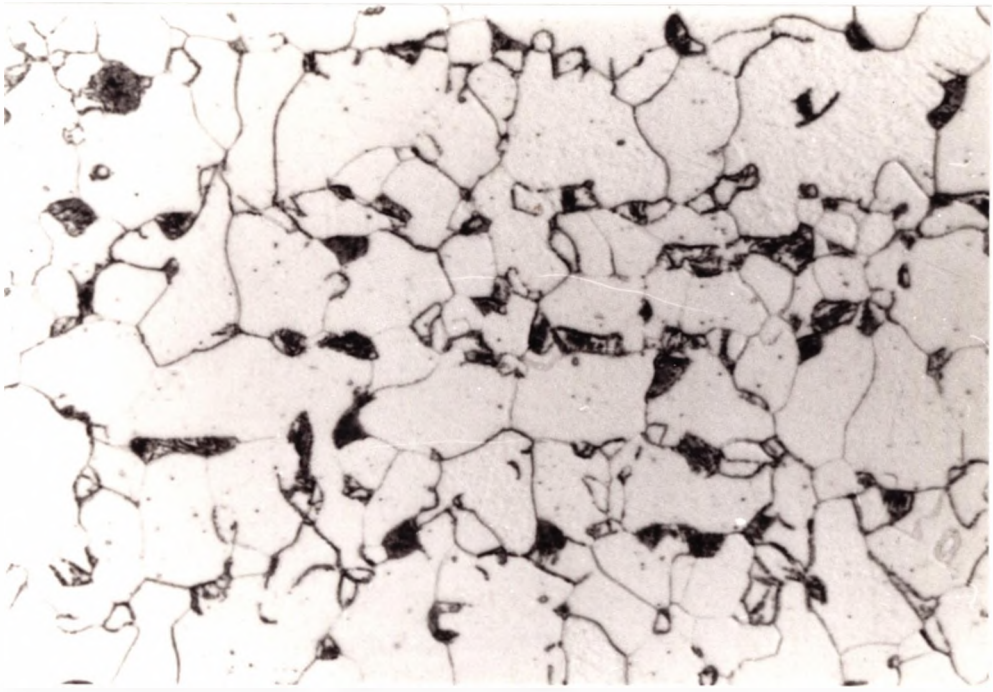

-c- x 900

Fig.4.16c- Microstructure of the 1.0%Mn Steel I.A. at 730°C for 15 Houres, Cooled at 7°C/min, Cooling Down Cycle.

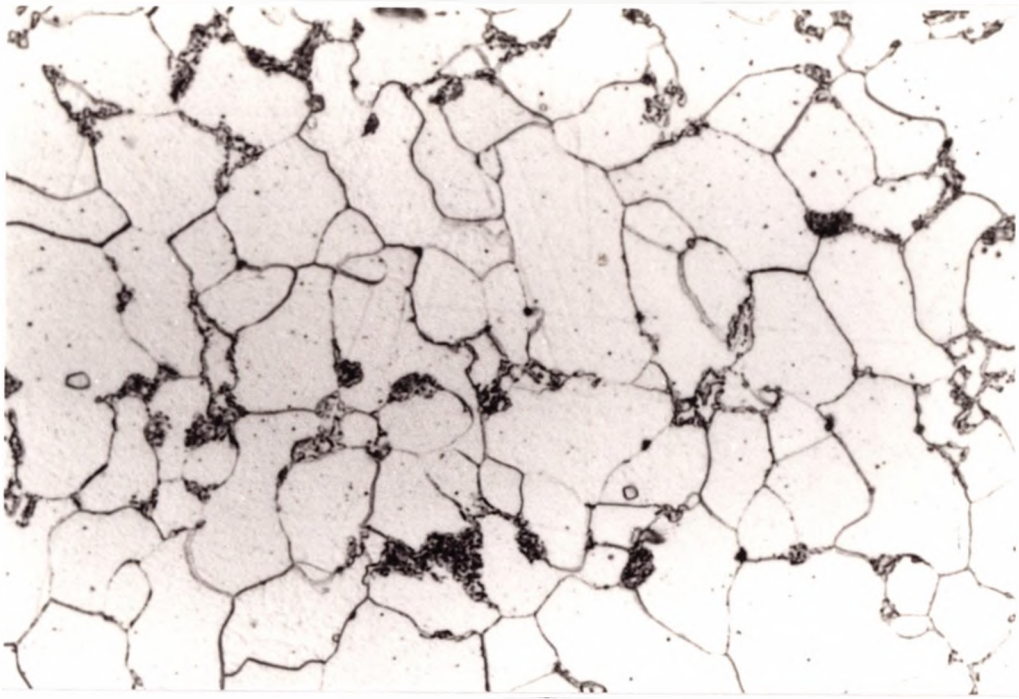

-a- x 900

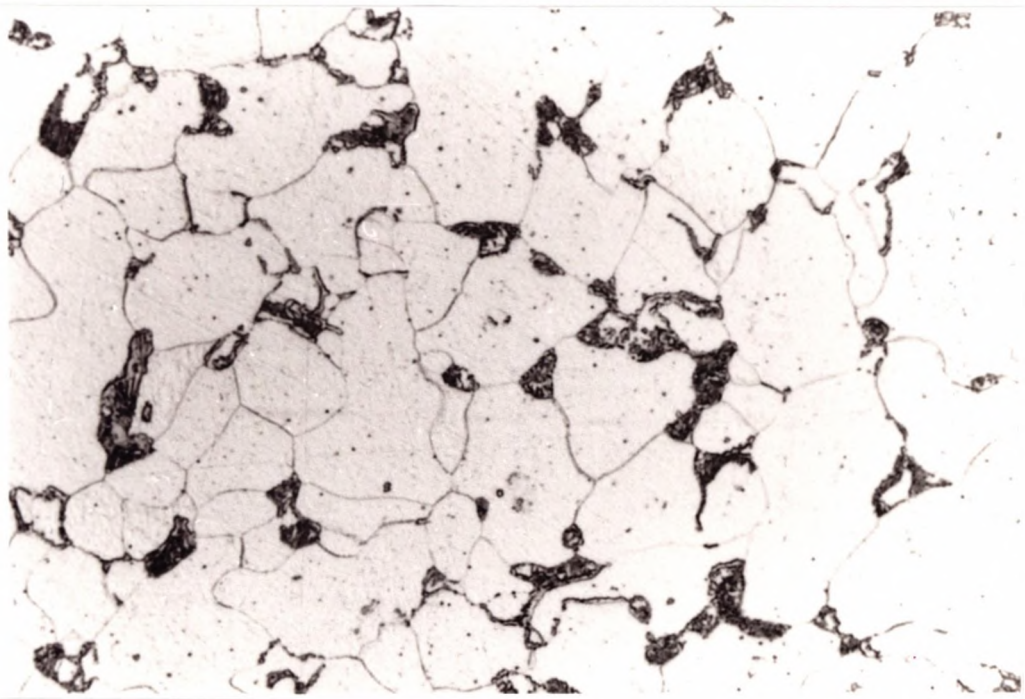

-b- x 900

Fig.4.17- Microstructure of 0.56%Mn Steel I.A. at 730°C, Cooled at 7°C/min, Heating Up Cycle.

a- for 30 min., b- for 15 hr.

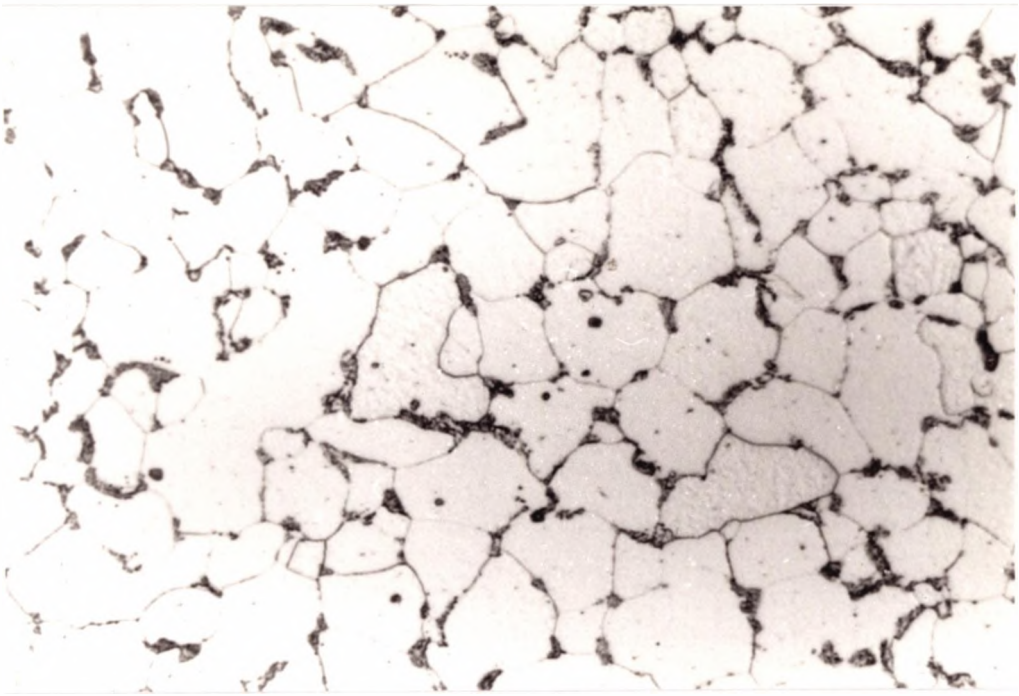

-a- x 900

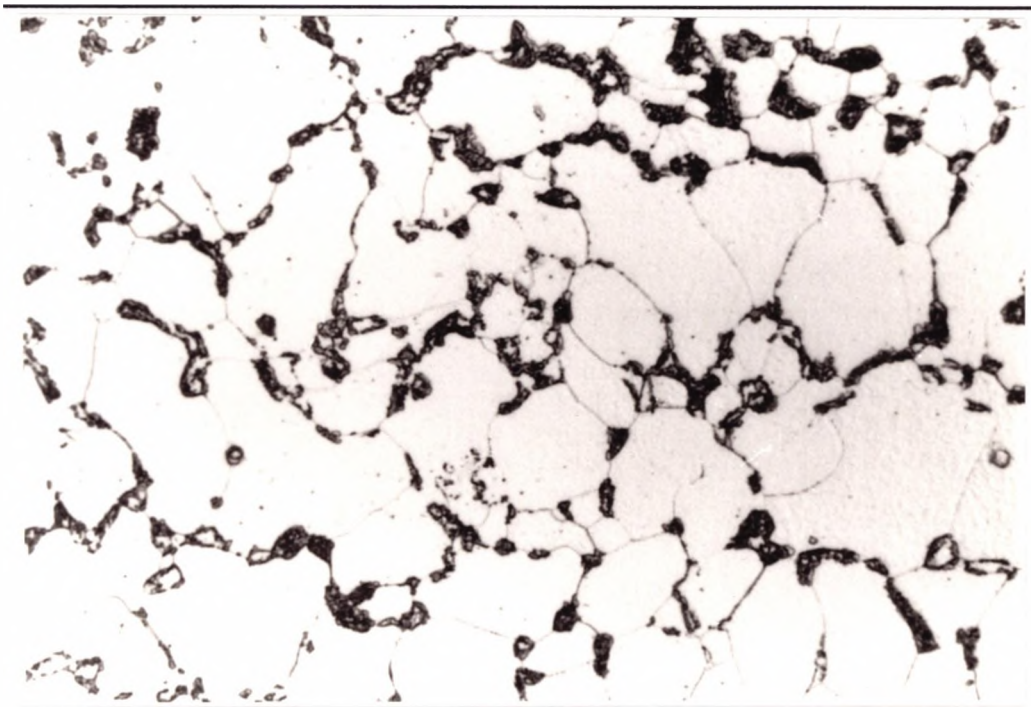

-b- x 900

Fig.4.18- Microstructure of 1.0%Mn Steel

I.A. at 730°C, Heating Up Cycle.

a- for 30 min., b- for 15 hr.

4.1.5.2- METALLOGRAPHY of the 1.49% Mn STEEL.

4.1.5.2.1-COOLING DOWN TO THE INTERCRITICAL ANNEALING TEMPERATURE.

Figure 4.19 (1 and 2) shows the microstructure of the 1.49% Mn steel after normalising and after intercritical annealing at 730°C for 30 minutes and 15 hours. Pearlite banding is evident in the normalised condition and this intensifies after intercritical annealing for 30 minutes.

The grains seem to be extended in the direction normal to the pearlite bands suggesting that these bands may be having some influence on the grain shape. Long time intercritical annealing seemed to reduced the pearlite banding. The long time intercritical annealing seemed to produce a more uniform distribution of pearlite. As well as the volume fraction of pearlite increasing, the size of the pearlite colonies also increased, with increasing intercritical annealing time.

4.1.5.2.2- HEATING UP TO THE INTERCRITICAL ANNEALING TEMPERATURE.

Figure 4.20 (1 and 2) shows the microstructure of the 1.49% Mn steel after intercritical annealing at 730°C for 30 minutes and 15 hours.

It can be seen that, the pearlite banding present in the normalised conditions is broken up on intercritical annealing. The pearlite phase first forms as a thin film round the ferrite grain. With increasing time, this film

thickens and extends producing a network around the ferrite phase.

After holding for 15 hours some martensite was found to be present at the edges of the pearlite colonies or as thin colonies along the boundaries as shown in Figure 4.21.

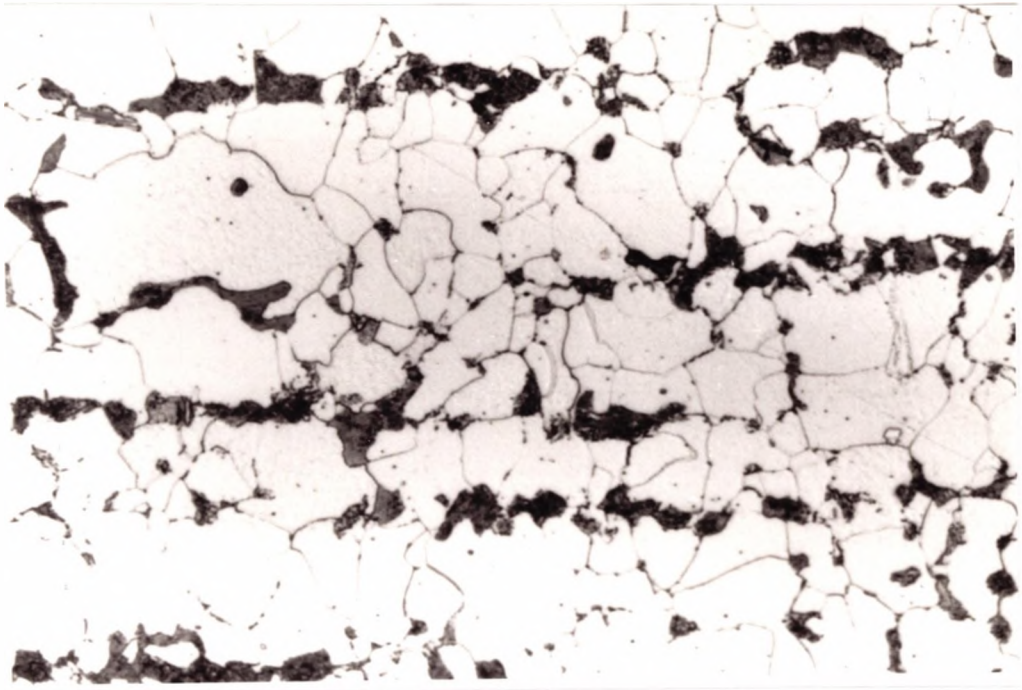

-a- x 900

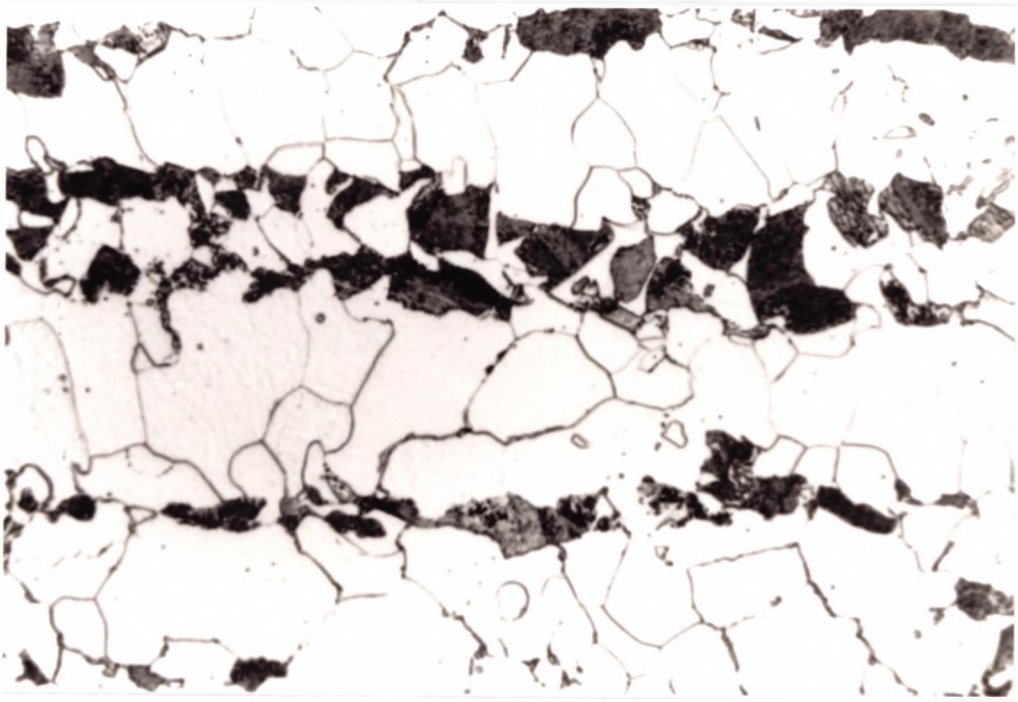

-b- x 900

Fig.4.19 (1)- Microstructure of the 1.49%Mn Steel, a- Normalised., b- I.A for 30 min at 730°C, Cooled at 7°C/min, Cooling Down Cycle.

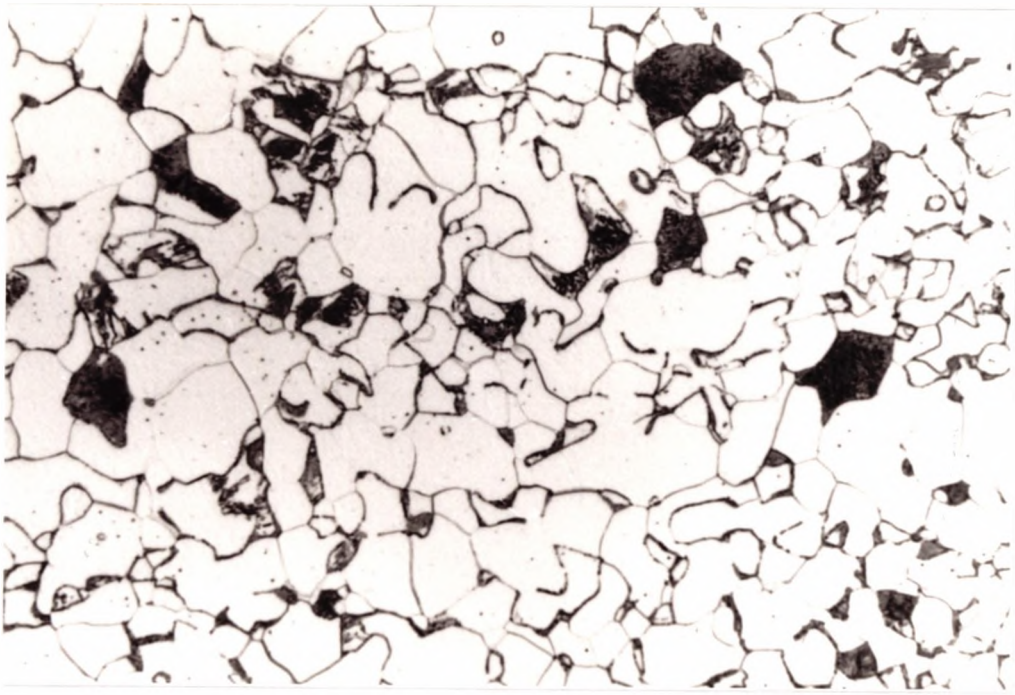

-c- x 900

Fig.4.19 (1)c- Microstructure of the 1.49%Mn Steel I.A. at 730°C for 15 Houres, Cooling Down Cycle.

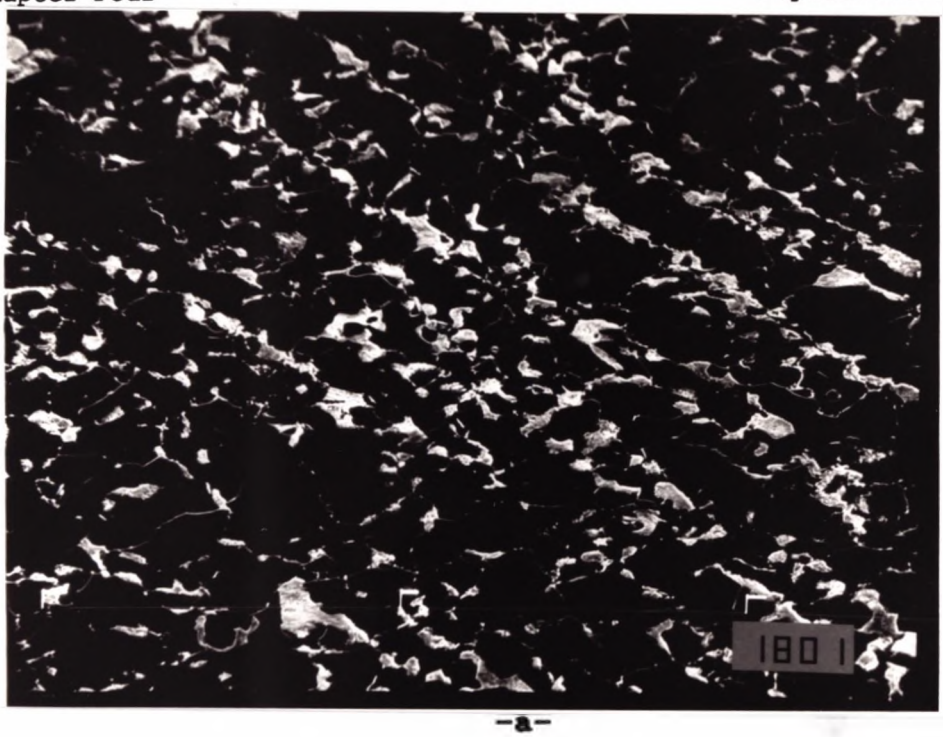

-a- x 1000

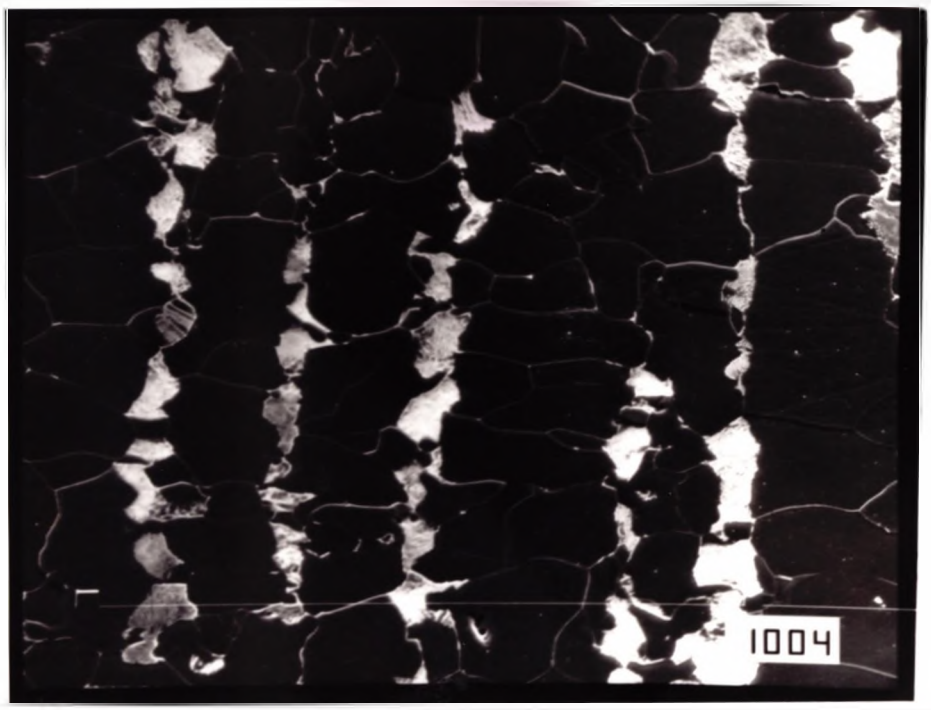

-b- x 1000

Fig.4.19 (2)- Microstructure of the 1.49%Mn Steel,

a- Normalised., b- I.A for 30 min at 730°C,

Cooled at 7°C/min, Cooling Down Cycle.

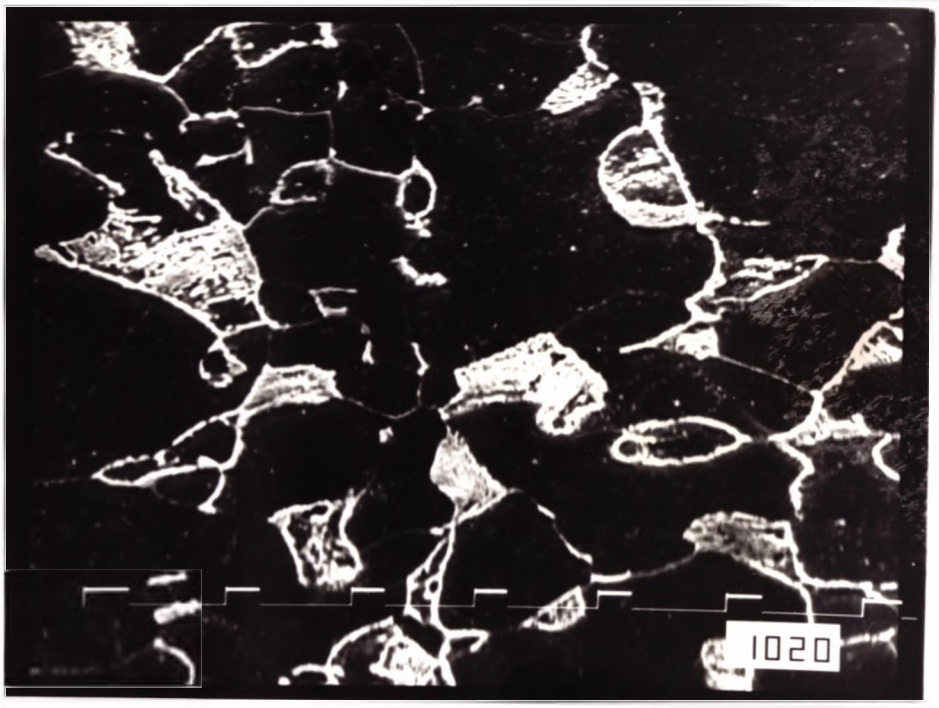

-c- x 900

Fig.4.19 (2)c- Microstructure of the 1.49%Mn Steel I.A. at 730°C for 15 Houres, Cooling Down Cycle.

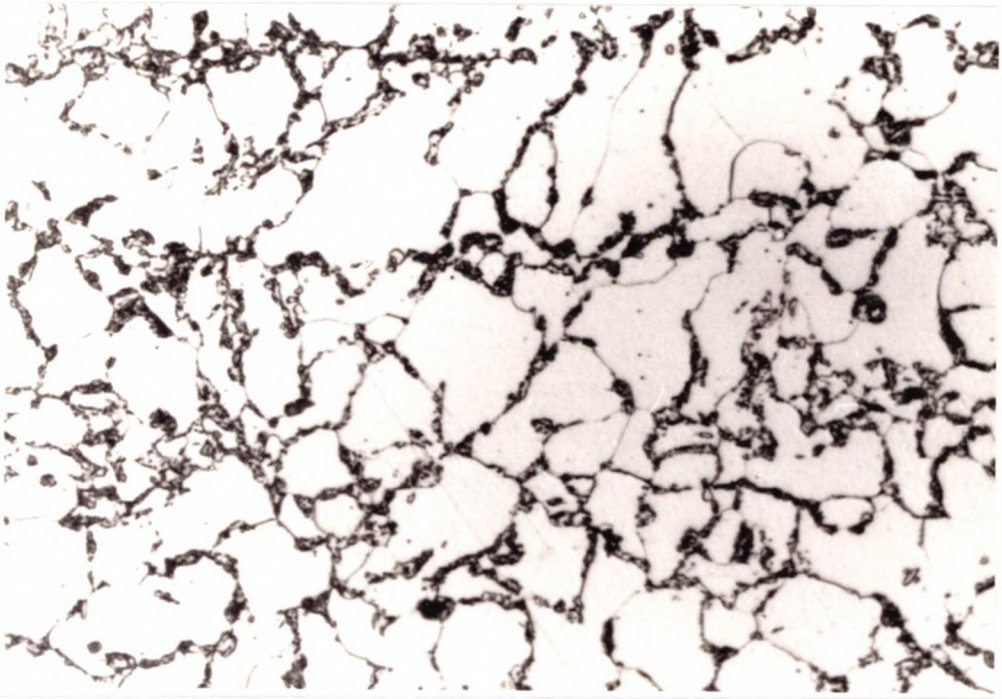

-a- x 900

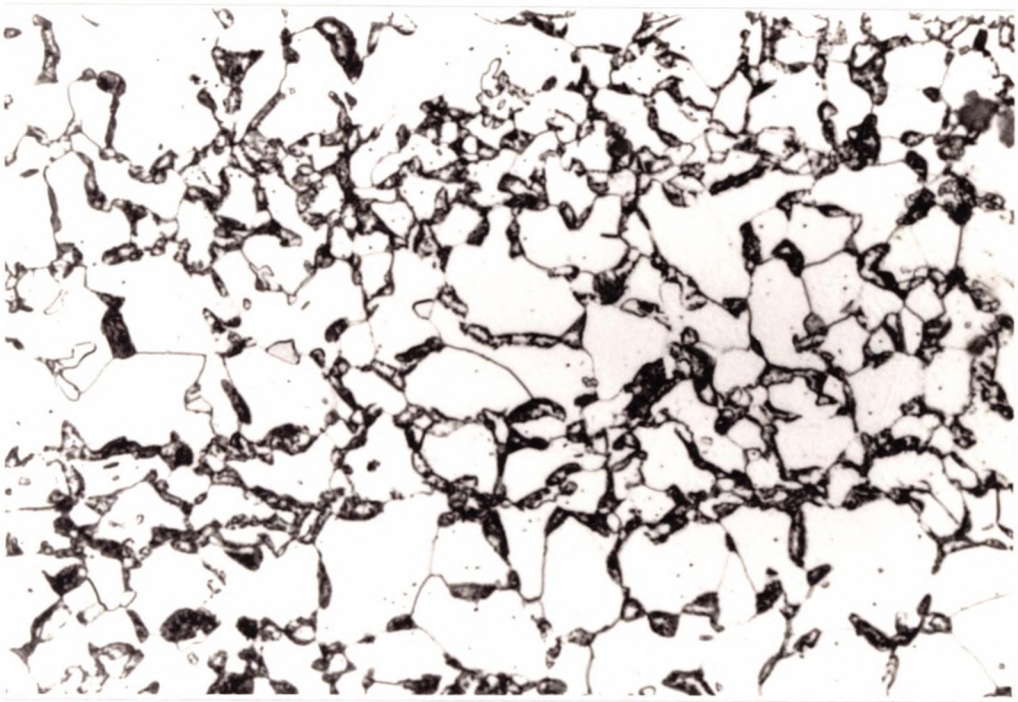

-b- x 900

Fig.4.20(1)- Microstructure of the 1.49%Mn Steel I.A. at 730°C, Cooled at 7°C/min, Heating Up Cycle a- for 30 min., b- for 15 hr.

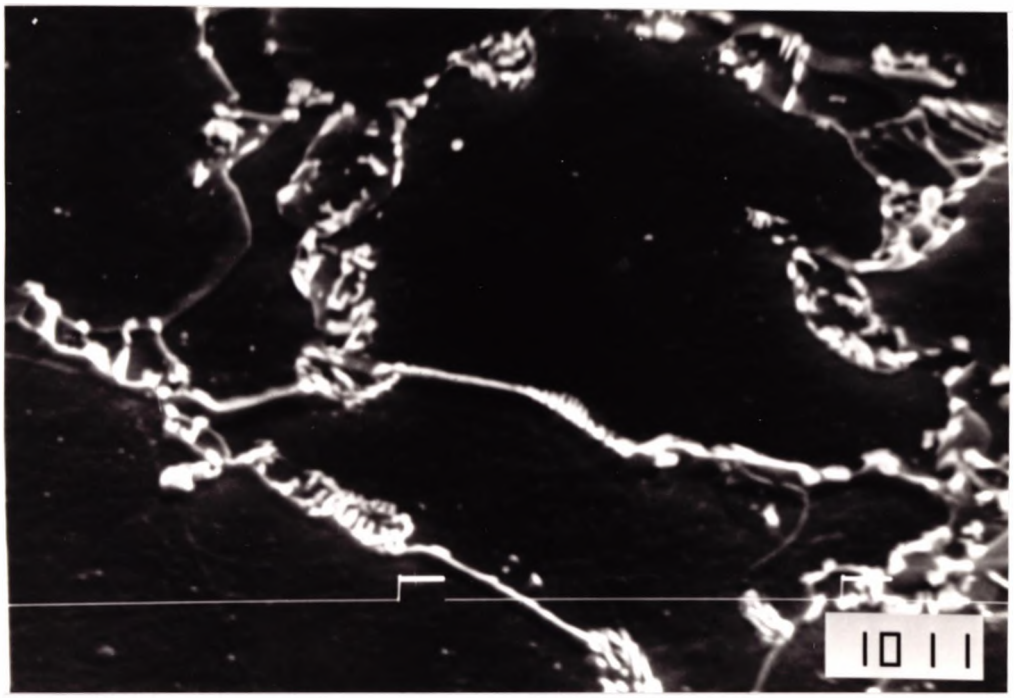

-a- x

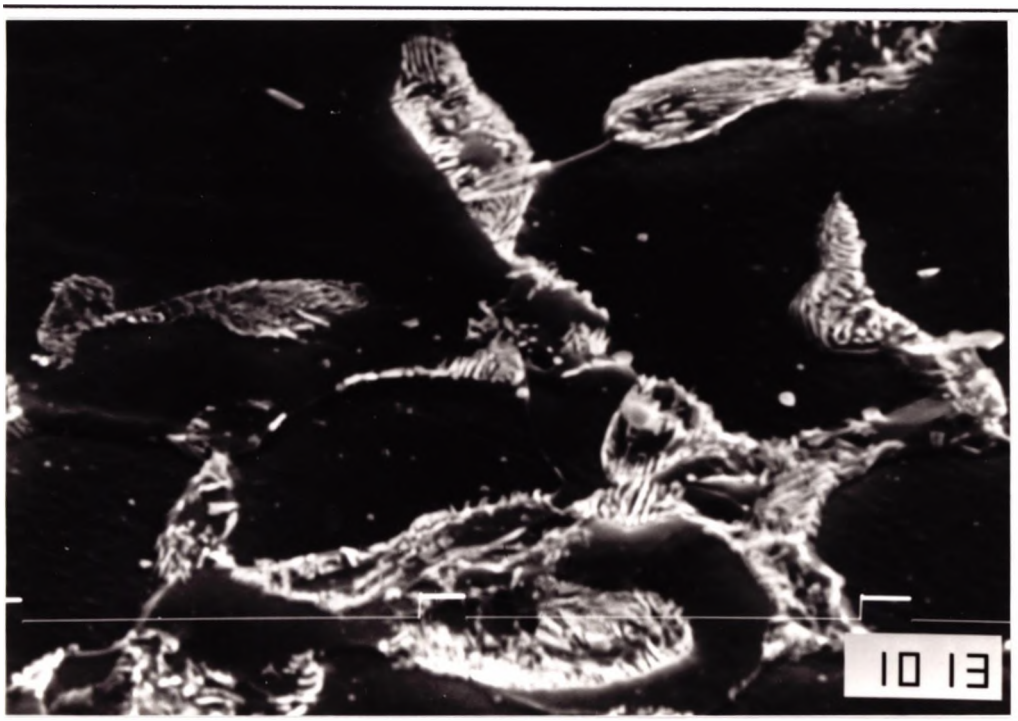

-b- x

Fig.4.20(2)- Microstructure of the 1.49%Mn Steel I.A. at 730°C, Cooled at 7°C/min, Heating Up Cycle

a- for 30 min., b- for 15 hr.

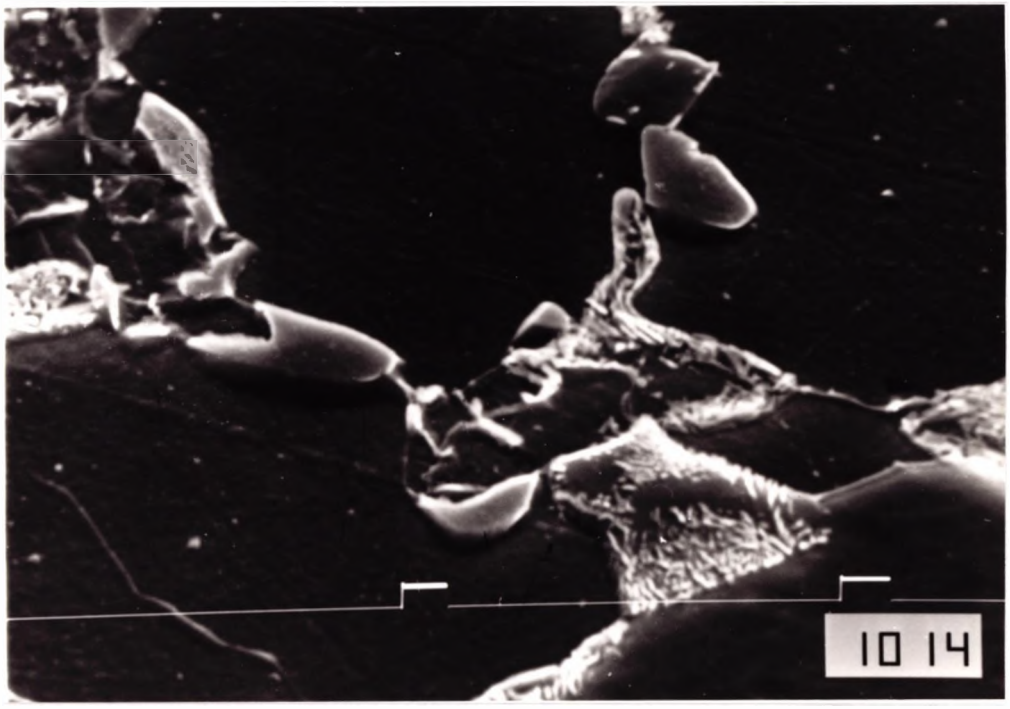

x 5 000

Fig.4.21- Martensite Formation After 15 Hours I.A., Heating Up Cycle.

4.1.6- METALLOGRAPHY, MARTENSITE VOLUME FRACTION, AND MICROHARDNESS OF 0.56%Mn AND 1.49% Mn STEEL INTERCRITICAL ANNEALED FOR VARIOUS TIMES AND QUENCHED.

4.1.6.1- METALLOGRAPHY OF 1.49%Mn STEEL.

The change in microstructure with intercritical annealing time was followed by taking a series of optical photographs of the microstructure of samples quenched from 730°C in ice brine after intercritical annealing for various times.

4.1.6.1.1- COOLING DOWN TO THE INTERCRITICAL ANNEALING TEMPERATURE.

Figure 4.22 shows the microstructure of the 1.49% Mn Steel after intercritical annealing at 730°C for 0, 15, 30, and 900 minutes.

It can be seen that the martensite volume fraction decreases after 15 minutes, but after 30 minutes the volume fraction of martensite again increases with intercritical annealing time as shown in Figure 4.22(d)..

4.1.6.1.2- HEATING UP TO THE INTERCRITICAL ANNEALING.

Figure 4.23 shows the microstructure of the 1.49% Mn steel after intercritical annealing at 730°C for 0, 15, 30, and 900 minutes.

It can be seen that, the martensite volume fraction increases with increasing intercritical annealing time. The martensite surrounds the ferrite and produces a continuous network around the matrix after 15 hours.

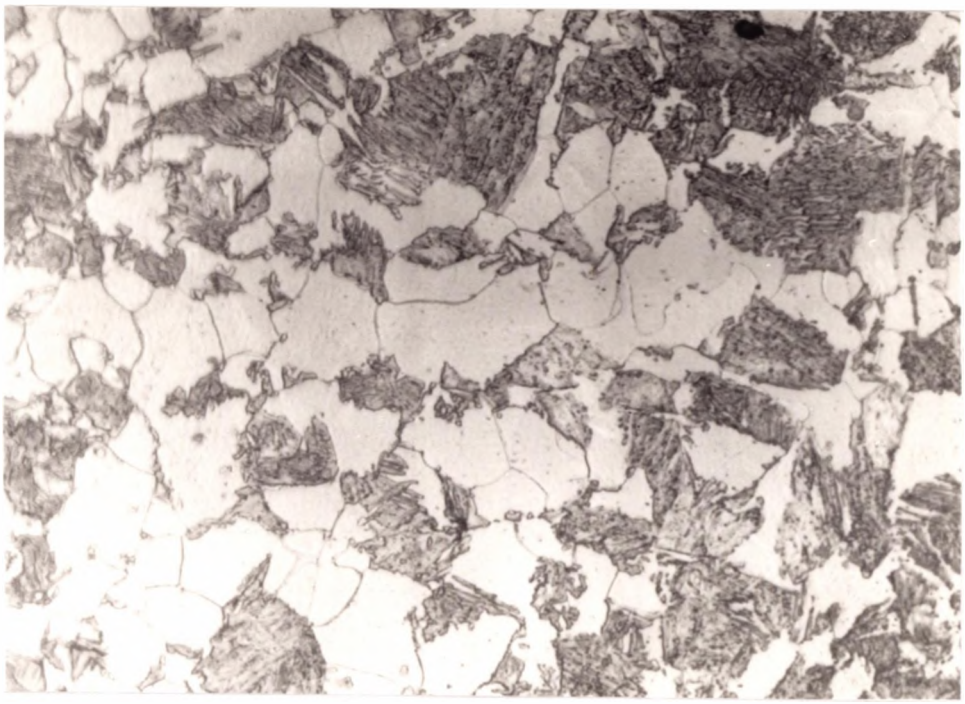

-a- x 1000

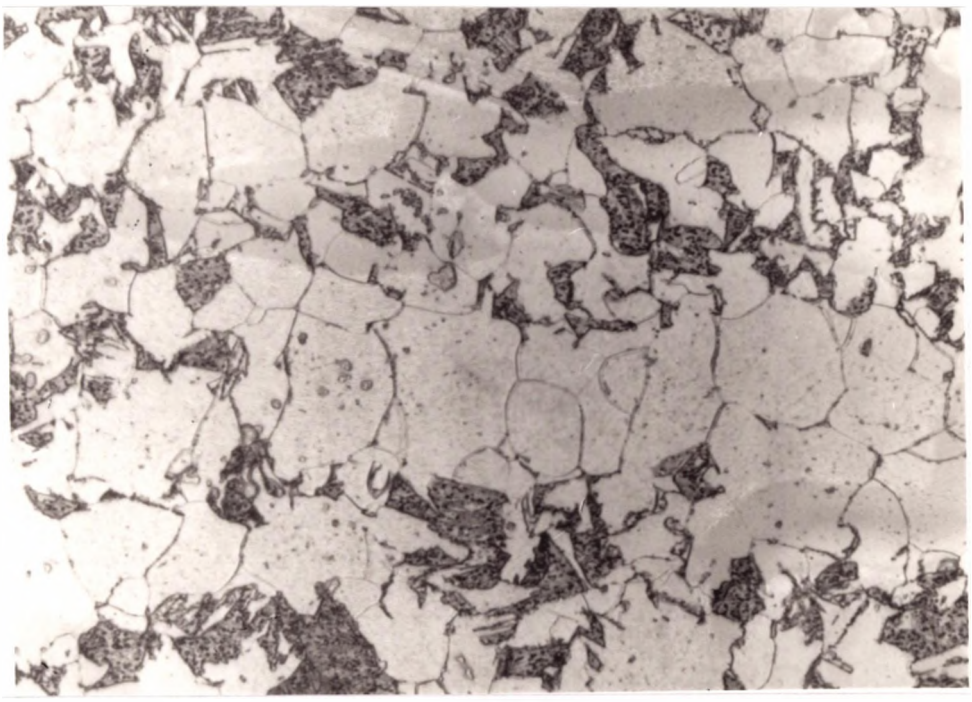

-b- x1000

Fig.4.22- Microstructure of 1.49%Mn Steel After I.A. at 730°C and Quenching, Cooling Down Cycle a- for 0 min., b- for 15 min.

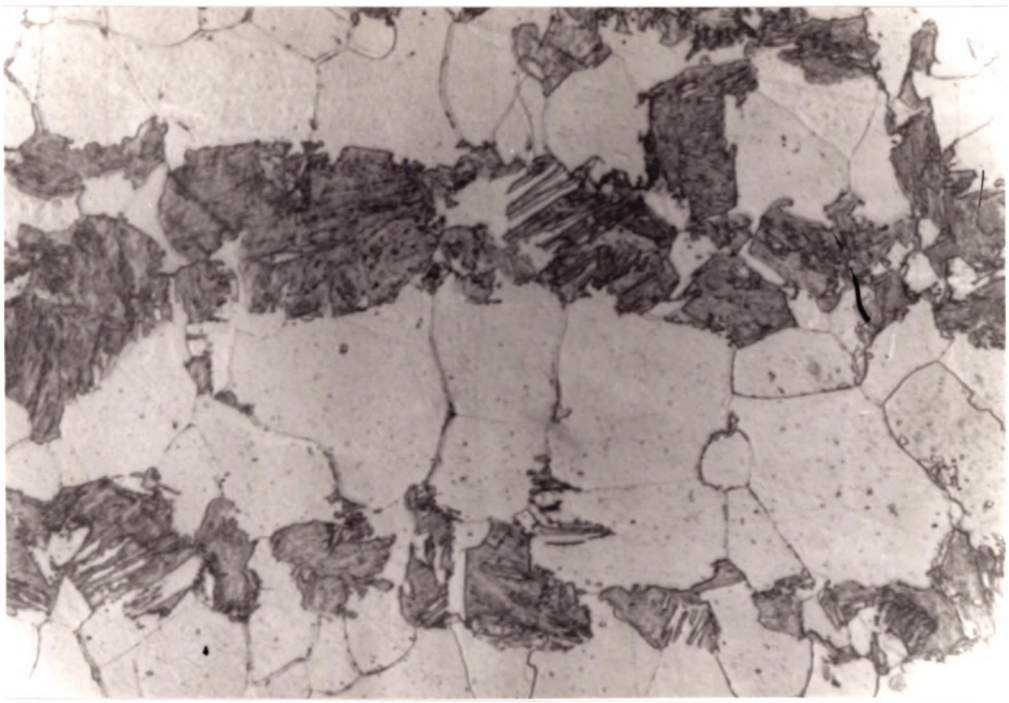

-c- x1000

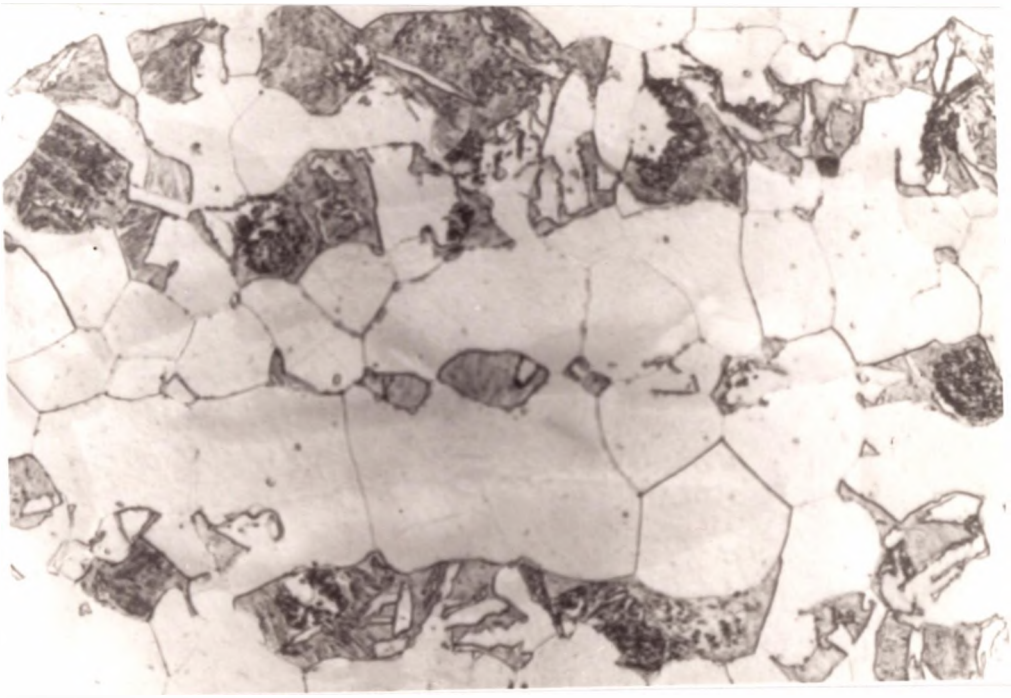

-d- x1000

Fig.4.22- Microstructure of 1.49%Mn Steel After I.A. at 730°C and Quenching, Cooling Down Cycle c- for 30 min., d- for 900 min.

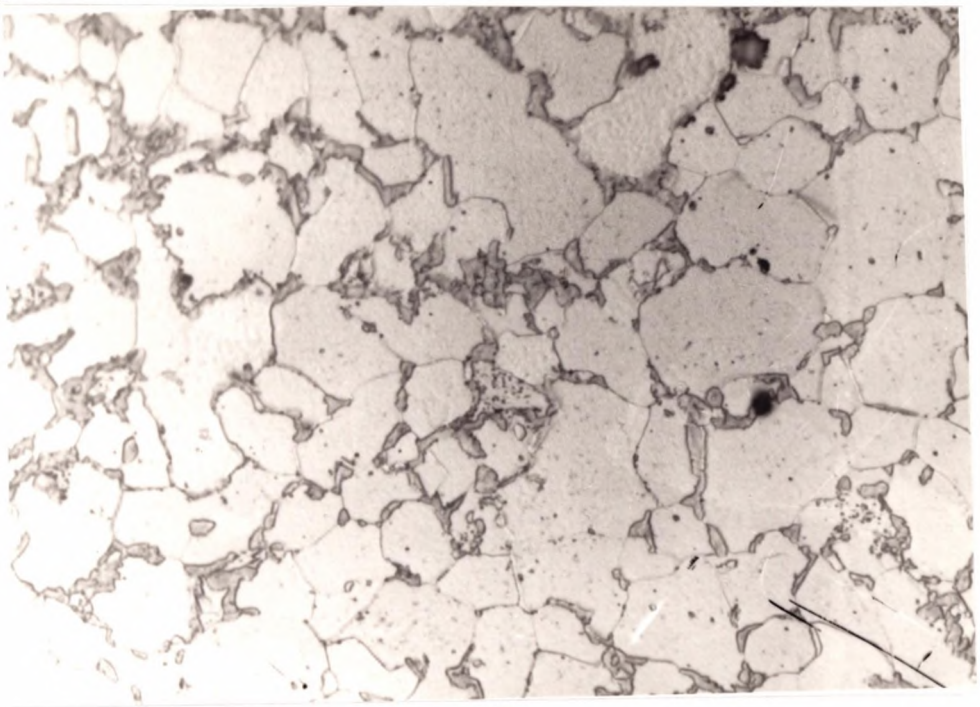

-a- x1000

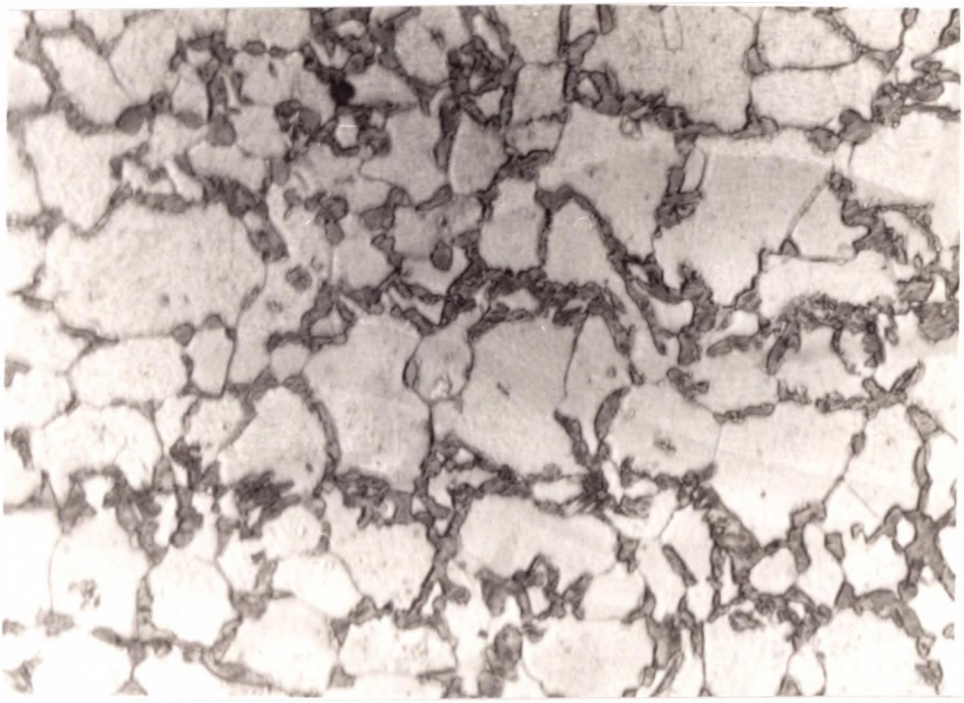

-b- x1000

Fig.4.23- Microstructure of 1.49%Mn Steel After I.A. at 730°C and Quenching, Heating Up Cycle a- for 0 min., b- for 15 min.

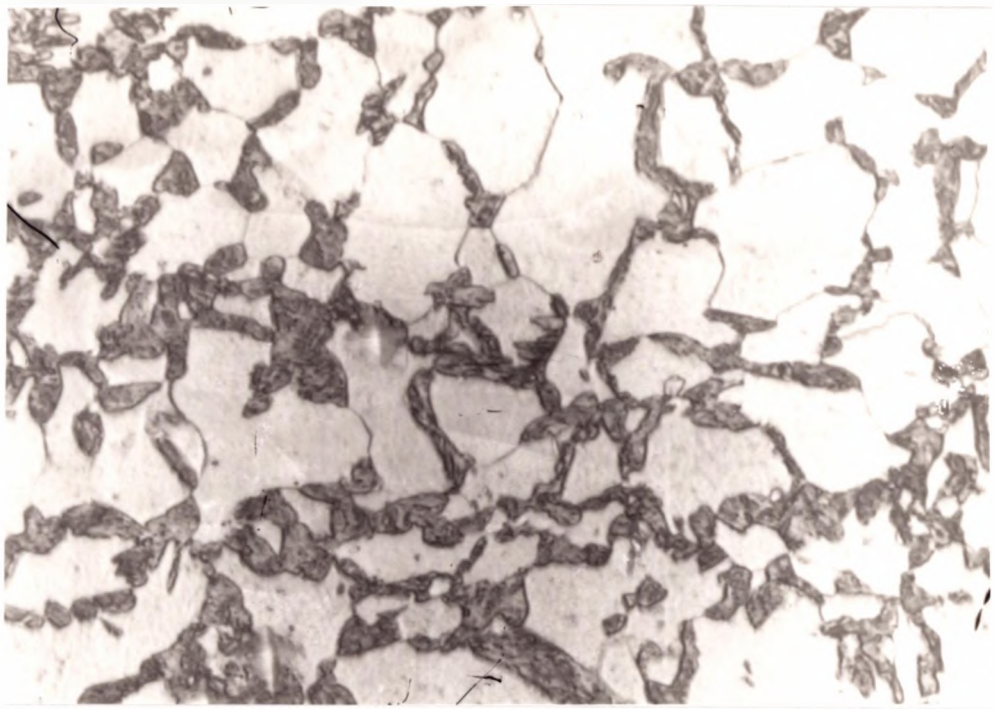

-c- x 1000

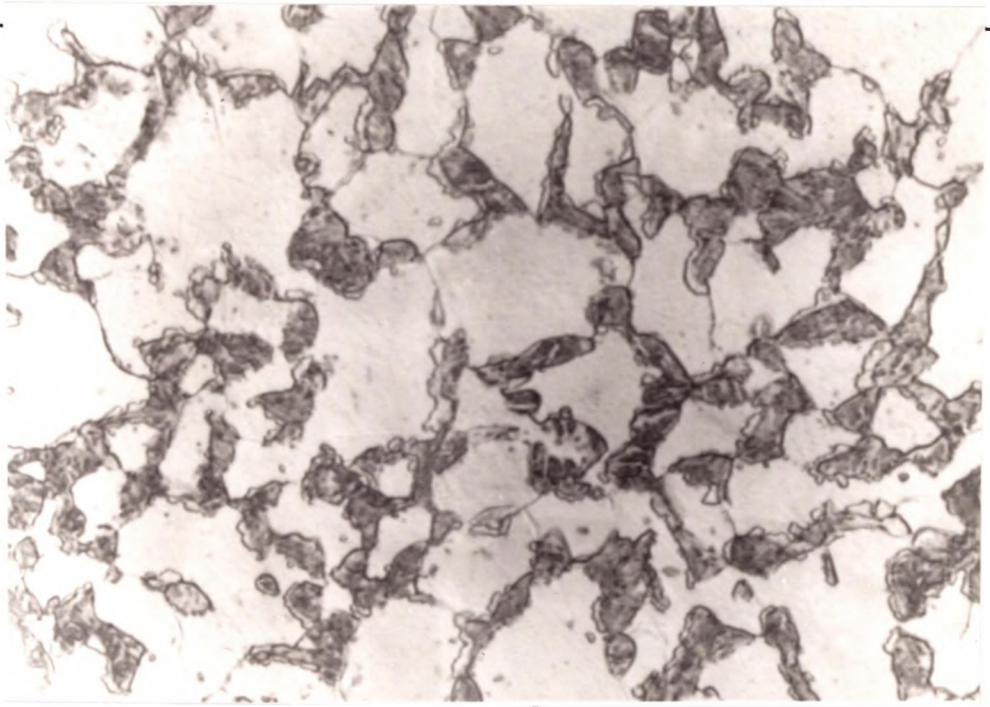

-d- x 1000

Microstructure of 1.49% Mn Steel I.A. at 730°C and Quenching, Heating up Cycle

c- for 30 min., d- for 900 min.

4.1.6.2- MARTENSITE VOLUME FRACTION.

The volume fraction of martensite after quenching from the intercritical annealing temperature, VmQ, as a function of intercritical annealing time are listed in table 4.6 for the 1.49% Mn and 0.56% Mn steel intercritically annealed at 730°C for 0, 15, 30, 60, and 900 minutes, for both heating up directly to the intercritical annealing temperature and cooling down to the intercritical annealing temperature.

Figure 4.24 shows the effect of intercritical annealing time on the volume fraction of austenite (measured from the martensite volume fraction) as a function of intercritical annealing time. It can be seen for both steels (0.56%, 1.49% Mn) during heating directly to the intercritical annealing temperature, increasing heating time leads to an increase in the austenite volume fraction. On cooling down to the intercritical annealing temperature, the austenite volume fraction for the two steels (1.49%Mn, and 0.56%Mn) first decreases, and then increases again gradually with increase in heating time.The changes in austenite volume fraction with intercritical annealing as might be expected are much reduced for the lower manganese steel.

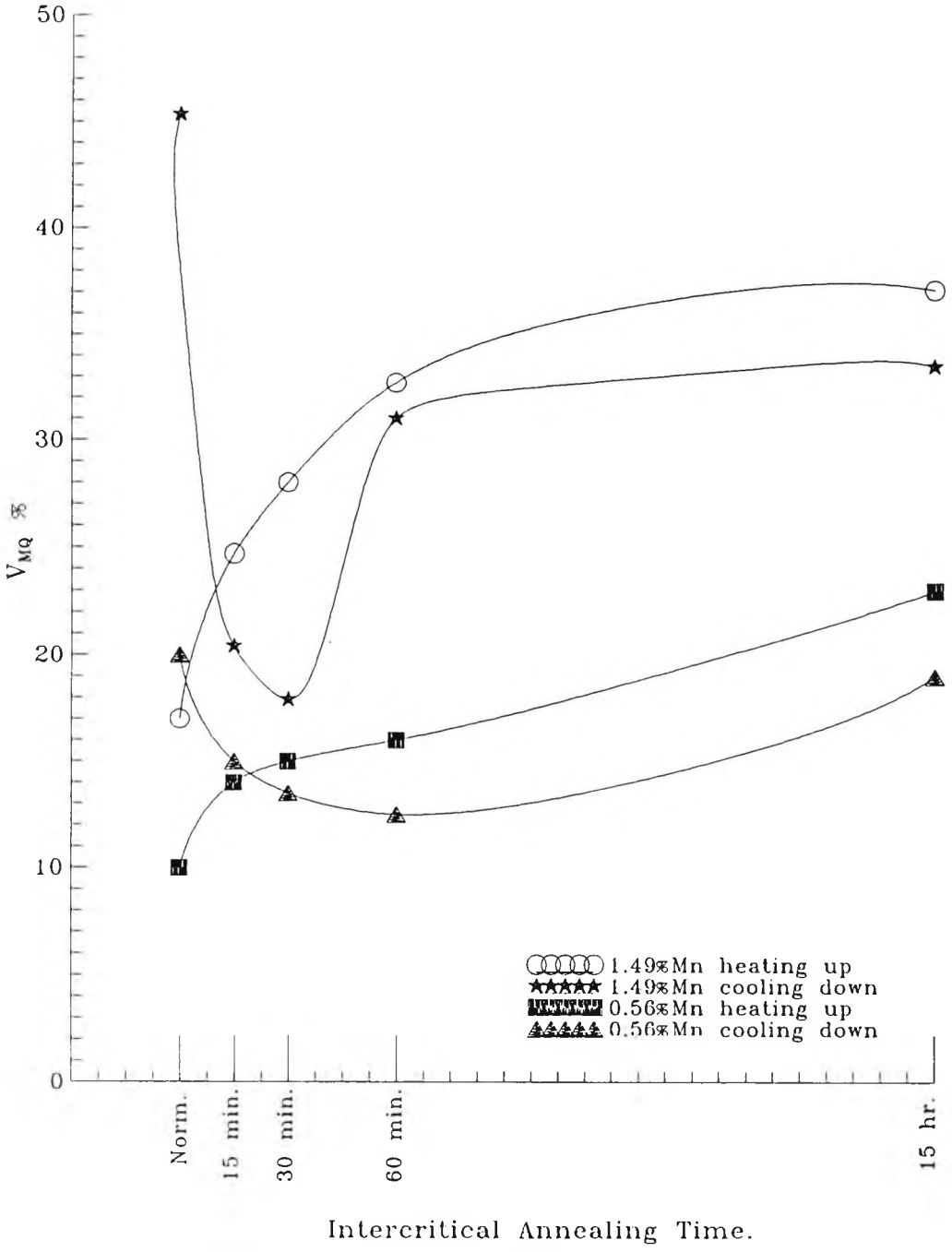

Fig. 4.24-Influence of I.A. Time on Volume Fraction of austensite (Measured from Volume Fraction of Martensite Produced on Quenching V_{MQ}) for 1.49%Mn Steel.

Table 4.6- Volume Fraction of Martensite, V_{MQ}, as a Function of I.A. Time.

(A)- Cooling Down.

Intercritical Annealing Time mins.	0	15	30	60	900
V_{MQ} 1.49% Mn Steel	45.0	20.0	18.0	32.0	34.0
V_{MQ} 0.56% Mn Steel	20.0	15.0	12.0	14.0	19.0

(B)- Heating Up.

Intercritical Annealing Time mins.	0	15	30	60	900
V_{MQ} 1.49% Mn Steel	17.0	25.0	26.0	33.0	37.0
V_{MQ} 0.56% Mn Steel	10	14.0	15.0	16.0	23.0

4.1.6.3- MICRO-HARDNESS MEASUREMENTS.

Microhardness values were obtained at the center of the ferrite grains and in the center of the martensite colonies for the 1.49% Mn steel after intercritical annealing followed by quenching and are listed in table 4.7.

Figure 4.25 shows the effect of intercritical annealing time on the microhardness of ferrite and martensite for the 1.49% Mn steel.

From this Figure it can be seen that, the microhardness of ferrite first increases slightly and then decreases as the intercritical annealing time increases, both on heating up directly to the intercritical annealing temperature and on cooling down to the intercritical annealing temperature.

The microhardness of martensite for samples heated directly to the intercritical annealing temperature decreases gradually as the intercritically annealing time increases. In contrast on cooling down to the intercritical annealing temperature the microhardness of martensite first increases and then decreases as the intercritical annealing time increases.

Table 4.7- Micro-Hardness of Ferrite and Martensite after quenching for the 1.49% Mn.

1-HARDNESS OF FERRITE.

Time, mins.	0	15	30	60	900
Hardness Cooling down $Hv_{0.005}$	109	113	101	105	104
Hardness Heating Up $Hv_{0.005}$	114	120	114	100	99

2-HARDNESS OF MARTENSITE.

Time, mins	0	15	30	60	900
Hardness Cooling Down $Hv_{0.005}$	238	283	298	272	243
Hardness Heating Up $Hv_{0.005}$	315	310	295	290	285

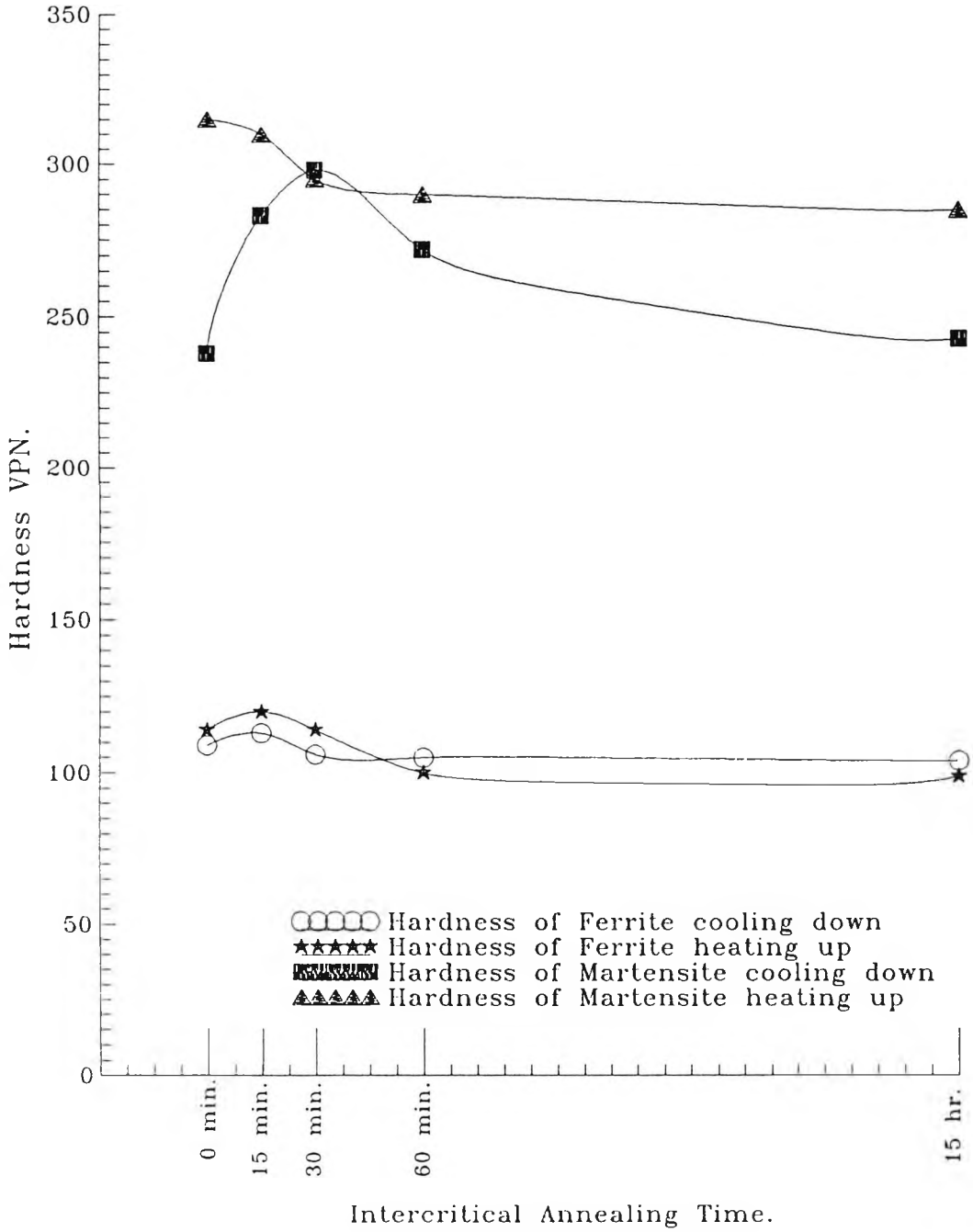

Fig.4.25- The Influence of I.A. Time on Hardness of Ferrite and Martensite for 1.49%Mn Steel (Heating up and Cooling Down Cycle).

4.1.6.4- CARBIDE DENSITY MEASUREMENTS.

The curves of carbide density as a function of intercritical annealing time are shown in Figure 4.26 for the 0.56, 1, and 1.49%Mn steels. It can be seen that raising the Mn level increases the carbide density, and that intercritical annealing causes the density to increase. Density increases rapidly on heating up, but there is a delay on cooling down and there is little evidence for any increase in density in the first half an hour.

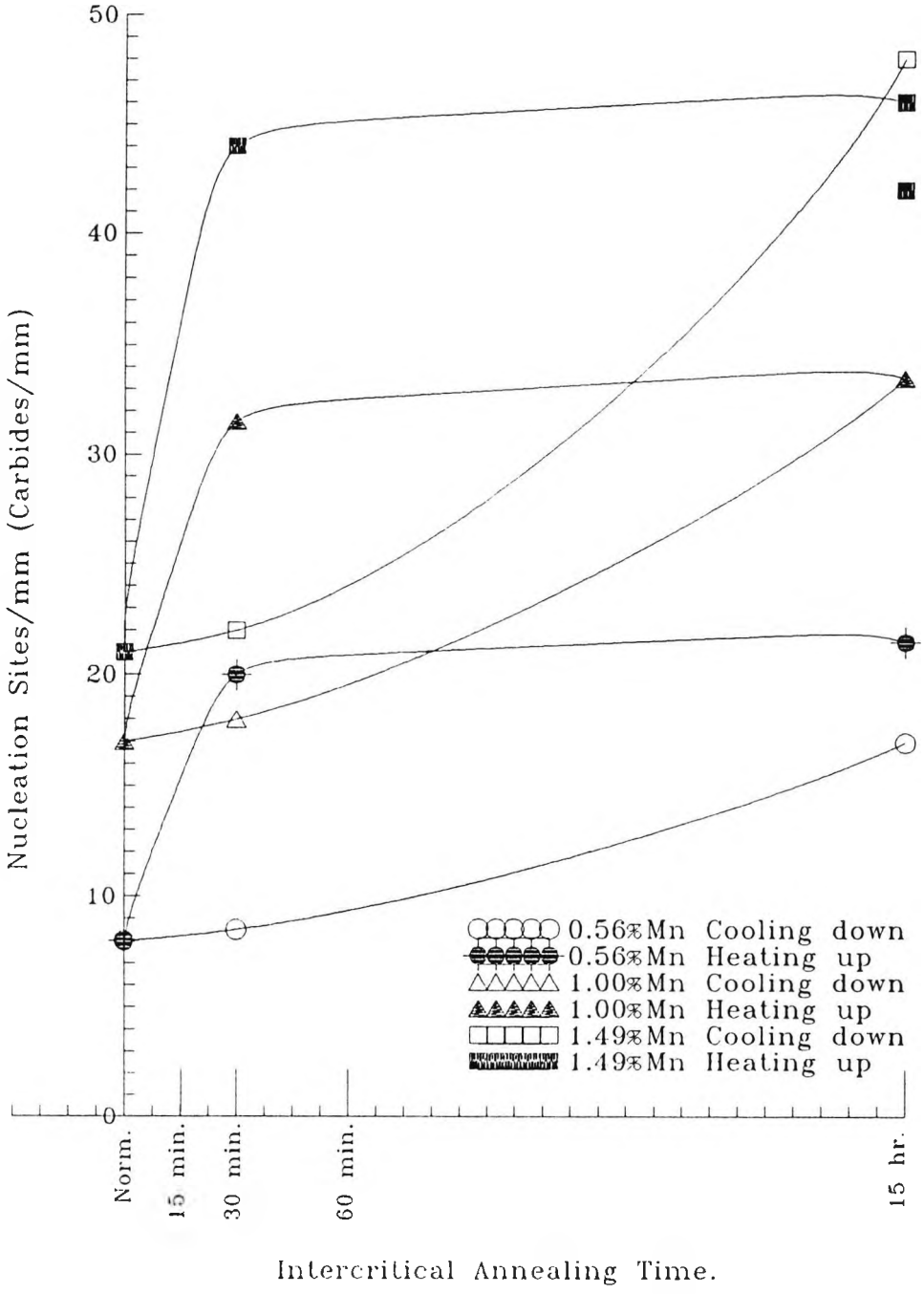

Fig.4.26- The Effect of I.A. Time on the Nuclution Sites for 1,49% MnSteel.

4.2- THE EFFECT OF COOLING RATE AND HOLDING TIME ON IMPACT AND TENSILE PROPERTIES.

4.2.1- INTRODUCTION.

As discussed in chapter (2.3.3) the cooling rate is one of the most important factors for achieving optimum properties of dual-phase steels, and the results from section (4.1) have shown that, the impact properties of an 0.56% Mn steel and 1% Mn steel improved after intercritical annealing with no loss in strength. In contrast, for the 1.49% Mn steel, the impact and tensile properties deteriorated on intercritical annealing. There are two possibilities to account for the poor impact performance of the 1.49%Mn steel. One is that, the cooling rate may be too fast, introducing too much martensite into the structure. The other is that, the carbon content may be too high favouring martensite. These two possibilities will be examined in the next two sections.

The aim of this investigational section, is to study the effect of cooling rate on the impact and tensile properties of 1.5% Mn (C-Mn-Al-Nb) steels.

The chemical composition of two steels used in this investigation are listed in table 4.8. The steels have similar base compositions. One steel, 1.49% Mn (which had been examined in the previous section) was heated directly from room temperature to the intercritical annealing temperature, and the other steel 1.51% Mn was cooled down to the intercritical annealing temperature.They were

intercritically annealed at 730°C for a various times and then cooled to room temperature at a slow cooling rate of 0.8°C/min. The results will be compared with the results from the 1.49%Mn steel, which has been studied in the previous section 4.1, and had been intercritically annealed at 730°C but cooled at the faster rate of 7°C/min. Plates were also austinetised at 920°C for 45 min, and cooled at 0.8°C/min to room temperature.

4.2.2- MICROSTRUCTURAL MEASUREMENTS.

The microstructural data, i.e, grain size, pearlite volume fraction and grain boundary carbide thickness measurements for the two steels cooled at 0.8°C/min are listed in tables 4.9 and 4.10.

The microstructural measurements for the 1.49% Mn steel cooled at 0.8°C/min were compared to the same steel cooled at 7°C/min which had been studied in the previous section(4.1).

As was expected the grain size was very fine for the Al and Nb grain refined steels. The intercritical annealing had little influence on the grain size as has been found by Leslie et.al [103].

For heating up directly to intercritical annealing temperature, and cooling at 7°C/min, the pearlite volume fraction was found to increase markedly from 14% to 30% on increasing the holding time from 0 to 900 minutes, Table 4.2. In contrast, heating up directly to the intercritical

annealing temperature and cooling at 0.8°C/min, the pearlite volume fraction was found to increase slightly from 14% to 15% as the holding time increased from 0 to 900 minutes, Table 4.9. At the slow cooling rate of 0.8°C/min, Tables 4.9 and 4.10, changes in pearlite volume fraction with intercritical annealing time seemed to be less marked both on heating up and cooling down. The grain boundary carbide thickness as well as decreasing with increasing intercritical annealing time, also decreased with increase in cooling rate.

On heating up to the intercritical annealing temperature, Table 4.2, the carbide thickness for a cooling rate of 7°C/min, decreased from 0.23 μm to 0.16 μm as the intercritical annealing time increased from 15 minutes to 15 hours. However, for the slower cooling rate (0.8°C/min) Table 4.9, the carbides were thicker and decreased from 0.32 μm to 0.24 μm as the intercritical annealing time increased from 30 minutes to 15 hours.

For the same time interval on cooling down to the intercritical annealing temperature similar changes were noted, the carbide thickness decreasing from 0.24 μm to 0.15 μm for the cooling rate of 7°C/min, Table 4.2, and from 0.38 μm to 0.27 μm for the cooling rate of 0.8°C/min, Table 4.10.

Table 4.8- The Chemical Compsition of Steel Used for Examining the Influence of Cooling Rate on I.A.

Steel	C	Mn	Si	S	P	Al	Nb	N
1.51% Mn	0.10	1.51	0.43	0.005	0.011	0.040	0.020	0.0025
1.49% Mn	0.10	1.49	0.41	0.003	0.010	0.016	0.027	0.0050

Table 4.9.- Microstructural Measurements and Strength of the 1.49% Mn Steel.

Specimen No.	Ferrite Grain Size µm	Ferrite Grain Size d-1/2 $m.m^{-1/2}$	Pearlite Volume Fraction %	Grain Boundary Carbide Thicknes s um	54J ITT °C	σ_Y MPa	σ_s MPa
A1	9.8	10.1	14.0	0.4	-28	304	451
A2	10.2	9.9	9.0	0.32	-77	305	438
A3	10	10.0	15.0	0.24	-88	302	453

A1 = samples austenitised at 920°C for 45 minutes -cooled at 0.8°C/min to room temperature.

A2,A3 = samples heated directly to the intercritical annealing temperature and held for 30 and 900 minutes respectivly followed by cooling at 0.8°C/min to room temperature respectively.

Table 4.10- Microstructural Measurements and Strength of the 1.51% Mn Steel.

Specimen No.	Ferrite Grain Size µm	Ferrite Grain Size $d^{-1/2}$ $m.m^{-1/2}$	Pearlite Volume Fraction %	Grain Boundary Carbide Thicknes s µm	54J ITT °C	σ_Y MPa	σ_s MPa
Y1	11.1	9.5	23	0.38	-55	321	458
1GH	11.1	9.5	23	0.27	-80	322	460

Y1 = samples austenitised at 920°C for 45 minutes -cooled at 0.8°C/min to room temperature

1GH = samples cooled down to the intercritical annealing temperature and held for 60 minutes -then cooled at 0.8°C/min to room temperature.

4.2.3- IMPACT AND TENSILE BEHAVIOUR.

Impact transition curves and fibrous fracture curves for the two steels after normalising and intercritical annealing and cooling at 0.8°C/min are given in Figure 4.27, and Figure 4.28 for heating up directly to the intercritical annealing temperature and cooling down to the intercritical annealing temperature respectively. The effect of intercritical annealing holding time at 730°C on the 54J ITT °C for the 1.5% Mn steels cooled at 0.8°C/min is shown in Figure 4.29, for both heating up directly to the intercritical annealing temperature and for cooling down to the intercritical annealing temperature. In the former instance, the starting microstructure was ferrite plus pearlite (F+P), and for the latter case the starting microstructure was ferrite plus austenite (F+A).

The 54J ITT is observed to fall rapidly at first, and then further falls are small, Fig.4.29. Compared to the normalised state, for heating up directly to the intercritical annealing temperature and cooling at 0.8°C/min, a drop in impact transition temperature (ITT) of 50°C occurred after 30 minutes while only a further fall of 10°C was observed after 15 hours.

For cooling down to the intercritical annealing temperature and cooling at 0.8°C/min, a drop in impact transition temperature of 20°C after 1 hour was noted, Fig. 4.29.

From the previous section(4.1), the results show that,

for the same steel cooled at 7°C/min, the impact transition temperature (ITT) was found to rise both on heating directly to the intercritical annealing temperature (10°C rise),and cooling down to the intercritical annealing temperature (20°C rise) after holding for long times at the intercritical annealing temperature, Fig. 4.13.

Figure 4.30 shows the effect of cooling rate on impact transition temperature for the 1.5%Mn steels both on heating up directly to the intercritical annealing temperature and cooling down to the intercritical annealing temperature. Compared to the normalised condition, it can be seen that the slow cooling rate of 0.8°C/min lowers the impact transition temperature significantly (about 50°C lower after 30 minutes on heating up and 20°C lower on cooling down). This contrasts with a rise in impact transition temperature of between 10-20°C when the faster cooling rate of 7°C/min was used.

Tensile data (yield strength and ultimate tensile strength) are listed together with microstructural data in tables 4.9 and 4.10, for the 1.49%Mn and 1.51%Mn steels respectively using the slow cooling rate (0.8°C/min). Figure 4.31 shows the effect of intercritical annealing holding time on lower yield strength for the 1.5% Mn steels cooled at 0.8°C/min for heating up directly to the intercritical annealing temperature and for cooling down to the intercritical annealing temperature. It can be seen that, compared to a standard normalising treatment,

intercritical annealing gives improved impact performance with no significant change in yield strength, particularly on cooling down to the intercritical annealing temperature.

The yield strength results from the previous section (4.1), have shown that, for the same 1.49% Mn steel, using a cooling rate of 7°C/min a fall in yield strength occurs on intercritical annealing (about 12 and 40 Mpa for cooling down and heating up respectively after holding for 15 hours). Figure 4.32 shows the effect of cooling rate on yield strength on both heating up directly to the intercritical annealing temperature and cooling down to the intercritical annealing temperature.

It can be seen that, for the 1.5% Mn steel a cooling rate of 0.8°C/min gives some improvement in strength on intercritical annealing (about 10 Mpa for cooling down to the intercritical annealing temperature). In contrast at the faster cooling rate of 7°C/min some loss in yield strength (12-40 Mpa) occurred after holding for long times (15 hr) both for cooling down and heating up, Fig. 4.14.

4.2.4- COMPOSITIONAL CHANGES.

As with the high cooling rate of 7°C/min the Mn content of the pearlite was found to have increased after holding for 15 hours at 730°C as shown in Table 4.11. Again slightly more partitioning of manganese was observed on heating up than on cooling down. Silicon content was found to decrease in pearlite with intercritical annealing time.

Table 4.11- Average Mn and Si content of Ferrite and Pearlite Regions of C-Mn-Al-Nb Steels.

Heat Treatment	Holding Time Minutes	Mn %		Si %	
		In Ferrite	In Pearlite	In Ferrite	In Pearlite
1.51% Mn Steel					
Normalised	-	1.4	1.53	0.44	0.41
Reheated to 730°C	900	1.24	2.01	0.47	0.38
Cooled to 730°C	900	1.36	1.71	0.46	0.39

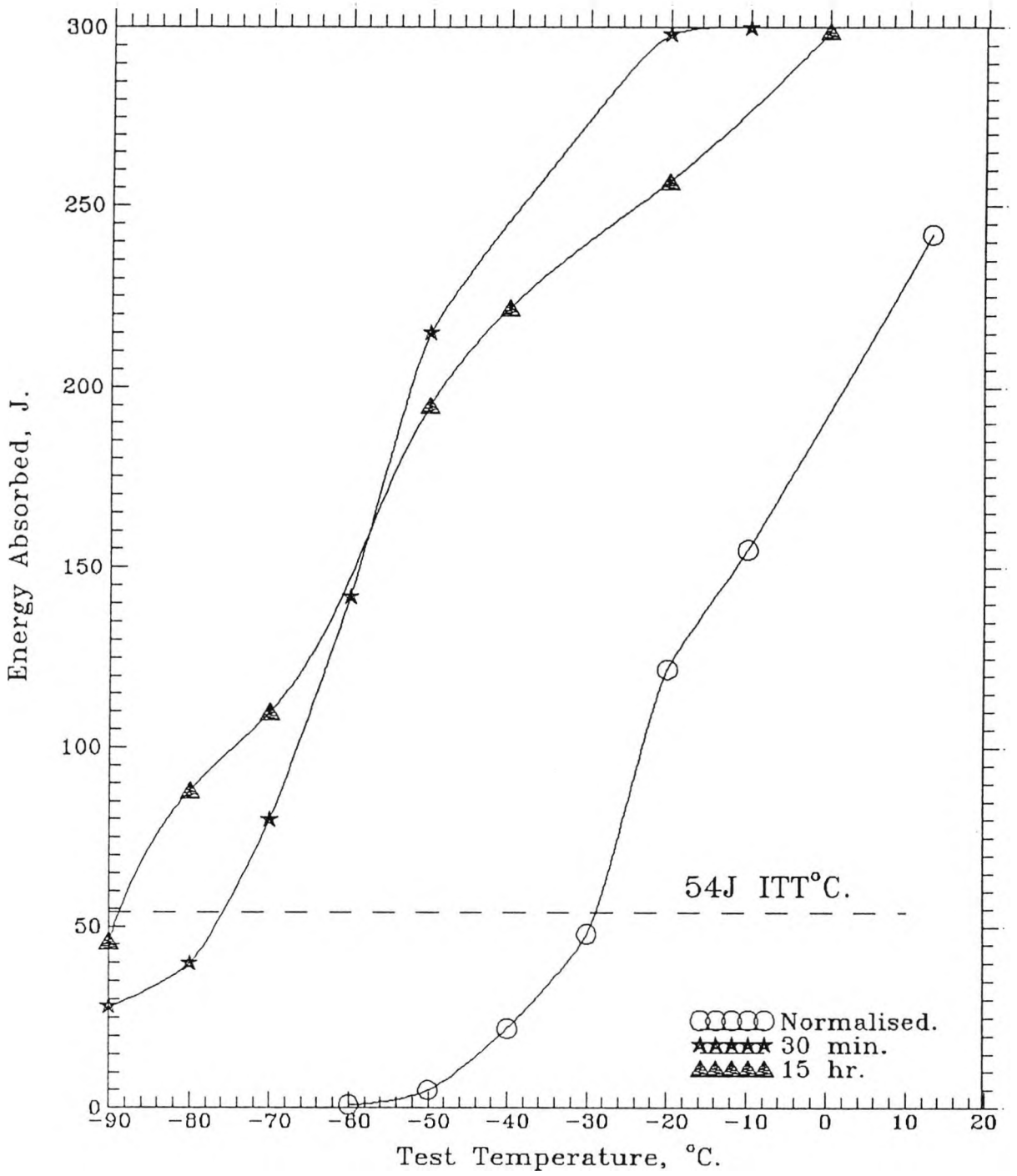

Fig.4.27a- Impact Transition Curves for the 1.49%Mn Steel I.A. at 730°C for Various Times, Cooled at 0.8°C/min, Heating Up Cycle.

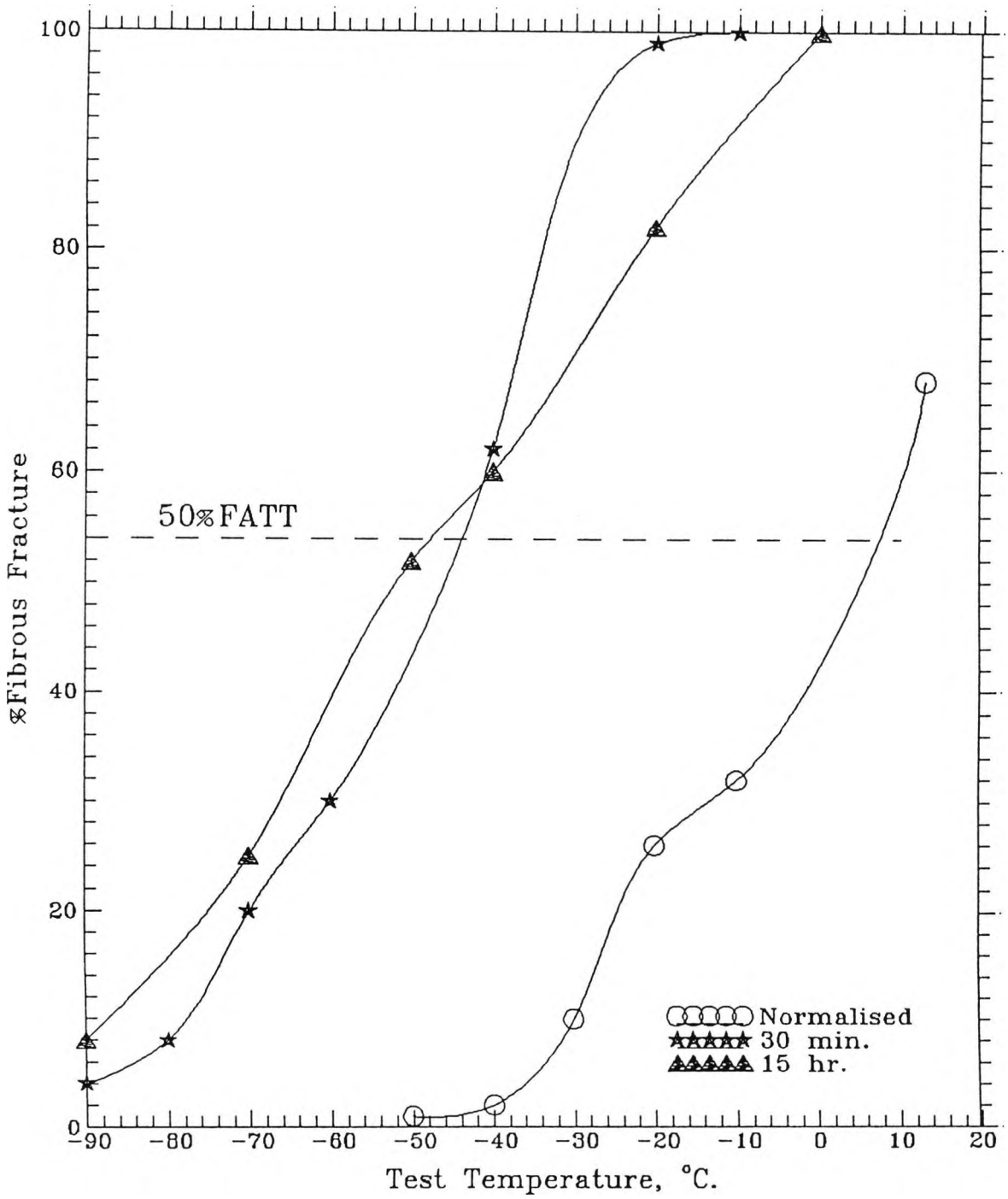

Fig.4.27b- Fibrous Fracture Curves for the 1.49%Mn Steel I.A. at 730°C for Various Times, Cooled at 0.8°C/min, Heating Up Cycle.

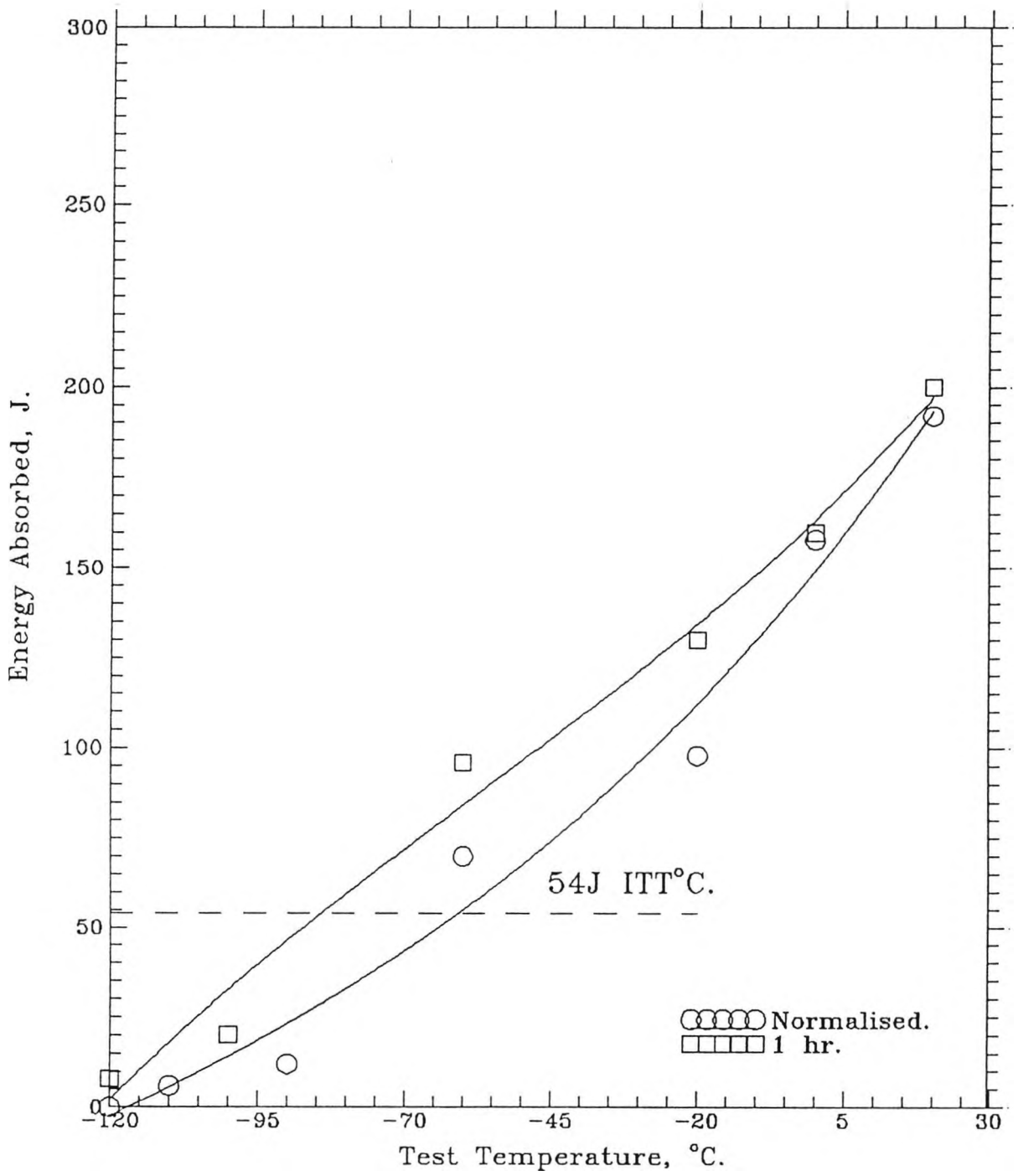

Fig.4.28a- Impact Transition Curves for 1.51%Mn Steel I.A. at 730°C for Various Times, Cooled at 0.8°C/min, Cooling Down Cycle.

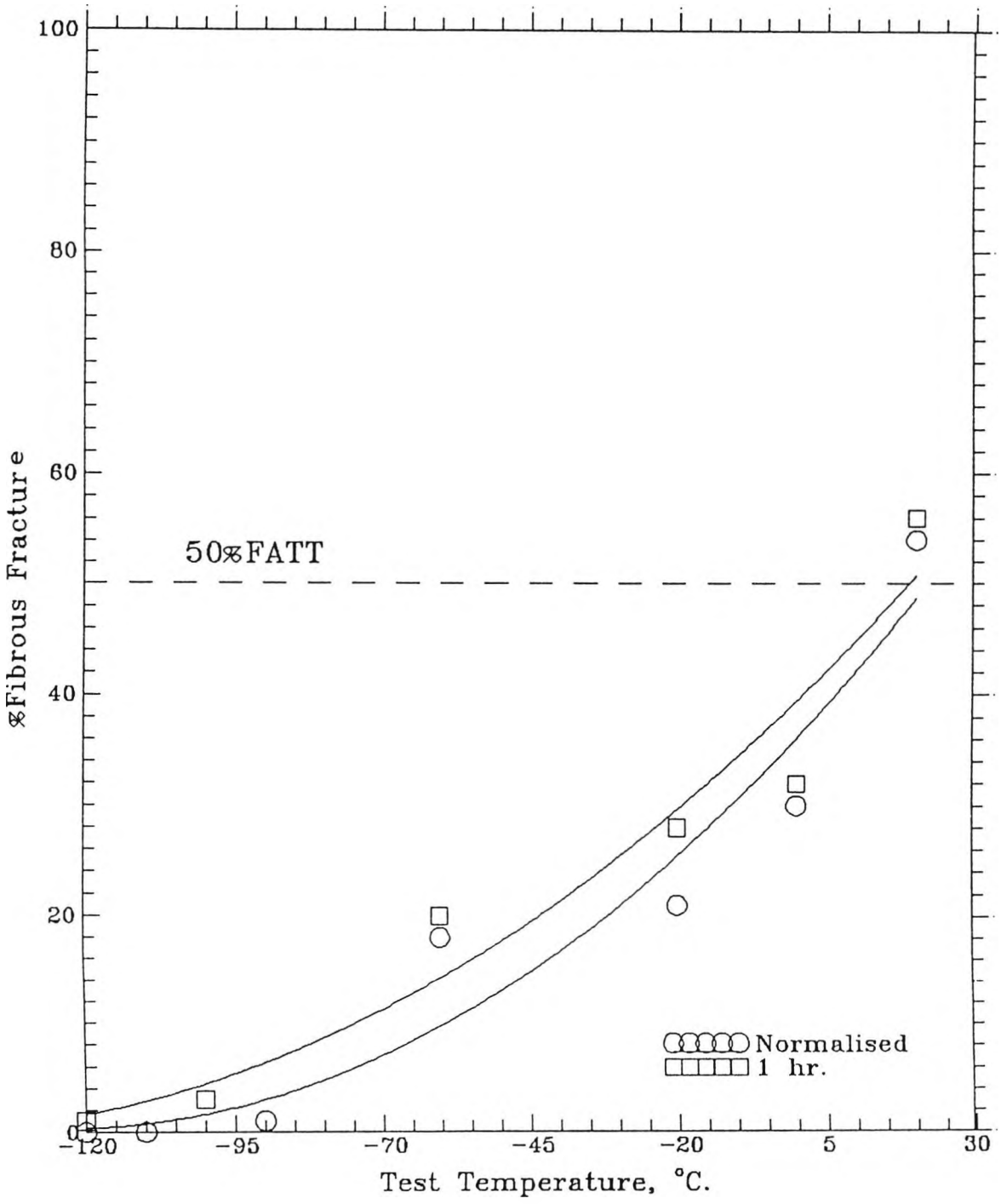

Fig.4.28b- Fibrous Fracture Curves for the 1.51%Mn Steel I.A. at 730°C for Various Times, Cooled at 0.8°C/min, Cooling Down Cycle.

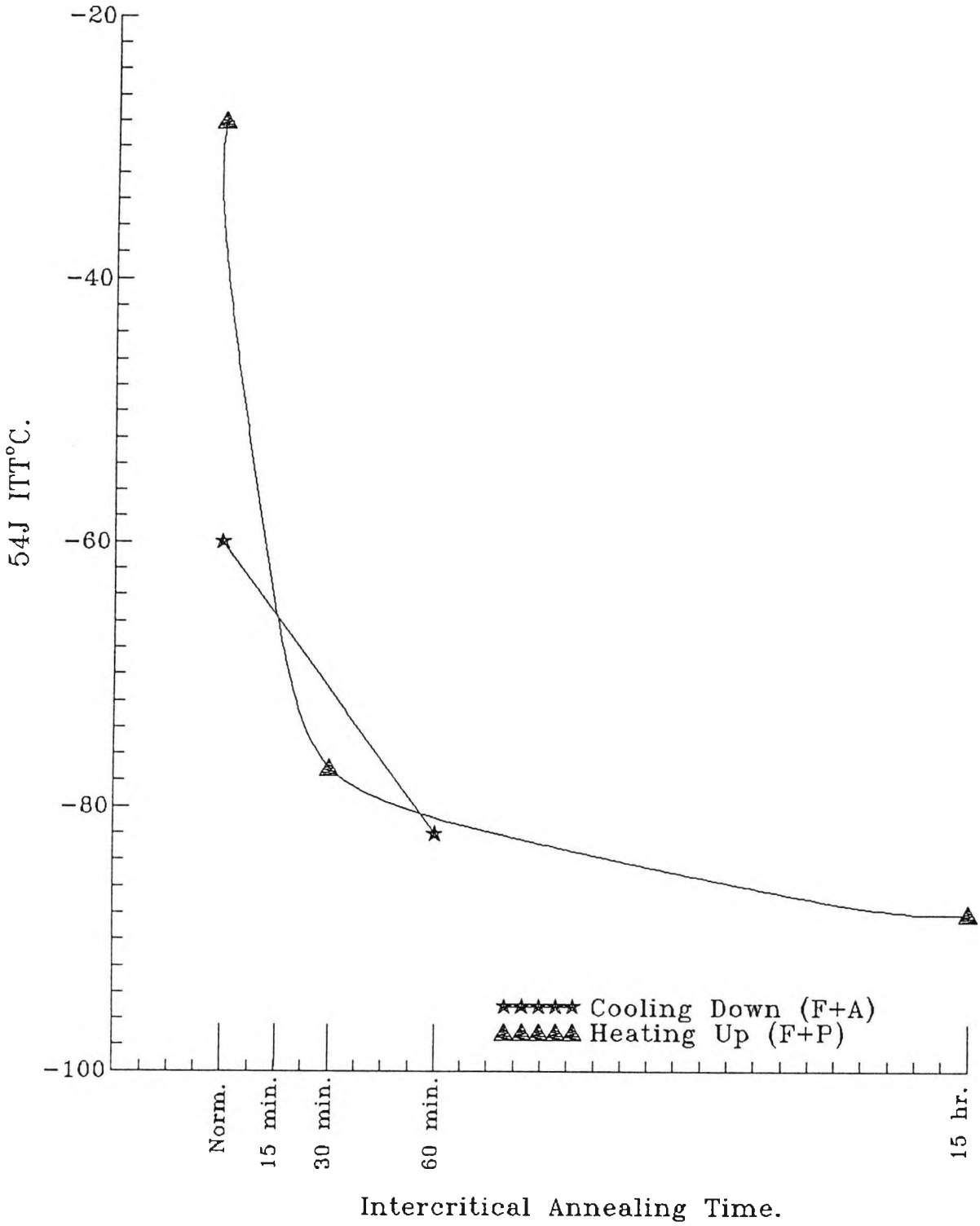

Fig.4.29- The Effect of I.A. Times on the 54J ITT°C for the 1.49%Mn Steel and the 1.51%Mn Steels, Cooled at 0.8°C/min.

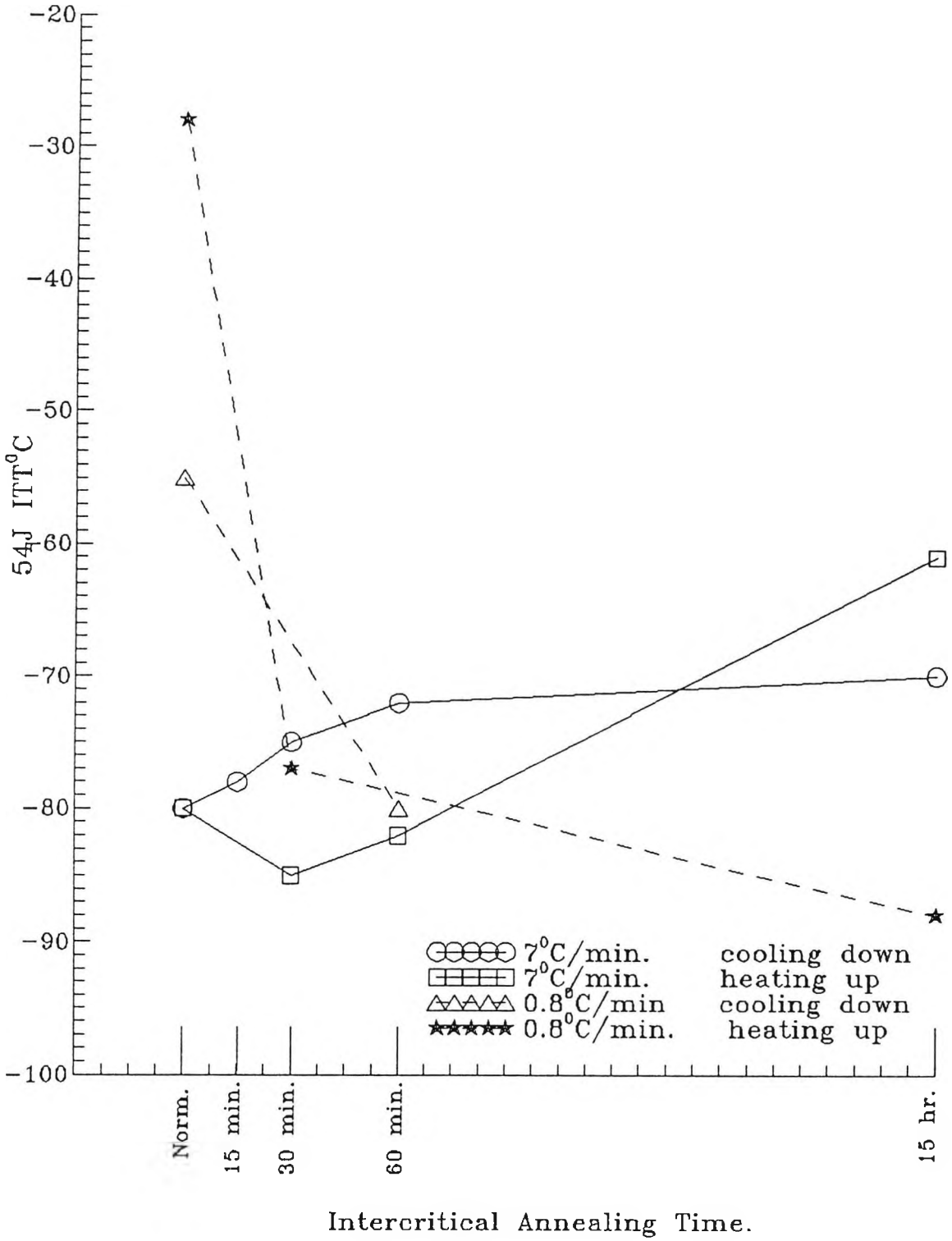

Fig.4.30- The Effect of Cooling Rate After Different I.A. Times on 54J ITT°C for the 1.5%Mn Steels.

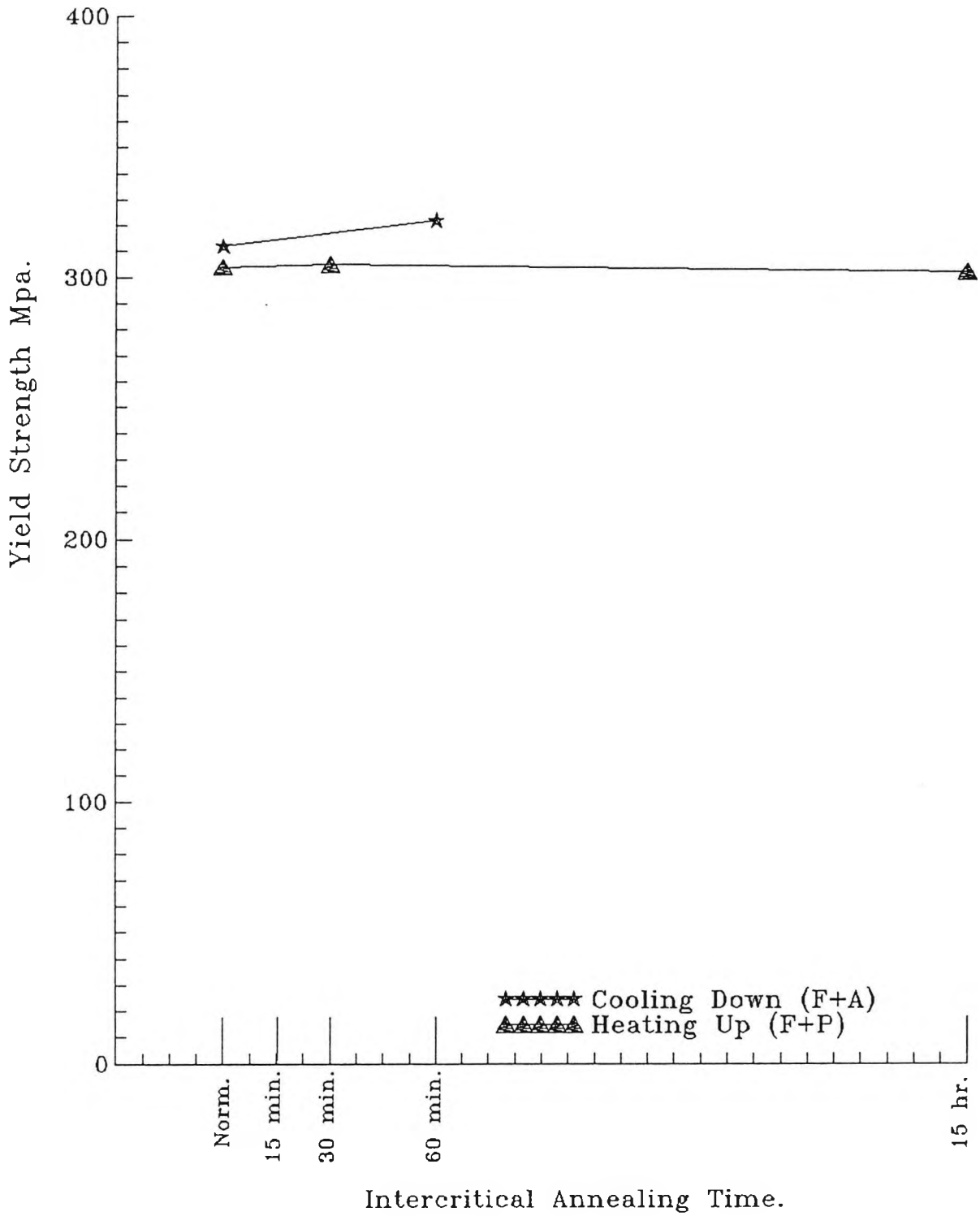

Fig.4.31- The Effect of I.A. Times on the Yield Strength for the 1.5%Mn Steels, Cooled at 0.8°C/min.

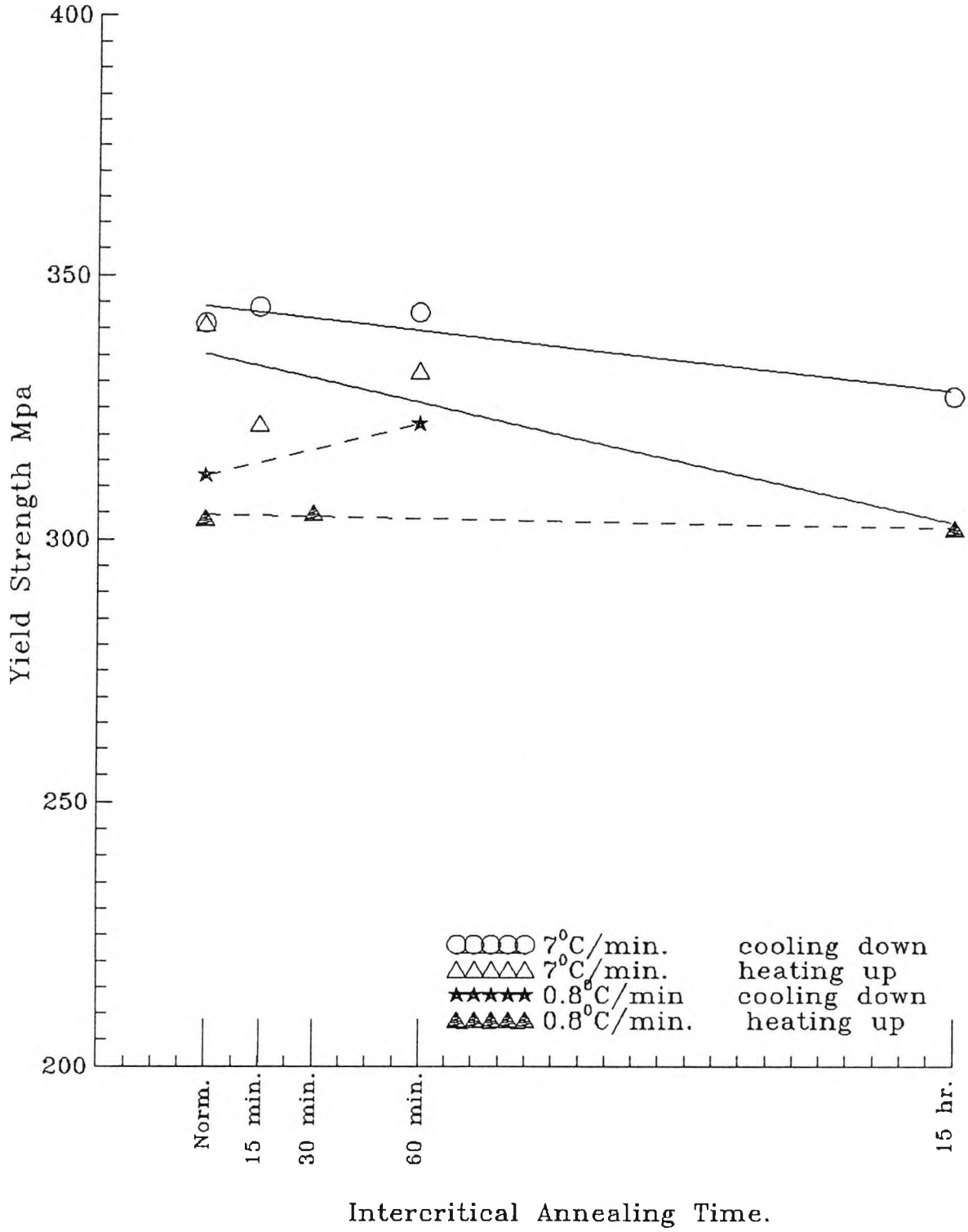

Fig.4.32- The Effect of Cooling Rate After Different I.A. Times on the Yield Strength for the 1.5%Mn Steels.

4.2.5- METALLOGRAPHY.

The change in microstructure with intercritical annealing time was followed by taking a series of optical photographs of the microstructure as a function of intercritical annealing time for samples cooled at 0.8°C/min to room temperature, Figs. 4.33 and 4.34.

4.2.5.1- COOLING DOWN

Figures 4.33 (1 and 2) show the microstructure of the 1.51% Mn steel after normalising and after cooling down to the intercritical annealing temperature of 730°C and holding for 1 hour, at two different magnifications. The microstructure after normalising consists of ferrite and heavily banded pearlite with a martensite band present at the center (thickness of band was 1 mm), Figure 4.33,1. After intercritical annealing the martensite band disappeared, the size of pearlite colonies decreased, and the pearlite phase became more evenly distributed, Figure 4.33,2.

4.2.5.2- HEATING UP.

Figures 4.34 (1 and 2) show the change in microstructure for the 1.49% Mn as a function of intercritical annealing time, after heating up to the intercritical annealing temperature at two different magnifications. The microstructure after normalising consists of ferrite plus banded pearlite.

The microstructure after 30 min of intercritical annealing, Figure 4.34.b consists of ferrite with a very thin film of pearlite surrounding the ferrite phase, the pearlite banding having been nearly removed. The microstructure after 15 hours again consists of ferrite and pearlite with the pearlite film surrounding the ferrite having become thicker and there being no evidence of any banding, Figure 4.34,2c.

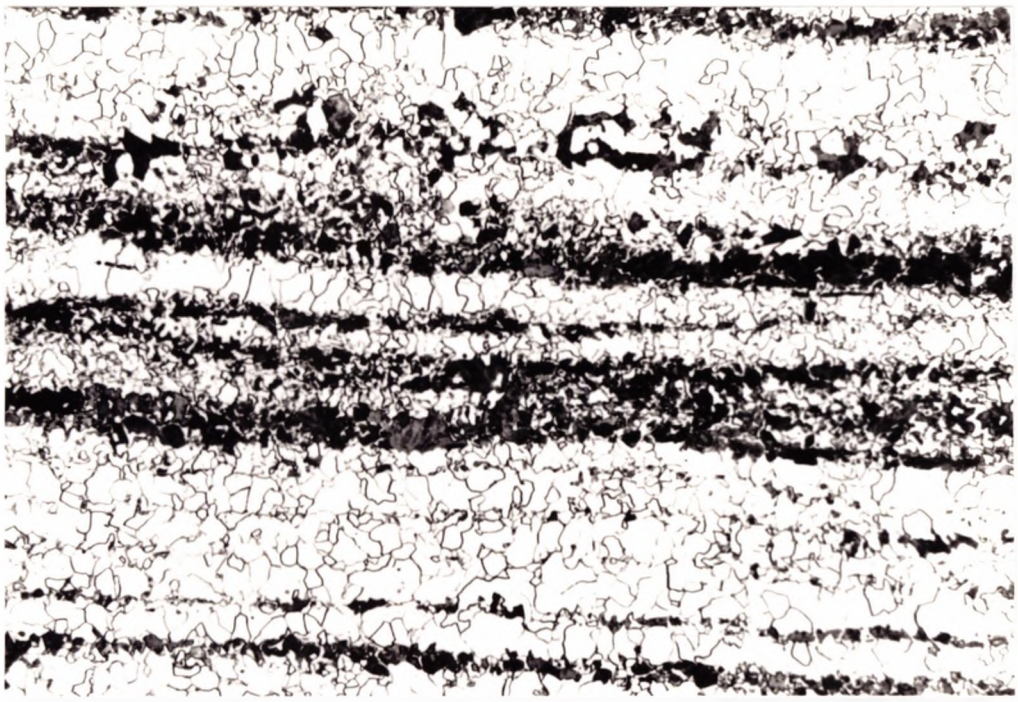

-a- x 450

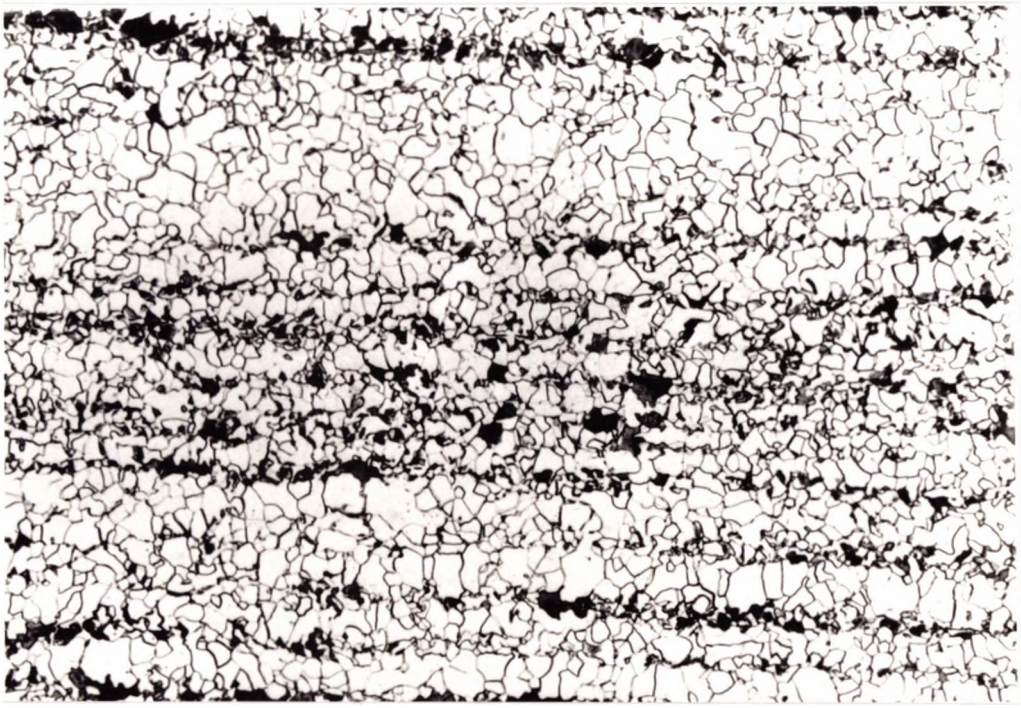

-b- x 450

Fig.4.33 (1)- Microstructure of the 1.51%Mn Steel

a- Normalised., b- I.A. for 1 hr at 730°C,

Cooled at 0.8°C/min, Cooling Down Cycle.

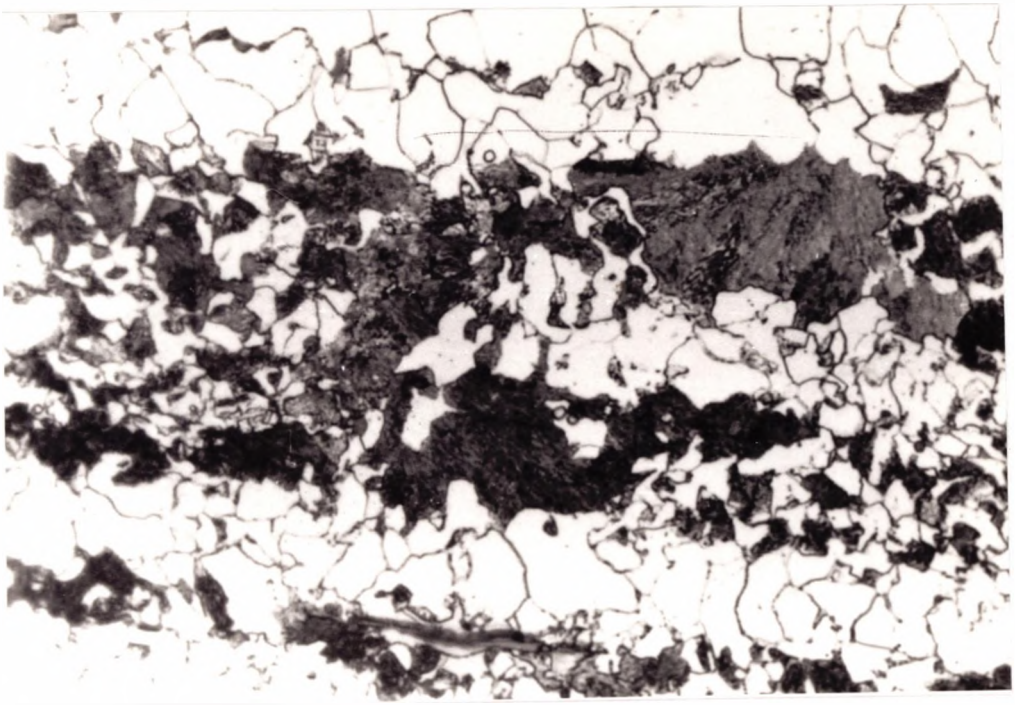

-a- x 900

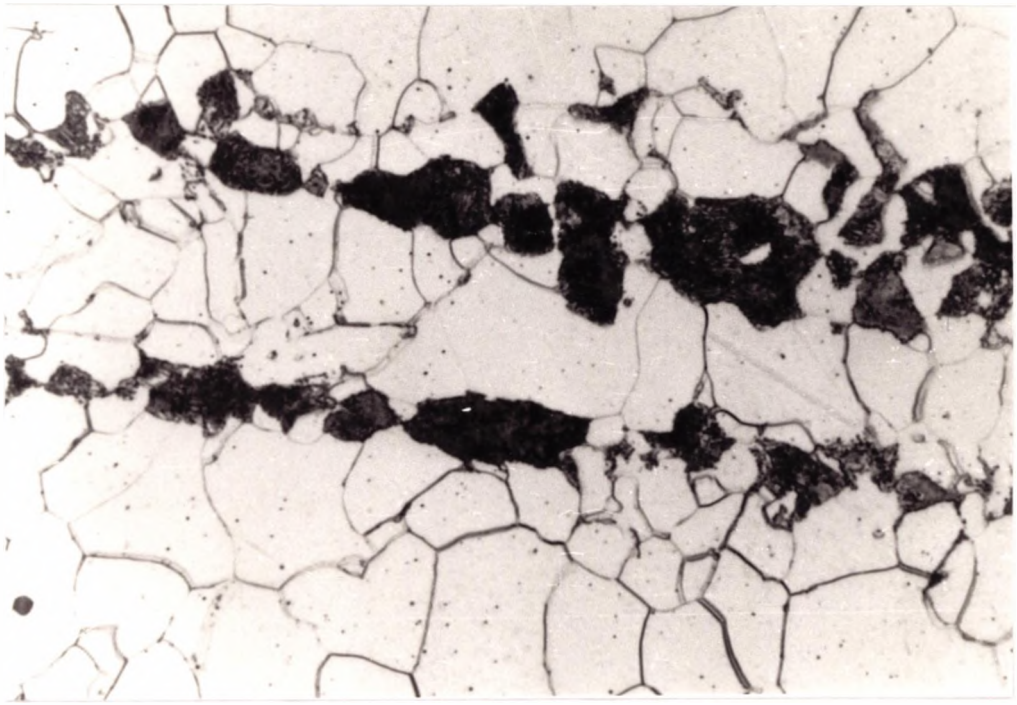

-b- x 900

Fig.4.33 (2)- Microstructure of the 1.51%Mn Steel

a- Normalised., b- I.A. for 1 hr at 730°C,

Cooled at 0.8°C/min, Cooling Down Cycle.

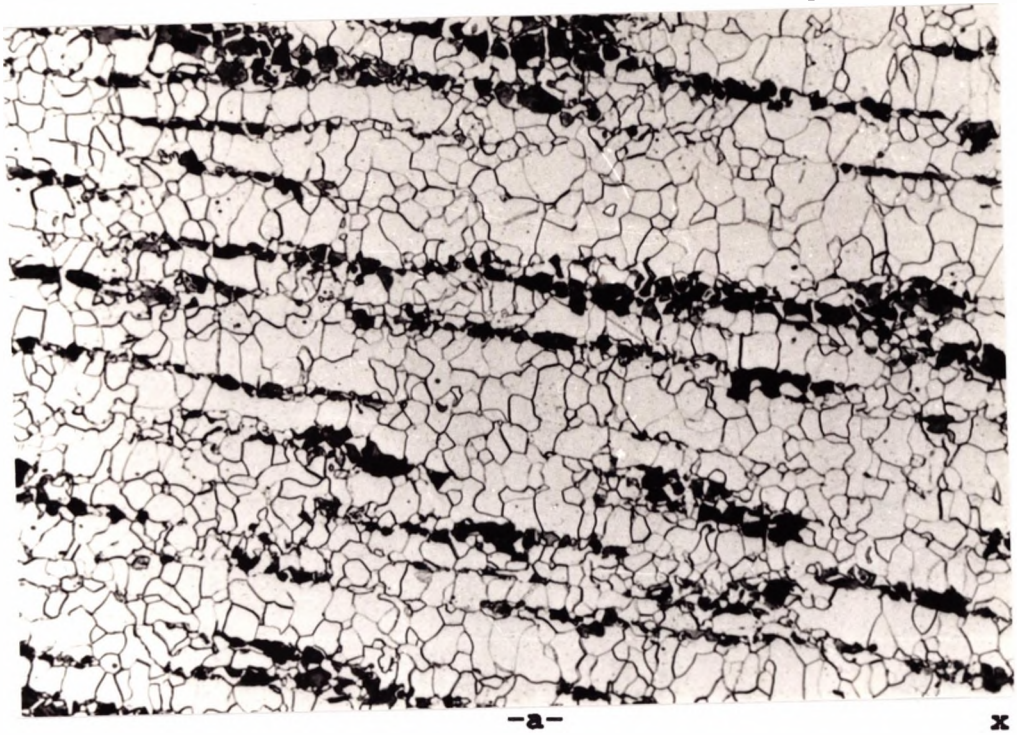

-a- x 450

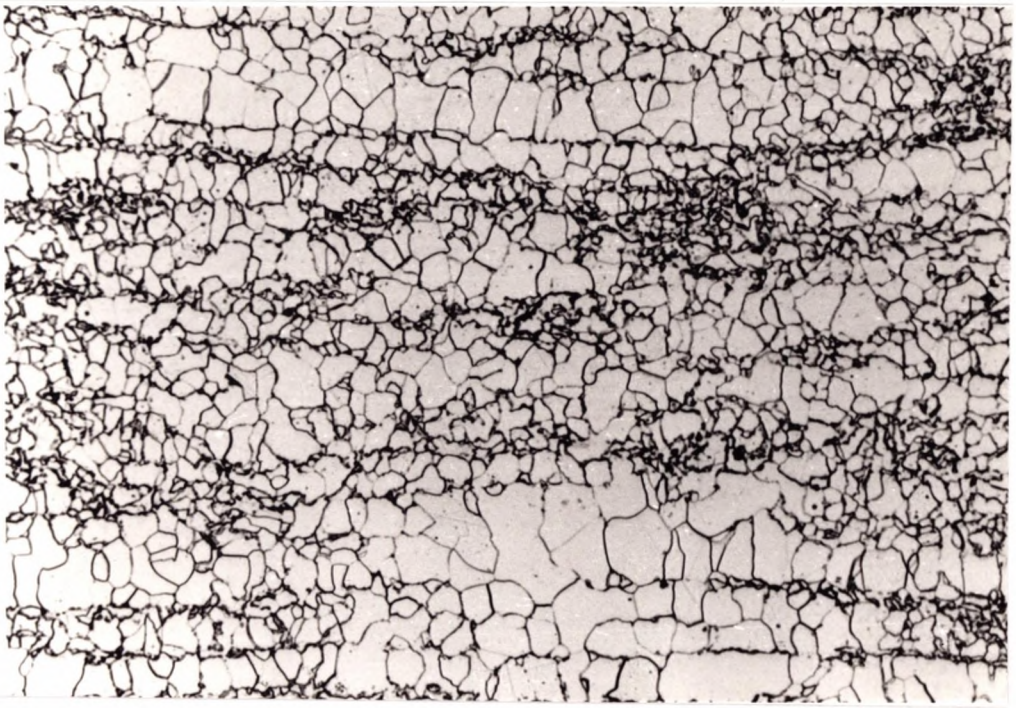

-b- x 450

Fig.4.34 (1)- Microstructure of the 1.49%Mn Steel

a- Normalised., b- I.A. for 30 min at 730°C,

Cooled at 0.8°C/min, (Heating Up Cycle.

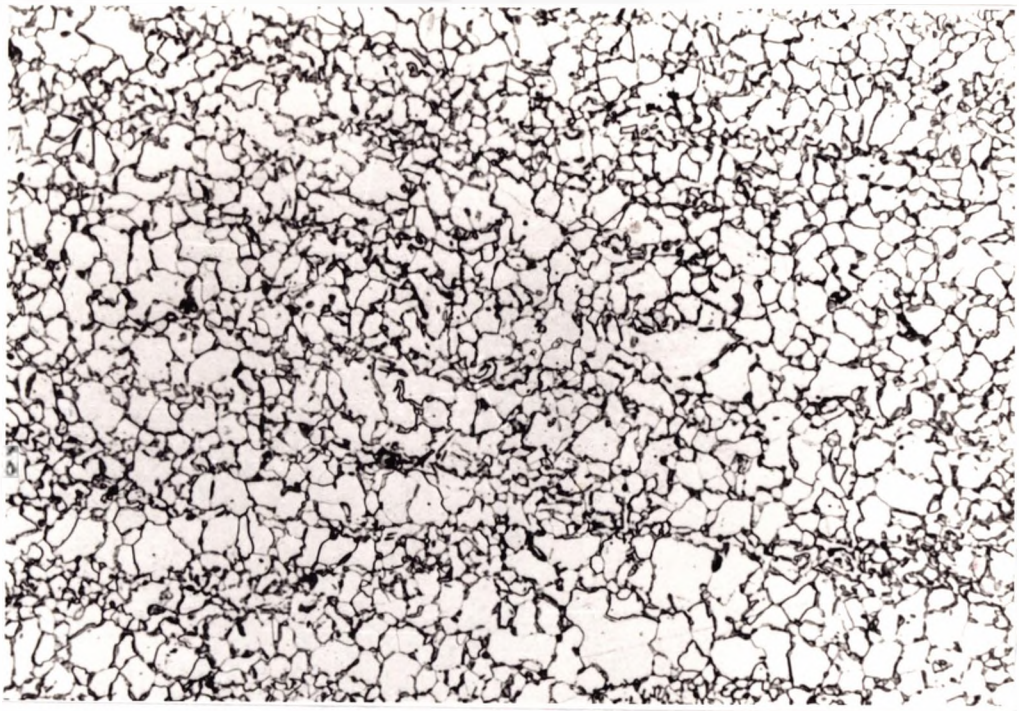

-c- x 450

Fig.4.34 (1)c- Microstructure of the 1.49%Mn Steel I.A. for 15 hr at 730°C, Cooled at 0.8°C/min, Heating up Cycle.

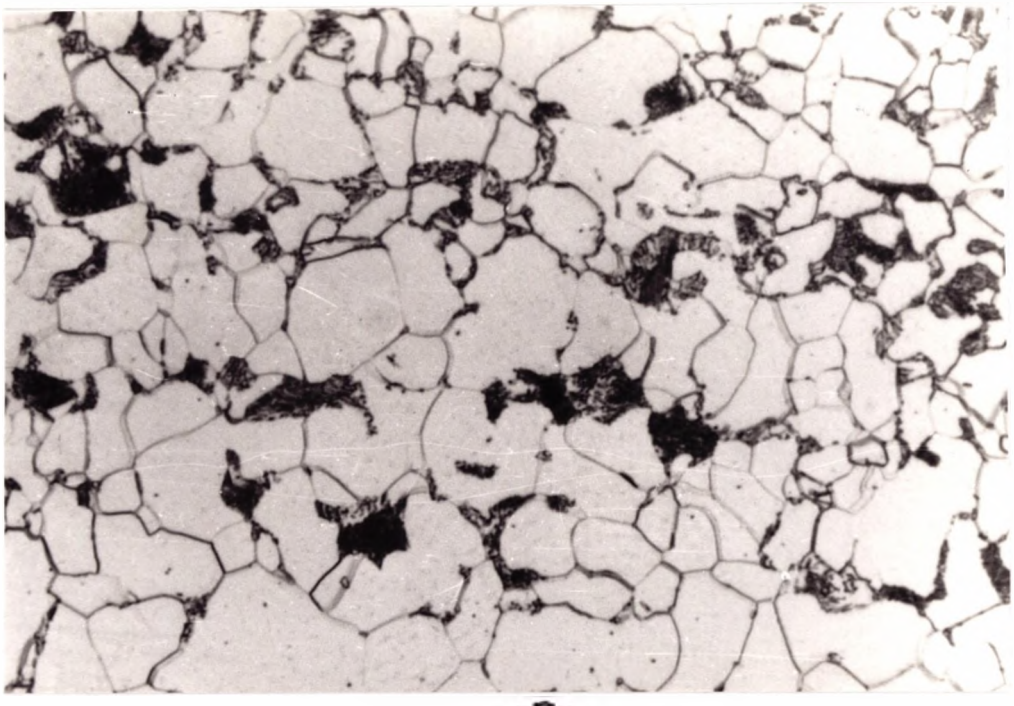

-a- x 900

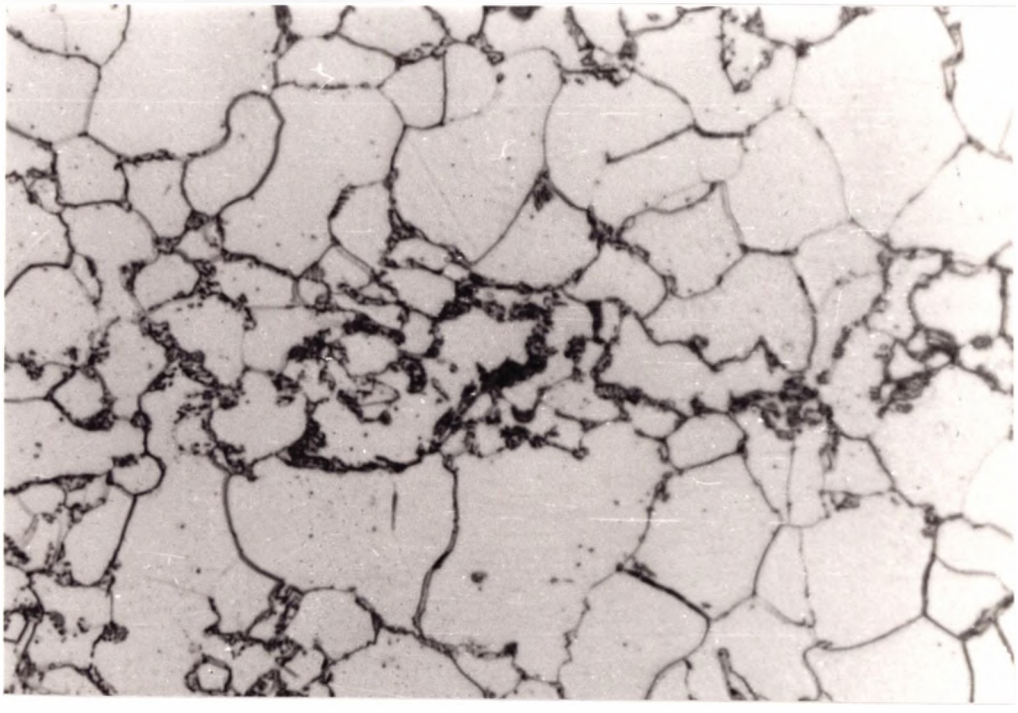

-b- x 900

Fig.4.34 (2)- Microstructure of the 1.49%Mn Steel

a- Normalised., b- I.A. for 30 min at 730°C,

Cooled at 0.8°C/min, Heating Up Cycle.

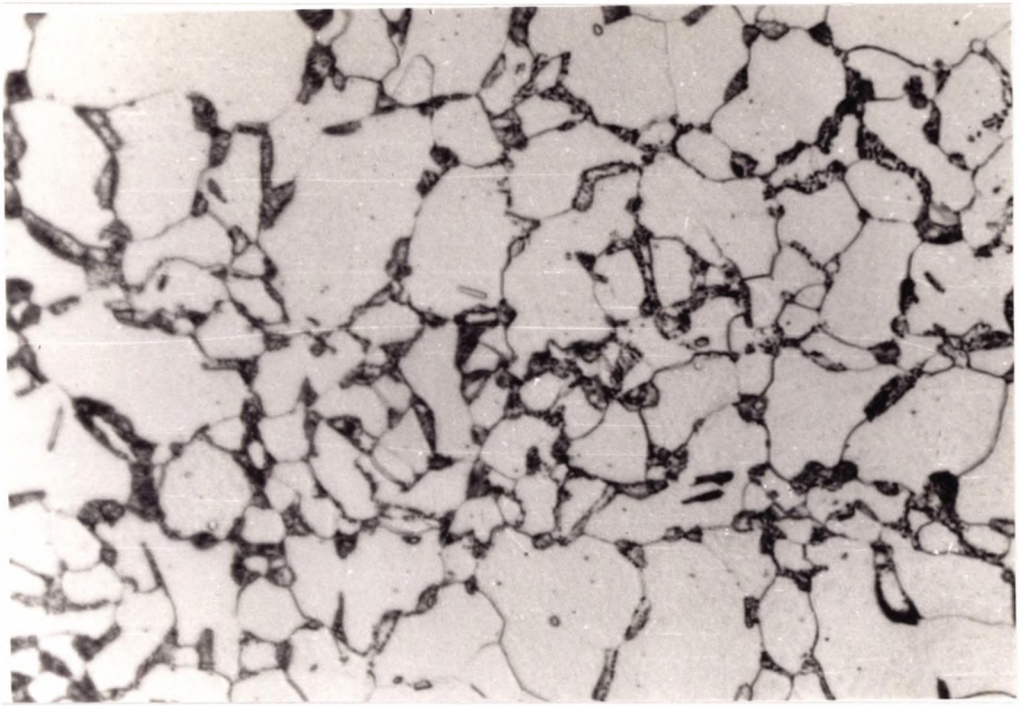

-c- x 900

Fig.4.34 (2)c- Microstructure of the 1.49%Mn Steel I.A. for 15 hr at 730°C, Cooled at 0.8°C/min Heating up Cycle.

4.3- THE EFFECT OF CARBON CONTENT AND HOLDING TIME ON IMPACT AND TENSILE PROPERTIES.

4.3.1- INTRODUCTION.

In section (4.1) it was shown that for a 0.1% C steel when the manganese level is 1.5%, the impact and tensile properties start to deteriorate after intercritical annealing for long times and this corresponds to a high volume fraction of the second phase. As the carbon content controls the volume fraction of the second phase in steel, it is very important to study the effect of the carbon level on impact and tensile properties during intercritical annealing.

The aim of this investigational section is to study the effect of carbon level and holding time on the impact and tensile properties for the 1.5% Mn steel. The chemical composition of steel used in this investigation had a low C level of 0.067% and a manganese level of 1.41% and it's full analyses is given in table 4.12. A cooling rate of 7°C/min was used for this steel. The results from this investigation will be compared with the results for the 1.49%Mn steel cooled at 7°C/min, which had been studied in the previous section 4.1. and contained 0.1%C.

Plates were also normalised and cooled at 7°C/min to room temperature.

4.3.2- MICRO-STRUCTURAL MEASUREMENTS:

The microstructural data; grain size, pearlite volume fraction and grain boundary carbide thickness measurements for the steel cooled at 7°C/min are given in table 4.13.

The microstructural measurements for this lower carbon steel was compared to the same base composition higher carbon steel cooled at the same cooling rate (7°C/min) which had been studied in the previous section (4.1), Table 4.2.

As in the previous work, intercritical annealing had little influence on the grain size. The grain size was found to decrease as the carbon level decreased (the average ferrite grain size being 9 µm and 8 µm for the 0.1% and 0.067% C steel respectively). This refinement may be related to the higher Al and N levels in the 0.067% carbon steel giving greater grain refinement on austenitising or normalising. For cooling down to the intercritical annealing temperature the pearlite volume fraction was found to decrease as the carbon level decreased (average of 14% and 8% for the 0.1% C and 0.067% C steel respectively). For heating up directly to intercritical annealing, the pearlite volume fraction was found to decrease from 25% to 10% as the C level decreased from 0.1%C to 0.067%C.

The grain boundary carbide thickness was found to be finer in the lower C steel and this again may be related to it's finer grain size. For this lower C steel, little

change in the thickness was noted with annealing time, on cooling down to the intercritical annealing temperature. The thickness refined from 0.15 to 0.14μm as the intercritical annealing time increased from 30 minutes to 15 hours, Table 4.13. This contrasts with the higher C steel in which the carbide thickness decreased from 0.23 to 0.15 μm as the intercritical annealing time increased from 15 minutes to 15 hours, Table 4.2.

Table 4.12- The Chemical Composition of Steel Used for Examining the Influence of Carbon Level on I.A.

C	Mn	Si	S	P	Al	Nb	N
0.067	1.41	0.28	0.006	0.009	0.041	0.030	0.0100

Table 4.13- Microstructural Measurements and Strength for the, 0.067% C Steel.

Specimen No.	Ferrite Grain Size µm	Ferrite Grain Size $d^{-1/2}$ $mm^{-1/2}$	Pearlite Volume Fraction %	Grain Boundary Carbide Thicknes µm	54J ITT °C	σ_Y Mpa	σ_s MPa
7N	8.1	11.0	7	0.17	-95	326	432
71C	7.8	11.3	8	0.15	-104	325	430
72C	8.0	11.2	7.5	0.14	-109	328	428
71H	7.7	11.4	8.0	0.16	-109	325	436
72H	7.7	11.4	10.0	0.15	-109	320	451

7N =normalised

71C,72C are for samples cooled down to the intercritical annealing temperature and held for 30 and 900 minutes respectively.

71H,72H are for samples heated directly to the intercritical temperature and held for 30 and 900 minutes respectively.

4.3.3- IMPACT AND TENSILE BEHAVIOUR.

Impact transition curves and fibrous fracture curves after normalising and intercritical annealing for the 0.067% C steel are given in Figure 4.35, and Figure 4.36 for heating up directly to the intercritical annealing and cooling down to the intercritical annealing temperature respectively.

The effect of intercritical annealing holding time at 730°C on 54J ITT °C is shown in Figure 4.37 both for heating up directly to the intercritical annealing temperature and cooling down to the intercritical annealing temperature.

For heating up directly to the intercritical annealing temperature, a fall in impact transition temperature (ITT) of 15°C after 30 minutes was noted.

For cooling down to the intercritical annealing temperature, a smaller drop in ITT of 10°C was noted. Increasing time at the intercritical annealing temperature had little further influence on ITT.

From the previous section (4.1),the results show that, for the steel with the higher C content (0.1%C), after holding for a long time, the ITT rises (20°C) both on heating directly to the intercritical annealing temperature and cooling down to the intercritical annealing temperature. Figure 4.38 shows more clearly the effect of carbon level on ITT for the 1.5% Mn steel both on heating up directly to the intercritical annealing temperature and

cooling down to the intercritical annealing temperature. Raising the C level can be seen to raise the ITT; and this is particularly marked after long holding times.

Tensile data (yield strength and ultimate tensile strength) are listed together with microstructural data in table 4.13, for the 0.067% C steel.Figure 4.39 shows the effect of intercritical annealing holding time on lower yield strength for the 0.067% C steel for both heating up directly to the intercritical annealing temperature and cooling down to the intercritical annealing temperature. It can be seen that, intercritical annealing gives a small improvement in ITT without any change in the yield strength.

This contrasts with results from the higher C steel, Fig. 4.13 and Fig. 4.14 (section 4.1) in which a deterioration in impact properties occurs and this is accompanied by a fall in yield strength (about 12 and 40 Mpa for cooling down and heating up respectively after holding 15 hours at the intercritical annealing temperature).

Fig 4.40 shows this effect of carbon level on yield strength for both heating up directly to the intercritical annealing temperature and cooling down to the intercritical annealing temperature.

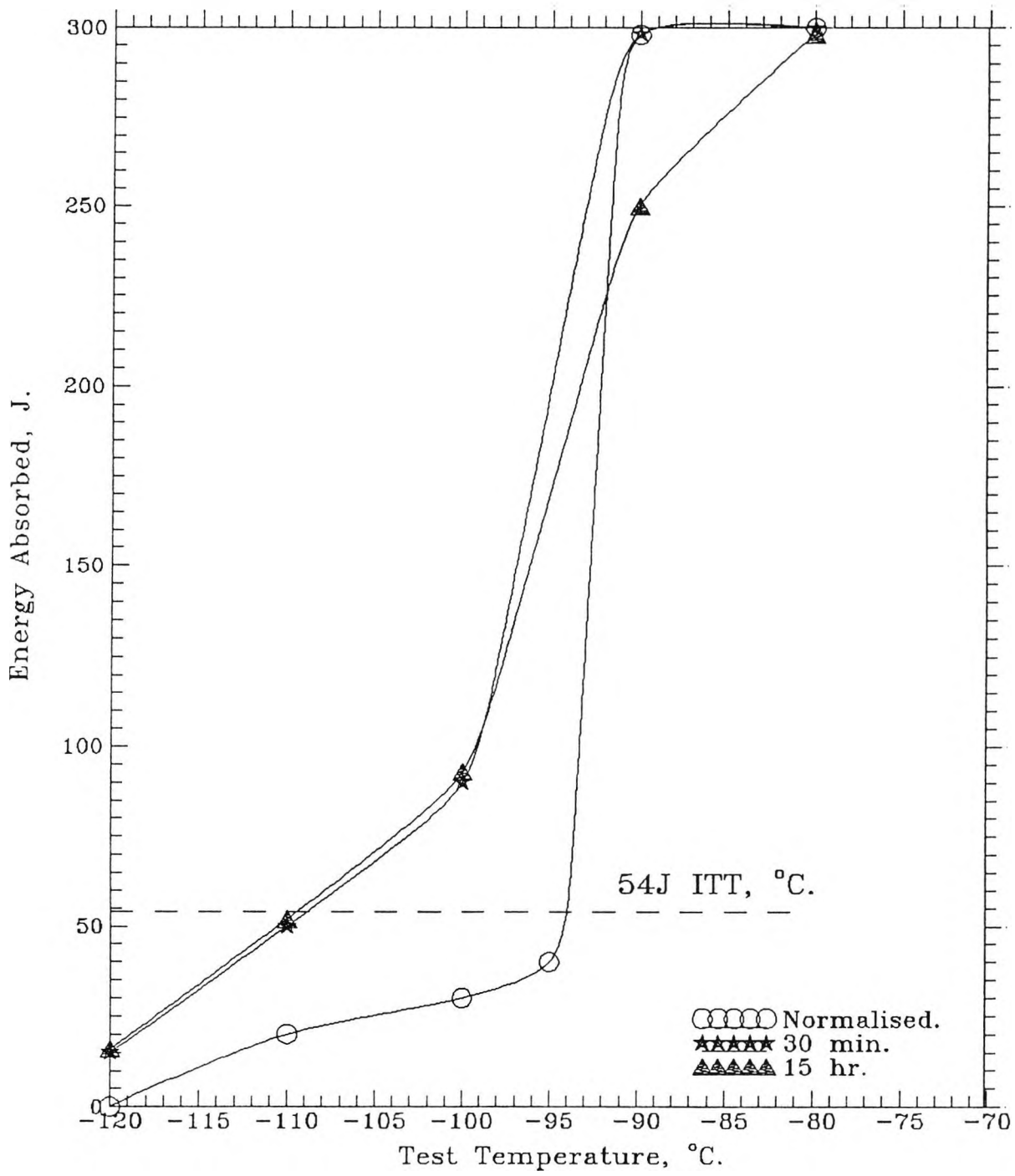

Fig.4.35a- Impact Transition Curves for the 0.067%C Steel I.A. at 730°C for Various Times, Cooled at 7°C/min, Heating Up Cycle.

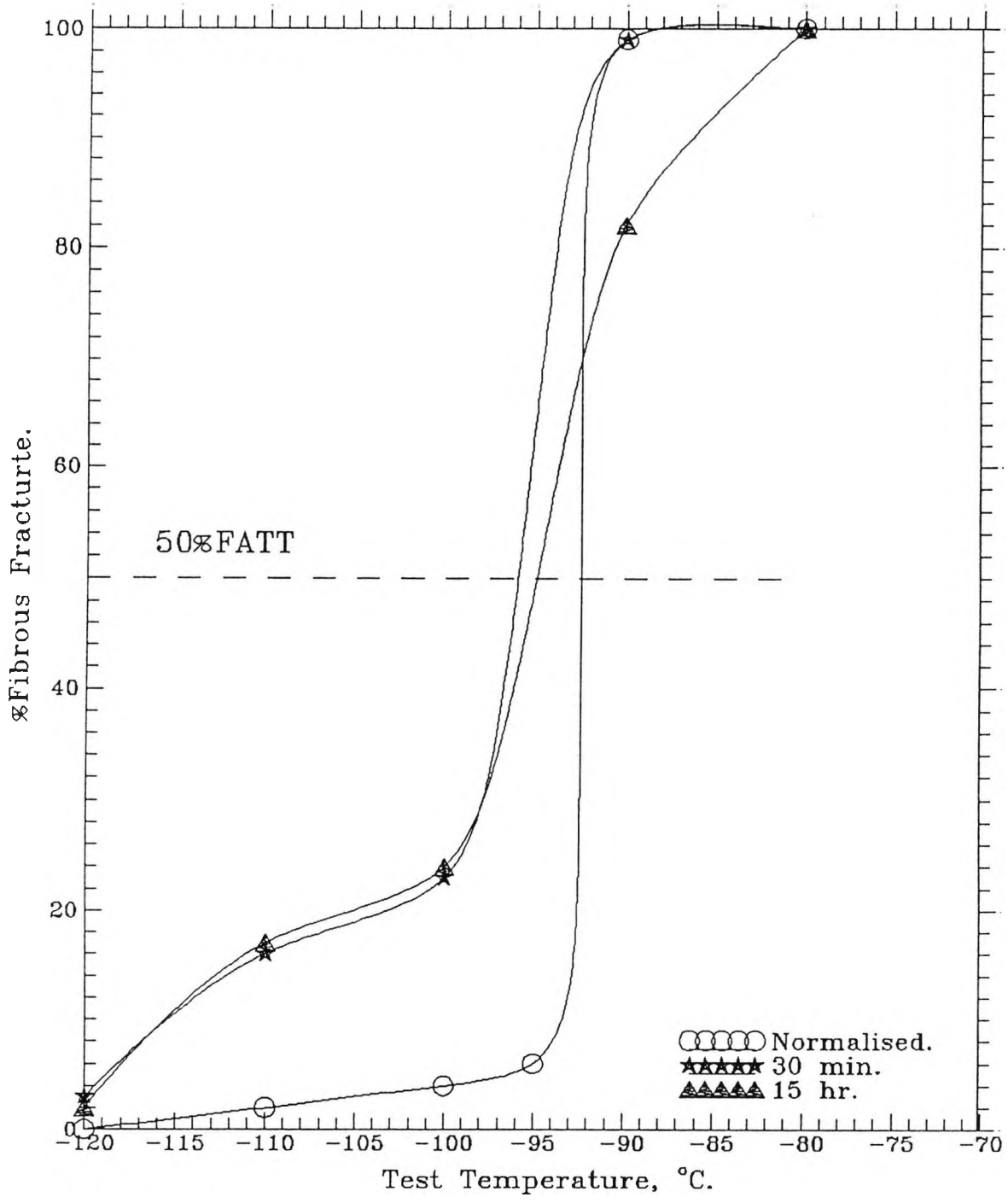

Fig.4.35b- Fibrous Fracture Curves for the 0.067%C Steel I.A. at 730°C for Various Times, Cooled at 7°C/min, Heating Up Cycle.

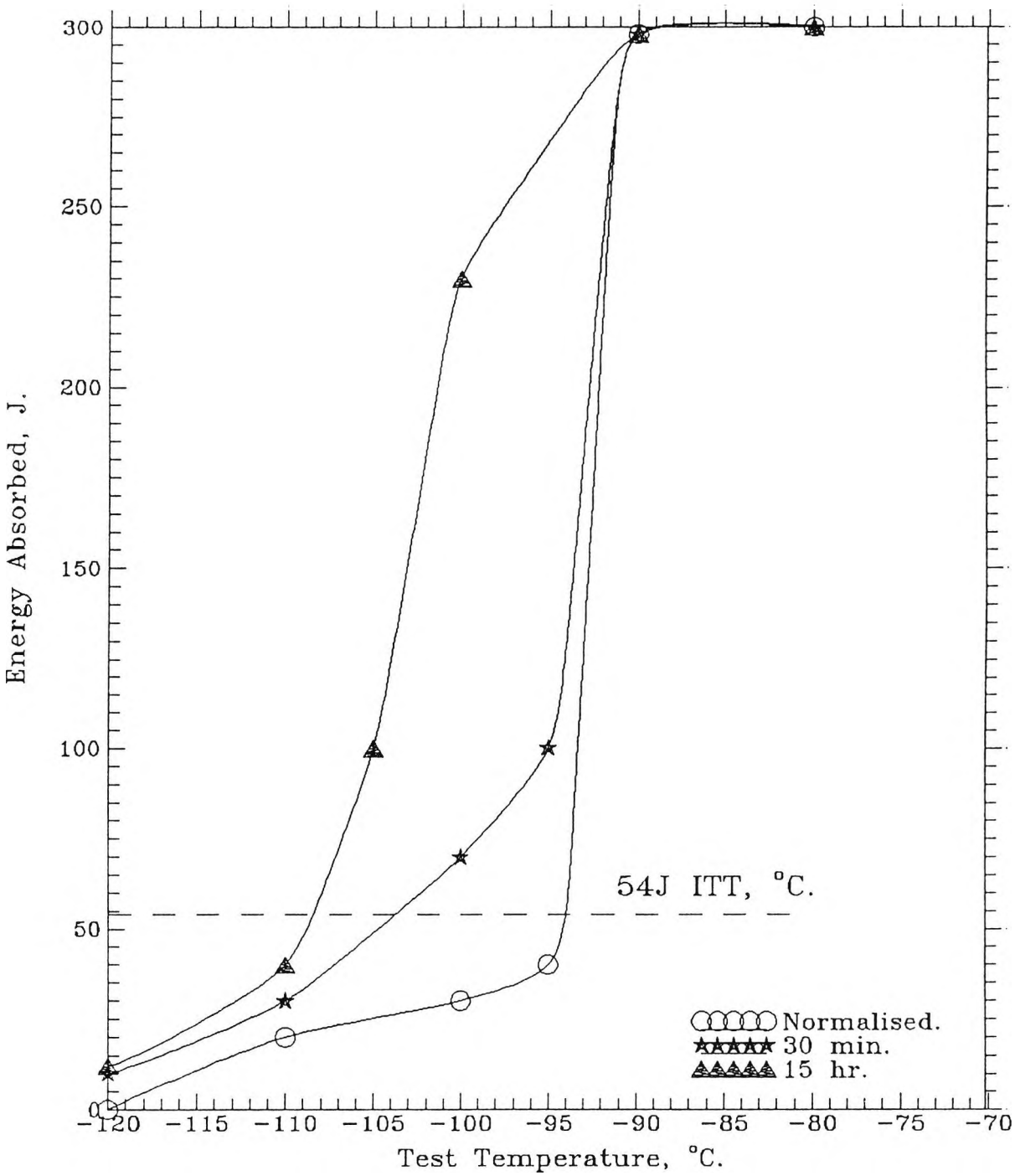

Fig.4.36a- Impact Transition Curves for the 0.067%C Steel I.A. at 730°C for Various Times, Cooled at 7°C/min, Cooling Down Cycle.

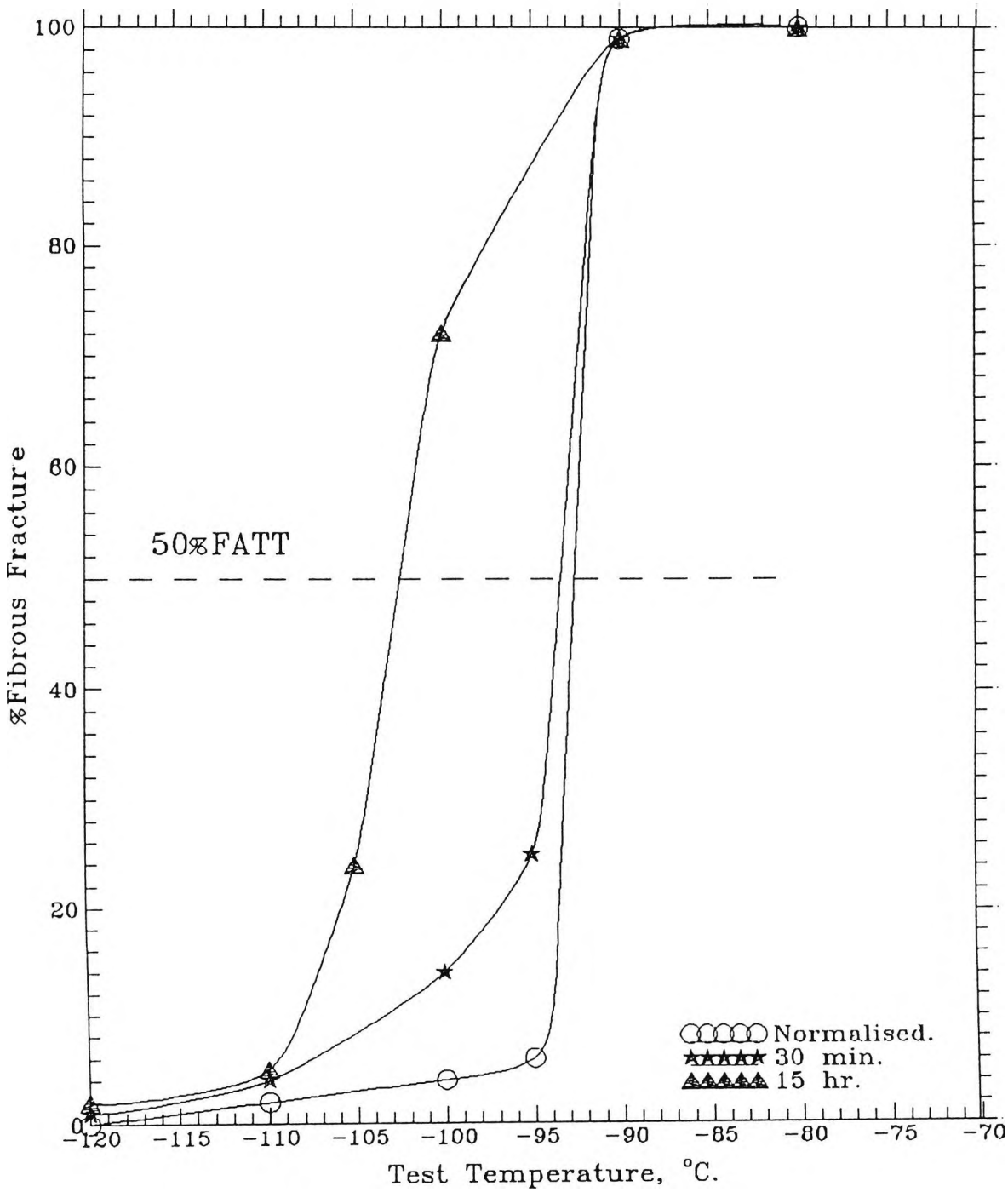

Fig. 4.36b- Fibrous Fracture Curves for the 0.067%C Steel I.A. at 730°C for Various Times, Cooled at 7°C/min, Cooling Down Cycle.

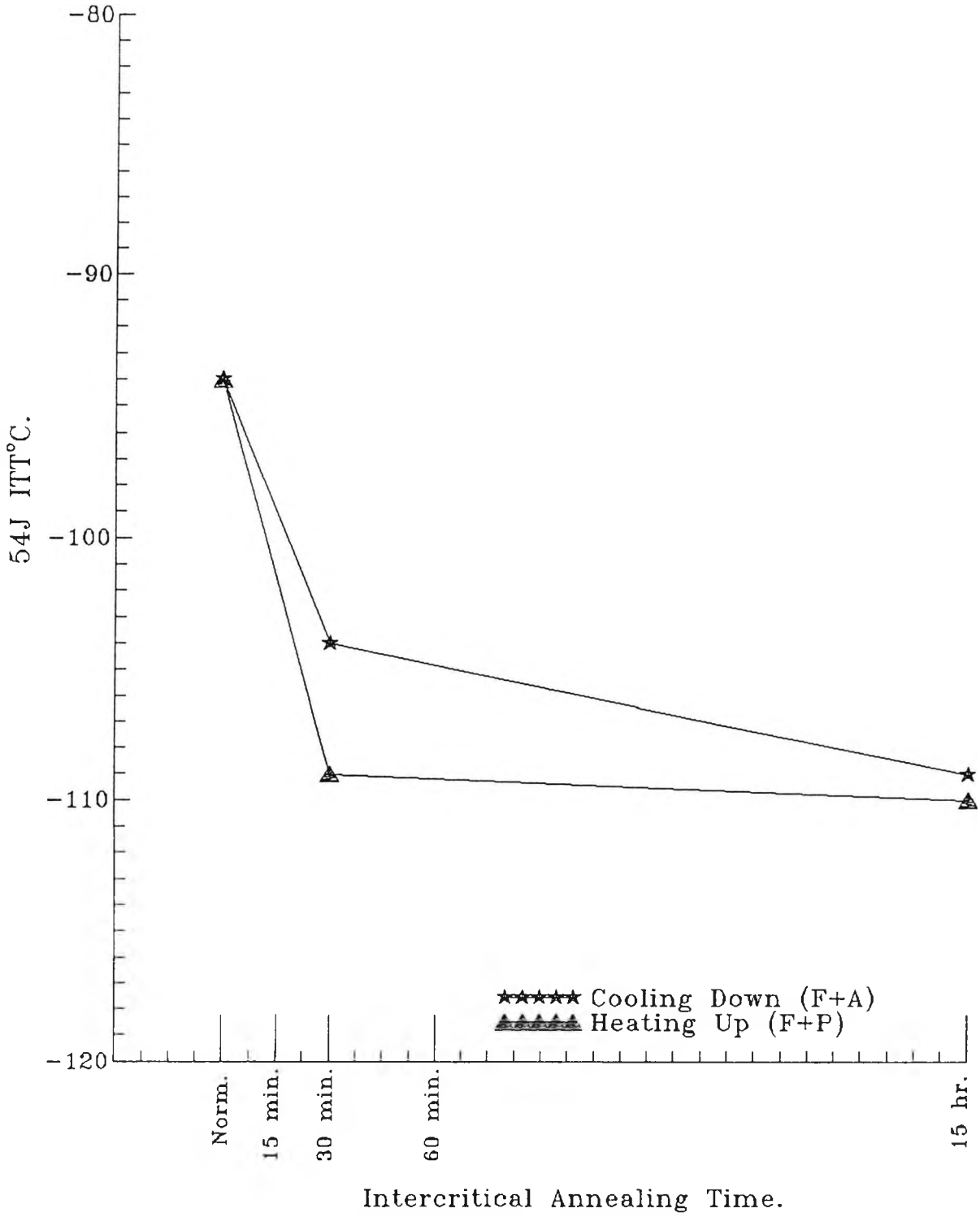

Fig.4.37- The Effect of I.A. on the 54J ITT°C for the 0.067%C Steel.

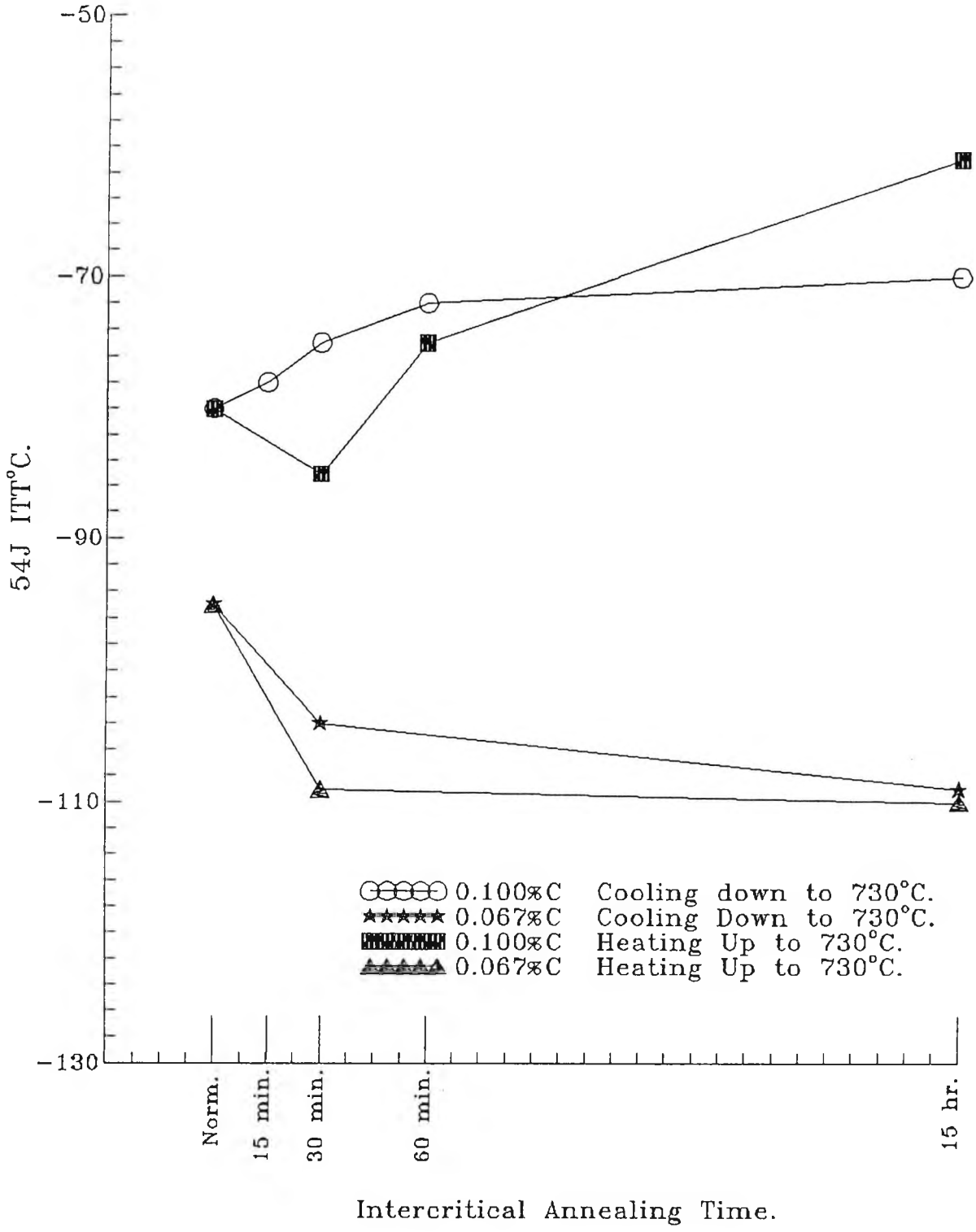

Fig.4.38- The Effect of Carbon Level on the 54J ITT°C After Different I.A. Times for the 1.5%Mn Steels.

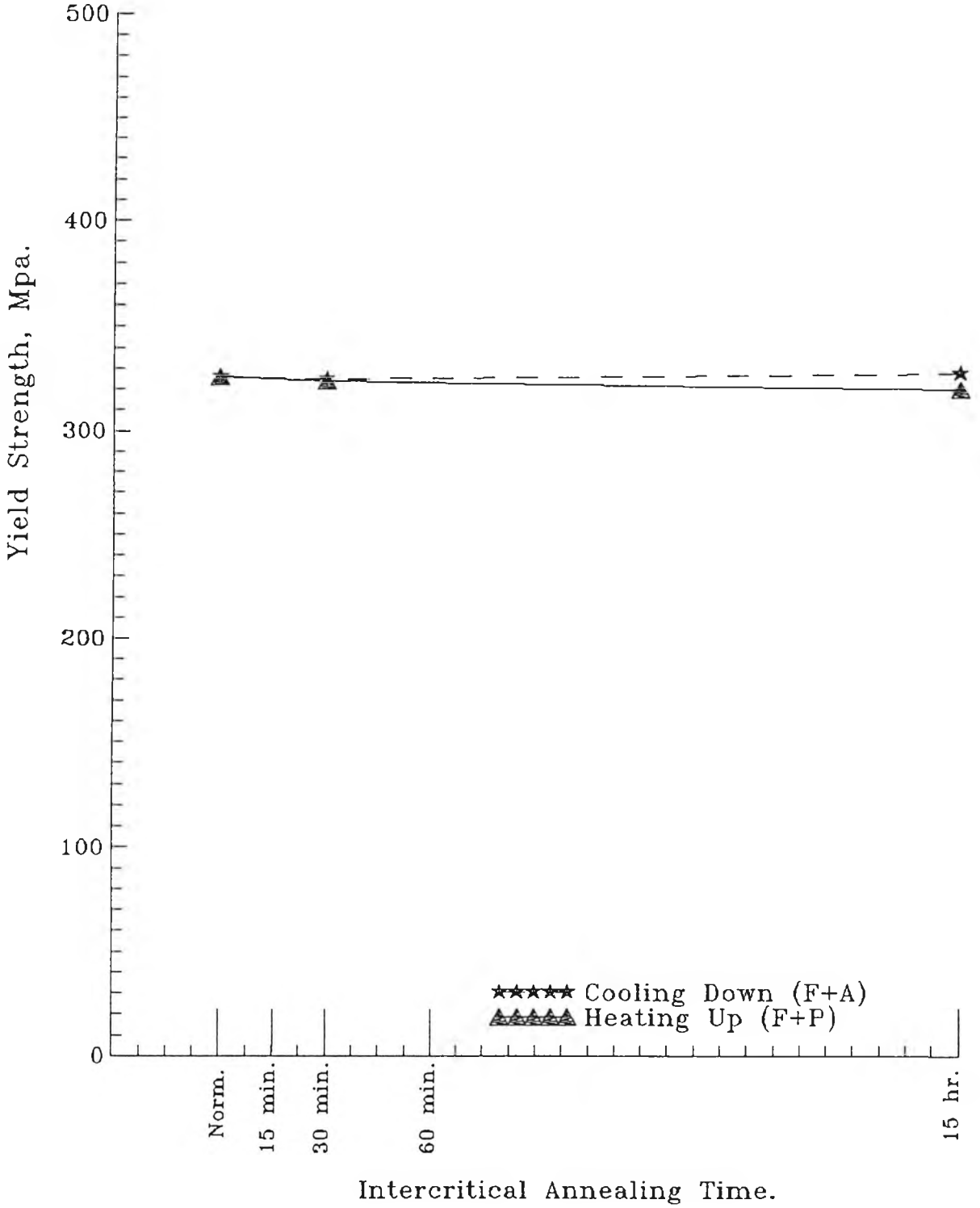

Fig.4.39- The Effect of I.A. Time on the Yield Strength for the 0.067%C Steel.

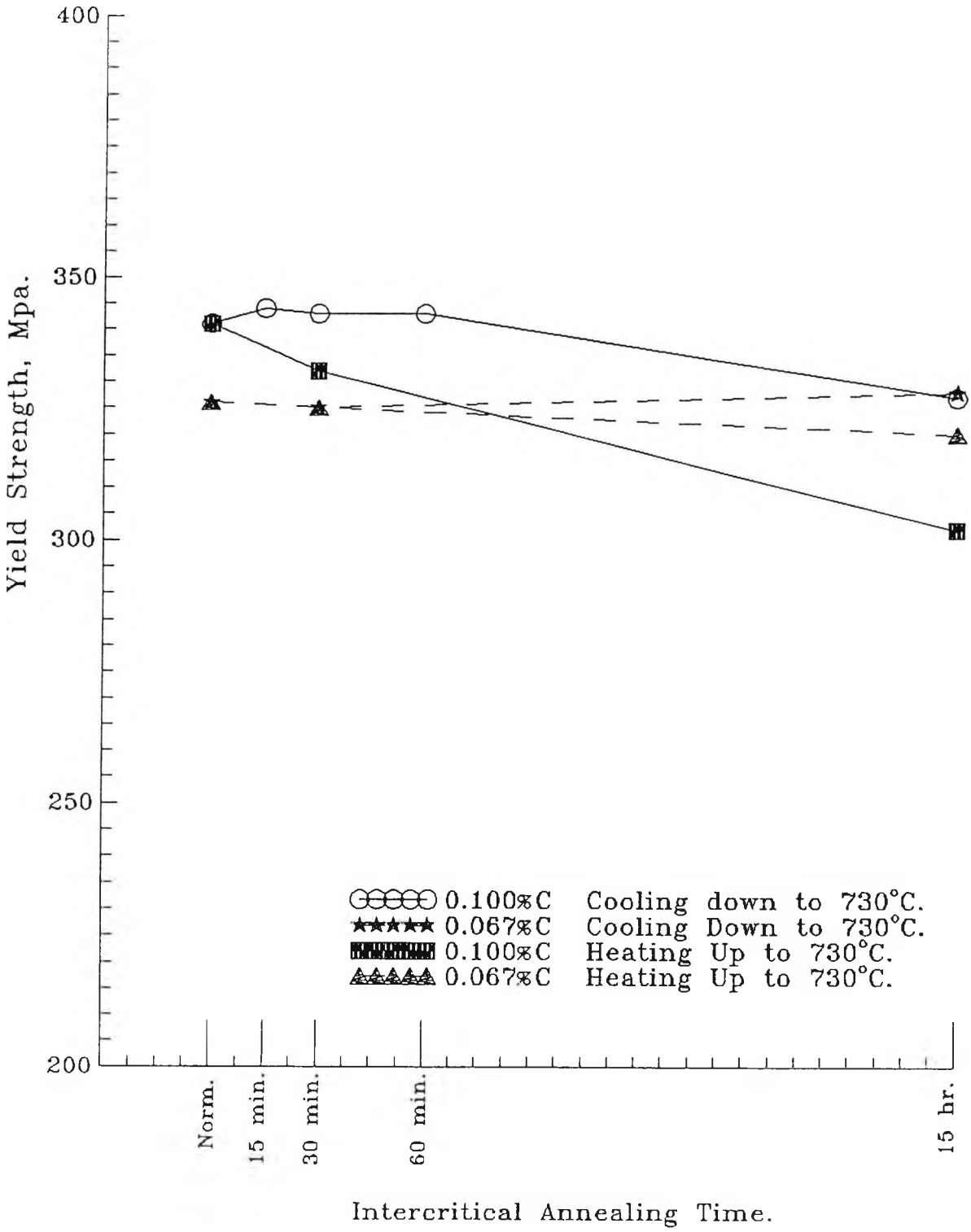

Fig.4.40- The Influence of I.A. Time on the Yield Strength for Two Different Carbon Levels for the 1.5%Mn Steel.

4.3.4- METALLURGY.

The change in microstructure with intercritical annealing time was followed by taking a series of optical photographs of the microstructure as a function of intercritical annealing time. Figs. 4.41 and 4.42.

4.3.4.1- COOLING DOWN.

Figure 4.41 shows the microstructure of 0.067% C steel after normalising and after intercritical annealing at 730°C for 30 minutes and 15 hours. The microstructure after normalising consists of ferrite and randomly dispersed pearlite. The microstructure after 30 minutes of intercritical annealing after cooling down from austenitising shows some reduction in the number of larger pearlite colonies and these are replaced by films of pearlite surrounding the grain boundaries. After very long holding times (15 hours), the structure again reverts back to the normalised but with some much coarser pearlite colonies.

4.3.4.2- HEATING UP.

Figure 4.42 shows the microstructure of the 0.067% C steel after intercritical annealing for 30 minutes and 15 hours. It can seen that, the pearlite colonies form as thin films round the ferrite grains. With increasing intercritical annealing time, this film thickens and extends producing a network around the ferrite phase.

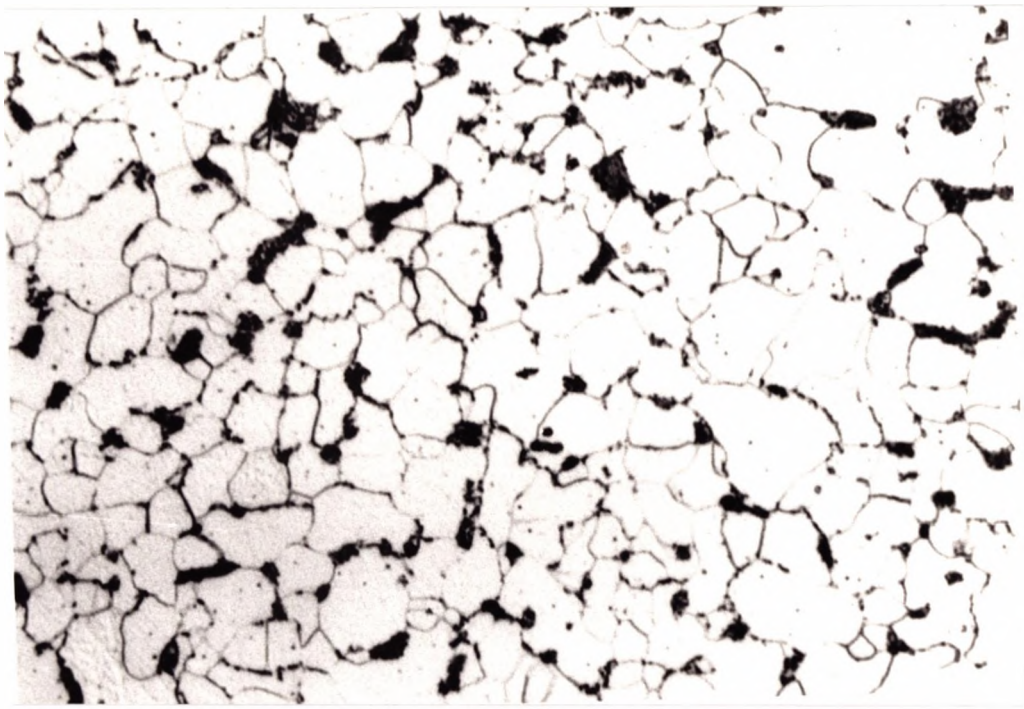

-a- x 900

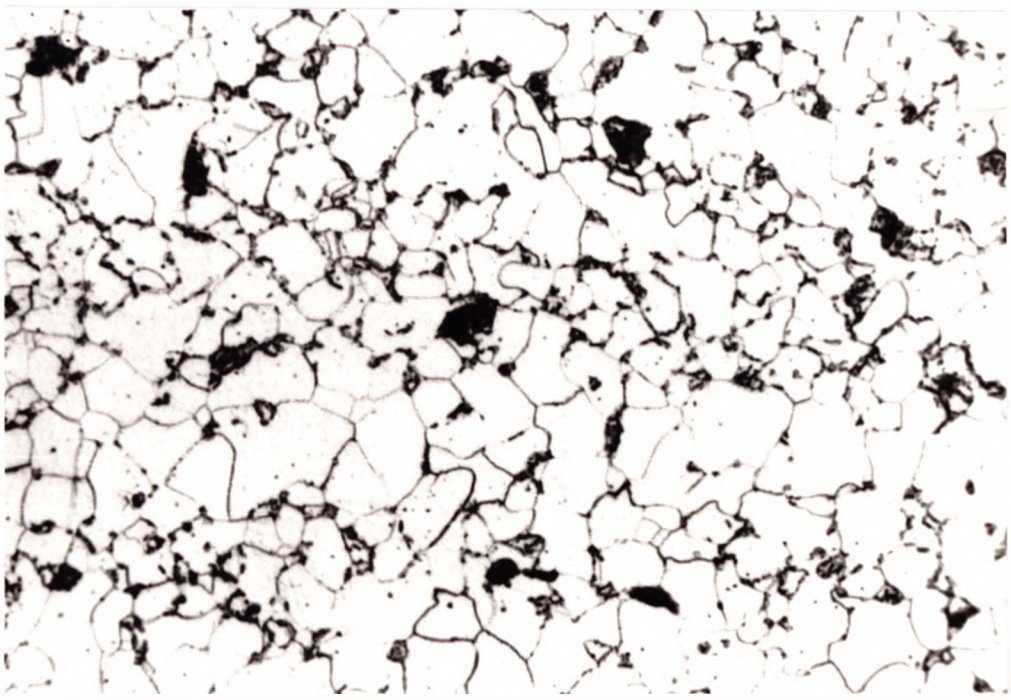

-b- x 900

Fig.4.41- Microstructure of the 0.067 % C Steel

a-Normalised, b-I.A. 30 min. Cooling Down Cycle.

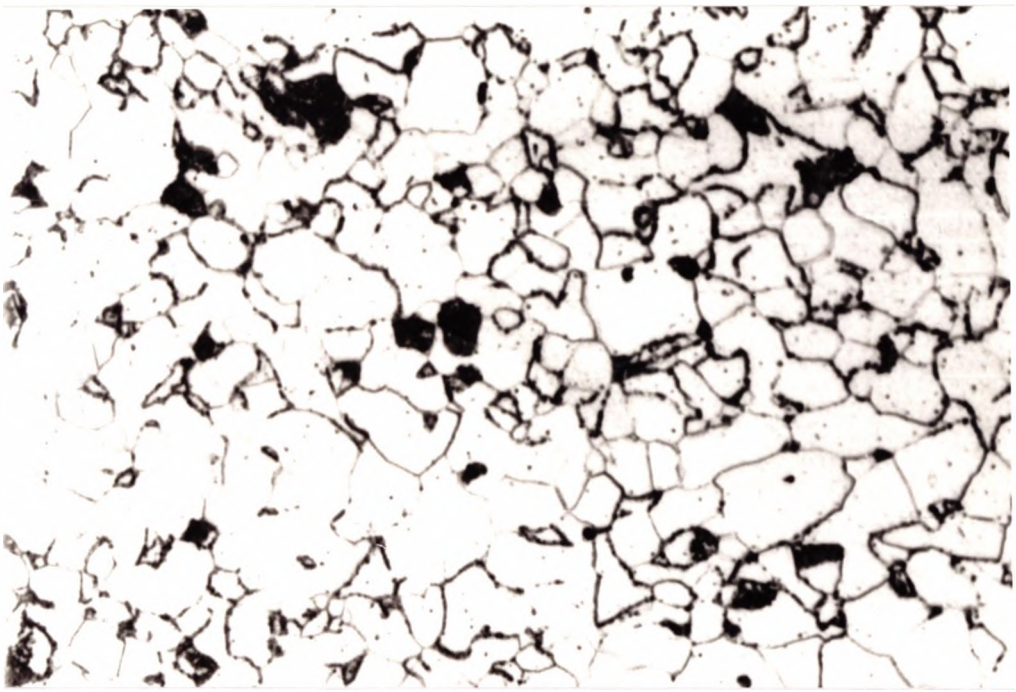

-c- x 900

Fig.4.41c- Microstructure of the 0.067%C Steel I.A. for 15 hr, Cooling Down Cycle.

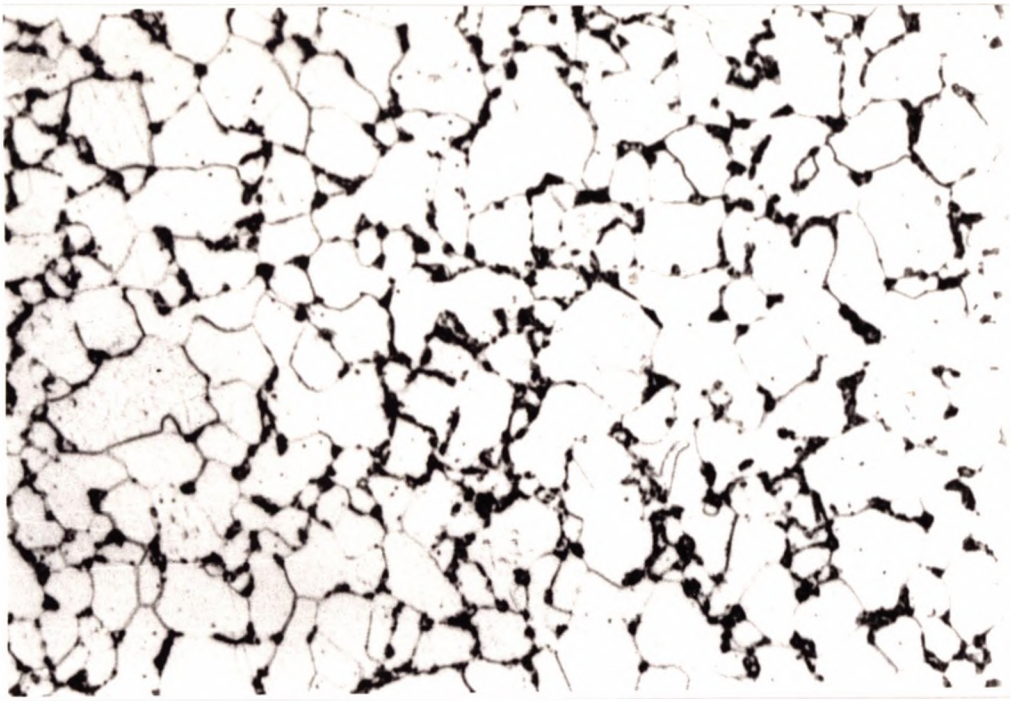

-a- x 900

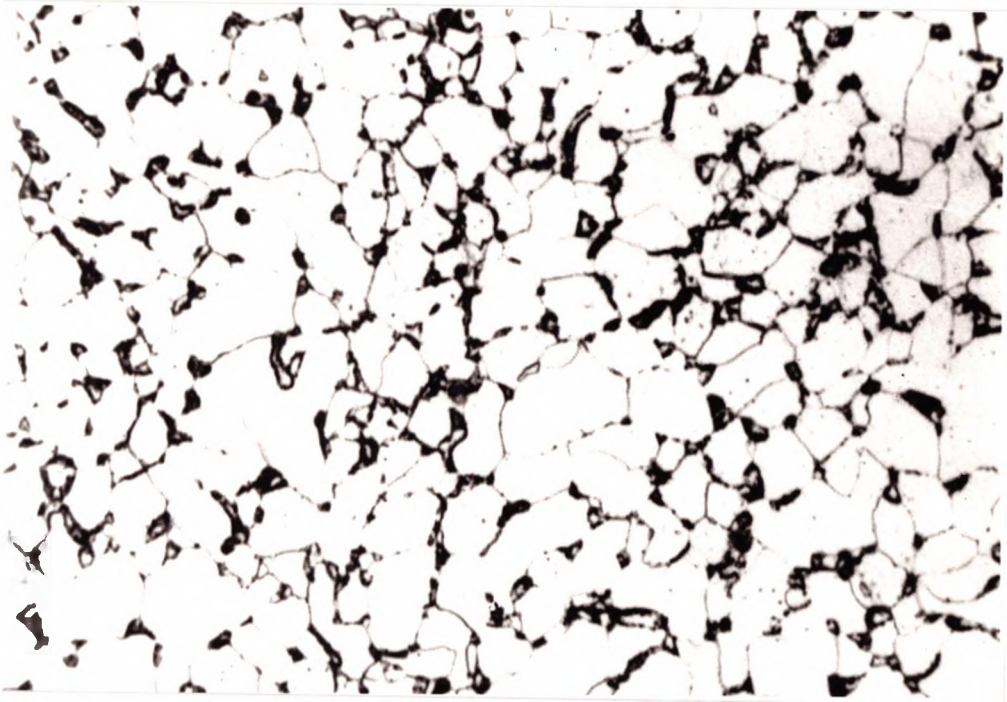

-b- x 900

Fig.4.42- Microstructure of the 0.067%C Steel

a- I.A. 30 min., b- I.A. for 15 hr,

Heating up Cycle.

4.4- THE EFFECT OF INTERCRITICAL ANNEALING TEMPERATURE AND HOLDING TIME ON IMPACT AND TENSILE PROPERTIES.

4.4.1- INTRODUCTION.

During intercritical annealing, the volume fraction of austenite is controlled by the heating temperature. As the heating temperature increases the volume fraction of austenite increases.

So far in the thesis a constant intercritical annealing temperature of 730°C has been used. In order to examine the influence of annealing temperature this investigational section extends the study to the higher temperature of 760°C. The 1% Mn steel has been chosen for examination in this excercise.

The chemical composition of this steel is listed in table 4.14. The results from this investigation will be compared with the results in section 4.1 for the same 1% Mn steel intercritically annealed at 730°C. The same cooling rate of 7°C/min was used as for the lower intercritical annealing temperature.

Plates were also normalised and cooled at 7°C/ min to room temperature.

Table 4.14- The Chemical Composition of Steel Used for Examining the Influence of Heating Temperature on I.A.

C	Mn	Si	S	P	Al	Nb	N
0.083	1.0	0.29	0.004	0.01	0.028	0.026	0.005

4.4.2- MICROSTRUCTURAL MEASUREMENTS.

The microstructural data; grain size, pearlite volume fraction, and grain boundary carbide thickness measurements for the steel after intercritical annealing at 760°C are given in table 4.14. Data at 730°C is given in Table 4.3.

As in the previous work, intercritical annealing had little influence on the normalised grain size. Only a slight coarsening of the grain size was found with increasing heating temperature (the average grain size being 10.3 μm and 10.7 μm for intercritical annealing at 730°C and 760°C respectively). Similarly, the pearlite volume fraction was found to only increase slightly with increasing heating temperature (average of 10% and 11% for intercritical annealing at 730°C and 760°C respectively).

There was a slight coarsening of the grain boundary carbide thickness as the heating temperature increased from 730°C to 760°C.

4.4.3- IMPACT AND TENSILE BEHAVIOUR.

Impact transition curves and fibrous fracture curves after normalising and intercritical annealing at 760°C for the 1%Mn steel are given in Figure 4.43 and Figure 4.44 for heating up directly to the intercritical annealing temperature and cooling down to the intercritical annealing temperature respectively.

The effect of intercritical annealing holding time at 760°C on the 54J ITT°C is shown in Figure 4.45 both for heating up and cooling down to the intercritical annealing temperature.

For heating up directly to the intercritical annealing temperature, a fall in (ITT) of 25°C was noted after 30 minutes. Increasing the intercritical annealing time had little further influence on the ITT.

For cooling down to the intercritical annealing temperature, a drop in ITT of 10°C occurred after 30 minutes and there was no further drop in ITT with increasing holding time.

Figure 4.46 shows the effect of intercritical annealing heating temperature on ITT for the 1%Mn steel intercritically annealed at 730°C and 760°C both on heating up and cooling down to the intercritical annealing temperature. It can be seen that; in case of cooling down to the intercritical temperature, increasing the intercritical annealing temperature from 730°C to 760°C raises the ITT by about 10°C after 30 minutes and by about

15°C after 15 hours. For heating up to the intercritical annealing temperature the ITT remains approximately constant.

Tensile data (yield strength and ultimate tensile strength) are listed together with microstructural data in table 4.15, for the 1%Mn steel intercriticaliy annealed at 760°C. Figure 4.47 shows the effect of intercritical annealing holding time at 760°C on lower yield strength for the 1%Mn steel for both heating up and cooling down to the intercritical annealing temperature. It can be seen that, intercritical annealing has no effect on yield strength.

Figure 4.48 shows the effect of intercritical annealing temperature on yield strength for both heating up and cooling down to the intercritical annealing temperature. It can be seen that, raising the intercritical annealing temperature from 730°C to 760°C causes a fall in yield strength of about 20 Mpa after 30 minutes on cooling down to the intercritical annealing temperature. For heating up to the intercritical annealing temperature, there is no significant change in yield strength with increasing intercritical annealing temperature.

Table 4.15- Microstructure Measurements and Strength of the 1% Mn Steel I.A at 760°C

Specimen No.	Ferrite Grain Size µm	Ferrite Grain Size $d^{-1/2}$ $mm^{-1/2}$	Pearlite Volume Fraction %	Grain Boundary Carbide Thicknes s µm	54J ITT °C	σ_Y MPa	σS MPa
2N	11	9.5	9	0.38	-60	290	432
21C	11.5	9.3	10	0.30	-70	288	430
22C	11	9.5	14	0.28	-70	290	428
21H	10.5	9.8	11	0.27	-85	295	436
22H	9.5	10.3	13	0.25	-89	285	541

2N =normalised.

21C, 22C are for samples cooled down to the intercritical annealing temperature and held for 30 and 900 minutes respectively.

21H, 22H are for samples heated directly to the intercritical annealing temperature and held for 30 and 900 minutes respectively.

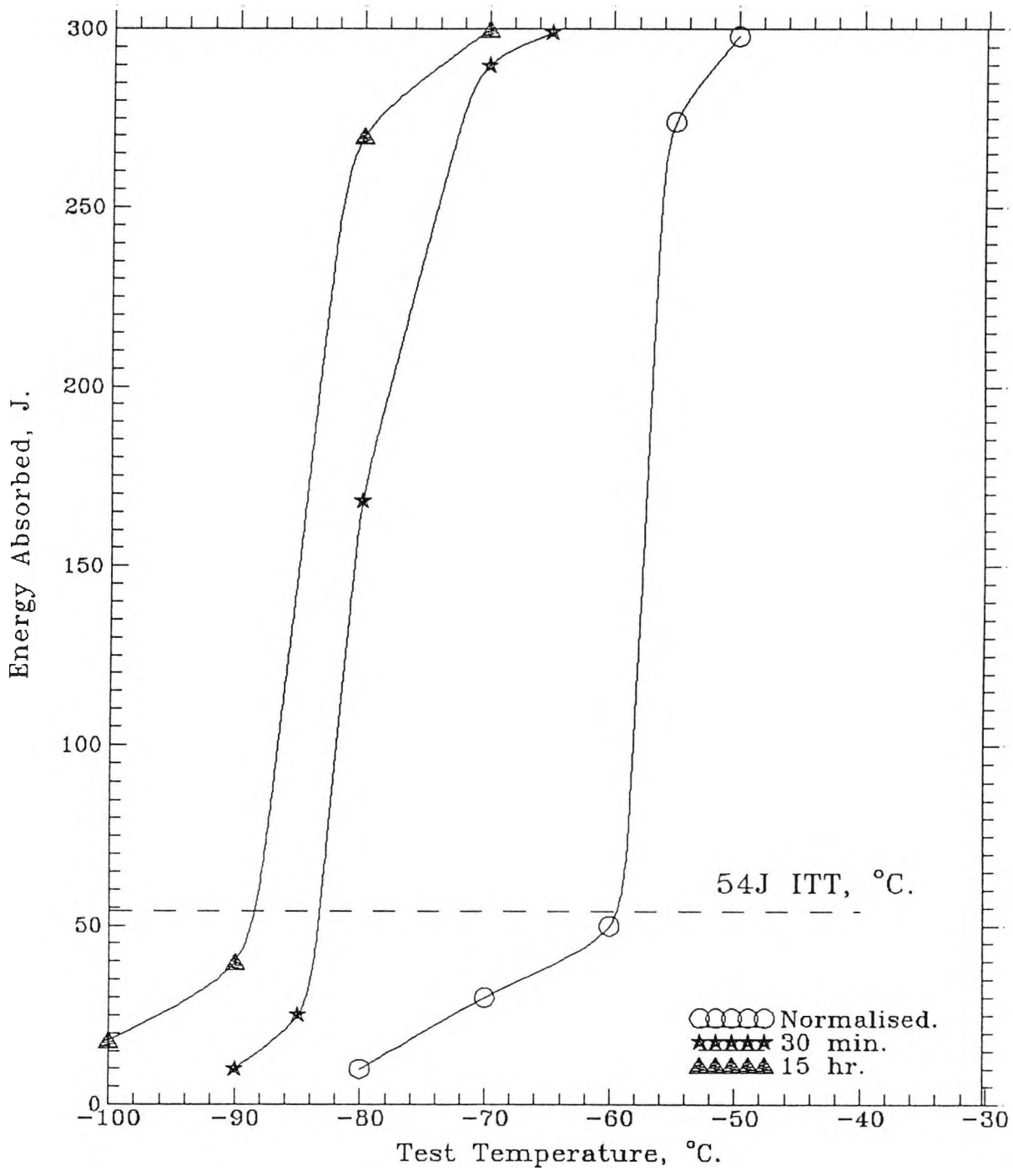

Fig.4.43a- Impact Transition Curves for the 1.0%Mn Steel I.A. at 760°C for Various Times, Cooled at 7°C/min, Heating Up Cycle.

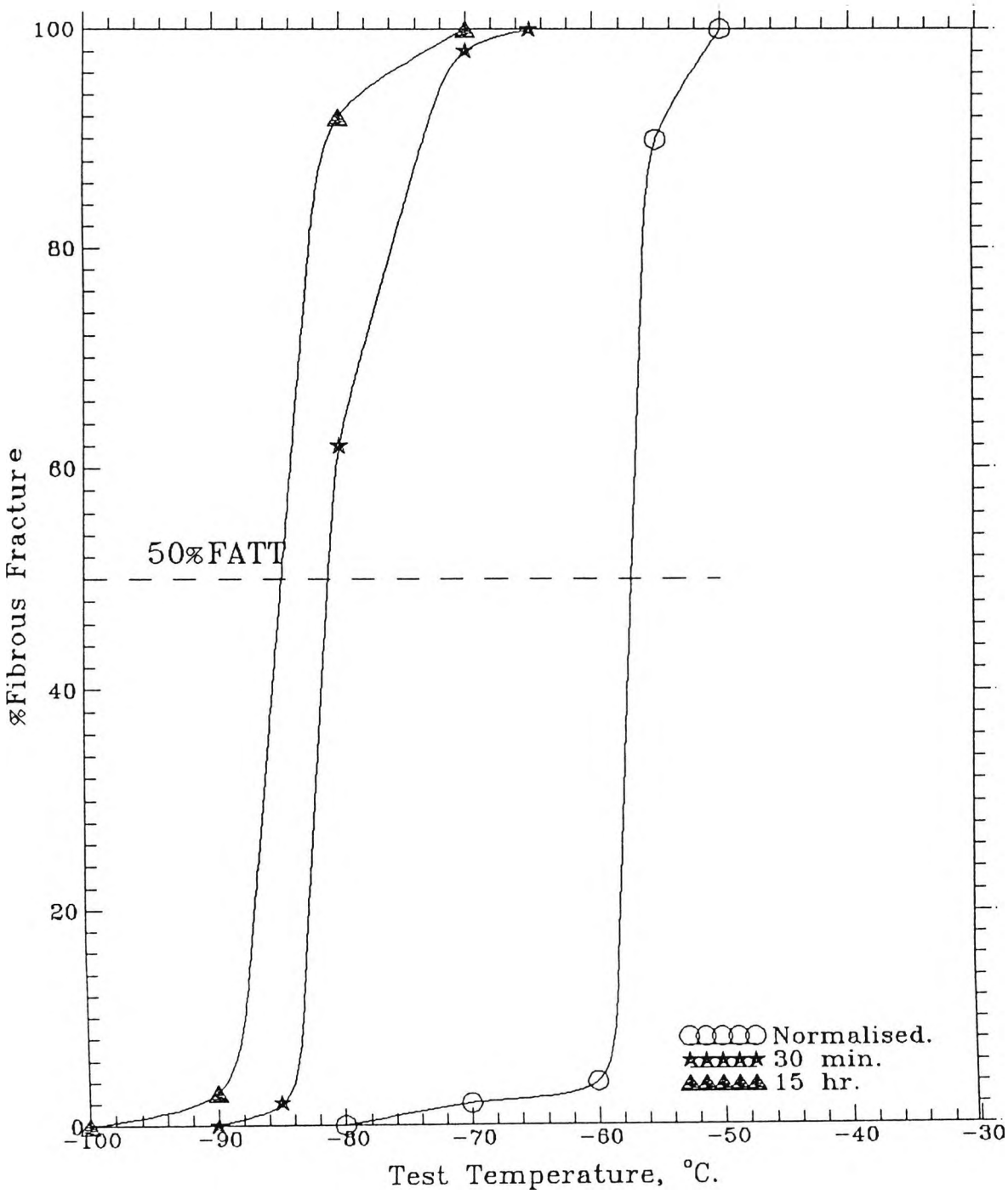

Fig.4.43b- Fibrous Fracture Curves for the 1.0%Mn Steel I.A. at 760°C for Various Times, Cooled at 7°C/min, Heating Up Cycle.

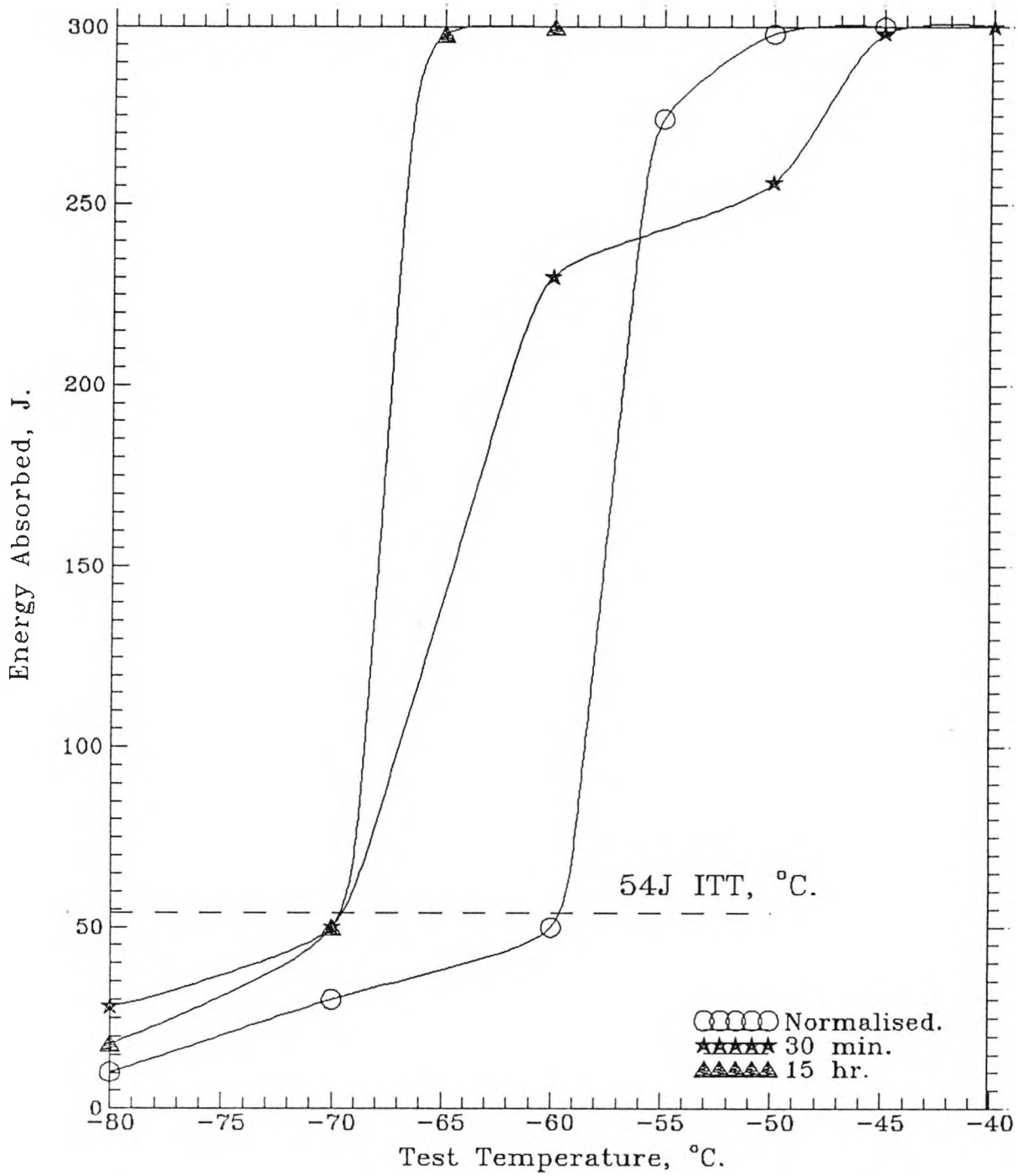

Fig.4.44a- Impact Transition Curves for the 1.0%Mn Steel I.A. at 760°C for Various Times, Cooled at 7°C/min, Cooling Down Cycle.

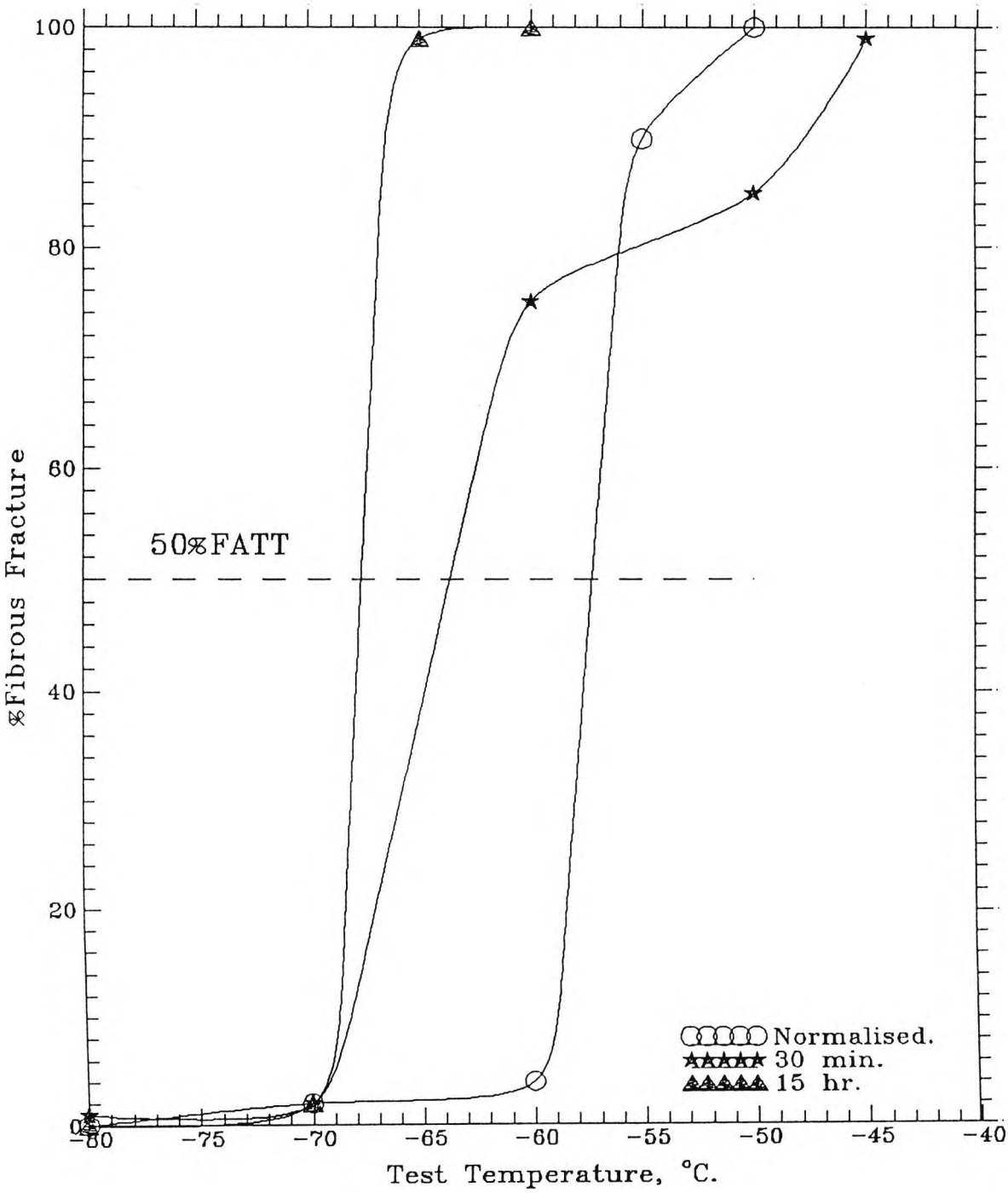

Fig.4.44b- Fibrous Fracture Curves for the 1.0%Mn Steel I.A. at 760°C for Various Times, Cooled at 7°C/min, Cooling Down Cycle.

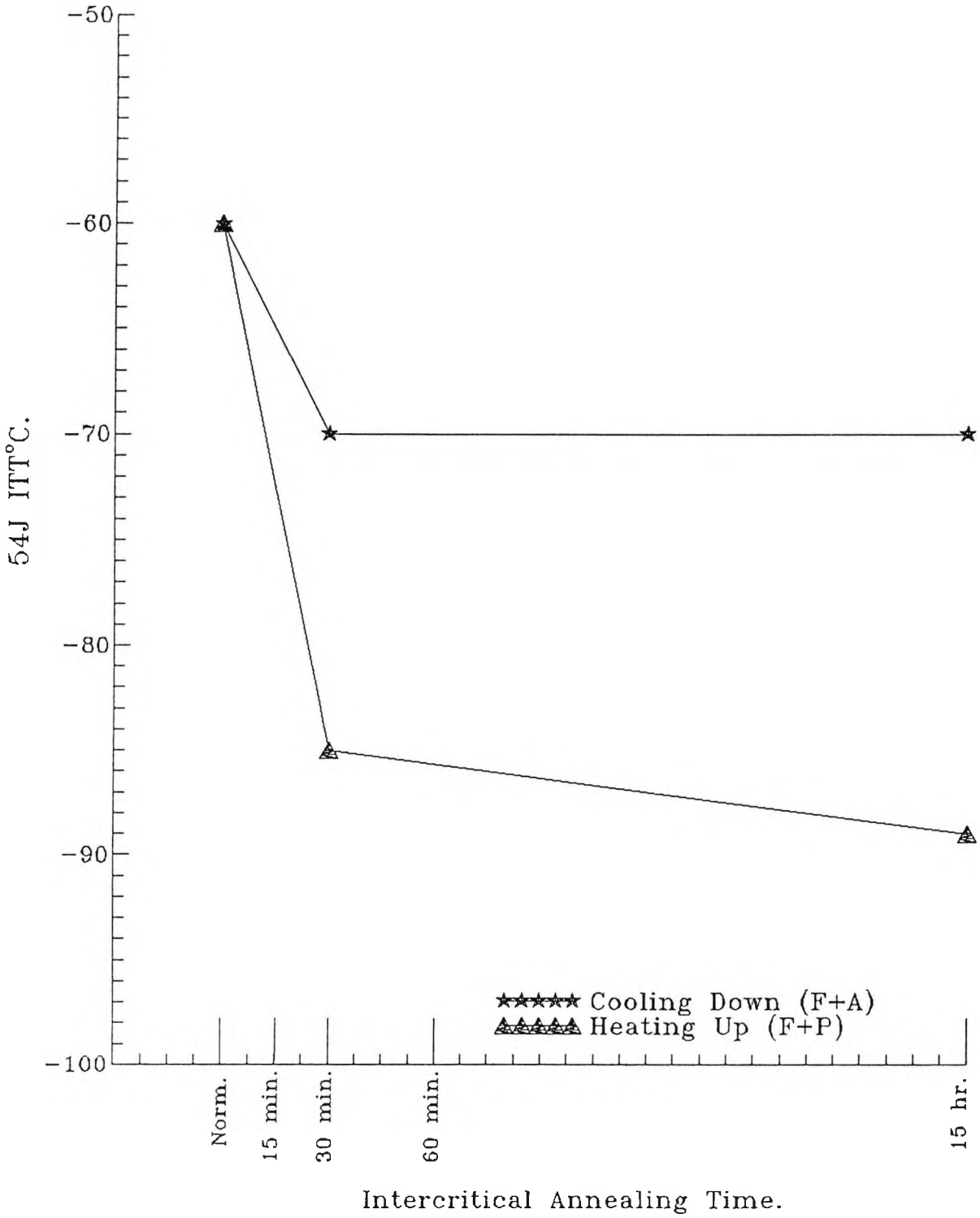

Fig. 4.45- The Effect of I.A. Times on the 54J ITT°C for the 1.0%Mn Steel I.A. at 760°C.

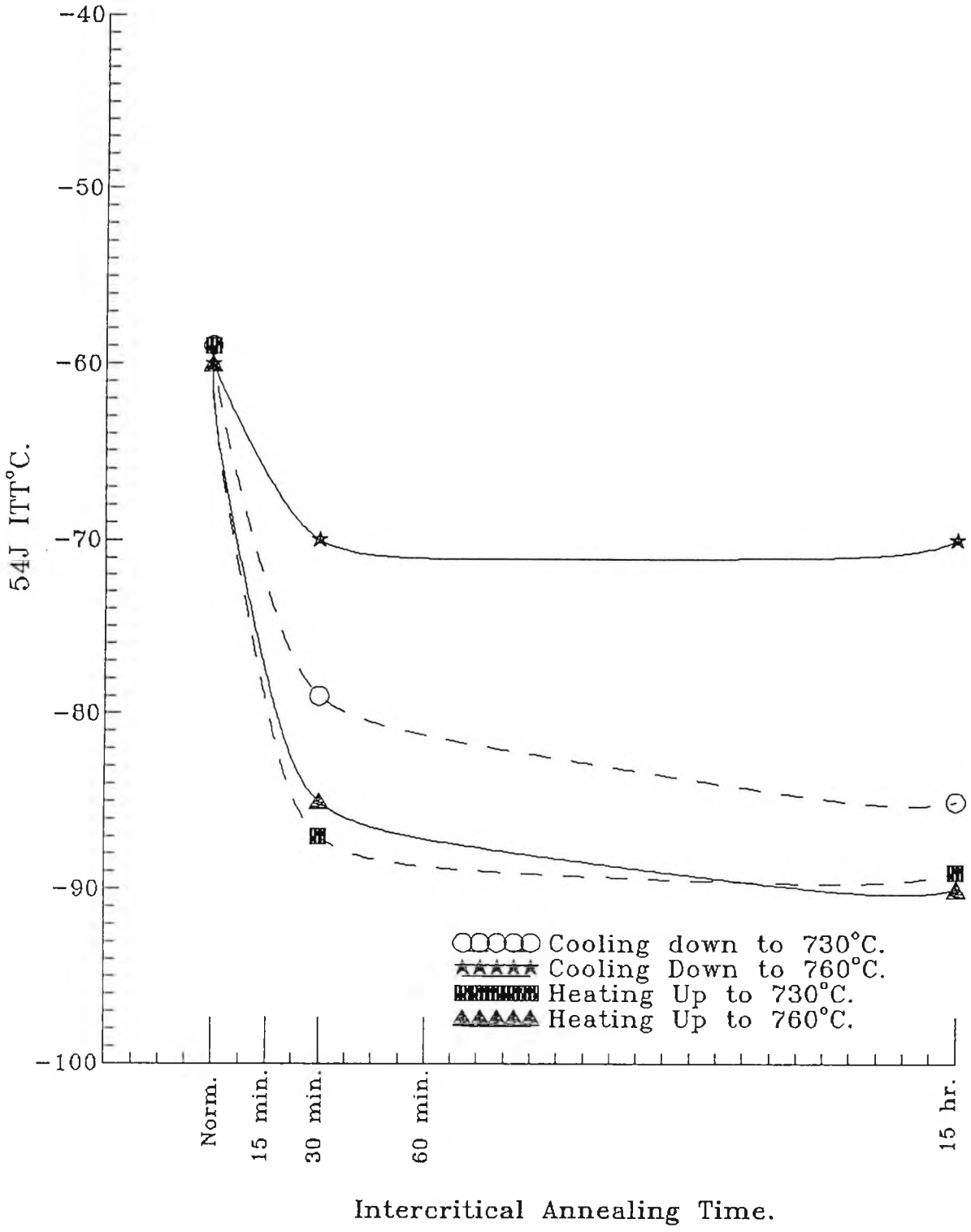

Fig.4.46- The Influence of Heating Temperature After Different I.A. Times on the 54J ITT°C for the 1% Mn Steel.

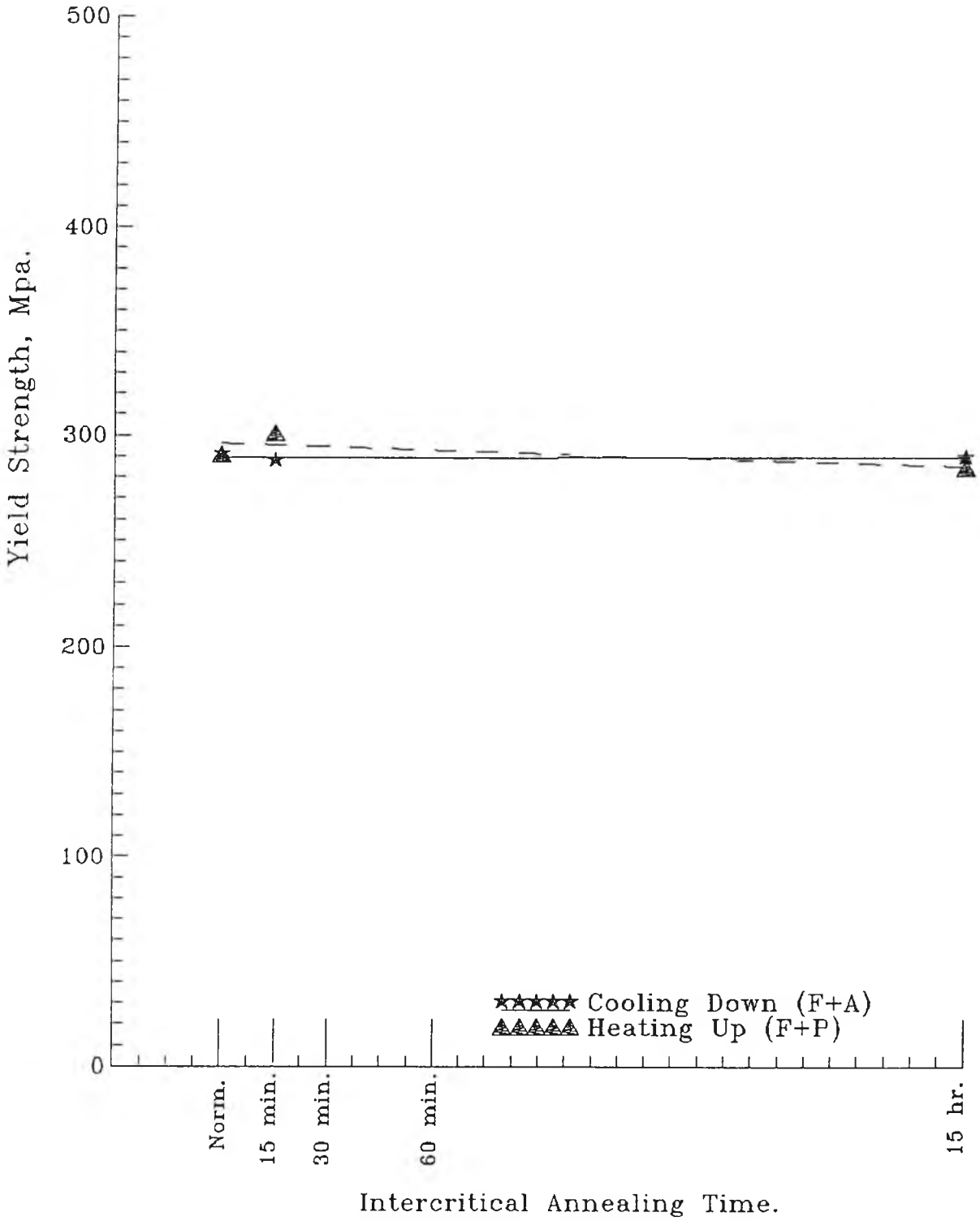

Fig.4.47- The Effect of I.A. Times on the Yield Strength of the 1.0%Mn Steel I.A. at 760°C.

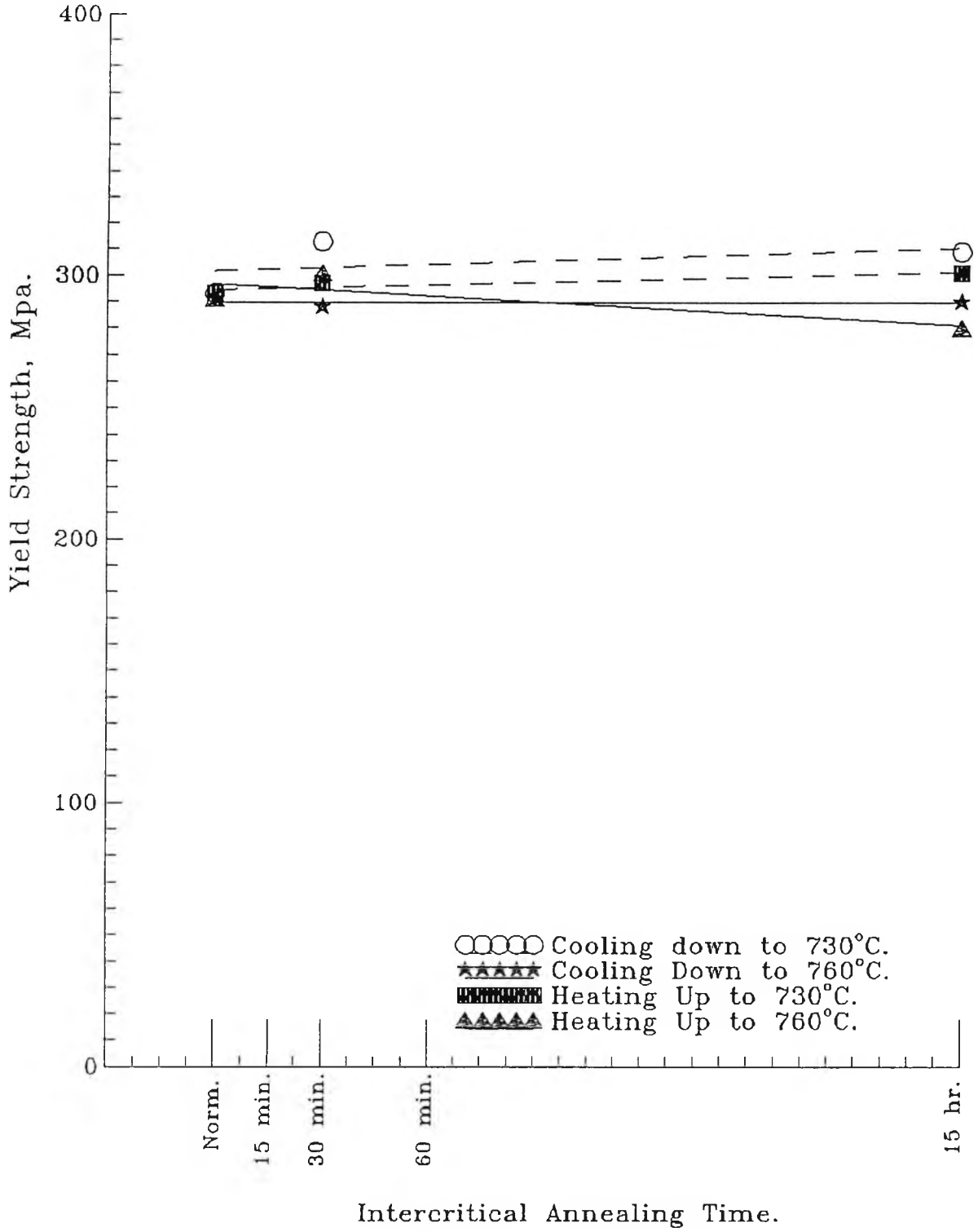

Fig.4.48- The Effect of Heating Temperature After Different I.A. Time on the Yield Strength of the 1.0%Mn Strength.

4.4.4- METALLOGRAPHY.

The change in microstructure with intercritical annealing time was followed by taking a series of optical photographs of the microstructure as a function of intercritical annealing time, Figs. 4.49 and 4.50.

4.4.4.1- COOLING DOWN.

Figure 4.49 shows the microstructure of the 1%Mn steel after normalising and after intercritical annealing at 760°C for 30 minutes and 15 hours. The microstructure after normalising consists of equiaxed ferrite grains plus banded pearlite colonies. The microstructure after 30 minutes of intercritical annealing after cooling down from austenitising temperature shows some coarser pearlite colonies than found after normalising. After holding for 15 hours , the pearlite phase becomes more distributed throughout the structure. Again there are some coarser pearlite colonies than found in the normalised condition.

4.4.4.2- HEATING UP.

Figure 4.50 shows the microstructure of the 1%Mn steel after intercritical annealing at 760°C for 30 minutes and 15 hours. It can seen that, the pearlite colonies form as thin films round the ferrite grains. Increasing the intercritical annealing time causes the pearlite films to extend and thicken. The pearlite colonies after intercritical annealing at 760°C for 30 minutes and 15

hours were thicker than after intercritical annealing at 730°C for the same times.

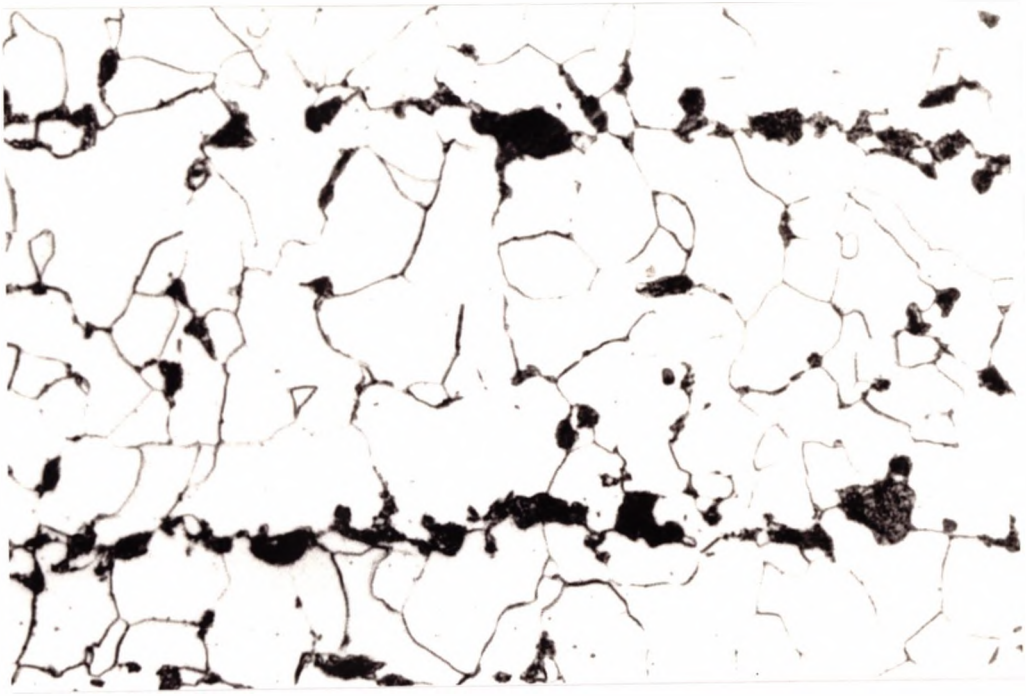

-a- x 900

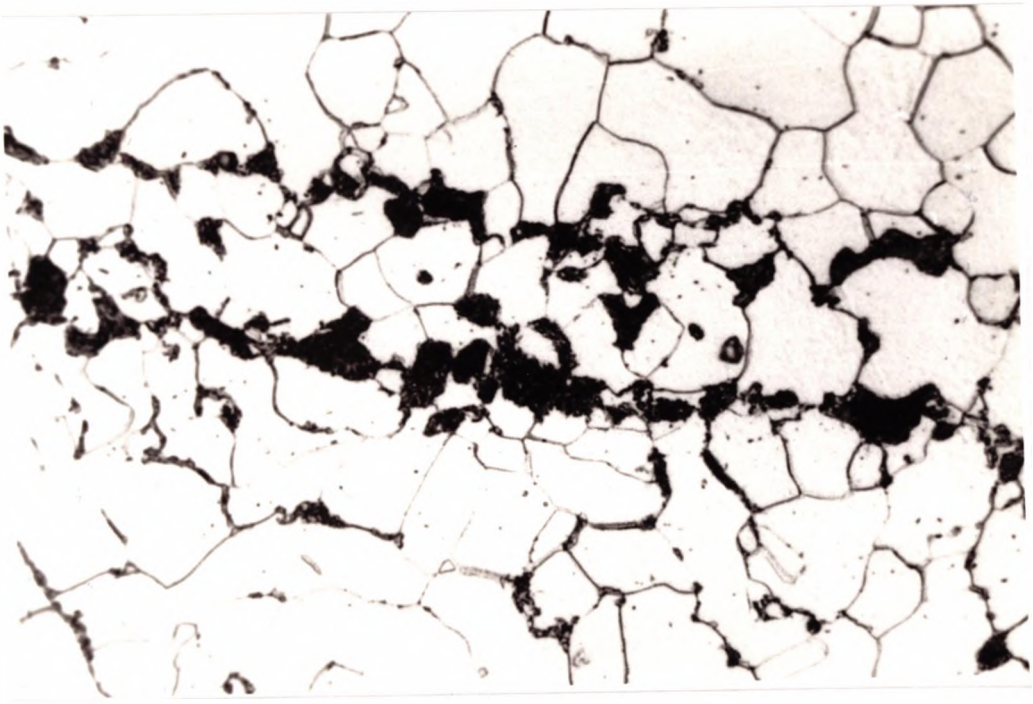

-b- x 900

Fig.4.49- Microstructure of the 1.0%Mn Steel

a- Normalised., b-I.A. for 30 min. at 760°C

Cooling Down Cycle.

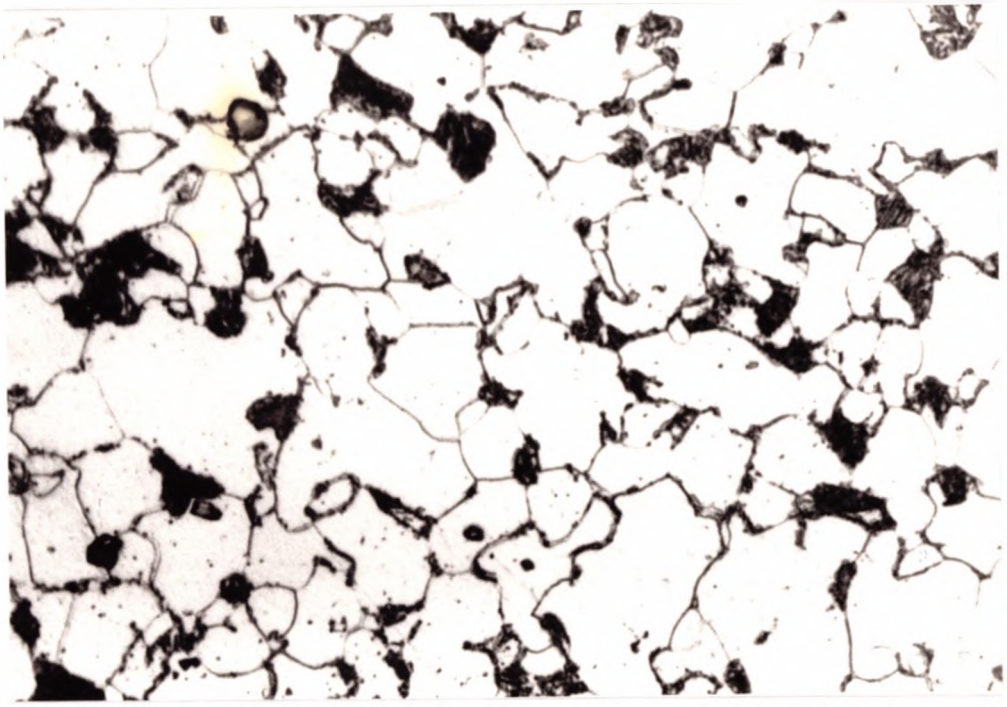

-c- x 900

Fig.4.49c Microstructure of the 1.0%Mn Steel

I.A. for 15 hr at 760°C.

Cooling Down Cycle.

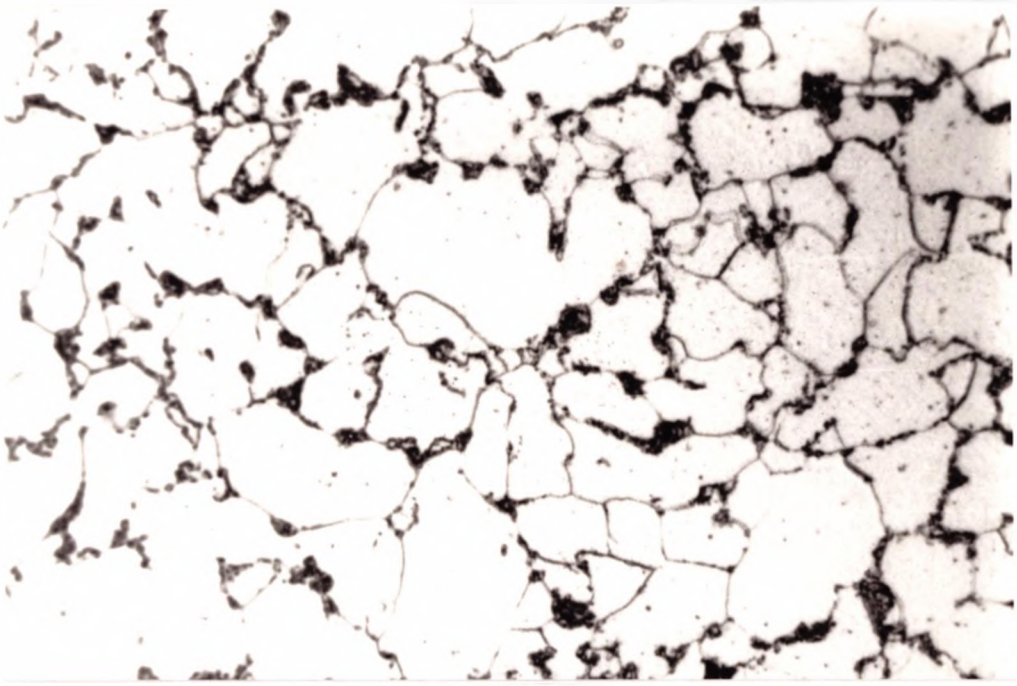

-a- x 900

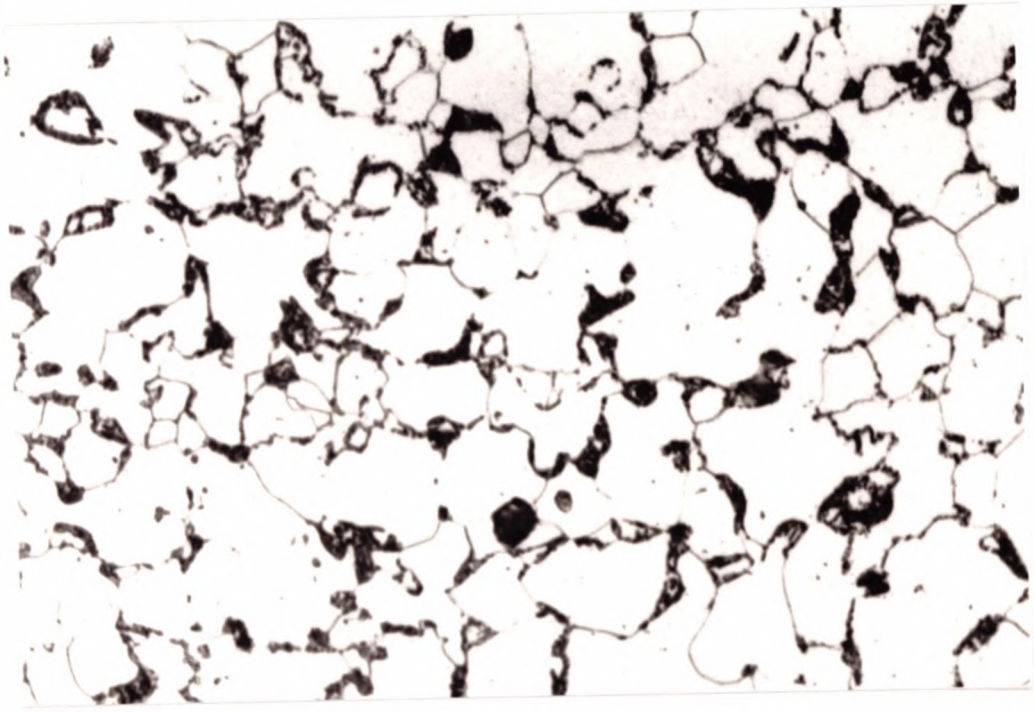

-b- x 900

Fig.4.50- Microstructure of the 1.0%Mn Steel

a- I.A. for 30 min., b- I.A. for 15 hr, at 760°C

Heating Up Cycle.

4.5- THE EFFECT OF GRAIN SIZE AND HOLDING TIME ON IMPACT AND TENSILE PROPERTIES.

4.5.1- INTRODUCTION.

Grain size is the most important factor dominating the impact and yield strength; a finer grain size increases the yield strength and lowers the ITT. The aim of this investigational section is to study the effect of grain size and holding time on the impact and tensile properties for a plain carbon manganese steel. Two grain sizes were examined (18 μm and 37 μm). The chemical composition of the steel used in this investigation is listed in table 4.16. A cooling rate of 7°C/min was used for all the intercritical annealing treatments time.

Plates were also normalised and cooled at 7°C/min to room temperature.

Table 4.16- The Chemical Composition of Steel Used for Examining the Influence of Grain Size on I.A.

C	Mn	Si	S	P	Al	Nb	N
0.11	0.62	0.32	0.005	0.009	0.008	-	0.0039

4.5.2- MICROSTRUCTURAL MEASUREMENTS.

The microstructural data; grain size, pearlite volume fraction, and grain boundary carbide thickness measurements are listed in table 4.17 for the plain carbon steel having a grain size of (18 μm), and in table 4.18 for the plain carbon steel having a grain size of of (37 μm) .

For the finer grain size (18 μm), there was no significant change in grain size and pearlite volume fraction with increasing intercritical annealing time.

For the coarser grain size (37 μm), the pearlite volume fraction was found to increase slightly, on intercritical annealing when comparisons were made with normalised condition. On cooling down to the intercritical annealing temperature, little change in grain size was observed compared to the normalised state, but for heating up to the intercritical annealing temperature the grain size was found to decrease after intercritical annealing for a long time.

The grain boundary carbides thickness for this steel decreased after intercritical annealing comparing to the normalising treatment, independent of whether the intercritical annealing temperature was approached by heating up or by cooling down. Compared to the normalised condition the grain boundary carbide thickness decreased on intercritical annealing from approximately 0.7 μm to 0.5 μm. The coarser grain size tended to give on average slightly coarser grain boundary carbides.

Table 4.17- Microstructural Measurements and Strength of the Finer Grained (18 μm) Plain Carbon Steel I.A.at 730°C.

Specimen No.	Ferrite Grain Size μm	Ferrite Grain Size $d^{-1/2}$ $mm^{-1/2}$	Pearlite Volume Fraction %	Grain Boundary Carbide Thicknes s μm	54J ITT °C	σ_Y MPa	σ_s MPa
6N	17.8	7.50	11	0.7	-25	280	422
61C	18.4	7.4	11	0.6	-28	278	408
62C	18.6	7.3	13	0.45	-35	275	414
61H	18.5	7.3	10	0.58	-29	273	400
62H	17.0	7.7	11	0.42	-42	277	404

6N =normalised.

61C, 62C are for samples cooled down to the intercritical annealing temperature and held for 30 and 900 minutes respectively.

61H, 62H are for samples heated directly to the intercritical annealing temperature and held for 30 and 900 minutes respectively.

Table 4.18- Microstructural Measurements and Strength of the Coarser Grained (37 μm) Plain Carbon Steel I.A.at 730°C.

Specimen No.	Ferrite Grain Size μm	Ferrite Grain Size $d^{-1/2}$ $mm^{-1/2}$	Pearlite Volume Fraction %	Grain Boundary Carbide Thicknes s μm	54J ITT °C	σ_Y MPa	σ_s MPa
8N	37.0	5.20	10.0	0.72	-5	224	396
81C	38.0	5.13	13.0	0.60	-10	219	394
82C	37.6	5.15	14.0	0.50	-10	220	402
81H	37.0	5.20	13.0	0.62	-5	215	393
82H	32.0	5.60	15.0	0.45	-7	226	398

8N =normalised.

81C, 82C are for samples cooled down to the intercritical annealing temperature and held for 30 and 900 minutes respectively.

81H, 82H are for samples heated directly to the intercritical annealing temperature and held for 30 and 900 minutes respectively.

4.5.3- IMPACT AND TENSILE BEHAVIOUR.

4.5.3.1- THE FINER GRAINED (18 μm) PLAIN CARBON MANGANESE STEEL.

Impact transition curves and fibrous fracture curves are given in Figure 4.51 and Figure 4.52 respectively for the plain carbon manganese steel for the normalised and intercritically annealed condition.

The effect of intercritical annealing holding time at 730°C on 54J ITT°C is shown more clearly in Figure 4.53 for both heating up and cooling down to the intercritical annealing temperature.

For heating up directly to the intercritical annealing temperature, a small fall in ITT of 4°C after 30 minutes was noted and this increased to 17°C after 15 hours.

For cooling down to the intercritical annealing temperature, changes were smaller, a small drop in ITT of 3°C occurred after 30 minutes and a 10°C fall occurred after 15 hours.

4.5.3.2- THE COARSER GRAINED (37μm) PLAIN CARBON MANGANESE STEEL.

Impact transition curves and fibrous fracture curves for the plain carbon steel are given in Figure 4.54 and Figure 4.55 respectively for the normalised and intercritically annealed conditions. The effect of intercritical annealing holding time at 730°C on the 54J ITT°C is shown in Figure 4.56 for both heating up and cooling down to the

intercritical annealing temperature.

For coarser grained (37 μm) plain carbon manganese steel, only very small falls in ITT were obtained (approximately 5°C after 15 hours).

Figure 4.57 shows more clearly the effect of grain size (18 μm and 37 μm) on 54J ITT for the plain carbon steel intercritically annealed at 730°C both on heating up and cooling down to the intercritical annealing temperature. It can be seen that, for the normalised state increasing the grain size from 18 μm to 37 μm raises the ITT by 20°C. In the case of the finer grained (18μm) plain carbon manganese steel, increasing the intercritical annealing time at 730°C to 15 hours lowers the ITT by about 17°C and 10°C, for heating up and cooling down to the intercritical annealing temperature respectively. In the case of the coarser grained (37 μm) plain carbon manganese steel, there was no significant change in ITT with intercritical annealing.

The tensile (yield strength and ultimate tensile strength) and microstructural data are listed in tables 4.17 and 4.18 for the finer and coarser grained (18 μm and 37 μm) conditions respectively for the normalised and intercritical annealing states.

Figures 4.58 and 4.59 summarises the effect of intercritical annealing holding time at 730°C on the lower yield strength for the the plain carbon manganese steel at grain sizes of 18 μm and 37 μm respectively, for both

heating up and cooling down to the intercritical annealing temperature. It can be seen that, for the grain size range examined intercritical annealing has no significant effect on the yield strength of the plain carbon manganese steel.

Figure 4.60 shows the effect of grain size on yield strength for both heating up and cooling down to the intercritical annealing temperature.

It can be seen that, increasing the grain size from 18 μm to 37 μm lowers the yield strength by about 50 Mpa.

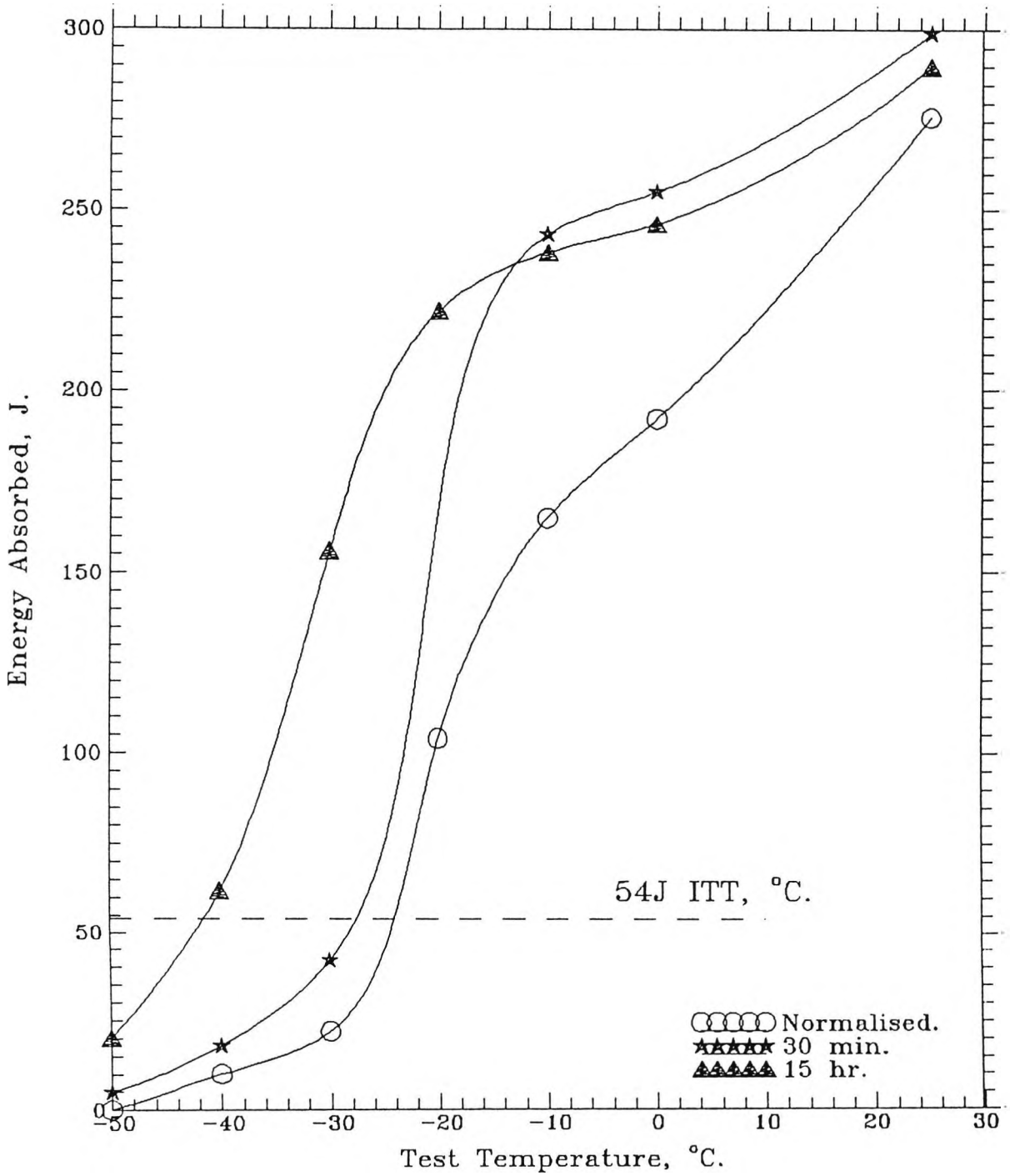

Fig.4.51a- Impact Transition Curves for the Plain Carbon Manganese Steel, (Fine Grain Size), I.A. at 730°C, Cooled at 7°C/min, Heating Up Cycle.

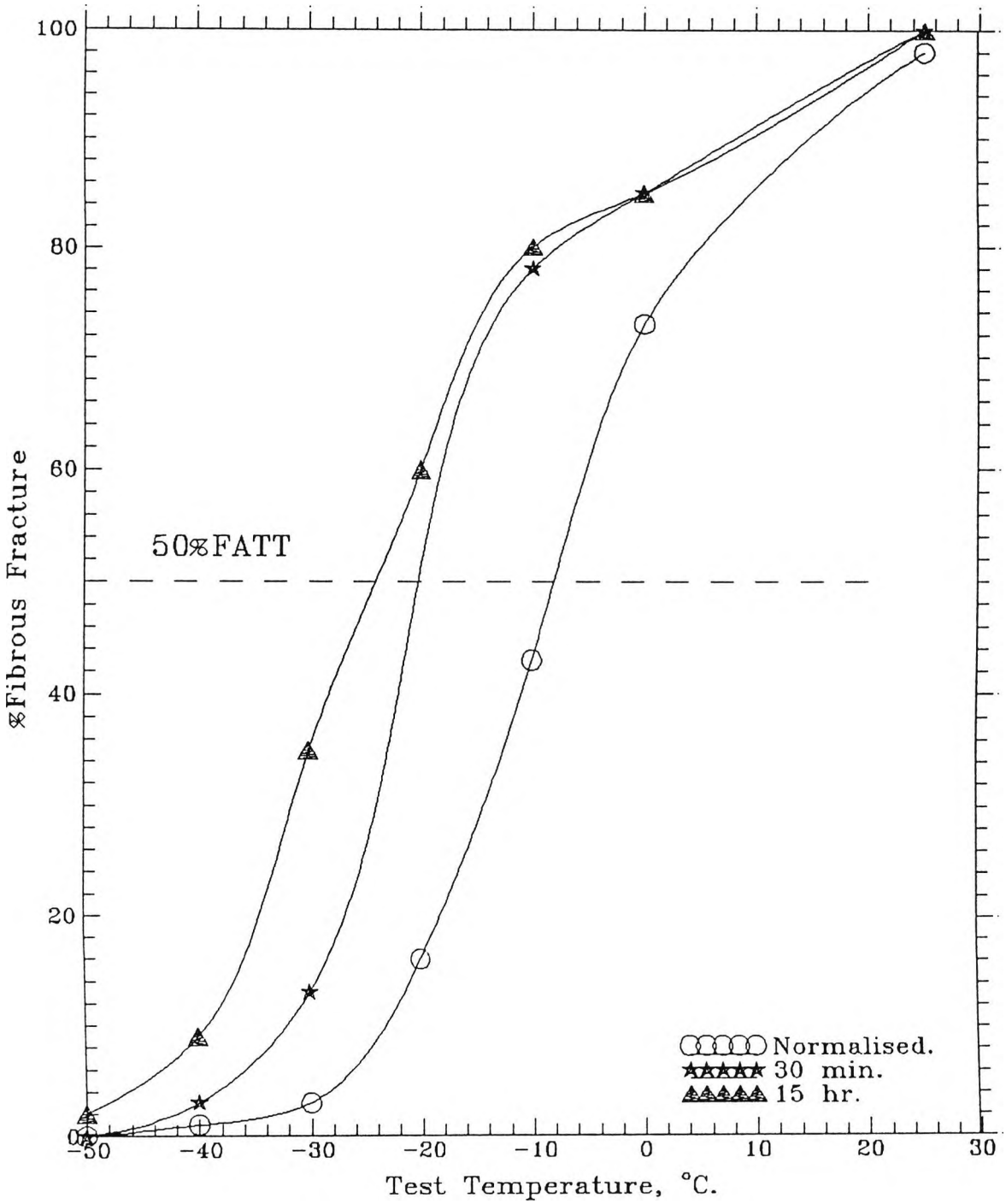

Fig.4.51b- Fibrous Fracture Curves for the Plain Carbon Manganese Steel, (Fine Grain Size), I.A. at 730°C, Cooled at 7°C/min, Heating Up Cycle.

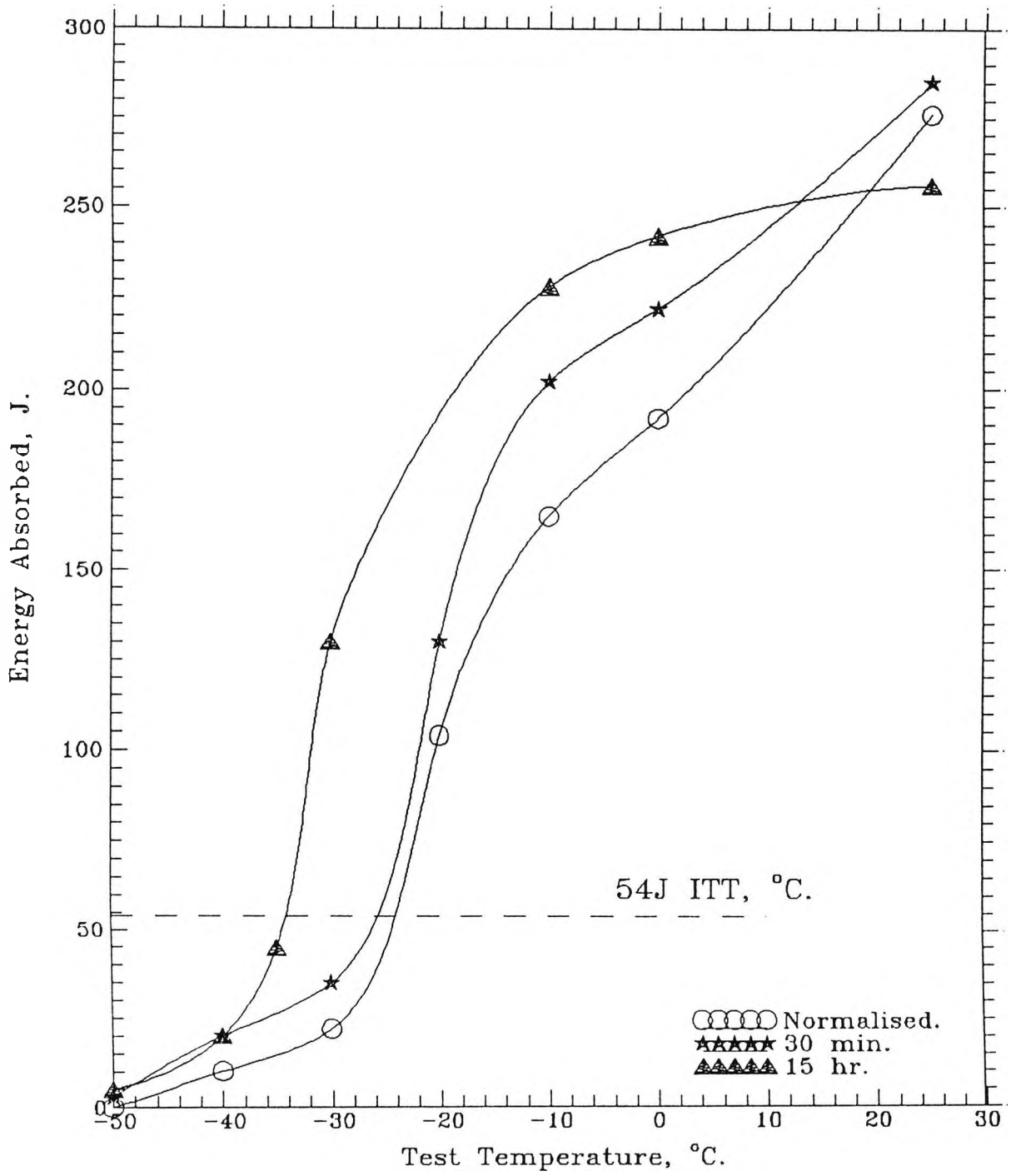

Fig.4.52a- Impact Transition Curves for the Plain Carbon Manganese Steel, (Fine Grain Size), I.A., at 730°C Cooled at 7°C/min, Cooling Down Cycle.

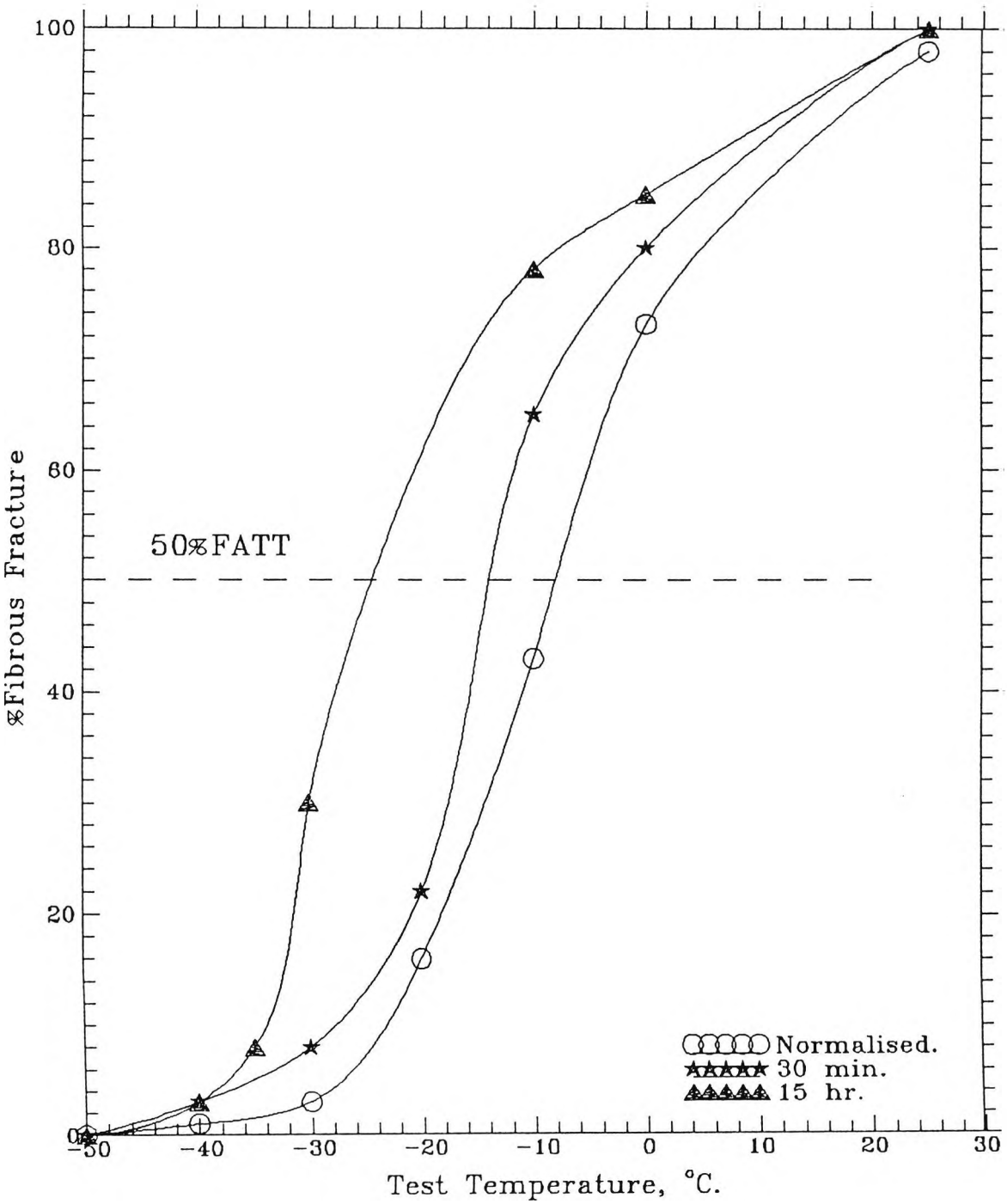

Fig.4.52b- Fibrous Fracture Curves for the Plain Carbon Manganese Steel, (Fine Grain Size), I.A., at 730°C, Cooled at 7°C/min, Cooling Down Cycle.

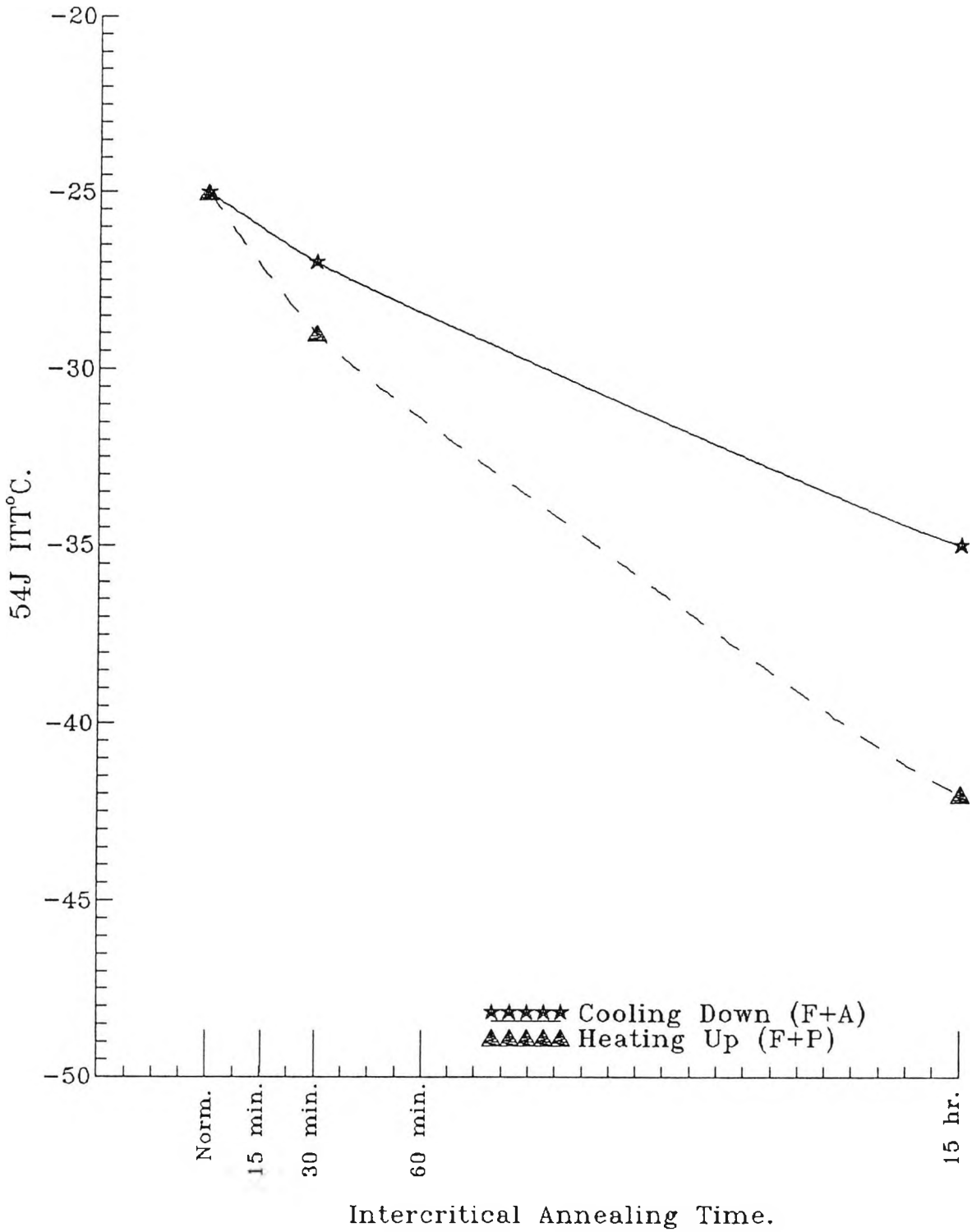

Fig.4.53- The Effect of I.A. Times on the 54J ITT°C for the Plain Carbon Mn Steel (Fine Grain Size).

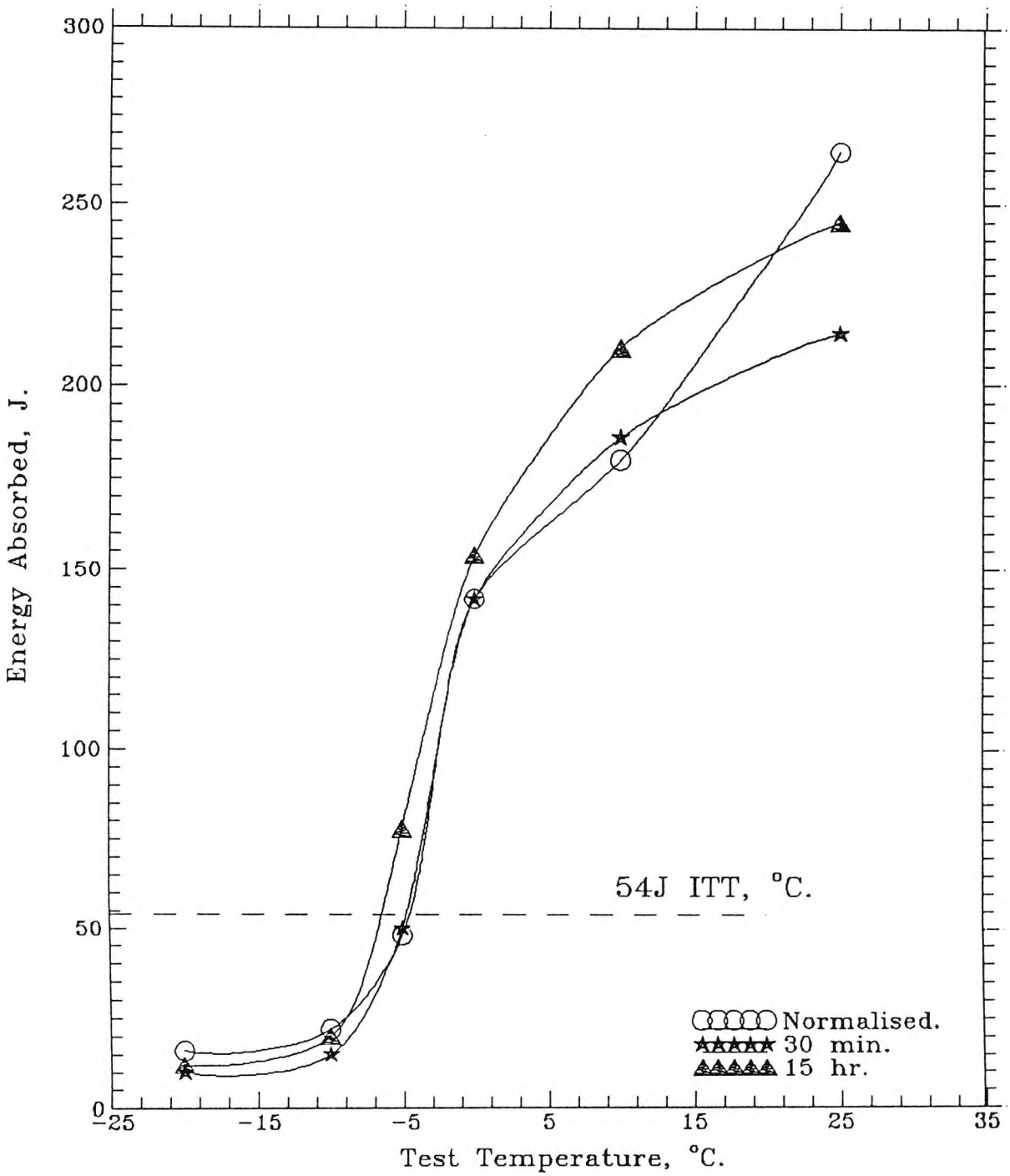

Fig.4.54a- Impact Transition Curves for the Plain Carbon Mn Steel (Coarse Grain Size), I.A. at 730°C, Cooled at 7°C/min, Heating Up Cycle.

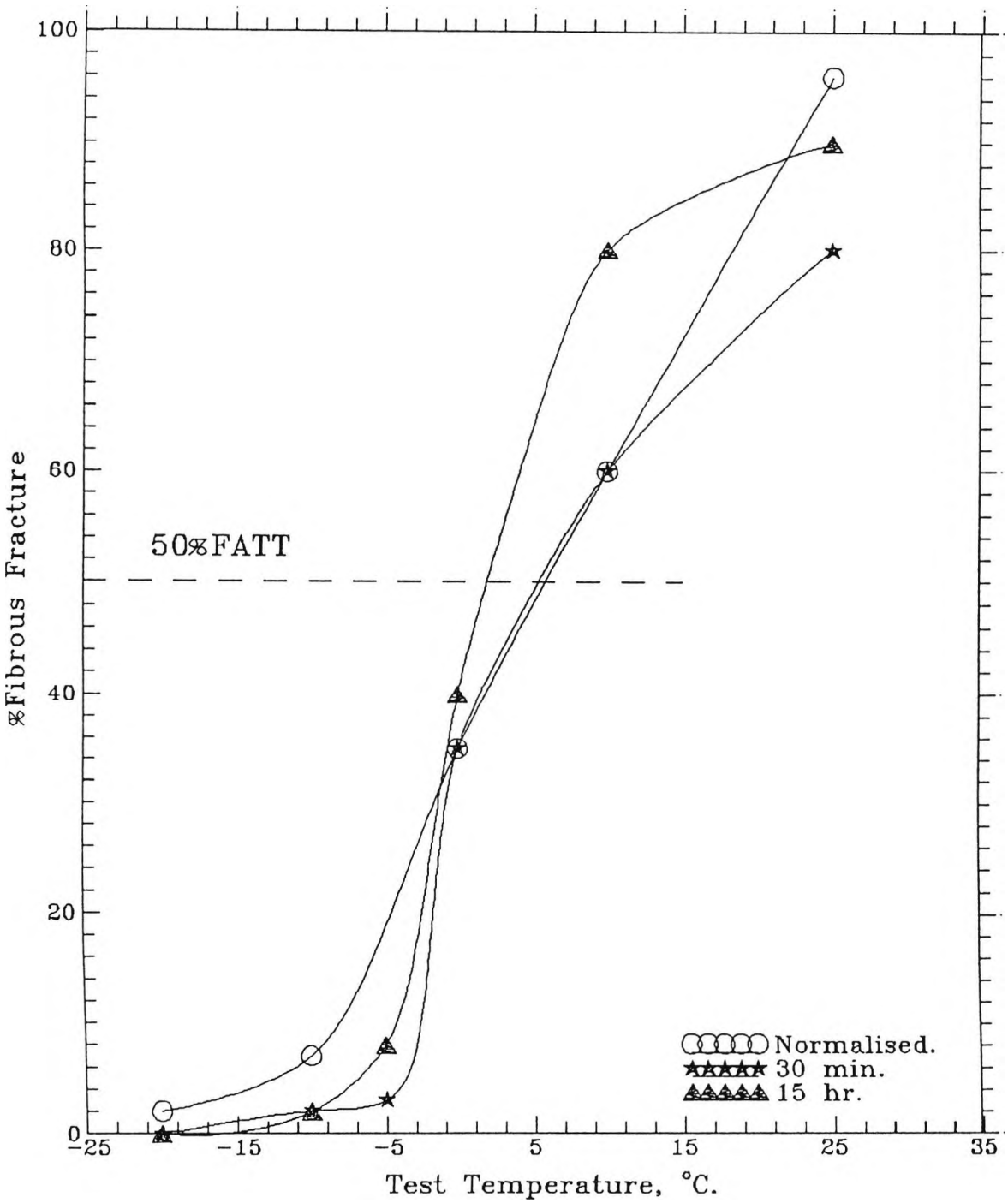

Fig.4.54b- Fibrous Fracture Curves for the Plain Carbon Mn Steel (Coarse Grain Size), I.A. at 730°C, Cooled at 7°C/min, Heating Up Cycle.

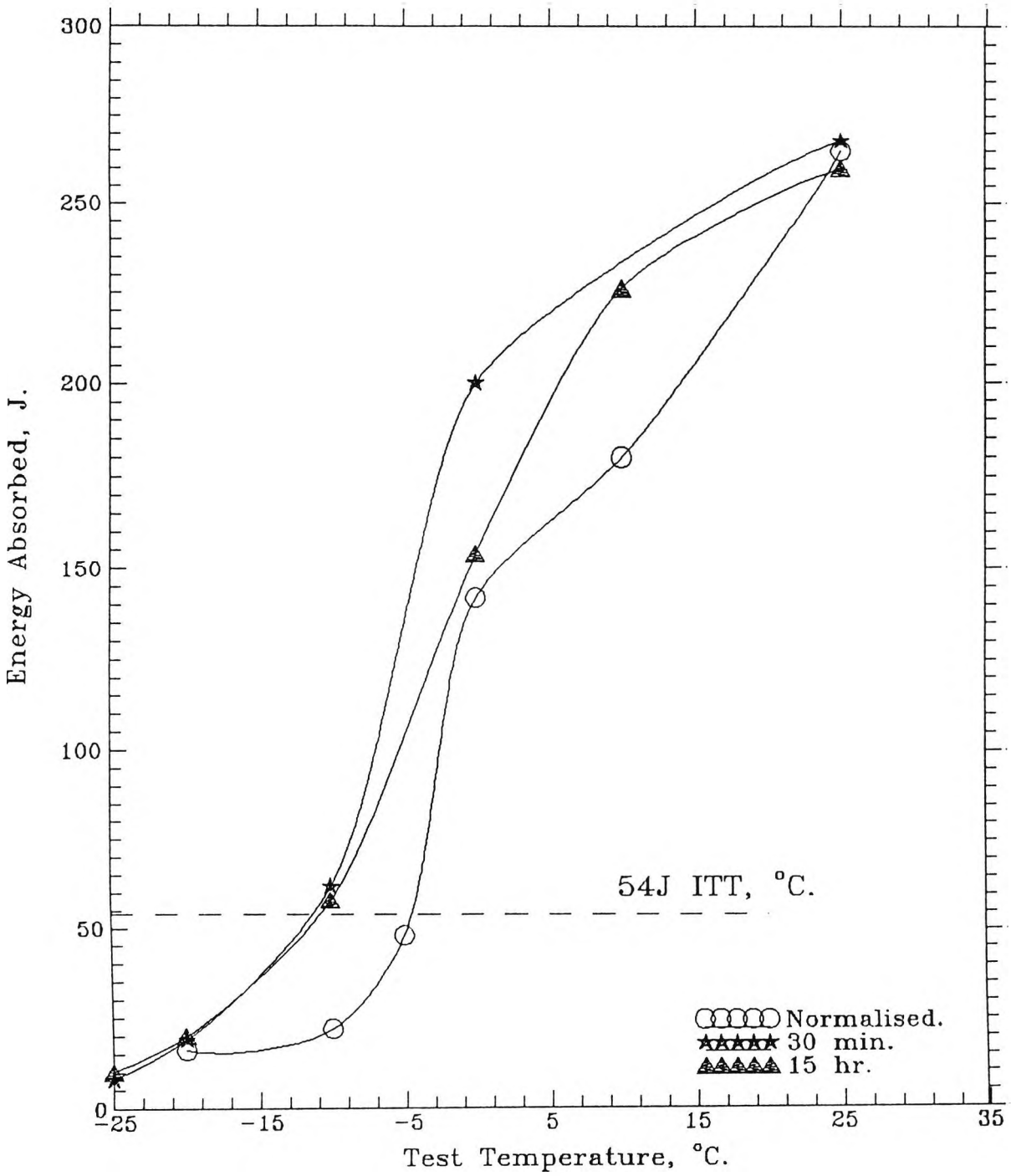

Fig.4.55a- Impact Transition Curves for the Plain Carbon Mn Steel (Coarse Grain Size), I.A at 730°C, Cooled at 7°C/min, Cooling Down Cycle.

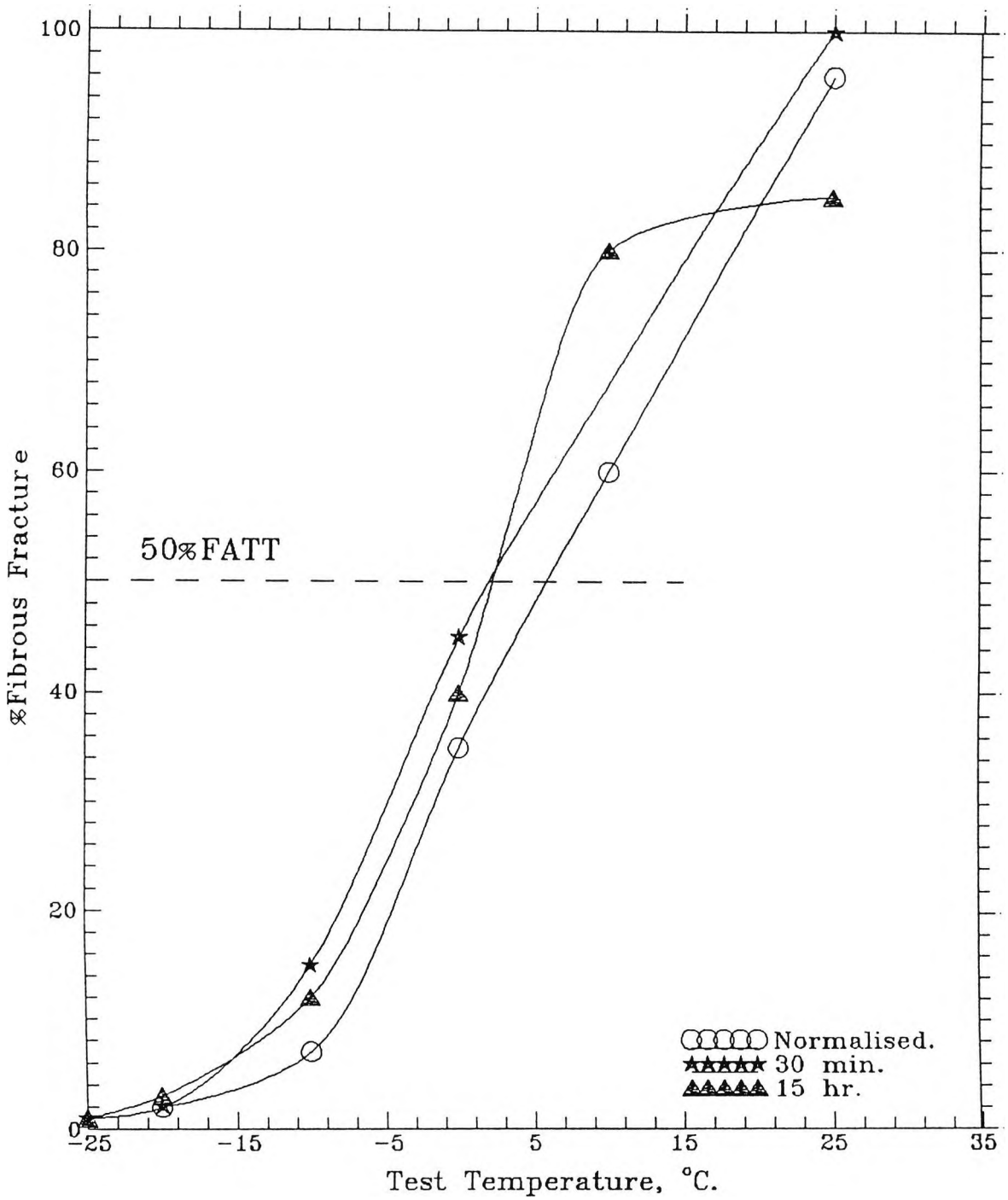

Fig.4.55b- Fibrous Fracture Curves for the Plain Carbon Mn Steel (Coarse Grain Size), I.A. at 730°C, Cooled at 7°C/min, Cooling Down Cycle.

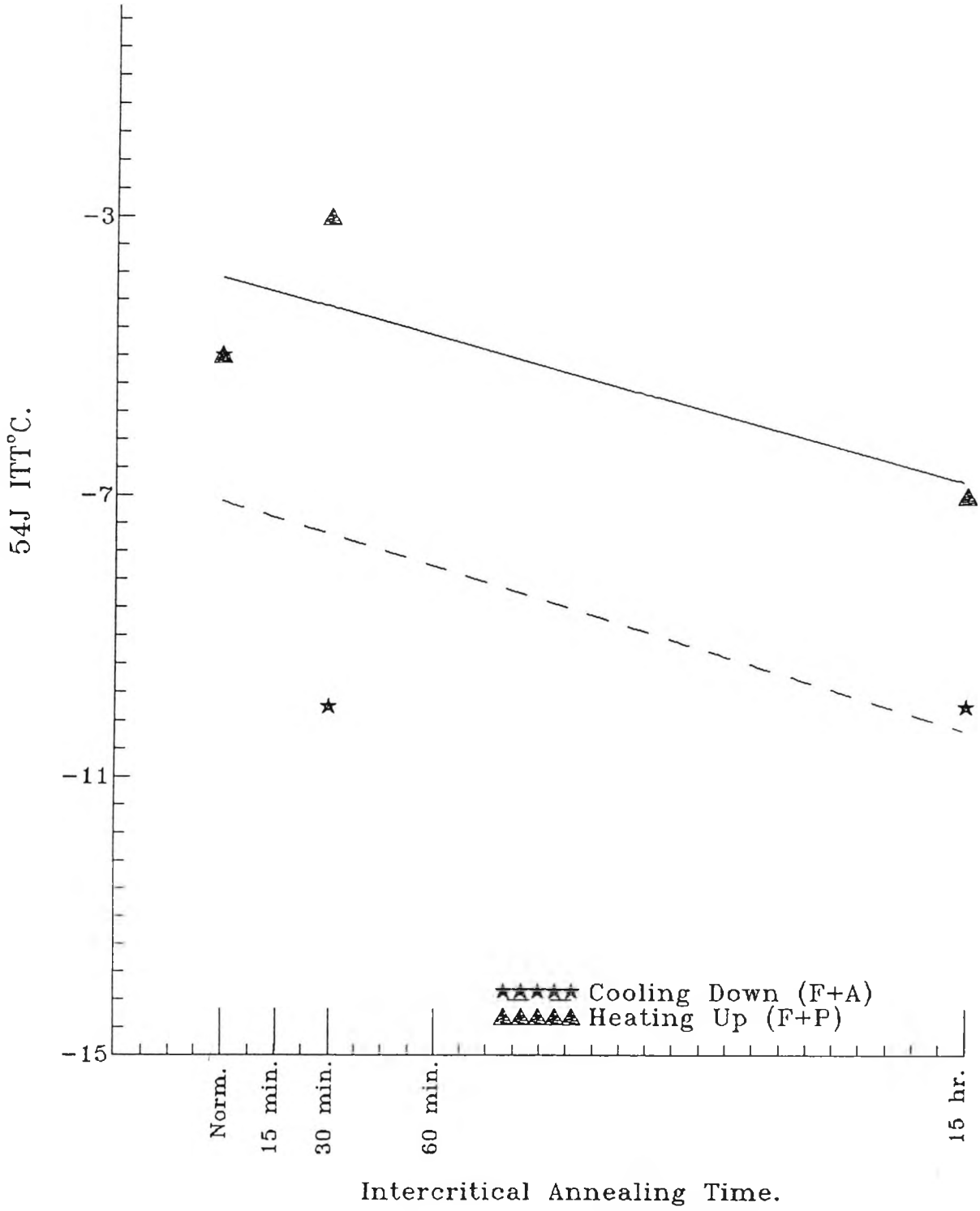

Fig.4.56- The Effect of I.A Times on the 54J ITT°C for the Plain Carbon Mn Steel, Coarse Grain Size.

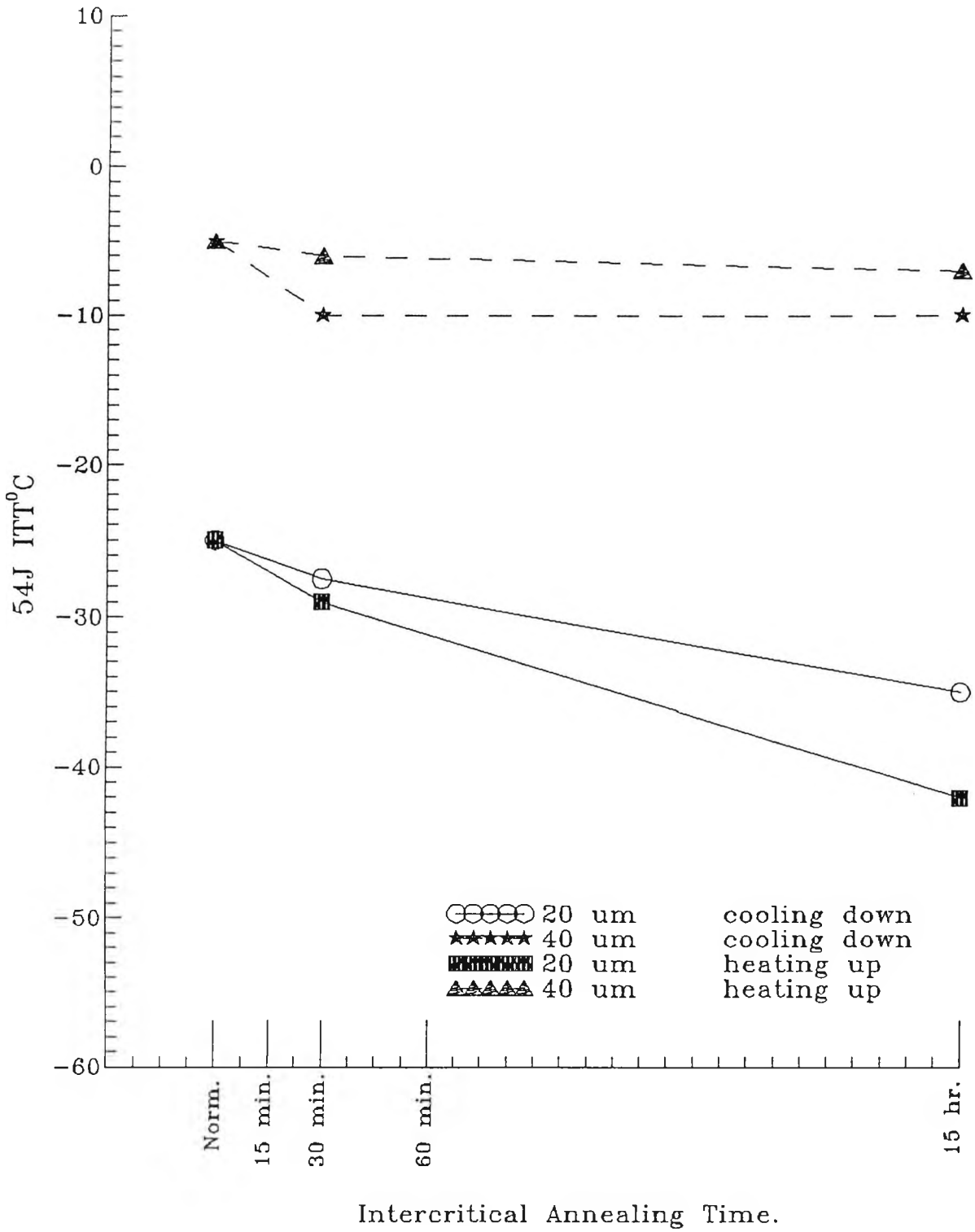

Fig.4.57- The Effect of Grain Size and I.A. Time on the 54J ITT°C of the Plain Carbon Manganese Steel.

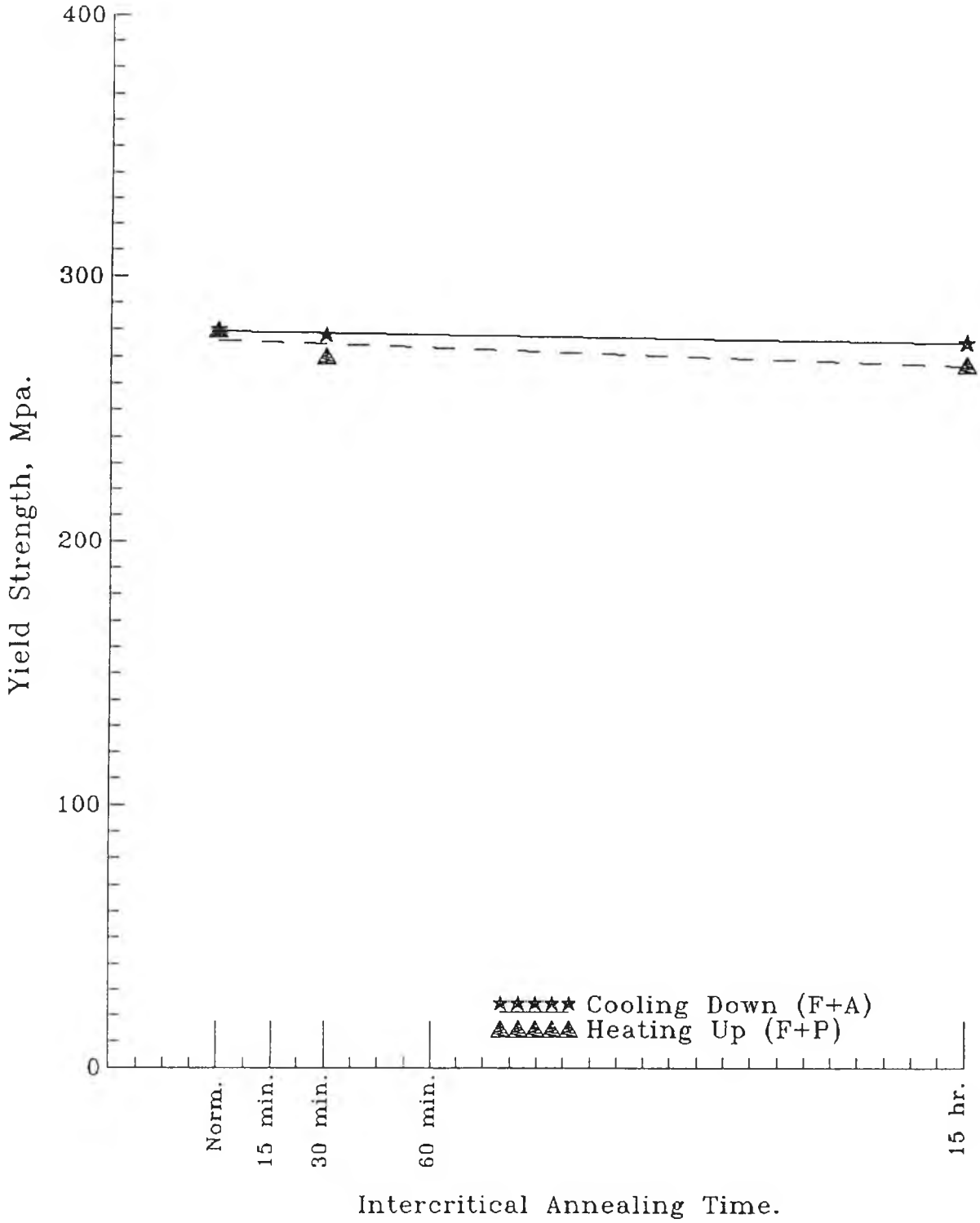

Fig.4.58- The Effect of I.A. Time on the Yield Strength of the Finer Grained Size Plain Carbon Mn Steel.

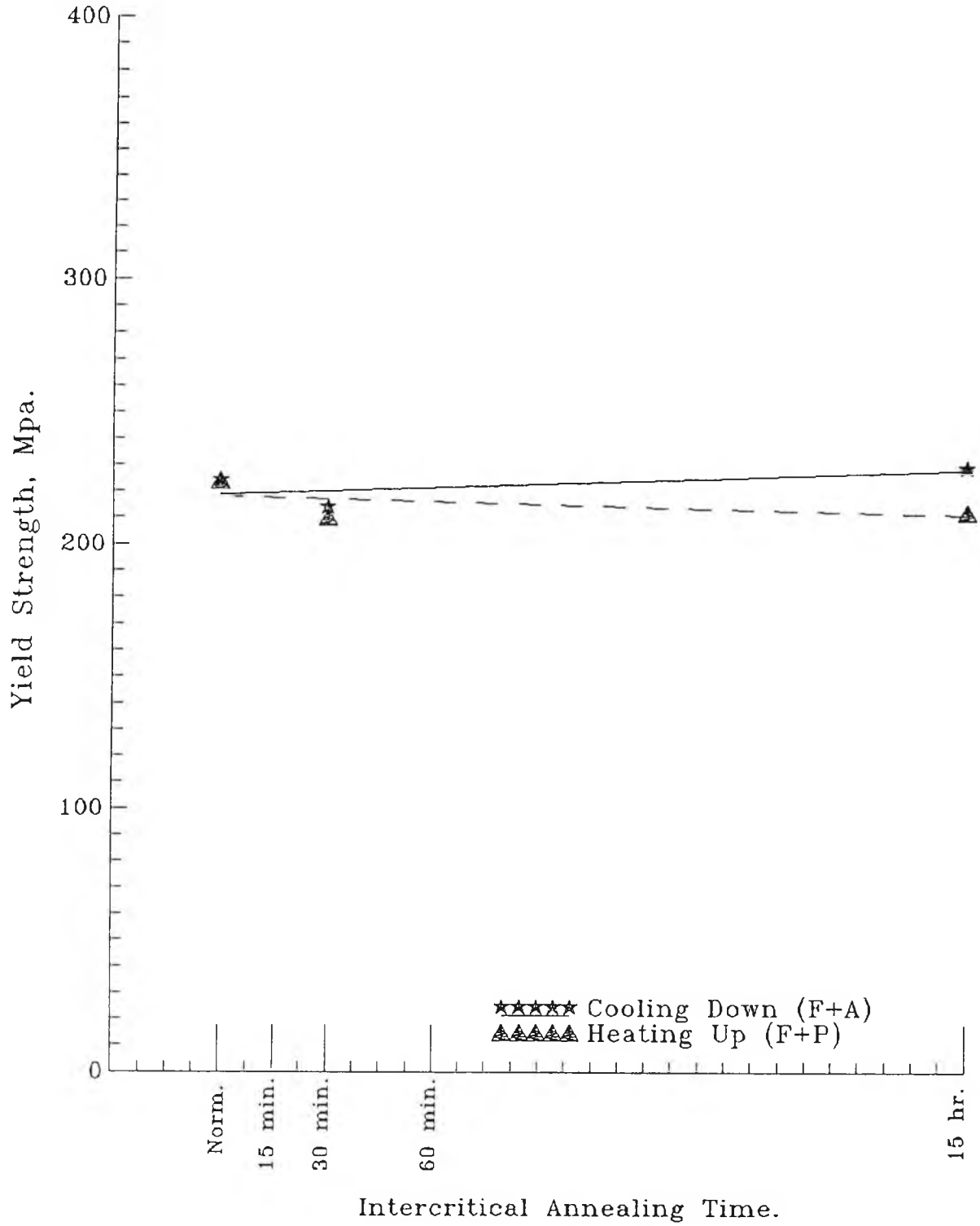

Fig.4.59- The Effect of I.A. Time on the Yield Strength of the Coarser Grained Size Plain Carbon Mn Steel.

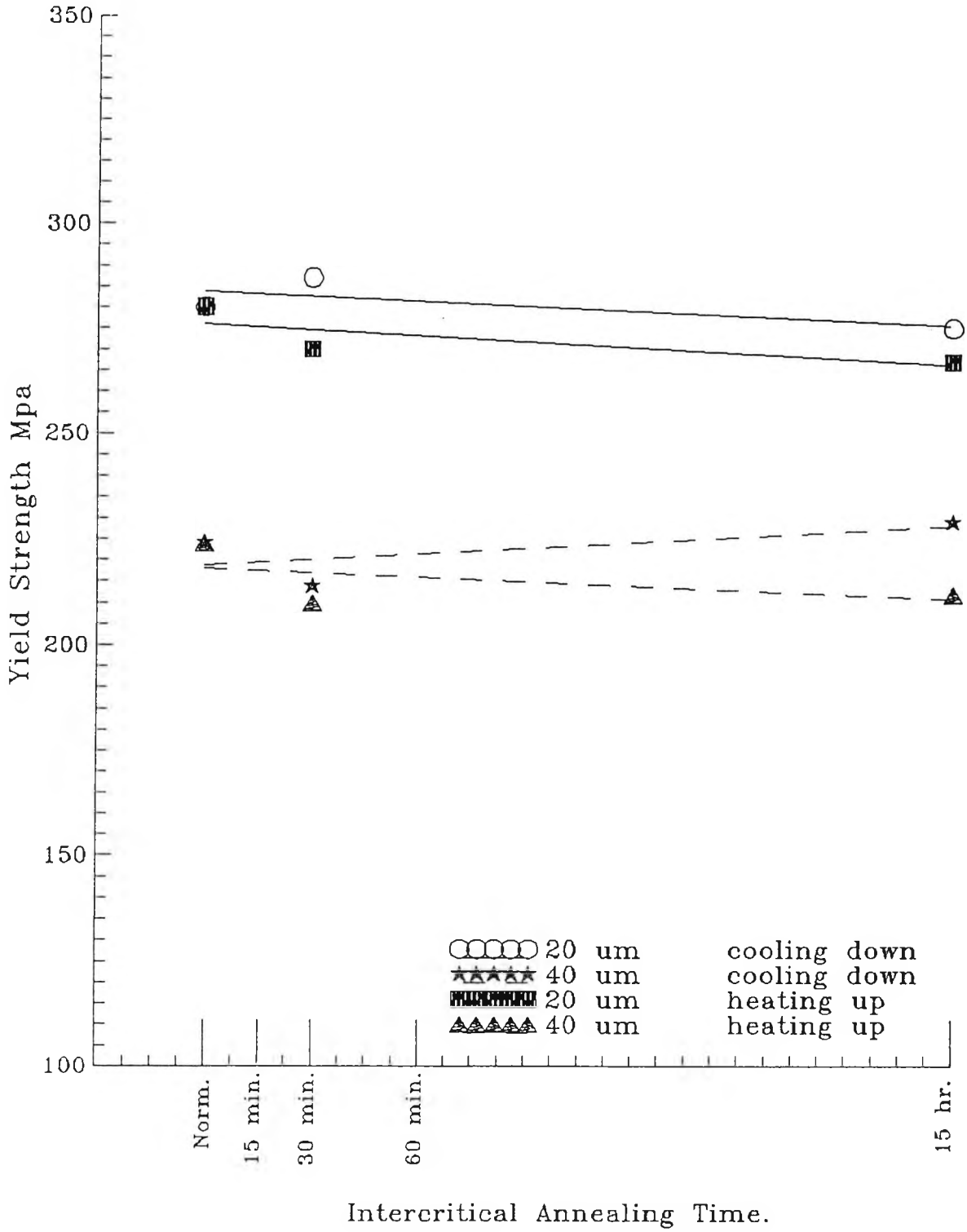

Fig.4.60- The Effect of Grain Size and I.A. Time on the Yield Strength of the Plain Carbon Mn Steel.

4.5.4- METALLOGRAPHY.

The change in microstructure with intercritical annealing time was followed by taking a series of optical photographs of the microstructure as a function of intercritical annealing time, Figs. 4.61 and 4.62.

4.5.4.1- Finer Grained (18 μm) Steel.

4.5.4.1.1- Cooling Down.

Figures 4.61(1 and 2) show the microstructure of the finer grained (18 μm) plain carbon manganese steel after normalising and after intercritical annealing at 730°C for 30 minutes and 15 hours at two different magnifications. The microstructure after normalising consists of equiaxed ferrite grains plus banded pearlite colonies. The colonies are elongated along the rolling direction. There is no change in microstructure after 30 minutes of intercritical annealing. However, after holding for 15 hours at 730°C, the pearlite phase becomes more dispersed and growth is more equiaxed.

4.5.4.1.2- HEATING UP.

Figures 4.62(1 and 2) show the microstructure of the finer grained (18 μm) plain carbon manganese steel after intercritical annealing at 730°C for 30 minutes and 15 hours at two different magnifications. It can be seen that, the microstructure after 30 minutes intercritical annealing seems to be similar to the normalised structure in that the

pearlite banding is intact. Increasing the intercritical annealing time disperses the pearlite and growth of the colonies is more equiaxed.

4.5.4.2- COARSER GRAINED (37 μm) STEEL.

4.5.4.2.1- COOLING DOWN.

Figures 4.63 (1 and 2) show the microstructure of the coarser grained (37 μm) plain carbon manganese steel after normalising and after intercritical annealing at 730°C for 30 minutes and 15 hours at two different magnifications . The microstructure after normalising consists of equiaxed ferrite grains plus banded pearlite colonies. It is intersting to note that there is no change in microstructure on intercritical annealing this steel.

4.5.4.2.2- HEATING UP.

Figure 4.64 shows the microstructure of the coarser grained (37 μm) plain carbon manganese steel after intercritical annealing at 730°C for 30 minutes and 15 hours. It can seen that, after 30 minutes of intercritical annealing the pearlite banding present in the normalised structure is partially broken up. Increasing the intercritical annealing time to 15 hours causes the pearlite to become more distributed within the structure.

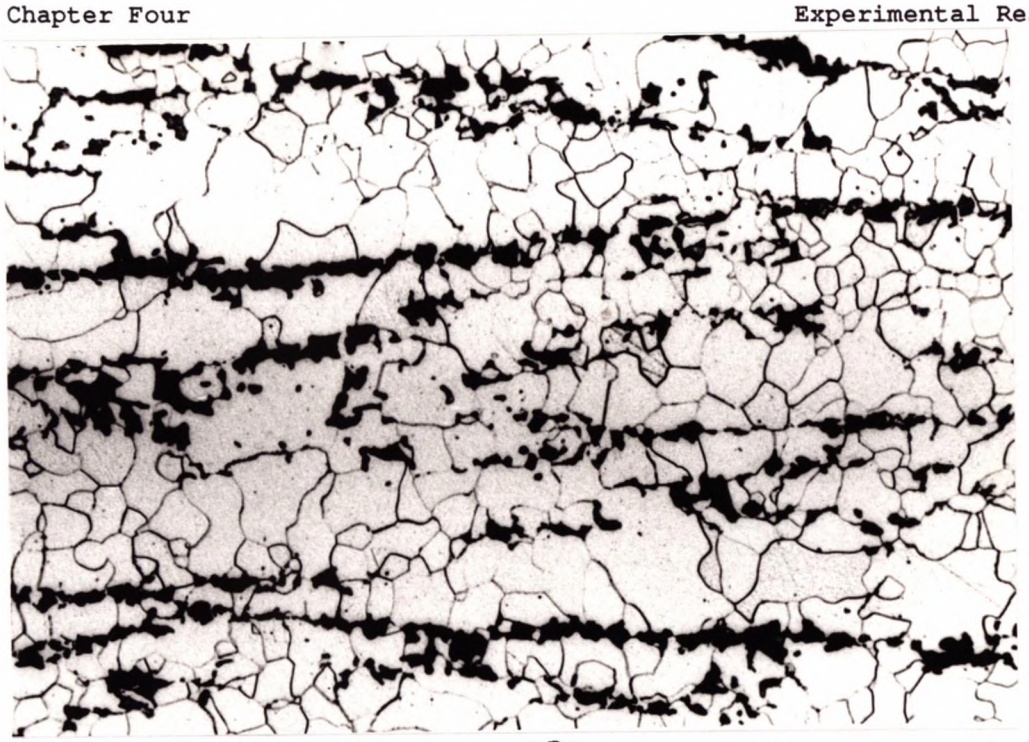

-a- x450

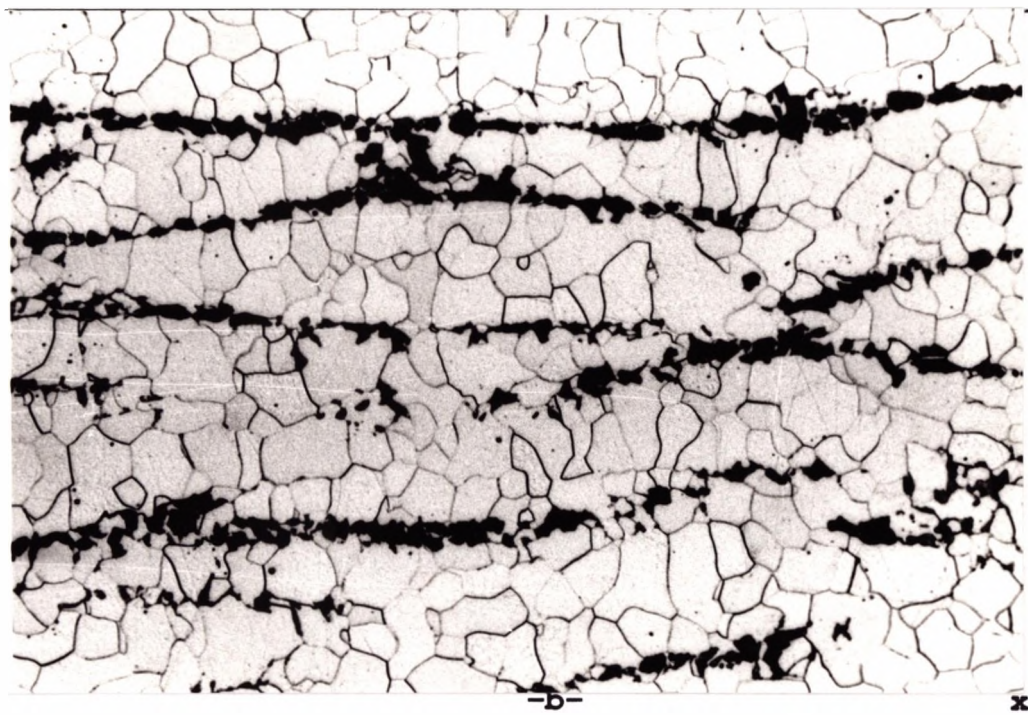

-b- x 450

Fig.4.61 (1)- Microstructure of the Finer Grained Plain Carbon Manganese Steel.

a- Normalised., b- I.A. at 730°C for 30min, Cooling Down Cycle.

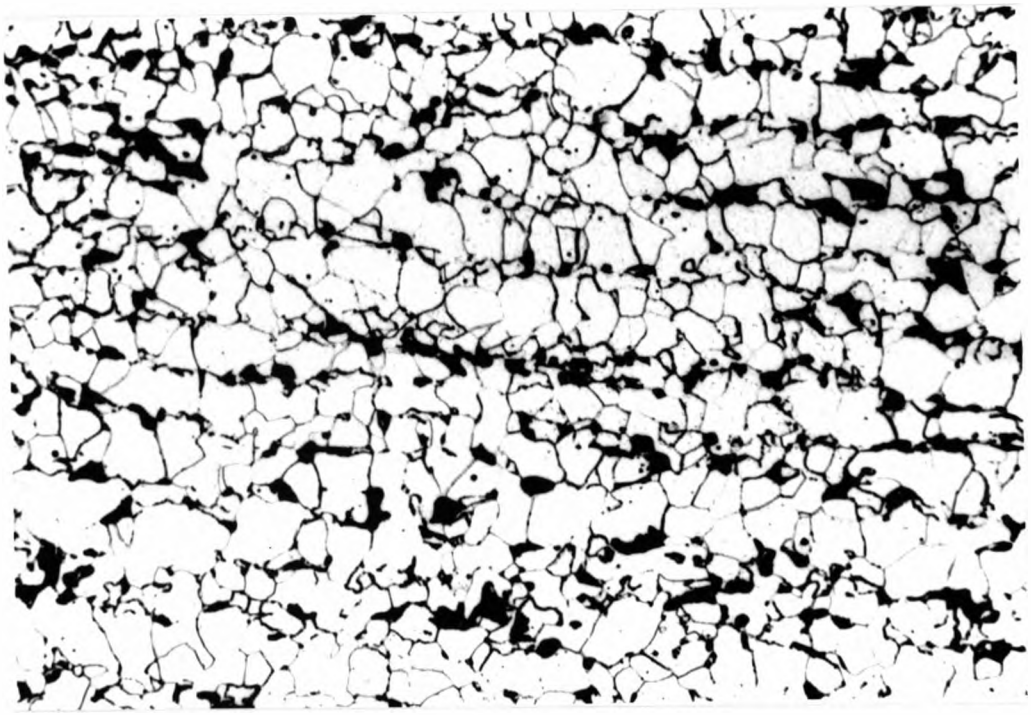

-c- x 450

Fig.4.61 (1)c- Microstructure of the Finer Grained Plain Carbon Manganese Steel.

I.A. at 730°C for 15 hr,

(Cooling Down Cycle).

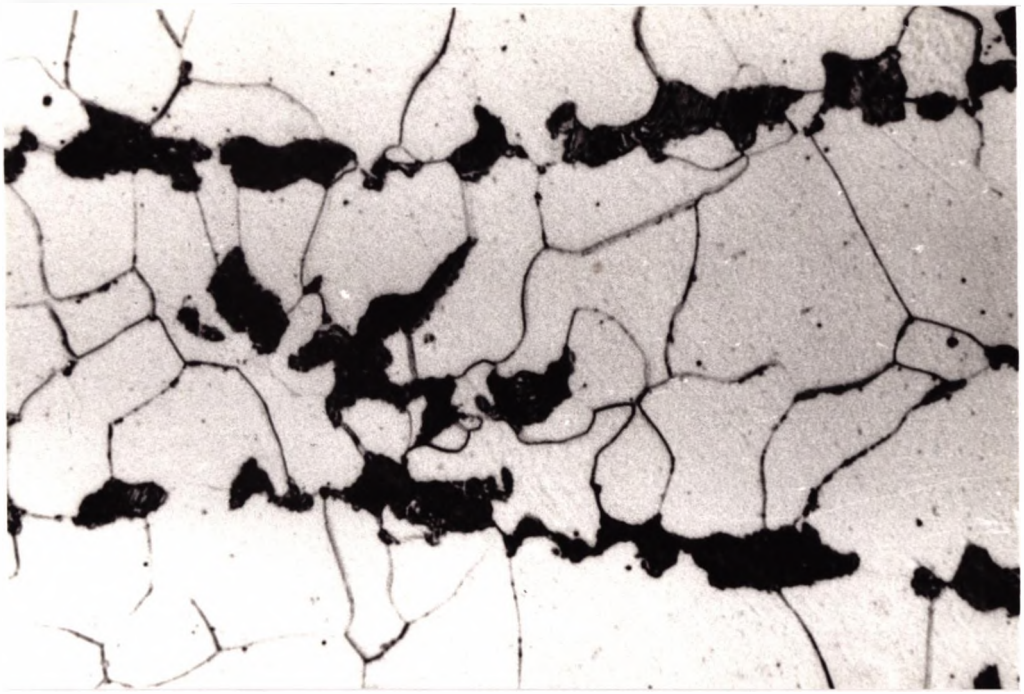

-a- x 900

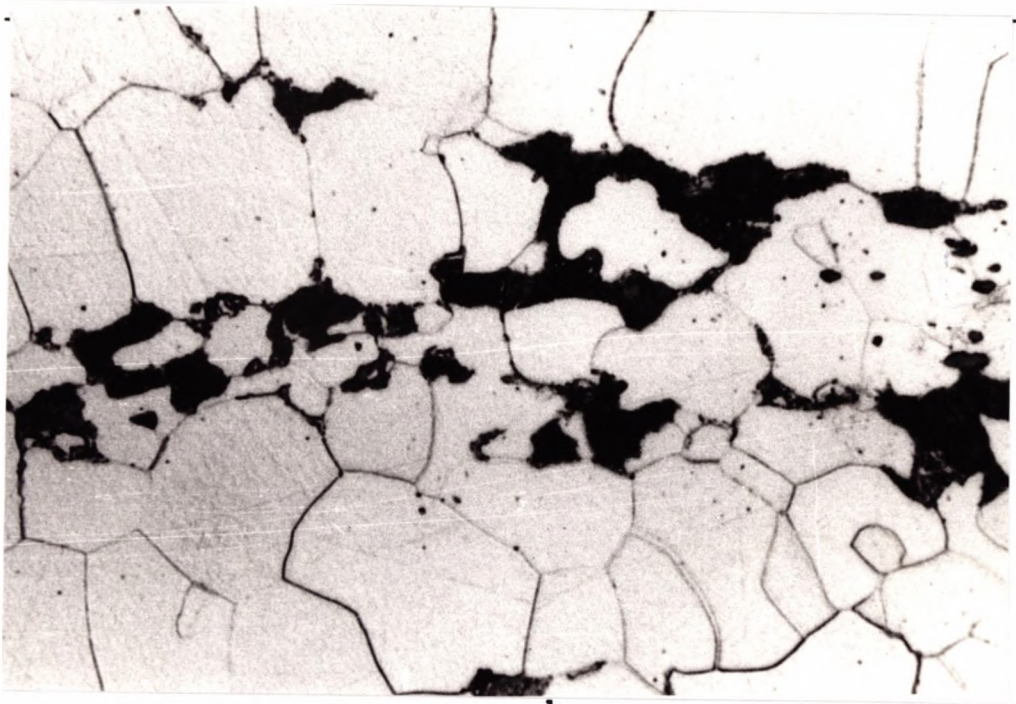

-b- x 900

Fig.4.61(2)- Microstructure of the Finer Grained Plain Carbon Manganese Steel.

a- Normalised., b- I.A. at 730°C for 30min, Cooling Down Cycle.

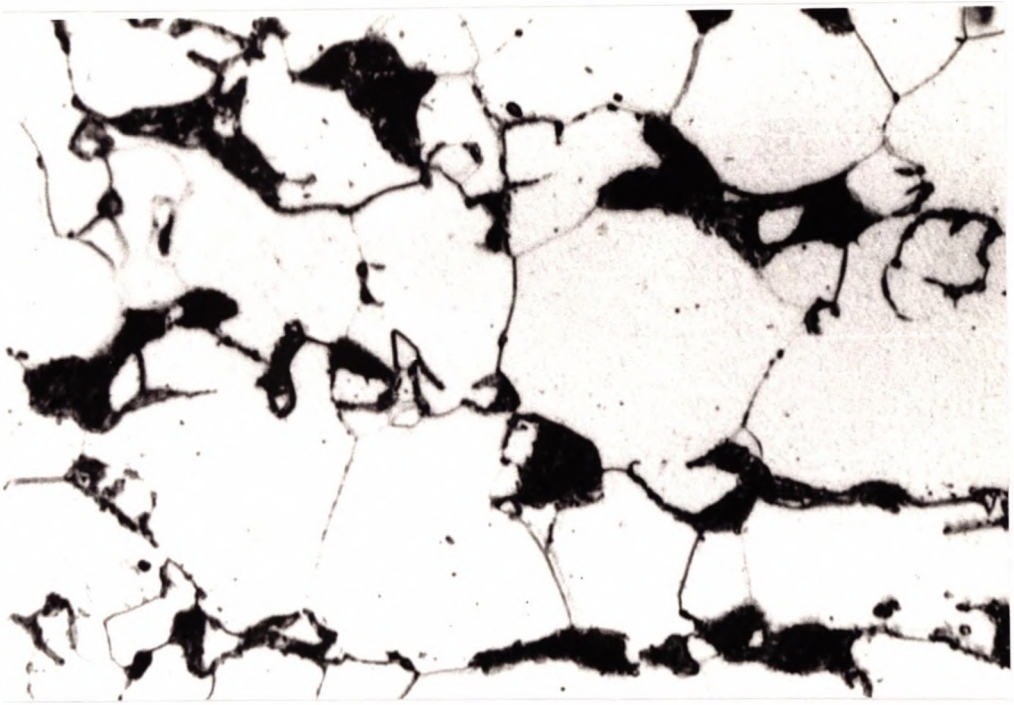

-c- x 900

Fig.4.61(2)c- Microstructure of the Finer Grained Plain Carbon Manganese Steel.

I.A. at 730°C for 15 hr,

(Cooling Down Cycle).

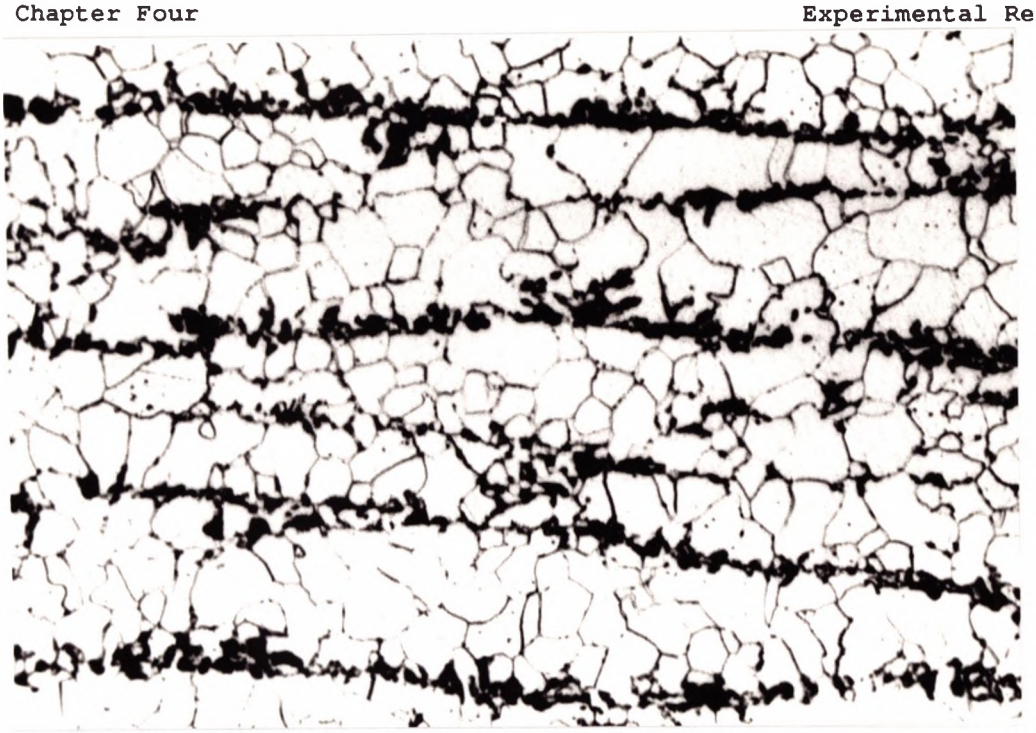

-a- x 450

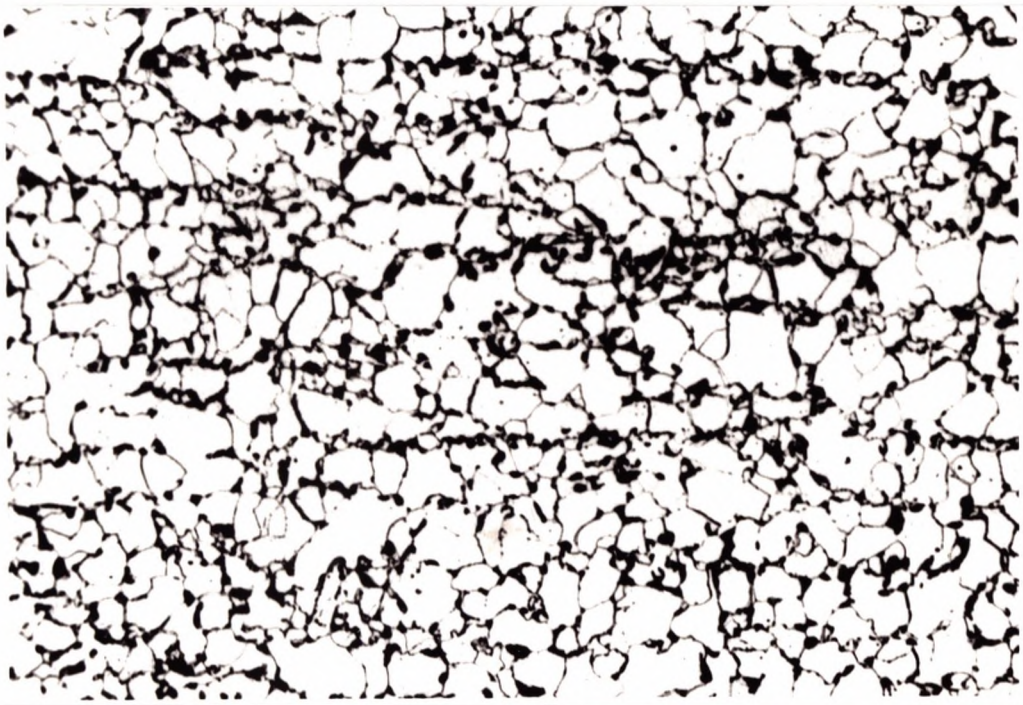

-b- x 450

Fig.4.62 (1)- Microstructure of the Finer Grained Plain Carbon Manganese Steel.

a-I.A. at 730°C for 30 min., b-I.A. at 730°C for 15 hr. Heating Up Cycle.

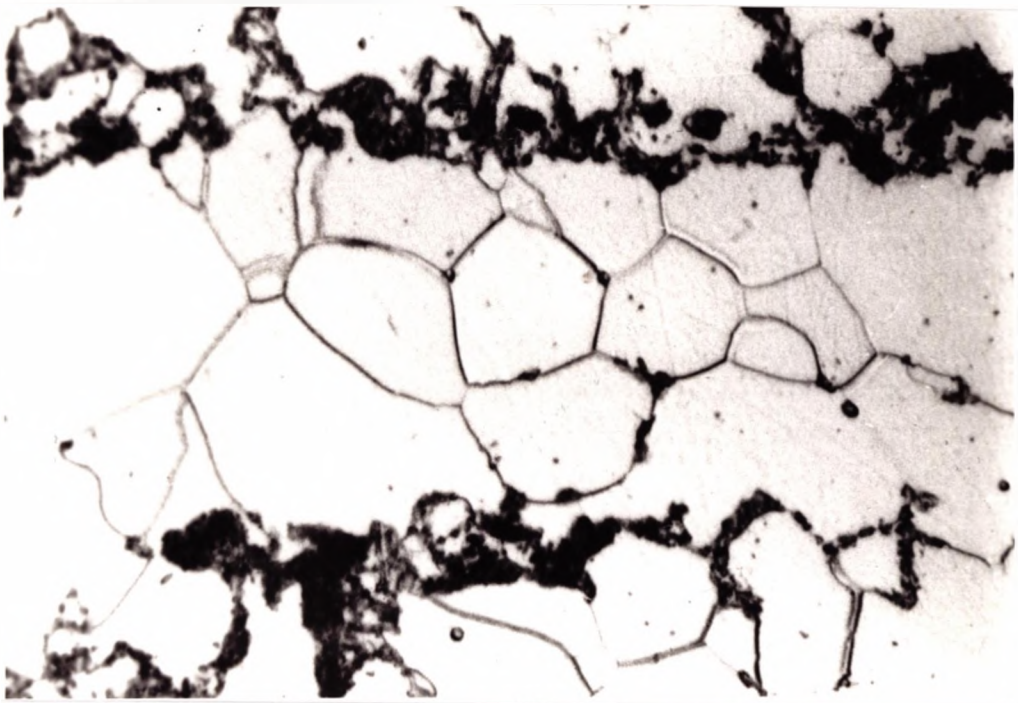

-a- x 900

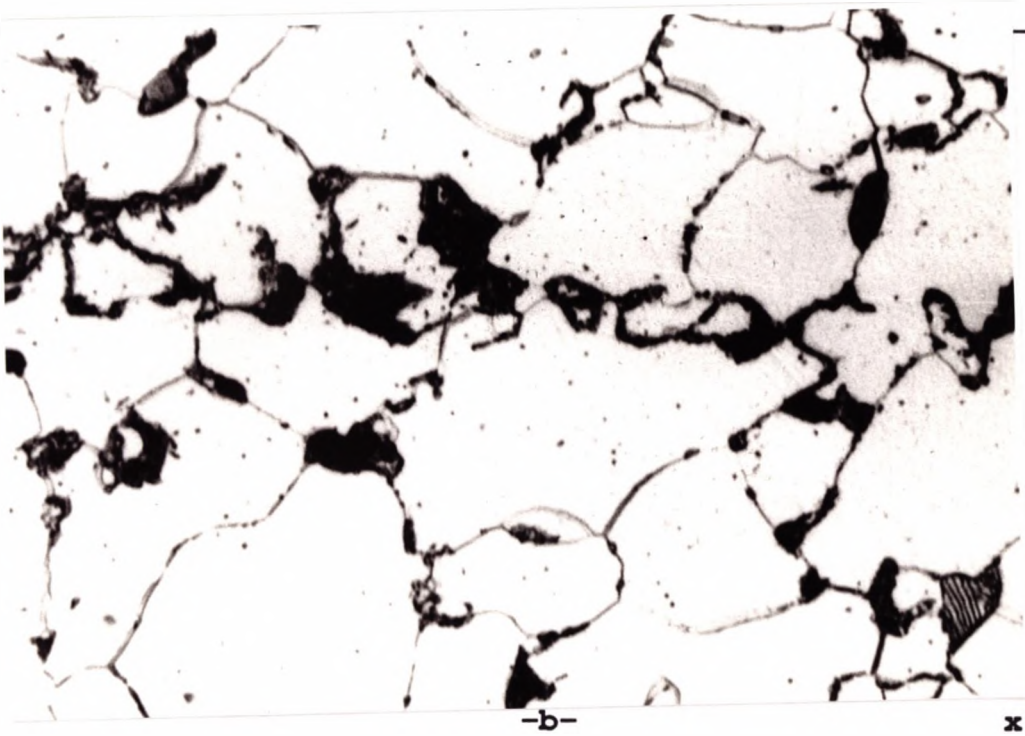

-b- x 900

Fig.4.62 (2)- Microstructure of the Finer Grained Plain Carbon Manganese Steel.

a-I.A. at 730°C for 30 min., b-I.A. at 730°C for 15 hr.

Heating Up Cycle.

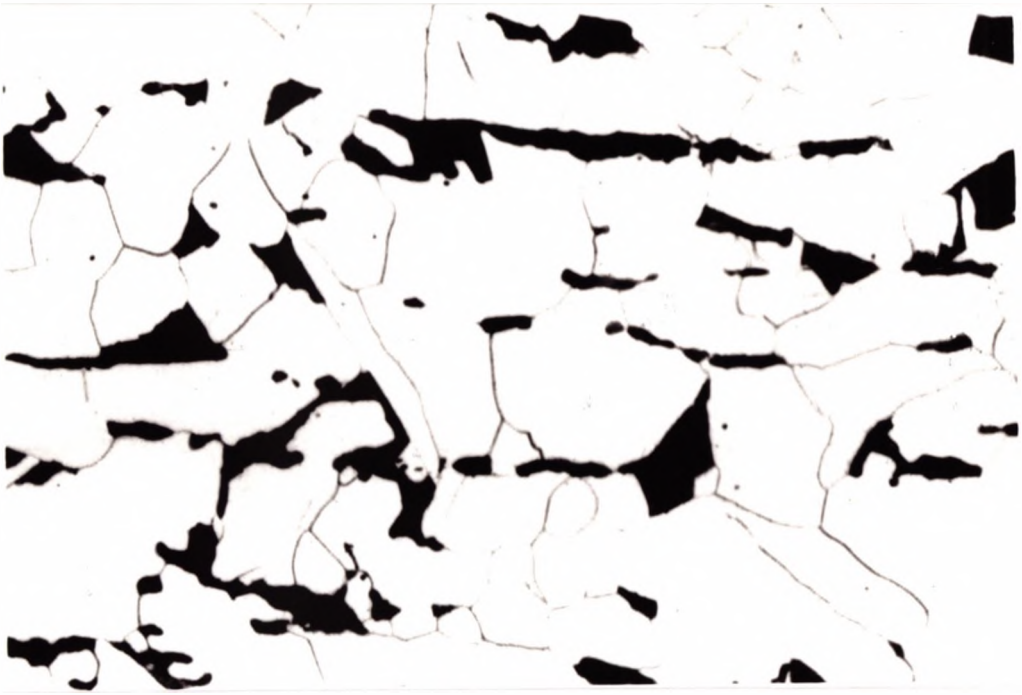

-a- x 225

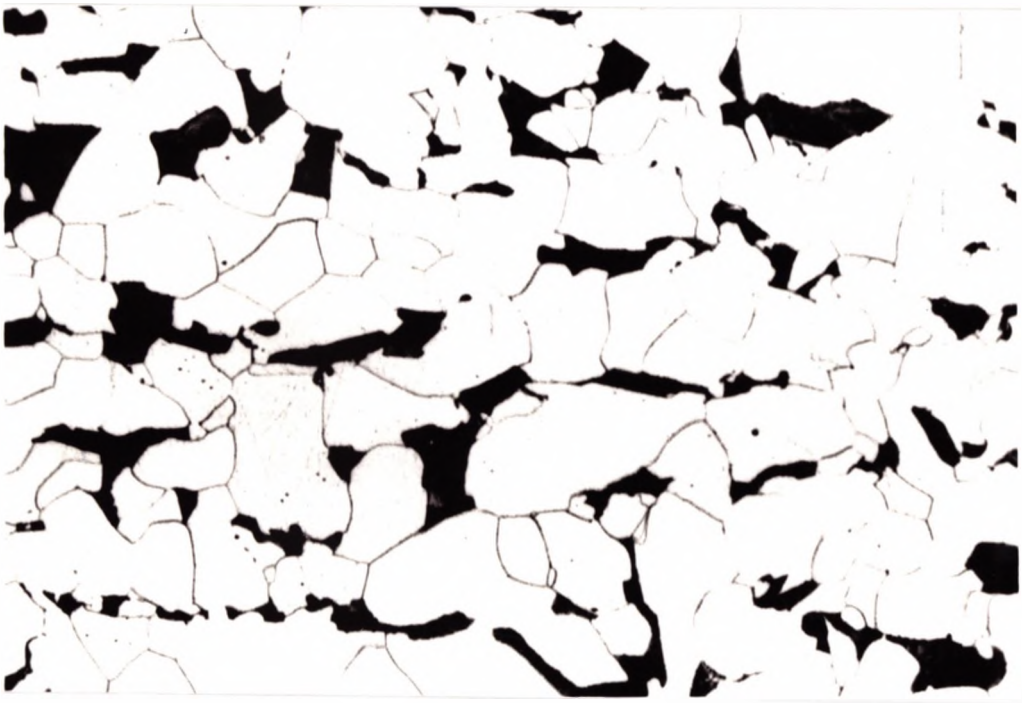

-b- x 225

Fig.4.63(1)- Microstructure of the Coarser Grained Plain Carbon Manganese Steel.

a- Normalised., b- I.A. at 730°C for 30min, Cooling Down Cycle.

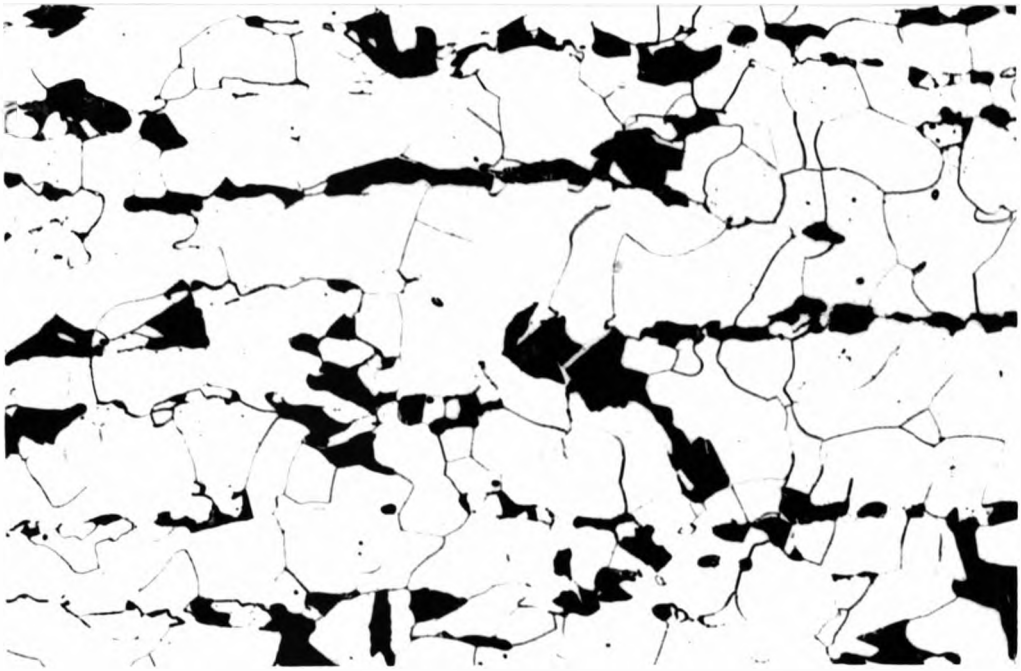

-c- x 225

Fig.4.63(1)c- Microstructure of the Coarser Grained Plain Carbon Manganese Steel. I.A. at 730°C for 15 hr, Cooling Down Cycle.

-a- x 450

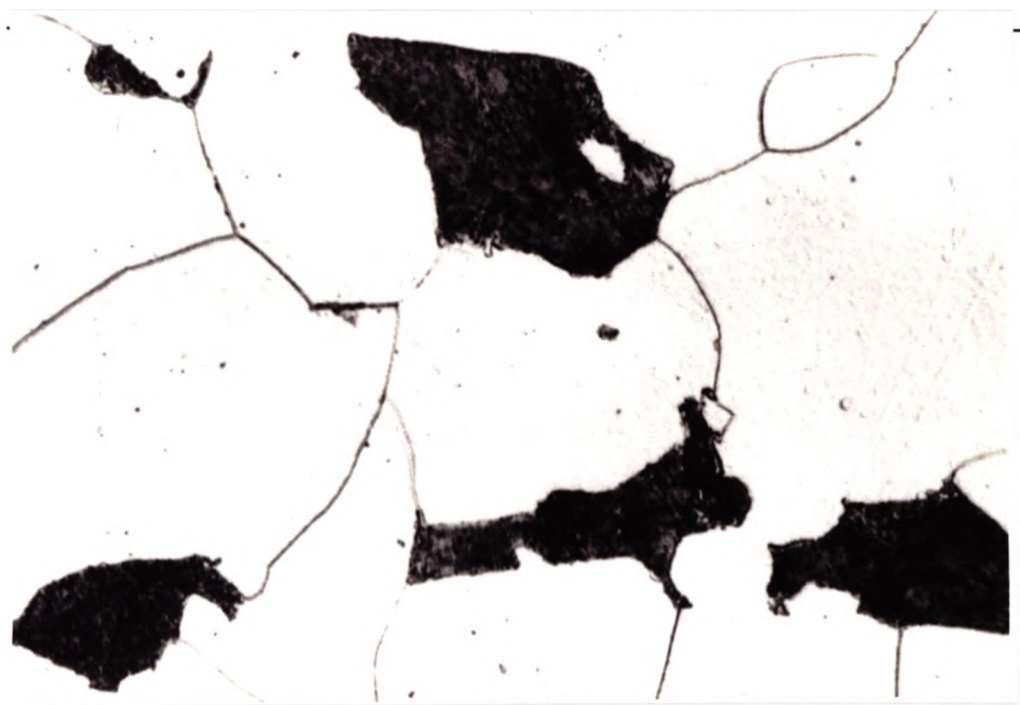

-b- x 450

Fig.4.63 (2)- Microstructure of the Coarser Grained Plain Carbon Manganese Steel.

a- Normalised., b- I.A. at 730°C for 30min, Cooling Down Cycle.

-c- x 450

Fig.4.63 (2)c- Microstructure of the Corser Grained Plain Carbon Manganese Steel.

I.A. at 730°C for 15 hr,

(Cooling Down Cycle).

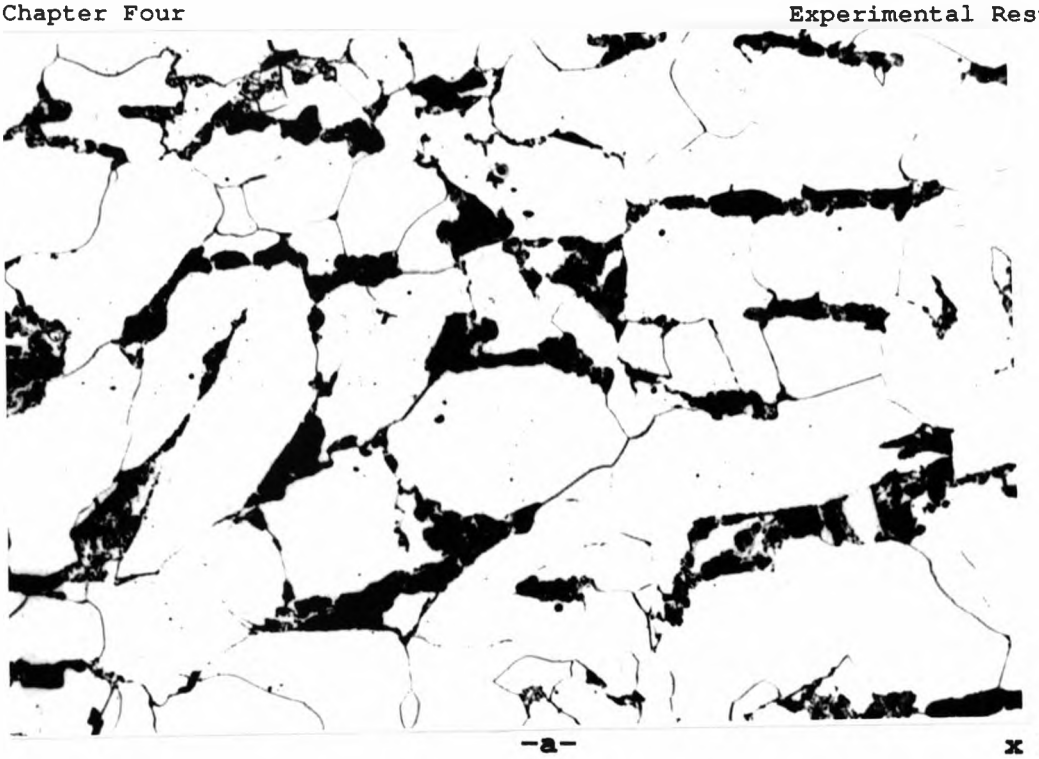

-a- x 225

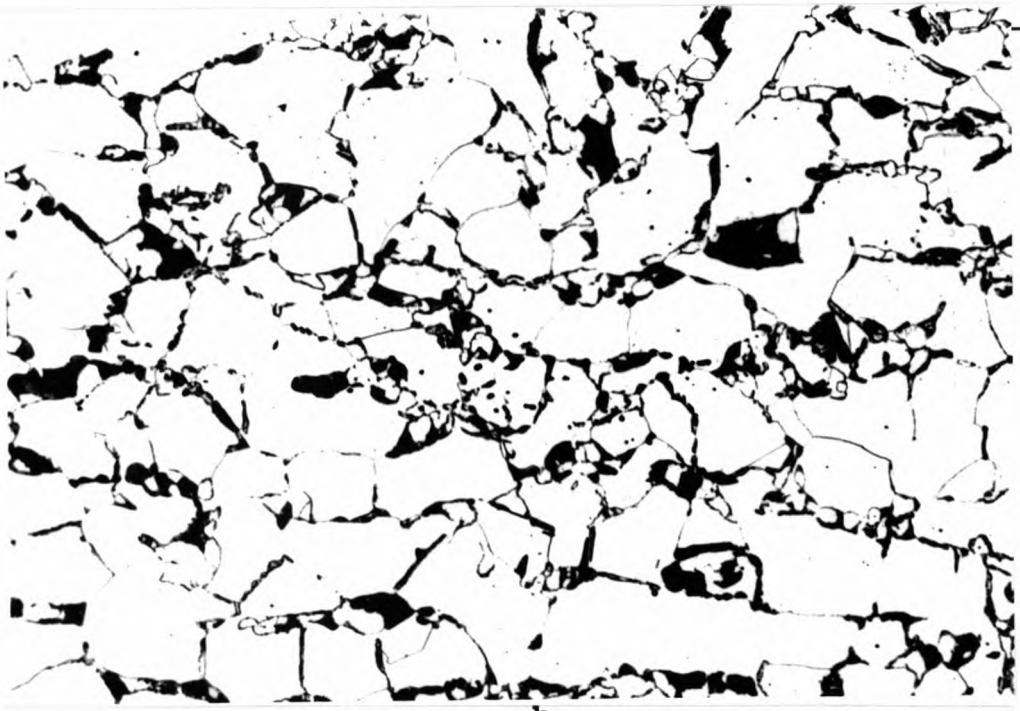

-b- x 225

Fig.4.64 (1)- Microstructure of the Corser Grained Plain Carbon Manganese Steel.

a-I.A. at 730°C for 30 min., b-I.A. at 730°C for 15 hr.

Heating Up Cycle.

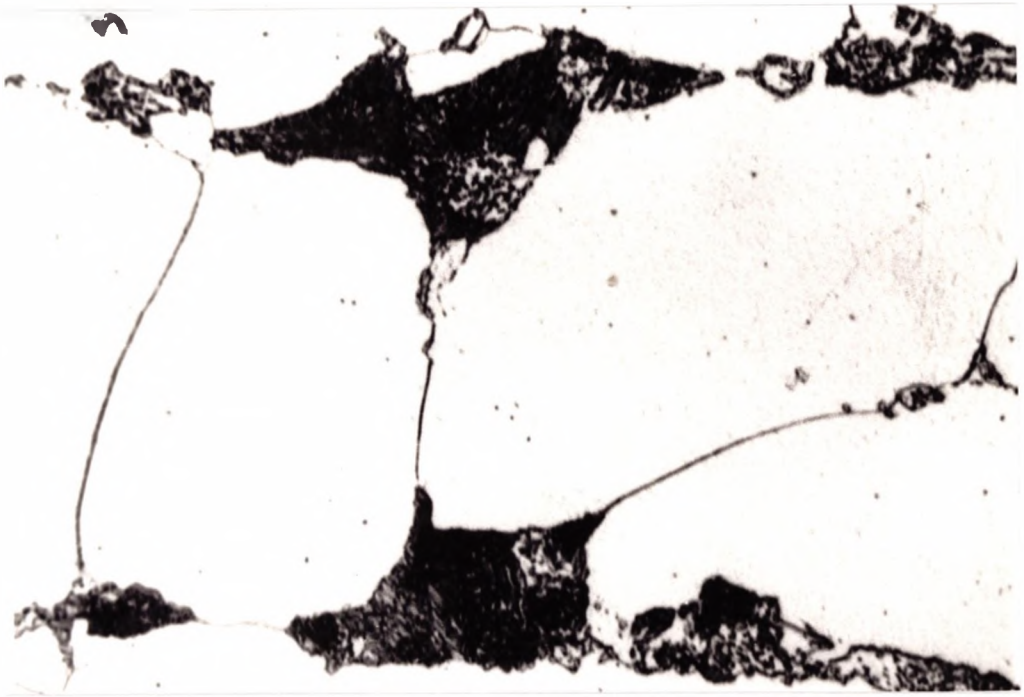

-a- x 450

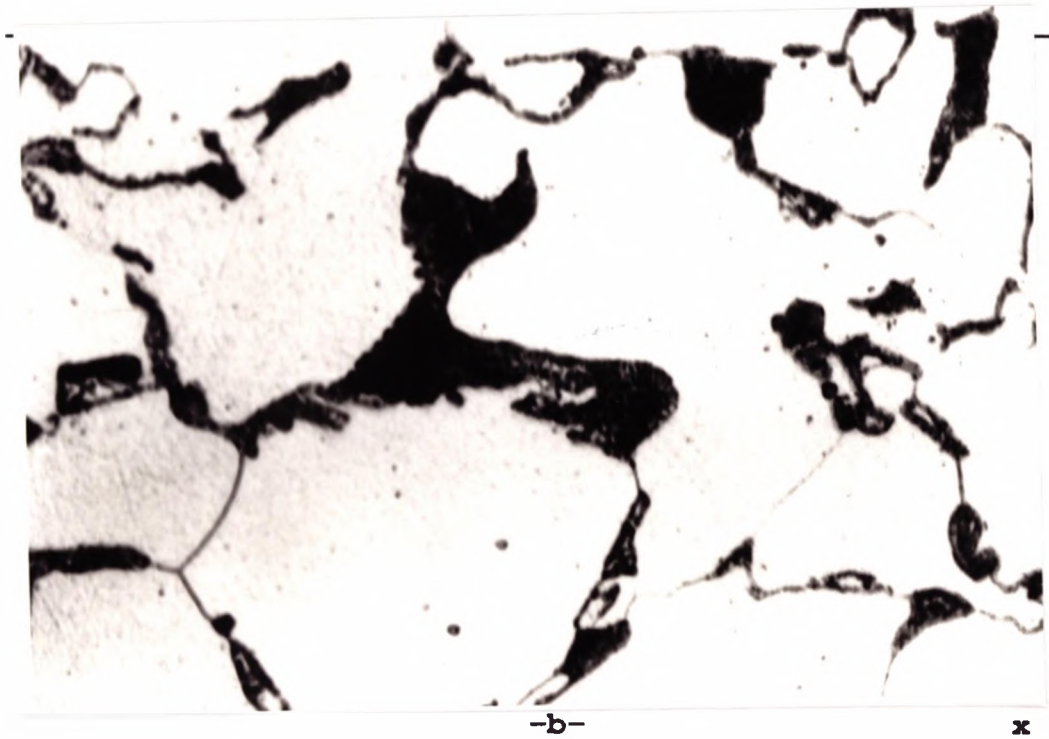

-b- x 450

Fig.4.64 (2)- Microstructure of the Corser Grained Plain Carbon Manganese Steel.

a-I.A. at 730°C for 30 min., b-I.A. at 730°C for 15 hr.

Heating Up Cycle.

CHAPTER FIVE

DISCUSSION

5.1- OVERVIEW.

In the previous chapter, it had been shown that intercritical annealing can improve the impact performance, with no significant change in strength (yield strength and ultimate tensile strength). However, this improvement in impact performance is critically dependent on the manganese level, cooling rate, carbon level,heating temperature, and grain size.

It had been pointed out, in the literature review of Chapter Two that, generally workers have reported that the mechanical properties of dual phase steels are a function of the volume fraction of martensite[123,124,125]. In their work, martensite is required to improve the formability of strip steel and impact behaviour is of secondary importance.

In the present work on plate steel, impact behaviour is of most importance and here the impact transition temperature (ITT) is mainly dependent on the grain boundary carbide thickness, grain size, and pearlite volume fraction, and twinned martensite is to be avoided[126]. Before discussing the details of the results obtained in this study, it should be pointed out that there are several

differences between the present work and most of the previously published work on intercritical annealing of steel and these are listed as follows:-

1- In the present work the steels examined are plate steels having thickness in the range 12 to 20 mm , while in most of the previous work, the steel used is a sheet or strip having a thickness of 2-4 mm. Hence cooling rates are much slower in the present work.

2- The current investigation covers impact performance and yield strength, while most of the previous work deals with ductility and tensile strength.

3- In the present work there are two starting microstructures {ferrite+ pearlite} and {ferrite+ austenite}, while in most of the previous work the starting microstructure was {ferrite+ pearlite}.

4- Most of the final microstructures in this examination are ferrite plus pearlite. In previous studies on dual phase steels the final microstructure was mainly ferrite plus martensite. Fortunately, both yield strength and impact behaviour have been quantified for plate steel and the empirical structure/ property relationships are detailed below as these will be used in the following sections to interpret the changes in ITT and strength that occur on intercritical annealing.

The impact transition temperature (ITT) for steels can generally be described by empirical regression equations of the following type[115]

$$54J\ ITT = 161t^{1/2} - 11.7d^{-1/2} + 0.47\Delta y + 18p^{1/3} - constant \quad .....5.1$$

Where:

54J ITT = the impact test temperature which gives an impact energy of 54 joules in a charpy impact test.

p = is the pearlite volume fraction, %.

t = grain boundary carbide thickness, μm.

d = grain diameter (mean linear intercept), mm.

Δy = the difference between the actual lower yield stress (LYS) and that calculated from the following regression equation which was calculated for non-precipitation hardening steels.

$$LYS\ N/mm^2 = 105 + 43.1\%Mn + 83\ \%Si + 1540\ \%N_f + 15.4\ d^{-1/2} \quad .....5.2$$

N_f = the free nitrogen content taken to be zero for the Al-containing steel and 0.004% for the plain C- Mn steels.

These two equations 5.1 and 5.2 can be used to calculate both the ITT and yield strength and these values are listed in tables 5.1 to 5.9 together with the observed values.

The constant obtained in the original regression equation (5.1) was -40°C and this represents the average constant for the steels examined at that time. The steels were hot rolled and generally contained higher C and S levels. More recent work[115] has indicated that for normalised steels with C levels of 0.1% and S levels below 0.01%, the

constant is considerably lower by at least 30°C (-70°C to -100°C).

It should also be noted that the $t^{1/2}$ relationship in the regression equation for ITT is only an approximation. The true relationship is believed to be as shown in Figure 5.1. Thus the constant obtained will depend on the range of carbide thickness covered.

Modern day steels with these lower C and S levels have been found to have Shelf energies which are twice as high as those examined in the original regression analysis, and this would be expected to lower the transition temperatures for impact criteria based on impact energies.

In analysing the present results a "variable" constant has been chosen. The constant has been taken as the value which gives the best fit to the data for each individual steel and condition. Thus, in the Mn excercise the constant changes from 78 to 90°C as the Mn level increases from 0.56% to 1.5%. This method has the advantage of clarifying changes in impact behaviour that occur on intercritical annealing. For example for the 0.56% and 1%Mn steels, the calculated changes in impact behaviour agree reasonably well with the observed, tables 5.1 and 5.2. As it is mainly the carbide thickness that changes this illustrates that the impact behaviour is being controlled by the grain boundary carbides.

For the high Mn steel, table 5.3, the correlation is good to start with but it is clear that as the intercritical

annealing time increases the calculated ITT is considerably lower than the observed, indicating martensite is influencing the results.

An alternative method for comparison is to compare all the changes in ITT on intercritical annealing with reference to the normalised condition, i.e. in tables 5.1 to 5.9, Δ ITT has been used as a means of comparison, where ΔITT = ITT in the normalised condition - ITT after intercritical annealing. It can be seen that, the calculated change in ITT is generally less than the observed. This most likely arises because of the changes in commercial plate steel compositions that have occurred since the original regression equations were obtained. Notwithstanding these differences, the present results clearly show that, when improvements in impact behaviour occur, it is due to the refinement of grain boundary carbides.

5.2- CALCULATION OF LOWER YIELD STRENGTH (LYS).

The original equation for the LYS, equation 5.2, was obtained for steels in which the vast majority examined had a plate thickness of 12 mm i.e. corresponding to a cooling rate of 40°C/min. There is considerable evidence[127] to indicate that as the cooling rate decreases, there is a fall in the LYS at constant grain size and pearlite volume fraction. This is believed to be due to a reduction in the K_Y value[128]. For a change in the cooling rate from 40°C/min

to 1°C/min the K_Y value falls by between 2 to 2.5 N $mm^{-3/2}$[129]. Other work by Mintz also shows similar behaviour[129]. At a constant grain size of $d^{-1/2}$ 12 $mm^{-1/2}$, a fall in strength, (LYS), of approximately 15 Mpa occurred in C-Mn-Al and C-Mn-Al-Nb steels as the cooling rate was reduced from 40 to 10°C/min and a further 15 Mpa fall took place when the cooling rate was lowered from 10 to 1°C/min.

In the present study, the best agreement between calculated and observed LYS was obtained by subtracting from the calculated LYS in equation 5.2, a further term, $1.8d^{-1/2}$ for a cooling rate of 7°C/min, and $2.5d^{-1/2}$ for a cooling rate of 1°C/min. It can be seen from tables 5.1 to 5.7, that the agreement between calculated and observed LYS is in general excellent.

5.3- RELATIONSHIP OF CHANGES IN GRAIN BOUNDARY CARBIDE THICKNESS TO IMPACT BEHAVIOUR.

Again, as in previous work[115] it has been shown that intercritical annealing can lead to improvements in impact behaviour without loss in strength. These improvement can best be related to the refinement in grain boundary carbide thickness, Fig.5.2. However, as can be seen from the tables 5.1 to 5.7, the magnitude of the improvement and whether they occur or not, is related to the composition. If for example, the manganese level is high (1.4%) in a 0.1%C steel, compare Tables 5.3, 5.4, and 5.5, then unless the

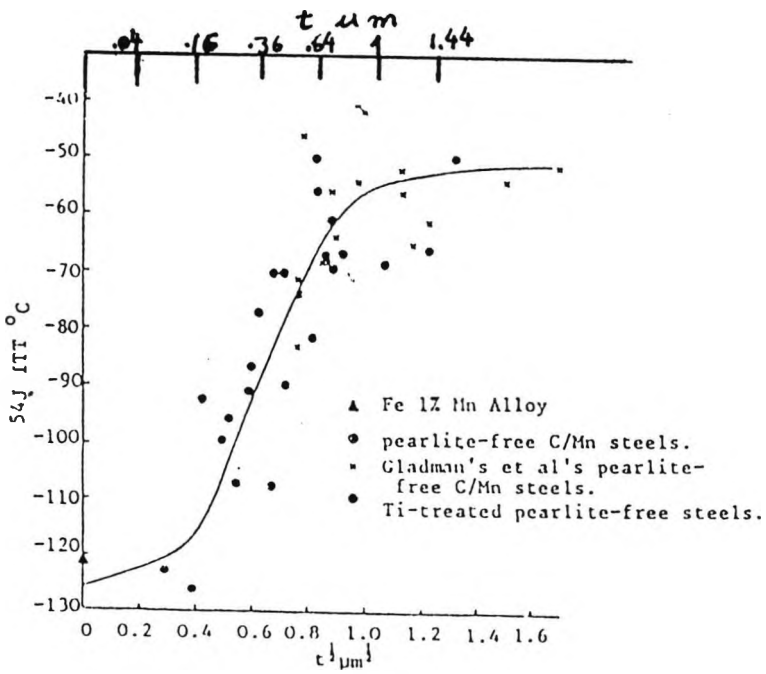

Fig.5.1- The Effect of Carbide Thickness on ITT.[130]

cooling rate is very slow, martensite can form on intercritical annealing as in Figure 4.21, with subsequent deterioration in impact behaviour. However, even when martensite does not form the improvement in impact behaviour can be variable. The low C high Mn steel Table 5.6, and the plain C-Mn steel Tables 5.8 and 5.9, give only minor improvements (5 to 15°C).

Leslie et.al[162] have also noted that the heat-treatment had compositional limitations in that it only seemed to be effective when the C level was between 0.05 to 0.15%C.

A probable explanation to account for this behaviour lies in the manner in which the ITT is related to the carbide thickness. As already mentioned, previous work by Mintz et. al[130] has shown that there is a maximum and minimum carbide thickness above and below which changes in carbide thickness have little influence on ITT, Figure 5.1. At coarse carbides the energy required to propagate micro-cracks from carbides is so low, that the critical event in fracture is the ability to propagate a grain size micro-crack over the ferrite boundary. At the other extreme below a certain carbide thickness (0.2μm), cracks can nucleate and propagate by the original Petch model without the help of carbides[131]. Mintz[132] also noted that the carbide thickness at which the curve reached its maximum was smaller at finer grain sizes.

If the improvement in ITT on intercritical annealing is measured by the difference between the normalised value and

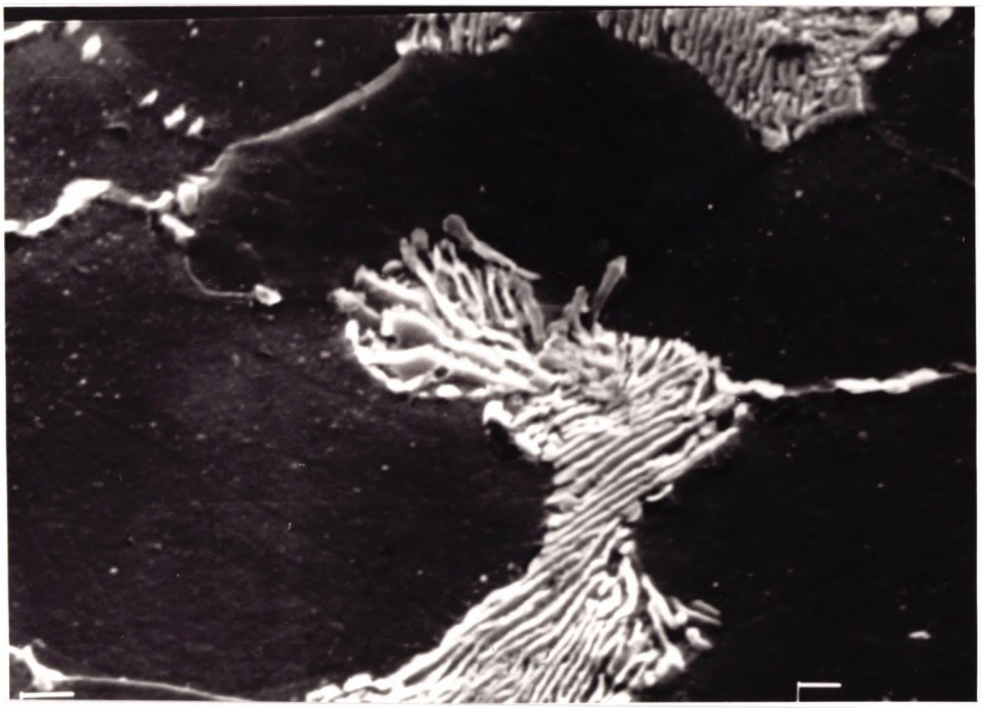

-a- X 5000

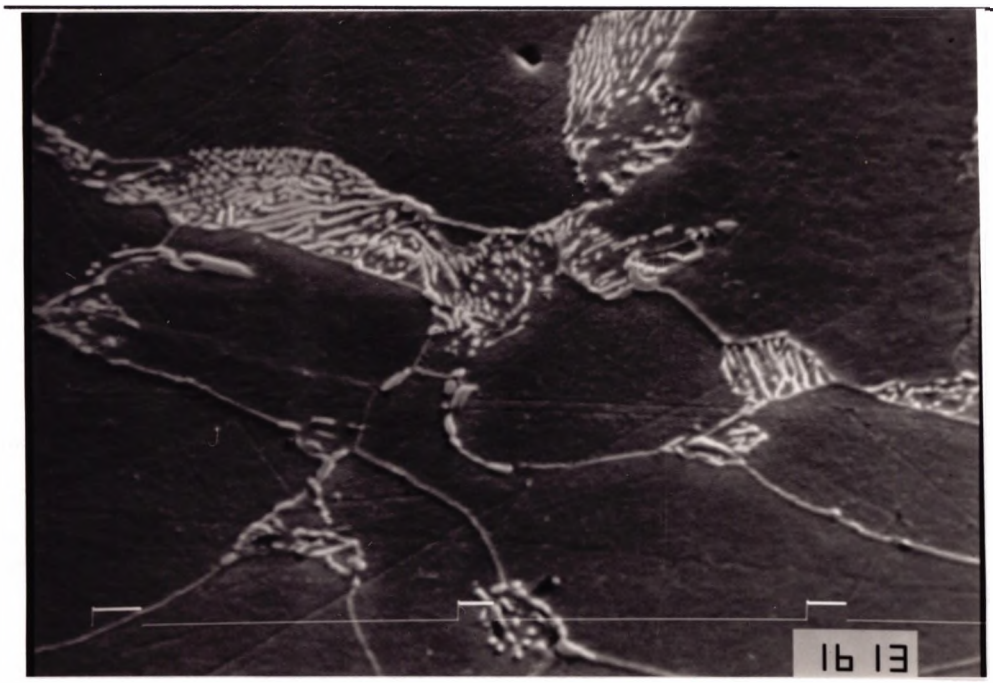

-b- X 5000

Fig.5.2- Refinement of Grain Boundary

a-After Normalising.

b- After 15 hr I.A.

that after intercritical annealing for 15 hr, and plotting this difference against the carbide thickness of the normalised condition the curve in Figure 5.3. is obtained. Although there is some scatter in the curve, the data fits reasonably well into the pattern noted in Figure 5.1. In the carbide thickness range 0.3 to 0.5 μm, intercritical annealing will give substantial improvements in impact behaviour (≥ 20°C). However, outside this range, changes in carbide thickness, t, will have a much smaller effect.

The value of carbide thickness depends to a large degree on the hardenability of the austenite and as such is related to the Mn and C levels. Raising either will lower the transformation temperature for the γ to Fe_3C reaction, and the lower the temperature at which the carbides precipitate, the finer they will be. Cooling rate also has an important influence, and its influence and that of hardenability on the carbide thickness of normalised steels is given in Figure 5.4.

Hardenability has been assessed here, by the simple (carbon equivalent value) CEV formula, C + Mn/6.

The steels in Leslie et al,s[11] work which showed marked improvements on intercritical annealing where low Mn (0.4%), 0.1%C steels, (CEV of 0.17). The steels which showed only small improvements on intercritical annealing where either high CEV (>0.32) or very low CEV (0.08). The cooling rate used in Leslie et al's[12] work after austenitising to room temperature were generally in the

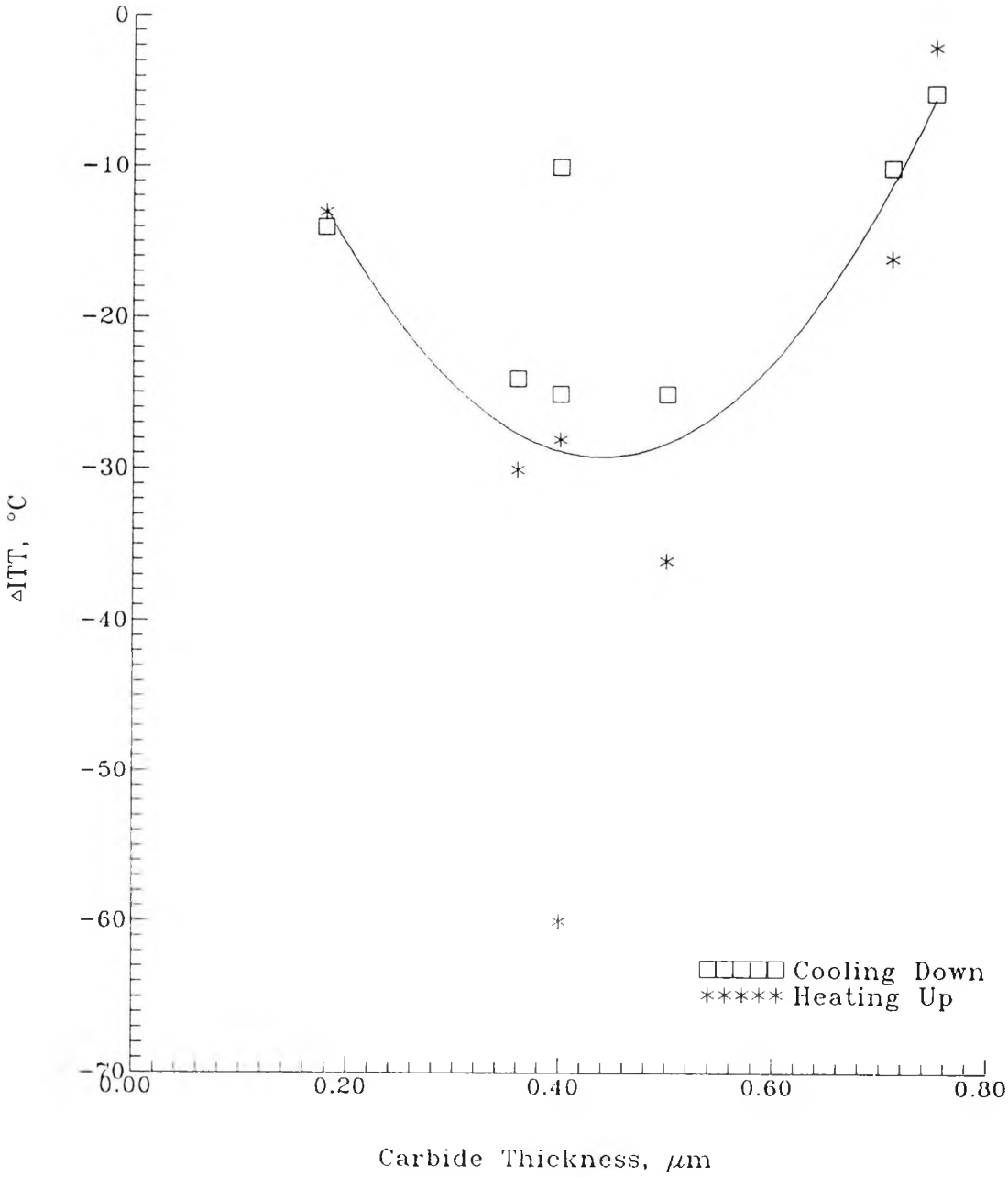

Fig.5.3- The Effect of Carbide Thickness on ΔITT.

range 25 to 50°C/min, and hence would most appropriately relate to curve C in Figure 5.4, in which significant improvements on intercritical annealing would only be expected in the CEV range > 0.08 to < 0.25, i.e in the carbide thickness range 0.25 to 0.55 μm.

5.4- REFINEMENT of the GRAIN BOUNDARY CARBIDE.

Because of the obvious importance of carbides in controlling impact behaviour it is necessary to examine the factors that influence the thickness of the grain boundary carbides. Mintz and Campbell[133] have shown that growth of carbides does not occur unless the cooling rate through the γ to Fe_3C transformation is very slow. For the cooling rate of 7°C/min used in most of this investigation growth would not be likely. The thickness then depends on how much of the C in solution in the ferrite can precipitate out on the carbides that are present on transformation. These carbides are always believed to be associated with pearlite colonies and indeed may trigger off the pearlite reaction. Carbon is able to diffuse very fast and for the natural air cooling rates of plate steel all the carbon in solution is able to come out of solution and precipitate out on the tails of the pearlite colonies. Because of the high rate of diffusion of C, the amount of C available for precipitating out can be calculated from the equilibrium solubility at transformation. A model developed by Mintz and Tajik[134] is shown in Fig. 5.5. Two factors can be seen

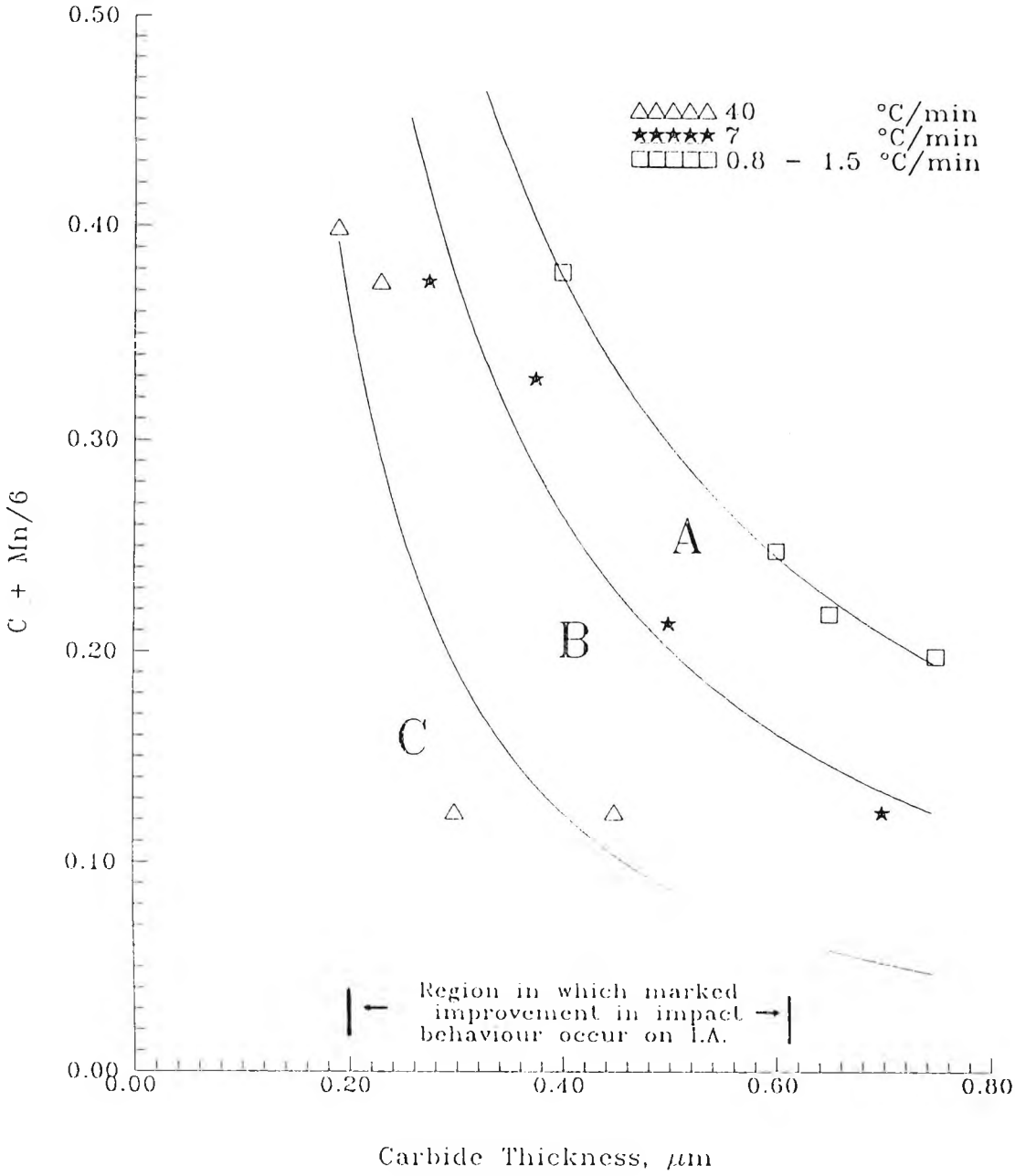

Fig.5.4- The Effect of Hardenability on Carbide Thickness[139].

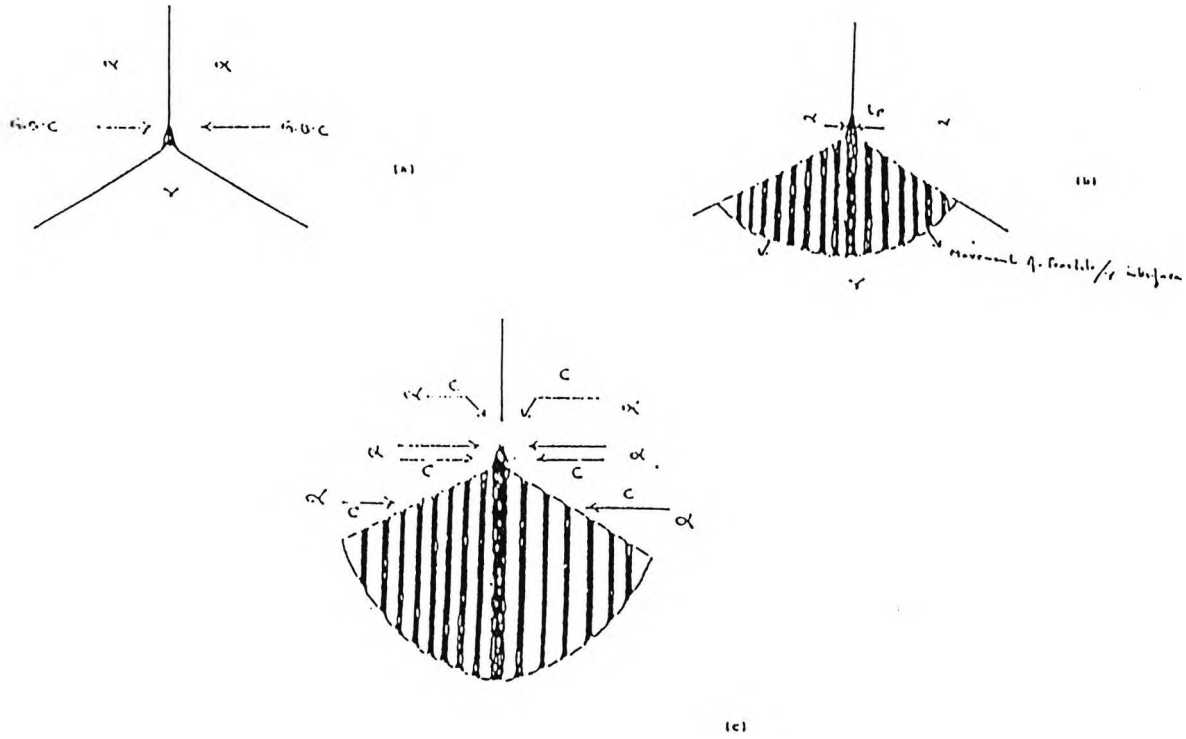

(a) Precipitation of grain boundary carbide from the austenite. Carbon comes from the austenite.

(b) Carbide nucleates pearlite reaction. Grain boundary carbide is now cut off from supply of carbon in the austenite.

(c) Further growth of grain boundary carbide occurs by carbon diffusing from ferrite to the grain boundary. Amount of carbon available from the ferrite for precipitation on existing carbides is dependent on the solubility drop that occurs between the temperatures for the start of the pearlite reaction and room temperature.

Fig.5.5- The Proposed Mechanism for G.B.C Formation, and Growth.[134]

to be very important in controlling thickness. One is the transformation temperature for the pearlite reaction which is controlled by composition, cooling rate, and grain size. The more hardenable the γ, the lower will be the transformation temperature and the less carbon will be available for precipitating out on the existing pearlite tails, leading to finer carbides. The other factor of great importance is the number of nucleation sites or tails of the colonies available for precipitating the carbon onto. The number of nucleation sites increases as the pearlite colony size decreases and this is favoured by fine austenite grain sizes and higher cooling rates. The greater the number of nucleation sites the more "mouths there are to feed" and hence the thickness is decreased.

Using these concepts it is possible to explain how changes in composition, cooling rate, grain size, and intercritical annealing temperature and time influence carbide thickness. Manganese for example lowers the transformation temperature and hence produces thin carbides.

However, it has been observed with grain refined steels[134] that provided the cooling rate through the transformation is constant the carbide thickness remains the same independent of prior γ grain size. This can be explained on the basis that the coarser the γ grain size the more hardenable is the steel, hence transformation temperatures are lowered but this is balanced by having

fewer nucleation sites as a result of the coarser γ grain size. Thus, the final thickness is a complex function of hardenability and number of nucleation sites.

In the present work the simplest explanation is just to assume that Mn is able to segregate to the boundaries very quickly and lower the transformation temperature locally so that the pearlite reaction is delayed to lower temperatures. In this way the very rapid improvements in impact behaviour with time (15 min) and the correspondingly rapid change in carbide thickness can be explained. This may not, however, be possible as there may not be sufficent driving force to set off the pearlite reaction. As the carbides are attached to the pearlite colonies, it may actually require the Mn to enter into the austenite colonies and lower the transformation temperature for the austenite pearlite reaction to occur. The hardenability of the γ may be the overriding factor which controls the pearlite transformation.

Therefore, another possible explanation can be found from the observation that as intercritical annealing proceeds Mn is absorbed into the γ and this causes the volume fraction of γ to increase, see Figure 4.24. However, on heating up this does not occur by growth of the old pearlite colonies but by the formation of new γ colonies most probably at the ferrite/ ferrite boundaries as suggested by Navara[55] et.al. Thus on heating up, not only the hardenability of γ increases as Mn gets absorbed, but

so does the number of nucleation sites for C to precipitate out on during transformation Figure 4.26.

On cooling down, the volume fraction of austenite first decreases to its equilibrum volume as carbon diffusion is controlling the transformation but after 30 minutes the austenite starts to grow as Mn is again absorbed. Although some of this volume increase occurs by growth of the old austenite, there is no doubt that new γ colonies are formed in the same way as on heating up, as is indicated by the increase in grain boundary coverage after 15 hour as shown in Figure 4.26. Thus, hardenability is increasing as well as the coverage of the boundaries by carbides, both of which could account for the thinner carbides. However, it is noticeable that the improvements in impact behaviour are less than on heating up in accord with the delay noted in Figure 4.13.

Nevertheless, there are some indications that changes in carbide thickness are taking place even after a short time as 15 minutes, and it is possible that both explanations are required to thoroughly explain the results.

5.5- MECHANISMS FOR MANGANESE DIFFUSION TO BOUNDARIES AND INTO AUSTENITE.

Manganese has been shown to be very important in controlling the grain boundary carbide thickness and so some discussion is required as to how it is able to reach the boundaries and diffuse into the γ.

The driving force for Mn segregation into the γ is due to the fact that Mn is an austenite stabilizer and when the two phases are present, ferrite and austenite, it dissolves more readily in the γ lattice than the ferrite lattice. Mn also retards the precipitation of carbon from the γ as carbides and again this has the effect of stabilising the γ. Silicon in contrast is a ferrite stabilizer and will if given the opportiunity diffuse from the γ to the α phase. Si also diminishes the solubility of C in γ and in this way stabilises the ferrite.

Manganese diffusion in the austenite is extremely slow compared to the diffusion in the ferrite. At 740°C the diffusion coefficient is $6.8 \times 10^{-19} m^2/sec$[135] and $1.2 \times 10^{-16} m^2/sec$[136] respectively, and if the diffusion rate of Mn in austenite was the controlling variable in partitioning many weeks would be required for an appreciable build up of manganese to occur. Navara[135] reported that on heating up to the intercritical annealing temperature, heat treatment times of the order of 10 hours ought to bring about a considerable degree of partitioning, which is in reasonable agreement with Leslie et. al's work[112], which

indicated that times of the order of 24 hours were required to significantly improve impact behaviour.

The relative short times of 15 minutes to 1 hour in the present work, to give an improvement in impact behaviour, indicates that Mn diffusion in ferrite must be controlling "partitioning".

As discussed in chapter (2.4.1), there are three mechanisms for how the austenite forms during intercritical annealing.

The first mechanism was proposed by Speich et.al[48]. They postulated that the process of intercritical annealing can be separated into three stages;

1- Nucleation of austenite at ferrite/pearlite interfaces followed by rapid growth into the pearlite until all the pearlite has dissolved.

2- Slower growth of austenite into the ferrite at a rate controlled by Mn diffusion in the ferrite.

3- Very slow final equilibrium between the ferrite and austenite.

The second mechanism was proposed by Navara and Harrysson[54]. They suggest that the austenite forms by heterogeneous nucleation, most probably at grain boundary carbides, and subsequently grows by absorption of both C and Mn, supplied to the surface of the grain.

The third mechanism was proposed in a later paper by Navara et.al[55]. They suggest that the austenite nucleation occurs at the ferrite/ferrite boundaries and is not

dependent on the presence of cementite particles for nucleation. It is this mechanism which seems to apply to the present results.

5.6- IMPORTANCE OF PARTITIONING IN CONTROLLING TRANSFORMATION

5.6.1- COOLING DOWN FROM THE γ.

Gilmour et.al[137] have shown that in C-Mn steels, the speed at which the γ to α transformation takes place depends on whether transformation is controlled by the diffusion of C or Mn, and this in turn is dependent on the degree of undercooling below the Ae_3, Figure 5.6. For compositions well below the Ae_3, the transformation should be rapid and controlled by C diffusion, whereas for compositions close to the Ae_3 partitioning can occur and transformation is controlled by Mn diffusion which is much slower. The isotherms for the Fe-C-Mn system at 730°C and 760°C are shown in Figure 5.6.

Gilmour et.al[138] suggest there is a boundary line in the diagram above which partitioning occurs and below which no partitioning takes place, Fig 5.6. It can be seen that at 730°C the present compositions fits into the region in which transformation is controlled by C diffusion and so should be very rapid. Data from the present work indicates for the high Mn steel that in the region of 30 minutes is required for the full transformation to occur, Figure 4.24.

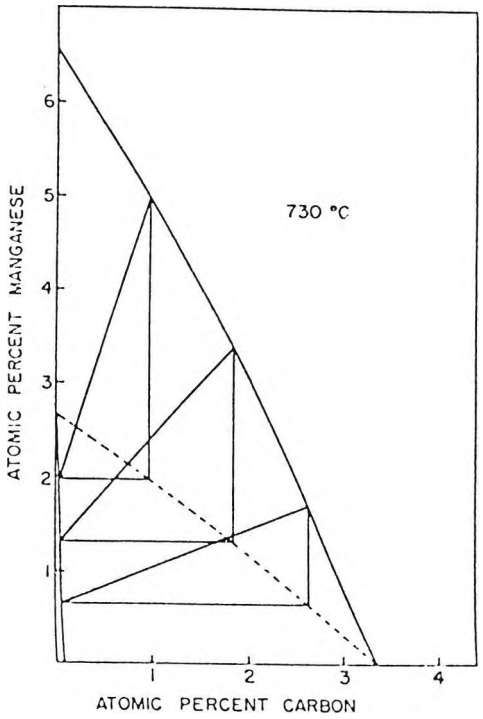

(a)

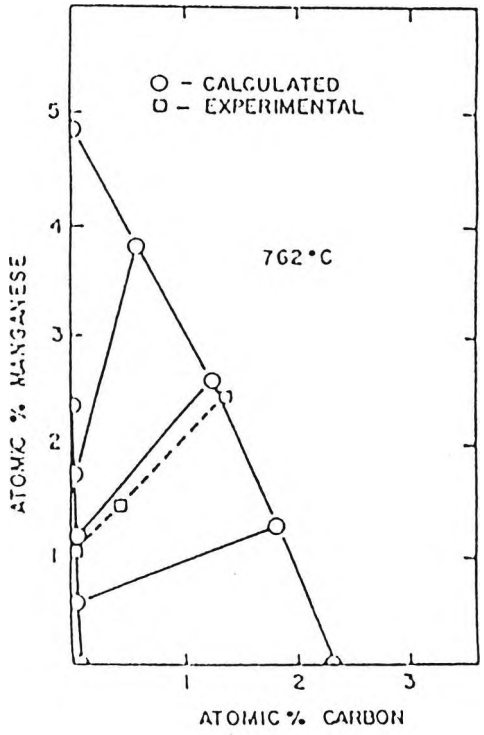

(b)

Fig.5.6- Isotherm of the Fe-Mn-C System[137]

a- at 730°C

b- at 760°C

5.6.2- HEATING UP TO THE ITERCRITICAL ANNEALING TEMPERATURE.

In contrast on heating up to the intercritical annealing temperature, the reverse behaviour occurs on the α to γ transformation, i.e. the region in Figure 5.6, which was high saturation now becomes low and vice versa. The present compositions now are close to the Ae_1, and hence transformation is controlled by Mn diffusion and hence will be slow.

5.7- LITERATURE EXPERIMENTAL EVIDENCE FOR Mn DIFFUSION TO BOUNDARIES OR INTO THE γ

Navara[54] has also suggested that, in case of cooling down from the austenite partitioning of manganese into the austenite can only occur by diffusion of manganese in austenite for the reasons given in previous section and because in this case ferrite is absorbing austenite. Diffusion of manganese would then be exceedingly slow. In accord with this, Gilmour et.al[46]. using electron-probe techniques have shown on transforming a steel with 1.5% Mn at 728°C from 1200°C that only interphase spikes high in manganese are obtained after many days at temperature i.e. no Mn is present within the γ.

It should also be noted that, Aaronson and Domaian[145] have shown using electron-probe techniques that the partitioning of manganese between austenite and proeutectoid ferrite on cooling down only occurs at high

temperatures in the temperature range 130°C below the Ae_3. Purdy et.al[44]. have shown that the criteria for partitioning depends on the degree of supersaturation on transformation. Only low supersaturation (where there is a very low growth rate) can give partitioning of substitutional solute elements. At higher supersaturation the transformation, while still maintaining complete local equilibrium at the interface, is much faster, the rate being controlled by carbon diffusion and the transformation being characterised by the absence of measurable manganese partitioning. Xue-Ling Cai et.al[144] have confirmed this by using a high resolution analytical STEM technique. They have shown that for a 0.11%C, 1.6%Mn steel, with a ferrite/pearlite microstructure heating into the two phase region (2 hours at 769°C) produces substantial segregation of Mn into the austenite. However, on step quenching from austenite to the intercritical annealing, 769°C, and holding for 2 hours no partitioning of manganese occurred, when measurements of the concentration profile were made at intervals of 0.5μm, transformation was now controlled by carbon diffusion. When the concentration of manganese was measured on a finer linear scale, intervals of 5 and 10 nm, a narrow spike (≈ 10nm) of high manganese concentration at the ferrite/austenite interface was obtained, ≈ 4% Mn (maximum value).

5.8- PRESENT EVIDENCE FOR Mn DIFFUSION TO THE BOUNDARIES AND SEGREGATION INTO γ.

In the present study using EDX techniques, substantial Mn segregation into the γ has been found both on heating and cooling to the intercritical annealing temperature after holding for 15 hours, table 4.5. Enrichment of the γ by Mn automatically involves growth of the γ and hence its volume fraction increases. Thus, the curve of martensite volume fraction against intercritical annealing time shown in Figure 4.24. is extremely important in interpreting the present results.

The curve for the high Mn steel (low Mn steels are similar but changes are smaller), again confirms that substantial segregation of Mn has occurred into the γ, both on heating up and cooling down to intercritical annealing temperature as is indicated by the marked increase in the γ volume fraction (i.e. martensite on quenching). However, whereas the γ volume fraction increases continually on heating up indicating that the Mn level is also increasing, on cooling down, the γ to α transformation has to be completed before the γ volume fraction starts to increase and Mn levels can rise, Figure 4.24. Equilibrium data for the non-partitioned diagram for a 1.5% Mn, 0.1 C steel at 730°C indicates that 19% γ should be present which is little higher than that observed experimentally (17%). The equilibrum diagram, Figure 5.6, indicates that when partitioning is complete about 2.5% Mn will be present and

the volume fraction of γ would be in the range of 27%. Thus a 1% increase in Mn is accompanied by an 8% increase in the percentage volume fraction of γ.

Quenching immediately after holding for various times at intercritical annealing temperature is also therefore an excellent technique for establishing the presence of Mn in the γ and the actual amounts can be estimated knowing the equilibrum and para-equilibrum γ volume fractions and Mn contents for these positions.

However experimentally the change in γ volume fraction with Mn level was more marked. On heating up, the Mn level increased to 2.2% and the γ volume fraction as shown by the quenched samples to 37% on intercritical annealing for 15 hours. On cooling down, the Mn level increased to 1.93% and the γ volume fraction to 34%.

A problem exists in the present work is explaining how Mn can diffuse into the γ after such short times on cooling down to the intercritical annealing temperature.

The results show that for cooling to the intercritical annealing temperature, the volume fraction of martensite first decreases to the equilibrium condition (after about 30 minutes), then increases in exactly the same way as on heating up to the intercritical annealing temperature (i.e increases as the intercritical annealing time increases).

This behaviour indicates a mechanism entirely different from that proposed by Speich et.al[48]. Recent work by Navara et.al[55]. has shown that on heating, austenite

nucleates randomly at the ferrite/ferrite boundaries, not at dissolved pearlite as suggested by Speich et.al[98]. or at grain boundary carbides as originally suggested by Navara and Harrysson[54] The austenite is thought to nucleate through a local build up of manganese in the boundary regions by grain boundary diffusion of manganese along ferrite/ferrite boundaries (this being more rapid than bulk diffusion), the feedstock coming from the ferrite grains. A nucleus of manganese enriched austenite then forms and enlarges into the ferrite by continued grain boundary diffusion.

This mechanism is capable of explaining the present results both on heating up to and cooling down to the intercritical annealing temperature.

Previous work by Cai et.al[141]. on step quenched samples has shown that although manganese diffuses to the boundary regions no partitioning of manganese into the austenite occurs except after very long times.

However, it is noticeable in their work that the transformation from austenite to ferrite takes place over a long time, i.e many hours, not minutes as in this work, where cooling from the austenite is slow. Because transformation from austenite to ferrite is so rapid, 30 minutes in this work, once the non-partitioned equilibrium has been achieved, the austenite is able to grow into the ferrite and the manganese enrichment again probably occurs by grain boundry diffusion of manganese along the

ferrite/ferrite boundaries. However, whatever the exact mechanism of austenite formation it is clear that considerable Mn enrichment of the austenite can occur and the presence of Mn either at the α/γ boundary or within the γ is responsible for the refinement of the grain boundary carbides.

It is now proposed to discuss the individual results.

5.9- THE EFFECT OF MANGANESE LEVEL ON IMPACT BEHAVIOUR.

5.9.1- CARBIDE THICKNESS After Normalising.

From the results shown in chapter (4.1), increasing the Mn level has the effect of making the steel more hardenable so lowering the γ to Fe_3C transformation temperature, as well as increasing the number of nucleation sites as can be seen from Figure 4.26. In consequence, the carbide thickness refined from 0.48 μm to 0.24 μm as the Mn increased from 0.56% to 1.5% in the normalised steels.

5.9.2- CARBIDE THICKNESS After Intercritical Annealing.

The effect of Mn level studied in the present work on impact performance (ITT) during intercritical annealing is shown in figure 4.13. It can be seen that for steels having 0.56%Mn and 1%Mn an improvement in impact performance (lower ITT) occurs on intercritical annealing. In contrast for the 1.49% Mn the ITT rises after intercritical annealing for long times.

5.9.3- IMPACT PERFORMANCE FOR THE 0.56% Mn AND 1% Mn STEEL.

Little change was found in grain size and pearlite volume fraction on intercritical annealing, Table (4.2), and Table (4.3).

However, during intercritical annealing the Mn is observed to increase in the austenite both on "heating up" and "cooling down". The transformation temperature is therefore lowered leading to refinement in the grain

boundary carbide thickness, (see Tables 4.3 and 4.4 for the 1% and 0.56% Mn steels respectively).

Using equation {5.1} to calculate the 54J ITT, it can be seen that in Tables 5.1 and 5.2 that there is reasonable agreement between the observed and calculated values. In these calculations the constant in the equation was taken as 78°C for 0.56% Mn steel, and 85°C for 1% Mn steel so as to give the best agreement to the data. Δy was taken as zero, i.e no precipitation hardening.

Because the change in grain size and in pearlite volume fraction is small, it seems reasonable to assume that the improvement in impact performance on intercritical annealing is due to the refinement in grain boundary carbides due to Mn segregation. Thus for example for the 0.56% Mn steel, the carbide thickness decreased from 0.48 μm on normalising to 0.35 to 0.34 μm after holding for 900 minutes, Table 4.4. This corresponded to an observed fall in ITT of 24°C to 36°C. During the 900 minutes hold, the Mn level in the γ was observed to increase by 10% from 0.7% to 0.77% Mn, Table 4.5. However, calculated changes in ITT on the basis of the changes in carbide thickness were in general less than the observed changes, Table 5.1.

Similar improvements in impact behaviour on intercritical annealing were noted in the higher 1% Mn steel but this time the calculated change was very closed to the observed, Table 5.2. The carbide thickness decreased from 0.35 μm on normalising to 0.23 μm and 0.22 μm on intercritical

annealing for long times. This corrosponded to an observed fall in ITT of 26°C to 30°C compared to calculated falls of 19°C to 25°C. During the 900 minutes hold the Mn level in the γ was observed to increase markedly by 60%. It should be noted that for both the 0.56% and 1% Mn steels the carbide thickness after normalising is in the range in which significant improvements in impact behaviour would be expected on intercritical annealing, Fig. 5.1.

This enrichment of Mn in the γ occurs on intercritical annealing due to "partitioning". However, the means in which Mn enrichment of the γ occurs is most likely by diffusion along the ferrite/ferrite boundaries causing a build up of Mn most likely at grain junctions and these regions then form the γ nuclei from which growth occurs.

Table 5.1- Observed and Calculated ITT°C to Give Impact Energy of 54J & Observed and Calculated Yield Strength for the 0.56% Mn Steel.

Holding time, minutes	54J ITT°C				Yield Strength σ_Y, Mpa		
	Obs.	Cal*	ΔITT°C		Obs.	Cal.	$\Delta\sigma_Y$ obs.- cal.
Normalised	-18	-26	obs	cal	265	272	-7
Cooled to 730°C							
15	-34	-28	16	2	287	270	17
30	-38	-31	20	5	287	269	18
60	-40	-35	22	9	272	269	3
900	-42	-43	24	17	289	274	15
Reheated to 730°C							
15	-36	-35	18	9	268	277	-9
30	-38	-39	20	13	270	275	-5
60	-43	-38	25	12	276	275	1
900	-54	-44	36	18	280	274	6

* Constant taken as 78.

Table 5.2- Observed and Calculated ITT°C to Give Impact Energy of 54J & Observed and Calculated Yield Strength for the 1% Mn Steel.

Holding time, minutes	54J ITT °C				Yield Strength σ_Y, Mpa		
	Obs.	Cal.*	ΔITT		Obs.	Cal.	$\Delta\sigma_Y$ obs. - cal.
Normalised	-59	-64	obs	cal	293	301	-8
Reheated to 730°C							
30	-87	-84	28	20	297	306	-9
900	-89	-89	30	25	301	306	-5
Cooled to 730°C							
30	-79	-79	20	15	313	305	8
900	-85	-83	26	19	309	312	-3

* Constant has been taken as 85

5.9.4- YIELD STRENGTH.

The effect of Mn level studied in the present work on yield strength during intercritical annealing is shown in fig 4.14. By using equation 5.2 to calculate the yield strength, it can be seen from table 5.1 and table 5.2 that there is a reasonable agreement between the observed and calculated yield strength. The yield strength is dominated by the composition of steel and its grain size. During intercritical annealing the composition does change but generally average changes are small and any fall in yield strength from the slight decrease in Mn in the ferrite is likely to be approximately compensated for by the small increase in Si in the ferrite. As the change in grain size is very small the yield strength remains approximately unchanged on intercritical annealing.

5.9.5- INTERCRITICAL ANNEALING OF THE 1.49% Mn STEEL.

5.9.5.1- IMPACT PERFORMANCE.

The impact behaviour of the 1.49% Mn steel is more complex because intercritical annealing for long times causes :

a- In the case of heating up, the introduction of a high volume fraction of the pearlite due to the increase of manganese segregation into the γ. This increase in pearlite, is in the form of a net work surrounding the ferrite matrix, Figure 4.20 .

b- For both heating up and cooling down, the presence of

small amounts of martensite in the form of small colonies sited along the boundaries, Figure 5.7.

All of these changes in microstructure may well influence impact and tensile properties. Koo has been shown that[78], the morphology (size, shape, and distribution) of the microstructural constituents influence the mechanical properties of dual phase steels. The calculated 54J ITT using equation 5.1 are given in Table 5.3. The constant was chosen as 82°C to give the best agreement to the data, and Δy was taken as zero, i.e no precipitation hardening. It can be seen that for short intercritical annealing times, little improvement was noted in the impact performance.

However, long holding times introduced large amounts of (pearlite/martensite mixture) resulting in poor impact resistance.

Other possible causes of the poor impact behaviour are the growth of a network structure of the brittle pearlite/ martensite phase surrounding the softer ferrite which occurs after holding for long times on heating up and the coarsening of the pearlite colonies which occurs during the cooling down cycle.

However, pearlite influences ductile failure rather than brittle. It does have some influence on brittle fracture by providing the grain boundary carbides which act as nucleation sites for cracks*. The thickness of these carbides has been shown to be controlled by the transformation temperature, and the number of carbides present. Thus if pearlite is formed at

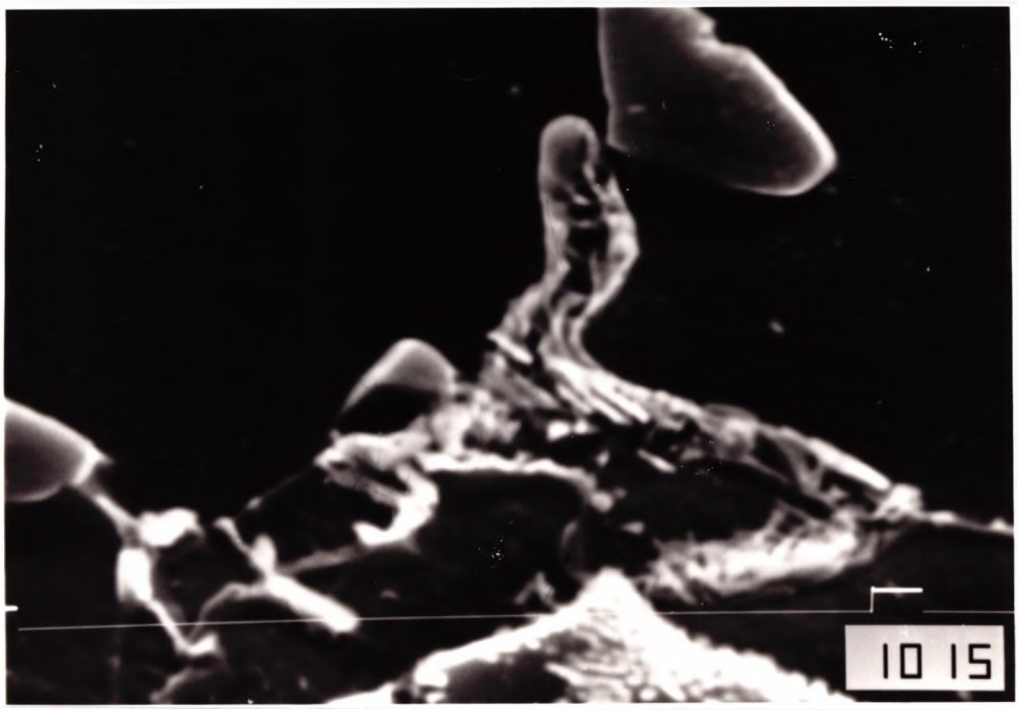

X 7500

Fig.5.7- Martensite Formation During Long Time I.A.(15hr), Heating Up Cycle.

a high temperature and their are few colonies present, there is a large amount of carbon in solution and few branches available for growth when this carbon precipitates out on cooling to room temperature. This large feedstock results in coarse carbides and poor impact behaviour. If however pearlite forms at low temperatures and there are many colonies, there is little C available to precipitate out on the pearlite arms and there are a large number of arms competing for the C, grain boundary carbides and impact behaviour is improved. In the present instance, the very similar impact behaviour shown after long holding times for both heating up and cooling down even though the pearlite distributions are so very different make it unlikely that it is pearlite which is responsible for the poor impact behaviour. However, carbide density measurements do indicate that γ growth along the ferrite grain boundaries which results in small pearlite colonies, form both on heating up and cooling down, and this would encourage finer carbides. It seems most likely that this poor impact behaviour arises because of the formation of small amounts of high C martensite, Fig. 5.7.

At the higher Mn level the enhancement of Mn in the γ is very marked (2.2%) and is high enough to cause a very small amount of martensite to form.

---

* It also reduces the impact energy criteria for fracture via lowering the shelf energy.

Tanaka et.al[14] have shown that the cooling rate (CR in Ks^{-1}) to give martensite can be related to the Mn content by the following empirical relationship

$$\log (CR) = 3.95 - 1.73 (\% Mn_{eq}) \quad \ldots\ldots\ldots\ldots\ldots\ldots\ldots\ldots \quad 5.3$$

This equation was obtained for steels containing. .05%C and does not take into account the influence of C on hardenability. A more comprehensive empirical equation which includes a vector for the influnce of C, has been derived by Messien et.al.[33].

$$\log (CR_{5\%M}) = 4.93 - 1.7 (\%Mn) - 1.34\% Si - 5.68\%C \quad \ldots\ldots\ldots \quad 5.4$$

where $CR_{5\%}$ is the cooling rate to give 5% martensite (again in Ks^{-1}).

The cooling rate of 7°C/min used in the present study is according to their equation an order of magnitude too low for 5% martensite to be formed (for a build up of 2.2% Mn the cooling rate needs to be 70 °C/min).

Neverthless, a few per cent of martensite is formed as laths along the grain boundaries as can be seen from Figure 5.7 and this probably indicates that the C content in these areas is very high according to Messiòn et.al[33] equation , 0.5%C. Martensite laths like grain boundary carbides are very brittle and if the average thickness of these laths (0.6 µm) is taken as the "carbide thickness" then this could well account for the poor impact behaviour of the steel.

In previous work[115] at a higher cooling rate (40°C/min), were amounts well in excess of 5% martensite where formed, even after short intercritical annealing times (1/2 hour), a

very small improvement in impact behaviour occurred. This was believed to be due to small amounts of martensite having no influence on impact behaviour; the impact behaviour improving through refinement of carbides. After very long holding times (24 hours), impact behaviour deteriorated because of the very high fraction of martensite (20%). Strength was also observed to increase with this large volume fraction of martensite.

These results contrast with those of the present work in which at the lower cooling rate only very small amounts of martensite form. There is no evidence for any improvement in impact behaviour with time, the impact behaviour starts to deteriorate after 1 hour and at the longest holding time there is a significant fall in strength (20 to 30 Mpa). Such differences in behaviour are not entirely understood but are probably related to the form and volume fraction of martensite present. The form of martensite is known to be important. For example high C twinned martensite is known to be very brittle compared to low C lath martensite which has a high density of dislocations. There is also evidence to indicate that small volume fractions of acicular ferrite (5%) may not influence impact behaviour in line pipe steels[73]. It is possible that at the lower cooling rate the volume fraction of γ prior to transformation is able to readjust itself to very low values giving a very brittle high C martensite. Clearly this is an area which requires further investigation.

5.9.5.2- YIELD STRENGTH.

By using equation 5.2 to calculate the yield strength, it can be seen from table 5.3 that there is a reasonable agreement between the observed and calculated yield strengths for short intercritical annealing times (15,30,60 minutes). However, after long holding times the observed yield strengths were very much less than the calculated values.

The fall in yield strength at long holding times on heating up is also not fully understood. In all cases a Luders extension was observed, Figure 5.8, and this was found on heating up to decrease with intercritical annealing time as the amount of pearlite increased. This is likely to be associated with the marked increase in work hardening rate that occurs with the presence of pearlite. The higher work hardening rate results in a smaller Luders extension, owing to the more rapid work hardening behind the front reducing the strain involved in reaching the stress required to propagate the front. The changes in pearlite volume fraction were very small on cooling down and in accord with this little change in Luders extension was obtained.

Small amounts of martensite have been shown to reduce the yield stress. This occurs because the volume expansion accompanying the martensite transformation causes pre yielding and the mobile dislocations formed are able to move at lower stresses. Work by Rigsbee and VanderArend[70] indicates that the yield strength decreases with increasing martensite volume fraction up to 4% volume fraction and then

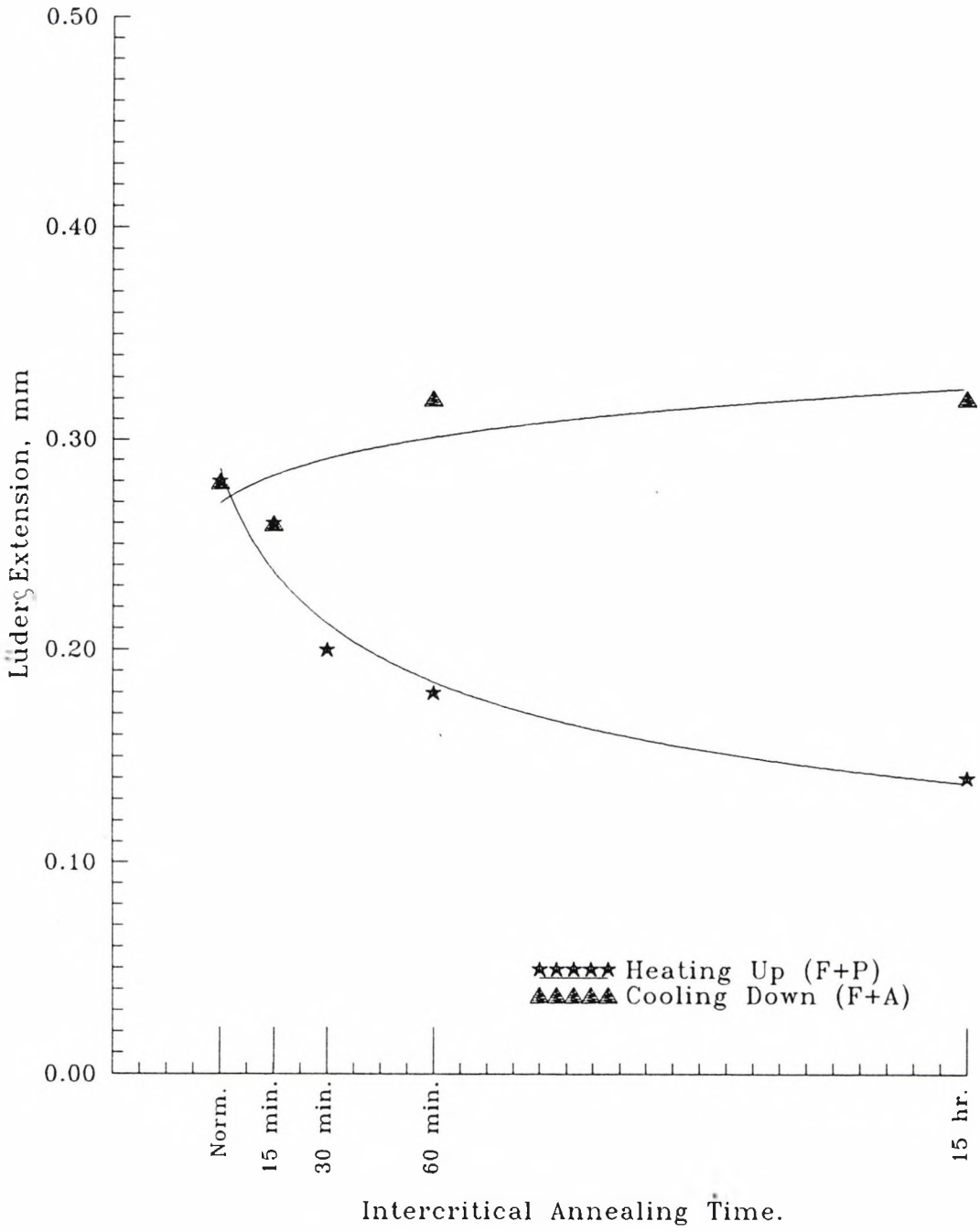

Fig.5.8- The Effect of I.A. on Luder Extension.

starts to increase again Figure 5.9. They also noted that the Luders strain decreased with with increasing volume fraction of martensite and the changeover to continuous yielding occured when the volume fraction of martensite exceeded 4%. The increase in strength for higher martensite volume fractions (> 6%) arises because it is believed that at these levels, the ferrite grain interiors become saturated with transformation induced dislocations. It may be possible that at this lower cooling rate in which only a very small amount of martensite is formed, mixed behaviour can occur, some regions yielding early, wherease in other regions, yield propagates by the movement of a Luders front.

Another possiblity is that, on heating for long times at the intercritical annealing temperature using the heating up, or cooling down cycles, the segregation of manganese and carbon to the austenite during intercritical annealing results in a softer ferrite matrix. Dislocation movement therefore becomes easier, resulting in a lower yield strength. However, if this was the explanation, one might have expected to see some fall in yield strength after one hour. Again further investigation is required.

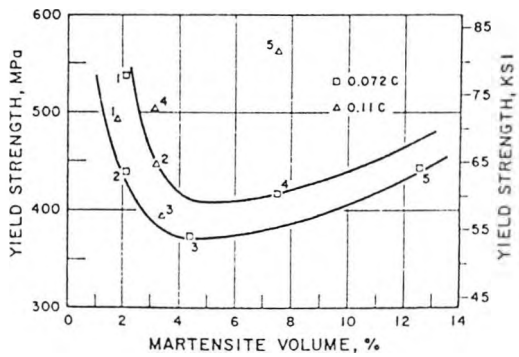

Fig.5.9- The Effect of Martensite Volume Fraction on Yield Strength[70].

Table 5.3- Observed and Caculated ITT'S to Give Impact Energy of 54J & Observed and Calculated Yield Strength for the 1.49% Mn Steel.

Holding time, minutes.	54J ITT °C				Yield Strength σ_Y, Mpa		
	Obs.	Cal*	ΔITT°C		Obs.	Cal.	$\Delta\sigma_Y$ obs. - cal.
Normalised	-80	-80	obs.	cal.	341	346	-5
Reheated to 730°C							
15	-85	-67	5	-13	322	337	-15
30	-85	-65	5	-15	332	345	-13
60	-78	-78	-2	11	332	344	-12
900	-61	-84	-19	17	302	353	-51
Cooled to 730°C							
15	-82	-94	2	14	344	348	-4
30	-82	-101	2	21	343	353	-10
60	-72	-106	-8	26	343	347	-4
900	-70	-110	-10	30	327	352	-25

* Constant taken as 90.

5.9.6- MICROHARDNESS.

When the microhardness of martensite is plotted as a function of intercritical annealing holding times, the curves shown in figure 4.26 are obtained. According to the microhardness testing results, for both heating up and cooling down to the intercritical annealing temperature the hardness of martensite is a linear function of martensite volume fraction, vmQ (i.e as the volume fraction of martensite increases so does the hardness decrease). This indicates that as the γ volume fraction increases the C content of the γ is reduced resulting in a softer martensite.

Changes in the ferrite microhardness were much smaller and may not be significant. As already noted although some changes in composition do occure they are unlikely to have any marked influence on the strength of the ferrite.

5.10- THE EFFECT OF COOLING RATE.

5.10.1- IMPACT PERFORMANCE.

As already noted for a 1.5% Mn steel, a cooling rate of 7°C/min causes a rise in ITT after intercritical annealing for a long time due to the presence of a large volume fraction of pearlite and martensite films. It was hoped that reducing the cooling rate would :

1) Prevent martensite formation.

2) Reduce the volume fraction of γ available for the pearlite transformation and both these aims were achieved. The effect of the two cooling rates studied in the present work for 1.5% Mn steels on the ITT is shown in figure 4.30.

For the lower cooling rate of 0.8°C/min, the improvement in ITT is noted for short and long time intercritical annealing treatments on both heating up and cooling down to the intercritical annealing temperature. As neither martensite formed nor was there an increase in pearlite volume fraction or grain size, the impact behaviour was controlled by changes in carbide thickness. Mn enrichment of the γ or Mn enrichment at the α/γ grain boundaries takes place on intercritical annealing reducing the transformation temperature resulting in finer carbides and better impact behaviour.

By using equation (5.1) to calculate the 54J ITT, and taking the constant in equation as 90°C for 1.49% Mn steel, and 100°C for 1.51% Mn steel to give the best agreement to the data, and taking $\Delta y = 0$, i.e no precipitation hardening, it can be seen from table 5.4 and table 5.5 that, there is a

reasonable agreement between the observed and calculated values.

The grain boundary carbides thickness after normalising were (0.4 and 0.38 μm) in the range in which large improvements in impact behaviour on intercritical annealing might be expected, Fig. 5.1.

5.10.2- YIELD STRENGTH.

The effect of cooling rate studied in the present work on yield strength during intercritical annealing is shown in fig 4.32.

By using the modified equation 5.2 to calculate the yield strength, it can be seen from table 5.4 and table 5.5 that there is very good agreement between the observed and calculated yield strength for 1.49% Mn steel, and 1.51% Mn steel cooled at the slower cooling rate of 0.8°C/min.

The lower yield stress (LYS) that is present in the slower cooled platesy is probably due to a lowering of the K_y value. It has been suggested that slower cooling rates in ferrite/pearlite steels reduce the amount of interstitials (mainly C) in solution at the grain boundaries[128].

Table 5.4- Observed and Caculated ITT'S to Give Impact Energy of 54J & Observed and Calculated Yield Strength for 1.49% Mn Steel Heating Up to the Intercritical Annealing Temperature and Cooled at 0.8°C/min.

Holding time, minutes	ITT °C				Yield Strength σ_Y, Mpa		
	Obs.	Cal *	ΔITT		Obs.	Cal.	$\Delta\sigma_Y$ obs. - cal.
Normalised	-28	-63	obs.	cal.	304	316	-12
Reheated to 730°C							
30	-77	-77	49	14	305	310	-5
900	-88	-85	60	22	302	312	-10

* Constant taken as 95.

Table 5.5- Observed and Caculated ITT'S to Give Impact Energy of 54J & Observed and Calculated Yield Strength for 1.51% Mn Steel Cooling Down to the Intercritical Annealing Temperature and Cooled at 0.8°C/min.

Holding time, minutes	ITT °C				Yield Strength σ_Y, Mpa		
	Obs	Cal*	ΔITT		Obs.	Cal.	$\Delta\sigma_Y$ obs. - cal.
Normalised	-55	-52	obs.	cal.	321	**325**	-4
Cooled to 730°C							
60	-80	-67	25	15	322	327	-5

* Constant taken as 100.

5.11- THE EFFECT OF CARBON LEVEL.

5.11.1- IMPACT PERFORMANCE.

From the previous two sections (5.4,5.5) it has been shown for high Mn steels that a cooling rate of 7°C/min causes a rise in ITT after intercritical annealing times, while a slower cooling rate of 0.8°C/min lowers the ITT without change in yield strength. In this section, the results of the effect of carbon level will be discussed.

The effect of carbon level studied in the present work for a 1.5% Mn steel on ITT is shown in figure 4.38. It can be seen that, whereas the high C steel gives poor impact performance after intercritical annealing for long times, the lower C steels shows improvements, although they where less than expected. This is probably related to the very fine carbide thickness (0.17 μm) of this steel in the normalised condition. It is believed that refinement of carbides below 0.2μm has little influence on impact behaviour, Fig. 5.1.

The regression equation 5.1 indicates that changes should have been more marked but this illustrates the limitations of linear regression analysis.

For heating up, lowering the C content seemed to prevent martensite formation and although a small increase in pearlite occurred with increase in intercritical annealing times it was minor compared to the large increase observed at the higher C level.

Hence, for both heating up and cooling down, because the

change in grain size and in pearlite volume fraction is small (Table 4.12), it seems reasonable to again assume that the improvement in impact performance on intercritical annealing is due to the refinement in grain boundary carbides due to Mn segregation.

5.11.2- YIELD STRENGTH.

The effect of carbon level studied in the present work on yield strength during intercritical annealing is shown in fig 4.40

By using equation 5.2 to calculate the yield strength, it can be seen from table 5.6 there is a reasonable agreement between the observed and calculated yield strength for the 1.41% Mn steel, 0.067%C containing steel.

The observed yield strengths were lower than the caculated yield strengths and this may be related to the lower pearlite content of the steel. The yield strength regression equation does not contain a term for the pearlite volume fraction but work by Mintz and Kolahi-Aval[128] have shown that a change in pearlite content by 1% corrosponds to approximately a change in strength by 1 Mpa.

Table 5.6- Observed and Caculated ITT'S to Give Impact Energy of 54J & Observed and Calculated Yield Strength for 0.067% C Steel.

Holding time, minutes	ITT °C				Yield Strength "σ_Y" Mpa		
	Obs.	Cal*	ΔITT		Obs.	Cal.	$\Delta\sigma_Y$ obs. - cal.
Normalised	-95	-98	obs.	cal.	326	334	-8
Reheated to 730°C							
30	-109	-101	14	3	325	329	-4
900	-109	-102	14	4	320	330	-10
Cooled to 730°C							
30	-104	-102	9	4	325	334	-9
900	-109	-107	14	9	328	337	-9

* Constant taken as 70.

5.12- THE EFFECT OF HEATING TEMPERATURE.

5.12.1- IMPACT PERFORMANCE.

The effect of the intercritical annealing temperature on the ITT for the 1% Mn steel is shown in figure 4.46. It can be seen that, in case of cooling down, intercritical annealing at 730°C reduced ITT's more than on intercritical annealing at 760°C. For heating up similar improvements were obtained.

From table 5.7, it can be seen that there is generally a reasonably agreement between the observed and calculated 54 J ITT values using a constant of 90°C.

For heating up, from table 4.15, because the change in grain size and in pearlite volume fraction is small, it seems reasonable to assume that the improvement in impact performance on intercritical annealing is due to the refinement in grain boundary carbides caused by Mn segregation.

Raising the intercritical annealing temperature would be expected to increase the volume fraction of γ, reducing its carbon content and hence reducing the hardenability. Coarser grain boundary carbides would therefore be expected. Coarser carbides were produced but differences were small.

High intercritical annealing temperatures would also be expected to enhance the diffusion of Mn along the γ boundaries, and this may account for the rather good impact behaviour observed on heating up in which improvements were

similar to those obtained at 730°C. The rather small improvements in impact behaviour noted on cooling down to 760°C are probably related to the longer time required for the γ to transform to ferrite. Examination of Figure 5.6 indicates that on cooling down for a given composition, raising the intercritical annealing temperature will favour transformation being changed from non- partitioned to the much slower partitioned. Ferrite/ ferrite boundaries are probably required for the growth of the small γ colonies and the accompanying Mn enrichment which gives rise to fine carbides. Hence this cannot occur until transformation is well developed. In contrast on heating up the ferrite/ferrite boundaries are already present.

5.12.2- YIELD STRENGTH.

The influence of heating temperature studied in the present work on yield strength during intercritical annealing is shown in fig 4.48.

By using the modified equation 5.2 to calculate the yield strength, it can be seen from table 5.7 that there is very good agreement between the observed and calculated yield strength for the 1% Mn steel intercritically annealed at 760°C.

Table 5.7- Observed and Caculated ITT'S to Give Impact Energy of 54J & Observed and Calculated Yield Strength for 1% Mn Steel Intercritically Annealed at 760°C.

Holding time, minutes	ITT °C				Yield Strength σ_Y, Mpa		
	Obs.	Cal*	ΔITT		Obs.	Cal.	$\Delta\sigma_Y$ obs. - cal.
Normalised	-60	-65	obs.	cal.	290	301	-11
Reheated to 760°C							
30	-85	-81	25	16	295	305	-10
900	-89	-84	29	19	285	307	-22
Cooled to 760°C							
30	-70	-74	10	9	288	297	-9
900	-70	-73	10	8	290	301	-11

* Constant=90

5.13- THE EFFECT OF GRAIN SIZE.

The effect of intercritical annealing on ITT as a function of grain size is shown in figure 4.57 for a plain C-Mn steel. It can be seen that, at a grain size of 18 μm intercritical annealing at 730°C lowers the ITT, while intercritical annealing has little effect on ITT when the grain size of the plain carbon steel is 37μm.

By using equation (5.1) to calculate the 54J ITT, and taking the constant in equation as 102°C to give the best agreement to the data, and taking $\Delta y = 0$, i.e no precipitation hardening, it can be seen from table 5.8, that there is reasonable agreement between the observed and calculated values.

For heating up, from table 4.17, because the change in grain size and in pearlite volume fraction is small, it seems reasonable to assume that the improvement in impact performance on intercritical annealing is due to the refinement in grain boundry carbides caused by Mn segregation.

Grain size would be expected to have an influence on the intercritical annealing process if austenite formation occurs by the rapid diffusion of Mn along the ferrite grain boundaries. Increasing the grain boundary surface area will provide more access of Mn to the boundaries and accommodate more readily the growth of γ as thin films along the boundaries. The rate of diffusion might be expected to be proportional the surface area to volume ratio, i.e. 1/d so

that having the grain size might be expected to halve the time taken for γ growth.

Certainly, reducing the grain size led to greater improvements in impact behaviour on intercritical annealing particularly if the C-Mn-Nb-Al steel results are included in the analysis. On intercritical annealing little improvement in impact behaviour occurred at the coarsest grain size. A small improvement was observed at 18 μm and at 12 μm, the ITT decreased by 25 to 30°C after holding 15 hours at the intercritical annealing temperature.

Again at the coarser grain sizes, the carbide thickness (approximately 0.7 μm after normalising) was too coarse for changes to have a large influence on ITT's. However at Fine grain size, the normalised grain boundary carbide thickness (0.4 μm) was in the range in which significant improvements in impact behaviour would occur on intercritical annealing.

Table 5.8- Observed and Caculated ITT'S to Give Impact Energy of 54J & Observed and Calculated Yield Strength for for Plain C-Mn Steel Intercritically Annealed at 730°C (Finer Grain Size).

Holding time, minutes	ITT °C				Yield Strength σ_Y, Mpa		
	Obs.	Cal*	ΔITT		Obs.	Cal.	ΔσY obs. - cal.
Normalised	-25	-15	obs.	cal.	280	267	13
Reheated to 730°C							
30	-29	-26	4	11	273	264	9
900	-42	-47	17	32	277	269	8
Cooled to 730°C							
30	-28	-23	3	8	278	265	13
900	-35	-38	10	23	275	264	11

* constant=102

Table 5.9- Observed and Caculated ITT'S to Give Impact Energy of 54J & Observed and Calculated Yield Strength for for Plain C-Mn Steel Intercritically Annealed at 730°C, (Coarser Grain Size).

Holding time, minutes	ITT °C				Yield Strength σ_Y, Mpa		
	Obs.	Cal*	ΔITT		Obs.	Cal.	$\Delta\sigma_Y$ obs. - cal.
Normalised	-5	5	obs	cal	224	235	-11
Reheated to 730°C							
30	-5	-2	0	7	215	235	-20
900	-7	-14	2	19	226	241	-15
Cooled to 730°C							
30	-10	-3	5	8	219	234	-15
900	-10	-14	5	19	220	235	-15

* Constant has been taken as 110

CHAPTER SIX

CONCLUSIONS

Based on the investigations in this research work the following conclusions are made:

1 - At a cooling rate of 7°C/min, intercritical annealing a 0.56%Mn and 1%Mn steel containing Nb and Al at 730°C improves the impact toughness (lowers the impact transition temperature) by 20-35°C without any significant change in yield and ultimate tensile strength.

2 - The improvements in impact toughness are due to a refinement in the grain boundary carbide thickness probably due to Mn segregation to the α-α grain boundaries from where the new γ nuclei are formed and/or to the α/γ boundaries. Enrichment of Mn at the boundaries or within the γ lowers the transformation temperature at which carbides form, resulting in finer carbides.

3 - Strength is generally little affected by intercritical annealing due to there being little change in grain size. Generally the regression equation obtained by Mintz et.al[] is satisfactory for describing yield behaviour. However, reducing the cooling rate produces

lower yield strengths than are calculated from this equation and there is a need to modify it to take account of cooling rate.

4 - Increasing the holding time at the intercritical annealing temperature, refines the grain boundary carbide thickness leading to a greater improvement in ITT.

5 - This refinement may be due to an increase in hardenability due to Mn enhancement. Also the dispersion of the second phase (pearlite) along the ferrite boundaries may contribute to the improvements in ITT, as on transformation a greater number of nucleation sites for carbide precipitation are formed and this will favour finer carbides.

6 - Significant improvements of impact toughness can occur after as short an intercritical annealing time as 15 minutes.

7 - Intercritical annealing the lower Mn steels improves the impact toughness both on reheating from room temperature to 730°C after normalising at 920°C or on cooling from the austenitising temperature of 920°C to 730°C, the former heat treatment being the most beneficial. Smaller improvements on cooling down would be expected as time is required for the γ to α transformation to occur before austenite enriched in Mn can form.

8 - In contrast, intercritical annealing the higher, 1.5%Mn

C-Mn-Nb-Al steel at 730°C gives a deterioration in impact behaviour. This is probably related to the increasing hardenability of the γ allowing the formation of very small martensite colonies at the boundaries as well as in the case of heating up an increased volume fraction of pearlite. This could be avoided by :

a- reducing the cooling rate from 7°C/minutes to a slower cooling rate of 0.8°C/minutes.

b- reducing the carbon level from 0.1% to 0.067%. However, improvements in this case were small, probably due to the very fine carbides present on normalising.

9 - For the 1% Mn steel containing Nb and Al, raising the intercritical annealing temperature to 760°C gives similar improvements to those obtained at 730°C on heating up but not on cooling down, when improvements were much reduced. This may be related to the higher intercritical annealing temperature delaying the γ to α transformation.

10- The benefits from intercritical annealing appear to be related to the grain size. A plain carbon manganese steel with a fine grain size (18μm) showed improved impact toughness (lowers the ITT) by about 5-15°C, whereas a coarser grain size of 37μm gave no significant change in the impact behaviour on intercritical annealing at 730°C. Assuming that

manganese enrichment along α/α boundaries leads to γ formation, then the higher the surface area/volume ratio of the ferrite grains the more readily this can occur, leading to finer carbides and improved impact behaviour.

11- Improvements in impact behaviour on intercritical annealing depend on the carbide thickness range which is covered. Increasing the carbide thickness on normalising above 0.55 μm or reducing carbide thickness below 0.2 μm has only a small influence on impact behaviour on intercritical annealing. Thus the greatest benefits to impact behaviour on intercritical annealing (assuming martensite can't form) are likely to occur when the carbide thickness on normalising falls into the 0.55 to 0.25 μm range. This limits the usefulness of the process for high Mn (1.4%) steels to very slow cooling rates i.e. thick plate.

CHAPTER SEVEN

FUTURE WORK

The present work is concerned with the effect of intercritical annealing treatment on the impact toughness and yield strength. It is hoped to extend the work to cover the following:

1- The effect of intercritical annealing on fracture strength needs to be established. This topic that has not been addressed in the literature. It is well known that increasing the grain boundary carbide thickness results in a lower fracture strength and a higher ITT[141]. Intercritical annealing does refine the grain boundary carbide thickness, so, it is expected that the intercritical annealing can also improve the fracture strength.

2- It is necessary to obtain the Mn content of the "pearlite" regions for all the conditions examined in this study i.e. on the lower C steel, the 1% Mn steel intercritically annealed at 760°C, and the plain C-Mn steel at the two grain sizes. Such information is required for a more complete picture.

3- More quenching experiments are required to examine how the γ forms and grows with intercritical annealing time.

This is particularly so for the higher intercritical annealing temperature of 760°C.

4- The influence of martensite on strength and impact behaviour needs to be more throughly examined. Steels having low and high Mn contents (0.56, and 1.4%) at two C levels (0.05 and 0.1%) need to be intercritical annealing for various times to give a variation in the γ volume fraction and quenched to form martensite, and the impact and strength determined.

5- The inter-relationship of carbide thickness to impact behaviour needs to be more clearly established over a wider range from 0.15 μm to 0.8 μm. This could be obtained by taking C-Mn-Nb-Al steels with low and high Mn levels and cooling at a variety of cooling rates through the transformation.

6- TEM on these dual- phase structures needs to be performed so as to establish the dislocation arrangements and the form of the martensite when present.

REFERENCES

1. R.S. Rashid, "GM 980X- Potential Application and Review", SAE Paper No 770211, Feb., 1977.
2. M.S. Rashid, "Manufacture of Automotive Components From Dual-Phase Steel", in Dual-Phase and Cold-Pressing Vanadium Steels in the Automobile Industry, Vanitec, Berlin, 1978, pp. 32-42.
3. A.M. Sage, "Dual-Phase and Cold Pressing Vanadium Steels in the Automobile Industry, Vanitec, Berlin, 1978, pp. 1-3.
4. S. Hayami and T. Furukawa, "A Family of High Strength, Cold-Rolled Steels", in Proceeding of Microalloying 75, 2A, Washington D.C, 1975, pp.78-87.
5. Formable HSLA and Dual-Phase Steels, Proceeding, AIME Symposium, Chicago, 1977.
6. P.R. Mould and C.C.Skena, "Structure and Properties of Cold-Rolled Ferrite-Martensite (Dual-Phase) Steel Sheets", in Formabile HSLA and Dual-Phase Steels, A.T. Davenport, ed.; AIME, New York, NY, 1979, pp.181-204.
7. A.F. Crawley et.al., "Processing Properties and Modelling of Experimental Batch-Annealed Dual-Phase Steels", in Funamental of Dual-Phase Steels, R.A. Kot and B.L. Bramfitt, ed.; AIME, New York, NY, 1981, pp.181-197.

8. A. Okamoto and M. Tanahashi, "Control of Strength and r-Value in Box-Annealed Dual-Phase Steel Sheet", in Funamental of Dual-Phase Steels, R.A. Kot and B.L. Bramfitt, ed.; AIME, New York, NY, 1981, pp.427-445.

9. J.M. Rigsbee et.al., "Structure-Processing and Structure-Property Dual-Phase Steels", in Structure and Properties of Dual-Phase Steels, R.A. Kot and J.W. Morris, ed.; AIME, New York, NY, 1979, pp. 304-329.

10. T. Matsuoka and K. Yamamori, "Metallurgical Aspects in Cold-Rooled High Strength Steel Sheets", Met. Trans., Vol. 6A, 1975, pp. 1613-1622.

11. K. Nakaoka et.al., "Reassessment of the Wter-Quench Process as a Means of Producing Dual-Phase Formable Steel Sheets", in Structure and Properties of Dual-Phase Steels, R.A. Kot and J.W. Morris, ed.; AIME, New York, NY, 1979, pp. 330-345.

12. T. Furukawa et.al.,"Process Factor for Highly Ductile Dual-Phase Sheet Steels", in Structure and Properties of Dual-Phase Steels, R.A. Kot and J.W. Morris, ed.; AIME, New York, NY, 1979, pp. 281-303.

13. M.S. Rashid, "Relationship Between Steel Micro-Structure and Formability", in Formabile HSLA and Dual-Phase Steels, A.T. Davenport, ed.; AMIE, New York, 1979, pp. 1-24.

14. T. Tanaka et.al., "Formation and Properties of Ferrite Plus Martensite Dual-Phase Structure", in Structure and Properties of Dual-Phase Steels, R.A. Kot and J.W.

Morris, ed.; AIME, New York, NY, 1979, pp. 221-241.

15. S. Hayami et.al., "Recent Developments in Formable Hot and Cold-Rolled HSLA Including Dual-Phase Sheet Steels", in Formabile HSLA and Dual-Phase Steels, A.T. Davenport, ed.; AMIE, New York, 1979, pp. 167-180.

16. J.H. Buchter and E.G. Hamburg, "High Strength Formable Sheet Steel", SAE Paper No. 770164, Jan. 1977.

17. A.P Coldren et.al., "Development and Mill Trial of As-Rolled Dual-Phase Steel", in Formabile HSLA and Dual-Phase Steels, A.T. Davenport, ed.; AMIE, New York, 1979, pp. 205-228.

18. T. Kato et.al., "Development of As-Hot-Rolled Dual-Phase Steel Sheet", in Fundamental of Dual-Phase Steels, R.A. Kot and B.L. Bramfitt, ed.; AIME, New York, NY, 1981, pp. 199-220.

19. A.P. Coldren and G. Tither, "Develoment of a Mn-Si-Cr-Mo As-Rolled Dual-Phase Steel", J.of Metals, April, 1978, pp. 6-9.

20. A.P. Coldren and G.T. Eldis, "Using CCT Diagrams to Optimize the Composition of an As-Rolled Dual-Phase Steel", J. of Metals, March, 1980, pp. 41-48.

21 T. Furukawa and M. Tanino, "Structure Formation and Mechanical Properties of Intercritically Annealed or As-Hot-Rolled Dual-Phase Steels", in Fundamental of Dual-Phase Steels, R.A. Kot and B.L. Bramfitt, ed.; AIME, New York, NY, 1981, pp. 221-248.

22. G.R. Speich and R.L Miller, "Mechanical Properties of

Ferrite-Martensite Steels" in Structure and Properties of Dual-Phase Steels, R.A. Kot and J.W. Morris, ed.; AIME, New York, NY, 1979, pp. 145-182.

23. J.W. Morrow et.al., "Intercritically Annealed Dual-Phase Steels for Automotive Applications", in Fundamental of Dual-Phase Steels, R.A. Kot and B.L. Bramfitt, ed.; AIME, New York, NY, 1981, pp. 151-167.

24. M.S. Rashid, "GM 980X- A Unique High Strength Sheet Steel With Superior Formability", SAE Preprint 760206, Feb. 1976.

25. Geib et.al, "The Effect of Intercritical Annealing Temperature on the Structure of Niobium Microalloyed Dual-Phase Steel" Met.Trans., Vol. 11A, 1980, pp. 1683-1689.

26. R.G. Davies, "The Deformation Behaviour of a Vanadium-Strengthed Dual-Phase Steel", Met. Trans., Vol. 9A, 1978, pp. 41-52.

28. R.G. Davies, "Influence of Martensite Composition and Content on the Mechanical Properties of Dual-Phase Steels", Met. Trans., Vol. 9A, pp. 671-679.

29. S. Asamura, "Automotive HSLA Steels Produced by Nippon Steel", in Dual-Phase and Cold-Pressing Vanadium Steels in the Automobile Industry, Vanitec, Berlin, 1978, pp.59-61.

30. P.E. Repas, "Metallurgy, Production Technology and Properties of Dual-Phase Steels", in Dual-Phase and Cold-Pressing Vanadium Steels in the Automobile

Industry, Vanitec, Berlin, 1978, pp. 13-22.

31. A.R. Marder and B.L. Bramfitt, "Processing of a Molybdenum-Bearing Dual-Phase Steel", in Structure and Properties of Dual-Phase Steels, R.A. Kot and J.W. Morris, ed.; AIME, New York, NY, 1979, pp. 242-259.

32. A.R. Marder, "The Structure-Properties Relationships in Chromium-Bearing Dual-Phase Steel", in Fundamental of Dual-Phase Steels, R.A. Kot and B.L. Bramfitt, ed.; AIME, New York, NY, 1981, pp. 145-160.

33. P. Messien et.al., "Phase Transformation and Microstructure of Intercritically Annealed Dual-Phase Steels", in Fundamental of Dual-Phase Steels, R.A. Kot and B.L.Bramfitt, ed.; AIME, New York, NY, 1981, pp. 161-179.

34. Metallurgy of Continuous-Annealed Sheet Steel, B.L. Bramfitt and P.L Mangonon, J.R., ed.; AIME, New York, NY, 1981.

35. Structure and Properties of Dual-Phase Steels, R.A. Kot and J.W. Morris, AIME, New York, NY, 1979.

36. Formable HSLA and Dual-Phase Steels, A.T Davenport, ed; AIME, New York, NY, 1981.

37. Fundamental of Dual-Phase Steels, R.A. Kot and B.L. Bramfitt, ed.; AIME, New Yok, NY, 1979.

38. A.E. Nehenberg, "The Growth of Austenite as Related to Prior, Structure", J. of Metals, Vol. 188, Ohio, 1950, pp. 162-174.

39. E.C Bain and H.W. Paxton, Alloying Elements in Steel,

2nd ed., 3rd Rev. Printing, ASM, Metals Park, Ohio, 1966.

40. R.R. Judd and H.W. Paxton, "Kinetics of Austenite Formation From a Spheroidized Ferrite-Carbide Aggregate", Trans. AIME, Vol. 242, 1968, pp. 206-215.

41. G.R. Speich and Szirmae, with Appendix by G.R. Speich and M.J. Richards, "Formation of Austenite from Ferrite and Ferrite-Carbide Aggregates", Trans. AIME, Vol. 245, 1969, pp.1063-1074.

42. M. Hillert et.al., "Effect of Alloying Ellement on the Formation of Austenite and Dissolution of Cementite", JISI, Jan. 1971, pp. 49-66.

43. M.Nemoto, "The Formation of Austenite From Mixtures of Ferrite and Cementite as Observed by HVEM", Met. Trans., Vol. 8A, 1977, pp. 431-437.

44. G.R. Purdy et.al., "The Growth of Proeutectoid Ferrite in Ternary Iron-Carbon-Manganese Austenite", Trans. AIME, Vol. 230, 1964, pp. 1025-1034.

45. J.B. Gilmour et.al.,"Thermodynamics Controlling the Proeutectoid Ferrite Transformations in Fe-C-Mn Alloys", Met. Trans., Vol. 3, 1972, pp. 1455-1464.

46. J.B. Gilmour et.al., "Partition of Manganese During the Proeutectoid Ferrite Transformation in Steel", Met. Trans., Vol. 3, 1972, pp.3213-3222.

47. G.R. Speich, "Physical Metallurgy of Dual-Phase Steels, in Fundamental of Dual-Phase Steels, R.A. Kot and B.L.Bramfitt, ed.; AIME, New York, NY, 1981, pp.

3-45.

48. G.R. Speich et.al., "Formation of Austenite During Intercritical Annealing of Dual-Phase Steels", Met. Trans., Vol. 12A, 1981, pp. 1419-1428.

49. A. Hultgren, "Isothermal Transformation of Austenite", Trans. ASM, Vol. 39, 1947, pp915-1005.

50. C.I. Garcia and A.J. DeArdo, "The Formation of Austenite in Low-Alloy Steels", in Structure and Properties of Dual-Phase Steels, R.A. Kot and J.W. Morris, ed.; AIME, New York, NY, 1979, pp. 40-61.

51. P. Wycliffe et.al., "Austenite Growth in the Intercritical Annealing of Ternary and Quaternary Dual-Phase Steels", in Fundamental of Dual-Phase Steels, R.A. Kot and B.L.Bramfitt, ed.; AIME, New York, NY, 1981, pp. 59-83.

52. D.P. Datta and A.M. Gokhale, "Austenitisation Kinetics of Pearlite and Ferrite Aggregates in a Low Carbon Steel Containing 0.15 Wt. Pct C", Met. Trans., Vol. 12A, 1981, pp. 443-450.

53. C.I. Garcia and A.J. De Ardo, "Formation of Austenite in 1.5Pct Mn Steels" Met. Trans., Vol. 12A, 1981, pp. 521-530.

54. E. Navara and R. Harrysson, "On the Mechanism of Austenite Formation During Inter and Subcritical Annealing of a C-Mn Steel", Scripta Meta., Vol. 18, 1984, pp. 605-610.

55. E. Navara et.al, "Austenite Formation in Manganese

Partitioning Dual-Phase Steel", Mater. Scie., Vol. 2, 1986, pp. 1196-1201.

56. R.G. Davies, "On the Ductility of the Dual-Phase Steels", in Formable HSLA and Dual-Phase Steels, A.T. Davenport, ed.; AIME, New York, NY, 1979, pp. 25-39.

57. R.G. Davies, "The Deformation Behaviour of a Vanadium-Strengthed Dual-Phase Steel", Met. Trans., Vol. 9A, 1978, pp. 41-52.

58. R.G. Davies, "Influence of Martensite Composition and Content on the Mechanical Properties of Dual-Phase Steels", Met. Trans., Vol. 9A, pp. 671-679.

59. R. Lagneborg, "Structure-Property Relationships in Dual-Phase Steels", in Dual-Phase and Cold Pressing Vanadium Steels in the Automobile Industry, Vanitec, Berlin, 1978, pp.43-54.

60. R.G. Davies and C.L. Magee, "Physical Metallurgy of Automotive High Strength Steels", in Structure and Properties of Dual-Phase Steels, R.A. Kot and J.W. Morris, ed.; AIME, New York, NY, 1979, pp. 1-19.

61. W.P. Morrison, "The Effect of Grain Size on the Stress-Strain Relationship in Low-Carbon Steel", Trans. ASM, Vol. 59, 1966, pp. 824-846.

62. W.C. Leslie, "Iron and it's Dilute Substitutional Solid Solution", Met. Trans., Vol. 3, 1972, pp. 5-26.

63. H. Masui and H. Takeshi, "On the Combination of Tensile Strength and Ductility in High Strength Cold Rolled Sheet Steels and the Metallurgical Factors

Responsible Therefore", Trans. ISI Japan, Vol. 16, 1976, pp.69-76.

64. D.K. Matlock et.al., "A Correlation of Processing Variables With Deformation Behaviour of Dual-Phase Steels", in Structure and Properties of Dual-Phase Steels, R.A. Kot and J.W. Morris, ed.; AIME, New York, NY, 1979, pp. 62-90.

65. M. Geib et.al., "The Effect of Intercritical Annealing Temperature on the Structure of Niobium Microalloyed Dual-Phase Steel", Met. Trans., Vol. 11A, 1980, pp. 1683-1689.

66. R.G. Davies, "Influence of Silicon and Phosphorous on the Mechanical Properties of Both Ferrite and Dual-Phase Steels", Met. Trans., Vol. 10A, 1979, pp. 113-118.

67. J.S. Gau et.al., "Microstructure and Properties of Dual-Phase Steels Containing Fine Precipitates, in Fundamental Dual-Phase Steels, R.A. Kot and B.L.Bramfitt, ed.; AIME, New York, NY, 1981, pp. 47-58.

68. J.M. Moyer and G.S. Ansell, "The Volume Expansion Accompanying the Martensite Transformation in Iron-Carbon Alloys", Met.Trans., Vol. 6A, 1975, pp., 1785-1791.

69. C.L. Magee and R.G.Davies, "On the Volume Expansion Accompanying the FCC to BCC Transformation in Ferrous Alloys", Acta Met., Vol. 20, 1972, pp. 1031.

70. J.M. Rigsbee and P.J. Vander Arend, "Laboratory Studies of Microstrusture-Property Relationships in Dual-Phase HSLA Steels", in Formable HSLA and Dual-Phase Steels, A.T. Davenport, ed.; AIME, New York, NY, 1979, pp. 56-86.

71. K.R. Kinsman et.al., "The Stability of Austenite in Very Small Particles", Acta. Met., Vol. 25, 1977, pp. 359-365.

72. P.R. Mould, "Methods for Producing High-Strength Cold Rolled Steel Sheet", Metals Eng. Quarterly, Aug. 1975, pp. 22-31.

73. G. Tither and M. Lavite, "Beneficial Stress-Strain Behaviour of Moly-Columbium Steel Line Pipe", J. of Metals, Sept. 1975, pp.15-23.

74. M.S. Rashid, "GM 980X-Potential Application an Review", SAE Paper No. 770211, Feb., 1977.

75. S. Hayami and T. Furukawa, "A Family of High-Strength, Cold-Rolled Steels", in Microalloying 75, Session 2A, Vanitec, London, 1975, pp. 78-87.

76. G. Thomas and J.Y. Koo, "Develoment in Strong, Ductile Duplex Ferritic-Martensitic Steels", in Structure and Properties of Dual-Phase Steels, R.A. Kot and J.W. Morris, ed.; AIME, New York, NY, 1979, pp. 183-201.

77. G.Thomas, Battelle Conf. on Fundamental Aspects of Structural Alloy Design, Richland, Wash., LBL-41/5, 1975.

78. B. Mintz, Met. Tech., 1974, p. 226.

79. W.B. Morrison et. al.,Conf. on Control Processing of HSLA Steels, York University, 1976, B.S.C. Report No. T/Prod/Misc/154/76/C.

80. F.B. Pickering, Microalloying 75, ed.; M. Korchynsky, Union Carbide Corporation, New York, p. 9.

81. B. Mintz and P.J. Turner, Met. Trans., 1978, 9A, p. 433.

82. B. Mintz, JISI, 1973, p. 433.

83. J.Y. Koo, Ph.D. Thesis, University of California, Berkeley, LBL-6657, Aug. 1977.

84. B. Harris, Composites, p. 152, July 1972.

85. K.D. Sibley and N.N. Breyer, "The Effect of Silicon on the Impact and Tensile Properties of Low-Carbon Steels", Met. Trans., Vol. 7A, 1976, pp. 1602-1604.

86. P. Abramowitz and R.A. Moll, "Silicon-Carbon Interaction and It's Effect on the Notch Toughness of Mild Steel", Met. Trans., Vol. 1, 1970, pp. 1773-1775.

87. Baumister, Mark's Standard Handbook for Mechanical Engineering McGraw-Hill, Inc. 1967.

88. A. Nakagawa et.al., ",Effect of Vanadium on Structure-Property Relationship of Dual-Phase Fe/Mn/Si/0.1C Steels", Met. Trans., Vol. 12A, 1981, pp.1965-1972.

89. G.T. Eldis and W.C. Hagel, "Effects of Microalloying on the Hatdenability of Steel", in Hardenability Concepts With Applications to Steel, D.V. Doane and J.S. Kirkaldy eds.; AIME, New York, NY, 1979, pp. 151-166.

90. T. Greday et.al., "About Different Ways to Obtain Multiphase Steels", in Formable HSLA and Dual-Phase Steels, A.T. Davenport, ed.; AIME, New York, NY, 1979, pp. 260-280.

91. J.W. Morrow et.al., "Intercritically Annealed Dual-Phase Steels for Automotive Applications", in Formable HSLA and Dual-Phase Steels, A.T. Davenport, ed.; AIME, New York, NY, 1979, pp. 151-166.

92. B. Mintz et.al., "Influence of Carbide Thickness on ITT of Ferrite Steels", Met. Tech., 1979, Vol. 6, p. 252.

93. M.R. Plichta and H.I. Aaronson, Met. Trans., Vol. 5, 1974, p. 2611.

94. N. J. Kim and G. Thomas, Met. Trans., Vol. 12A, 1981, p.483.

95. J.Y. Koo and G. Thomas, Mat. Sci. and Eng., Vol. 24, 1976, p. 187.

96. J.M. Hodge and M.A. Orehoski, "Relationships Between Hardenability and Percentage of Martensite in Some Low Alloy Steels", Trans. AIME, Vol. 167, 1946, pp. 627-638.

97. L.D. Jaffe and E. Gordon, "Temperability of Steels", Trans. ASM., Vol. 49, 1957, pp. 356-369.

98. J.Y. Koo and G. Thomas, "Design of Duplex Low Carbon Steels for Improved Strength : Weigth Applications", in Formable HSLA and Dual-Phase Steels, A.T. Davenport, ed.; AIME, New York, NY, 1979, pp. 40-55.

99. J.Y. Koo et.al., "Designing High Performance Steels With Dual-Phase Structures", Metal Progress, Sept. 1979, pp. 66.70.

100. J.Y. Koo et.al., "On the Low of Mixtures in Dual-Phase Steels", Met. Trans., Vol. 11A, 1980, pp. 852-854.

101. G.R. Speich and R.L. Miller, "Mechanicl Properties of Ferrite-Martensite Steels", in Structure and Properties of Dual-Phase Steels, R.A. Kot and J.W. Morris, ed.; AIME, New York, NY, 1979, pp. 145-182.

102. I.Tamura et.al., "On the Strength and Ductility of Two-Phase Iron Alloy", Trans. ISI Japan, Vol. 13, 1973, pp. 283-292.

103. W.C. Leslie and R.G. R.J. Sober, "The Strength of Ferrite and Martensite as Function of Composition, Temperature and Strain Rate", Trans. ASM, Vol. 60, 1967, pp. 459-484.

104. W.R. Cribband J.M. Rigsbee, "Work Hardening Behaviour and It's Relationship to the Microstructure and Mechanical Properties of Dual-Phase Steels", in Structure and Properties of Dual-Phase Steels, R.A. Kot and J.W. Morris, ed.; AIME, New York, NY, 1979, pp. 91-117.

105. A.R. Marder, "The Effect of Heat Treatment on the Properties of Structure of Molybdenum and Vanadium Dual-Phase Steels", Met. Trans., Vol. 12A, 1981, pp. 1569-1579.

106. P. Ostron, "Deformation Models for Two-Phase

Materials", Met. Trans., Vol. 12A, 1981, pp. 355-357.

107. A.R. Marder and B.L. Bramfitt, "Processing of a Molybdenum-Bearing Dual-Phase Steel", in Structure and Properties of Dual-Phase Steels, R.A. Kot and J.W. Morris, ed.; AIME, New York, NY, 1979, pp. 242-259.

108. S.S. Hanson and R.R. Pradhan, "Structure/Property Relationships and Continuous Yielding Behaviour in Dual-Phase Steels", in Fundamental Dual-Phase Steels, R.A. Kot and B.L.Bramfitt, ed.; AIME, New York, NY, 1981, pp. 113-144.

109. R.D. Lawson et.al., "The Effect of Microstructure on the Deformation Behaviour and Mechanical Properties of a Dual-Phase Steel", in Fundamental Dual-Phase Steels, R.A. Kot and B.L.Bramfitt, ed.; AIME, New York, NY, 1981, pp. 347-381.

110. G.T. Eldis, "The Influence of Microstructure and Testing Procedure on the Measured Mechanical Properties of Heat Treated Dual-Phase Steels", in Structure and Properties of Dual-Phase Steels, R.A. Kot and J.W. Morris, ed.; AIME, New York, NY, 1979, pp. 202-220.

111. J. Gerbase et.al., "The Mechanical Behaviour of Some Dual-Phase Steels With Emphasis on the Initial Work Hardening Rate", in Structure and Properties of Dual-Phase Steels, R.A. Kot and J.W. Morris, ed.; AIME, New York, NY, 1979, pp. 118-144.

112. W.C. Leslie et.al., Trans. AIME, 1960, Vol. 218, P

699.

113. United States Patent Office, 3042693, Nov. 1962.

114. B. Mintz and W.B. Morrison and A. Jones, Met. Technol., 1979, Vol. 6, pp. 252-260.

115. B. Mintz and J. Kolahi-Aval, Met. Trans., 1988, Vol. 19 A, pp. 1481-1490.

116. British Standrads 1041, Temperature Measurement.

117. D. Flemington B.Sc. Final Year Project, 1984, The City University, London.

118. British Standrads 18, Part 2, Tensile Test of Metals, Steels, 1971.

119. British Standrads 131, Part 2, Charpy V-Notch Impact Test on Metals, 1972.

120. British Standrads 131, Part 5, Determination of Crystallinity, 1965.

121. R.L. Ruben and T.N. Baker, Mat. Sci.& Eng., Vol. 62, 1984, p. 93.

122. F.B. Pickering, "The Basis of Quantitative Metallography", Inst. of Metallurogists, Monograph.

123. J.W. Morrow and G. Tither, J. Met., December 1978, p. 20.

124. J. Y. Koo and G. Thomas, Met. Trans. 8A, 1977, p. 525.

125. J.Y. Koo and Thomas, Mat., Sci. and Engr. 24, 1976, p. 187.

126. G. Thomas, Battelle Conf., "On Fundamental Aspects of Structural Alloy Design", LBL- 4175, 1975.

127. B. Mintz, Met. Tech. "The Influence of Cooling Rate

From Normalising Temperature and Tempering on the Strength of Ferrite/Pearlite Steels" 1984, vol. 11, pp.52-60

128. B. Mintz, Met. Tech.,"Importance of K_y (Hall Petch Slope) in Determining Strength of Steels" ,1984, Vol. 11 pp.265-272.

129. B. Mintz and J. Kolahi-Aval, Proc. 7th Inter. Conf. on Strength of Matels and Alloys, "Influence of Cooling Rate From the Normalising Temperature on the Hall-Petch Slop for Steels", 1985, Montreal, Canada, Pergamon Press, pp.207-212.

130. B. Mintz, W.B. Morrison and A. Jones, Met. Tech., "The Influence of Carbide Thickness on the Impact Transition Temperature of Ferritic Steel" 1979, vol.6, pp.252-260.

131. N. Petch, Acta Metall., "The Influence of Grain Boundary Carbide and Grain Size on the Cleavage Strength and Impact Transition Temperature on Steel", 1986, vol.34, pp.1387-1393.

132. B. Mintz et.al, Metals Soc. Book, " advances in Physical Metallurgy and Applications of Steels", 1981, 284, pp.222-228.

133. B. Mintz and P. Campbell, Mate. Sci. & Tech., portance of Carbide Density in Influencing Grain Boundary Carbide Thickness", 1987, vol. 3, pp. 845-848.

134. S. Tajik, M.Phi Thesis, The City University, London,1990.

135. G.R. Speich, V.A. Demarest & R.L. Miller, Met. Trans., 1981, 12A, p. 1419.

136. E. Navara, HSLA Steels Conf., Univ. Wollongong, Australia, Ed., D.P. Dunn & T. Chandra, 1984, p. 302.

137. J. Gilmour et.al, Met. Trans., "Thermodynamics Controlling the Proeutectoid Ferrite Transformations in Fe-C-Mn Alloys", 1972, vol. 3, pp.1455-1464.

138. J. Gilmour et.al, Met. Trans. "Partition of Manganese During Proeutectoid Ferrite Transformation in Steel", 1972, vol. 3, pp. 3213-3222.

139. B. Mintz, Private Communication, City University, London, 1992.

140. H.I. Aaronson and H.A. Domain, "Partition of Alloying Elements Between Austenite and Proeutectoid Ferrite or Bainite", Trans. of Metall. Soci. of AIME, 1966, Vol. 236, pp. 781-796.

141. X.L. CAI et.al, "The Development of Some Dual-Phase Steel Structure from Different Microstructure", Met. Trans., 1985, pp. 543-557.

PUBLICATIONS.

Some of the results in this thesis have already been published in "Materials Science & Technology" under the title "The Influence of Intercritical Annealing on Strength and Impact Behaviour of Niobium Containing Steels", Aug. 1991, vol. 7, pp. 699-706.